Multifunctional Nano Additives for High-Performance Drilling Fluids:

An Experimental Investigation for High-Temperature Applications

Thesis submitted in partial fulfillment

for the Award of Degree

Doctor of Philosophy

by

Anirudh Bardhan

RAJIV GANDHI INSITUTE OF PETROLEUM TECHNOLOGY

JAIS, UTTAR PRADESH-229304, INDIA

21PE0002 **2024**

CERTIFICATE

It is certified that the work contained in the thesis titled ***"Multifunctional Nano Additives for High-Performance Drilling Fluids: An Experimental Investigation for High-Temperature Applications"*** by ***Anirudh Bardhan*** has been carried out under our supervision and that this work has not been submitted elsewhere for a degree.

It is further certified that the candidate has fulfilled all the requirements of Comprehensive, Candidacy and SOTA.

Dr. Shivanjali Sharma
Thesis Supervisor
Associate Professor, PEGE
RGIPT Jais

Dr. Shailesh Kumar
Thesis Co-Supervisor
Assistant Professor, PEGE
RGIPT Jais

DECLARATION BY THE CANDIDATE

I, ***Anirudh Bardhan***, certify that the work embodied in this thesis is my own bonafide work and carried out by me under the supervision of **Dr. Shivanjali Sharma** & **Dr. Shailesh Kumar** from *August 2021* to *August 2024*, at Rajiv Gandhi Institute of Petroleum Technology, Jais. The matter embodied in this thesis has not been submitted for the award of any other degree. I declare that I have faithfully acknowledged and given credits to the research workers wherever their works have been cited in my work in this thesis. I further declare that I have not willfully copied any other's work, paragraphs, text, data, results, etc., reported in journals, books, magazines, reports dissertations, theses, etc., or available at websites and have not included them in this thesis and have not cited as my own work.

Date: **Anirudh Bardhan**

Place: RGIPT Jais Roll no. 21PE0002

CERTIFICATE BY THE SUPERVISORS

It is certified that the above statement made by the candidate is correct to the best of our knowledge.

Dr. Shivanjali Sharma **Dr. Shailesh Kumar**

Thesis Supervisor Thesis Co-Supervisor

Prof. Satish Kumar Sinha

Head, PEGE

CERTIFICATE

CERTIFIED that the work contained in the thesis titled ***"Multifunctional Nano Additives for High-Performance Drilling Fluids: An Experimental Investigation for High-Temperature Applications"*** by Mr. ***Anirudh Bardhan*** has been carried out under our supervision. It is also certified that he fulfilled the mandatory requirement of TWO quality publications arose out of his thesis work.

It is further certified that the two publications (copies enclosed) of the aforesaid Mr. ***Anirudh Bardhan*** have been published in the Journals indexed by –

(a) SCI

(b) SCI Extended

(c) SCOPUS

Dr. Shivanjali Sharma
Thesis Supervisor

Dr. Shailesh Kumar
Thesis Co-Supervisor

Dr. Hemant Kumar Singh
Convener, DPGC, PEGE

COPYRIGHT TRANSFER CERTIFICATE

Title of the Thesis: Multifunctional Nano Additives for High-Performance Drilling Fluids: An Experimental Investigation for High-Temperature Applications

Name of the Candidate: Anirudh Bardhan

Copyright Transfer

The undersigned hereby assigns to the Rajiv Gandhi Institute of Petroleum Technology Jais all rights under copyright that may exist in and for the above thesis submitted for the award of ***Doctor of Philosophy***.

Date: **Anirudh Bardhan**

Place: RGIPT Jais Roll no. 21PE0002

Note: However, the author may reproduce or authorize others to reproduce material extracted verbatim from the thesis or derivative of the thesis for author's personal use provided that the source and the Institute's copyright notice are indicated.

Dedicated to my anchor in life and beyond...

ॐ

असतो मा सद्गमय ।

तमसो मा ज्योतिर्गमय ।

मृत्योर्मा अमृतं गमय ।

ॐ शान्तिः शान्तिः शान्तिः ॥

Om

Lead us from the unreal to the real.

Lead us from darkness to light.

Lead us from death to immortality.

Om Peace Peace Peace.

— Brhadaranyaka Upanishad

Acknowledgment

The path to completing this thesis has been fraught with both professional challenges and personal adversities. As I reflect on my journey, I am overwhelmed with gratitude for the countless individuals who have touched my life, shaped my experiences, and supported me in innumerable ways. Each of them has contributed to the person I am today, and for that, I am deeply thankful.

First and foremost, I am profoundly grateful for the enduring support of my supervisor, Dr. Shivanjali Sharma, whose steadfast belief in my capabilities and academic potential encouraged me to persevere even during my lowest moments. Her guidance was a beacon of light in times of doubt. I am especially grateful for her efforts in ensuring I had all the necessary resources to complete my doctoral work. Her emphasis on integrity, professionalism, and respect has greatly shaped my approach to work and hopefully will remain a guiding principle throughout my career. I would also like to acknowledge my co-supervisor, Dr. Shailesh Kumar, for his unique contributions, which certainly added an unexpected dimension to this journey. Another person who deserves special mention is Dr. Amit Saxena, with whom I could reconnoitre the topology of the industry-academia interface through various projects and ideas.

I sincerely thank the Department of Petroleum Engineering and Geoengineering, and the institute as a whole, for providing a supportive and enriching environment that has greatly contributed to my research journey. The resources, facilities, and opportunities available here have been instrumental in my academic growth. I take immense pride in being associated with a prestigious institution like RGIPT. In this

regard, I would like to express my gratitude to Prof. Satish K. Sinha, our Head of the Department, Prof. Alok K. Singh, our Director, and Prof. A. S. K. Sinha, our Ex-Director, whose leadership and sustained support have made this journey possible. Appreciation to all the faculty members for their constructive feedback, and insightful suggestions. Thanks to Mr. Ramu, the Office assistant and Dr. Iltaf Zafar, technical superintendent from the department for being of assistance in times of dire need. Special credit also goes to the Dr. Anuj Prajapati, and Dr. Zahoor Alam from the Central Instrumentation Facilities at RGIPT, who have always helped me with timely analysis and acquisition of data from sophisticated equipment, and brotherly advices which enabled me with the analytical characterization in this thesis. This acknowledgment is also incomplete without mentioning Dr. Krishna Raghav Chaturvedi because of whom I got deeply interested in academic publishing and planning research methodologies for scientific investigations.

A heartfelt thanks to my incredible team at the Drilling Fluids Design, Net Zero and Sustainability, and Reservoir Laboratories. My journey began with an introduction to the laboratory by Dr. Mukarram Beg over a call, followed by a physical induction by Dr. Himanshu Kesarwani. The onboarding process was made seamless by the support of Fahad, Govind, Apoorv, and Vishnu, and later enriched by the companionship of Deepak, Abhilasha, and Shivam in the following year. A special shoutout to my immediate senior, Mr. Anurag Pandey and my junior, Mr. Darshan Halari, for making this experience truly memorable. My gratitude also extends to Zeya and Shahzar for being supportive and enthusiastic members of our team. Special thanks to the Manish duo, Jayant, Ashim, Ashwini, Muntasir, Prateek, Manoj, Ramaswamy, and everyone else I had the pleasure of meeting and sharing great moments with. I must also profess recognition to my students, especially Soumyl, Harshwardhanam, Sushipra, Farheed, Somprity, Arhaan, Akangkhsa, Hayensa, and Kritika whom I had the opportunity to teach and guide.

This journey was also enriched by the presence of individuals with whom I could openly discuss everything—from research challenges and personal frustrations

to abstract philosophies. I am grateful to Vidit, Gourab, and Suvadeep Sir for the engaging and thought-provoking discussions we shared sitting at Rambharose. A special thanks to Bidesh Sir for being the elder brother I never realized I needed. I also extend my heartfelt appreciation to Mr. Ankit Singh for collaborating with me and sharing his expertise in nanomaterial synthesis and characterization. My gratitude also goes to Sk. Mehebub Rahaman, Prof. Bidyut Saha (Burdwan University), Mr. Aniket Singh, Dr. Asheesh Kumar (CSIR-IIP), Prof. Jayati Sarkar (IIT Delhi), Dr. Prithu Mukhopadhyay (IPEX Technologies Inc.), and Dr. Chetna Tewari (KIST) for their invaluable collaboration from their respective institutes. Each of these individuals played a crucial role in my research journey, reminding me that the pursuit of knowledge is not a solo expedition but a communal effort.

Heartfelt thankfulness to my mentors, teachers, and guides, right from my school who have been my inspiration, nurturing my curiosity and igniting a passion for learning. Their guidance, both in academics and in life, has been a gift beyond measure. Special thanks to the two most important teachers of my life - Ananta sir and Asutosh Mama, whose memories and teachings have walked with me during my entire academic journey.

Aknowledgment to my friends, old and new, near and far—who are the laughter that fills my days and the solace during life's storms. Mousumi, Archchi di, Sirshendu, Sanjeev, Piyush, and Shahrukh have stood by me in moments of celebration and during my trials, offering words of wisdom, humor, and care. Each shared memory is a treasure I carry in my heart.

This is to Poulomi, as I am forever grateful for her presence in my life. She has been my constant source of happiness, love and inspiration.

I am indebted to my family, the bedrock of my existence — for their unwavering love, patience, and encouragement. This is for my parents who instilled in me the passion for excellence, tolerated my idiosyncrasies, offered constant support, motivation, and life lessons till this day. Whenever I feel like giving up I find myself getting up and moving again because of my Maa. My relentless pursuit of knowledge

is credited to me looking up to my Baba as I am always awed with his tenacity and knowledge on virtually everything. I owe everything to them as much as I owe my life to God. Also, thanks to my grandparents, aunts and uncle for their constant warmth and cheer. Exclusive appreciation to my Thakurma who imbued in me the passion of reading during my early years.

This is also to acknowledge those I've crossed paths with, even briefly—whether a kind stranger, a classmate from years ago, or a fellow traveler on life's journey, each interaction has left an imprint on me, teaching me lessons I hope to never forget. Thanks to those who challenge me, question me, or push me beyond my comfort zone—they've helped me grow stronger, wiser, and more perseverant. I am grateful for the opportunity to learn from these experiences.

This acknowledgement is lastly for everyone I may have missed by name but not in spirit for being part of my story. Each of them holds a unique place in my life, and I cherish the roles they have played in shaping it.

...Anirudh

Preface

The quest for energy in the 21st century has driven the oil, gas, and geothermal industries to explore greater depths, where extreme temperatures pose unprecedented challenges to conventional drilling technologies. In this high-stakes arena, water-based drilling fluids (WBDFs) have long been the preferred choice over non-aqueous drilling fluids due to their cost-effectiveness, environmental friendliness, and superior cooling properties. However, as wellbore temperatures go beyond 149°C, these fluids often falter, suffering from thermal degradation, viscosity loss, and excessive fluid invasion into formations. At the heart of this technological crucible are high-performance drilling fluids (HPDFs)—formulations engineered with nanomaterials that can withstand and perform in such harsh conditions.

The advent of nanomaterials in drilling fluid technology marks a paradigm shift, offering solutions to problems that have vexed engineers for decades. Nanomaterials, by virtue of their minuscule size and colossal surface area-to-volume ratio, interact with drilling fluids at a molecular level, bestowing properties that were once thought unattainable, especially in high-temperature regimes. The integration of nanomaterials into WBDFs is not merely an incremental improvement but a transformative leap. When dispersed in WBDFs, they form stable colloidal suspensions that dramatically enhance rheological stability, reduce fluid loss, mitigate shale swelling, and even improve lubricity—all without compromising the inherent benefits of WBDFs. Notably, nanomaterials are extensively researched as a multifunctional additive for WBDFs. However, to maximize the benefits and ensure the safe and effective application of the HPDFs, the optimal selection of nanoma-

terials, dosage, and compatibility with other additives present in the formulations still needs consideration. Therefore, the current work focuses on applying various nanomaterials each addressing a particular objective set at the beginning of the investigation.

This thesis begins with the urgency, fundamentals, and foundation of the research by clearly defining the problem, purpose, research objectives, and structure of the thesis. Also, a thorough review of the literature is presented, offering a critical analysis of existing knowledge and identifying gaps that the current research aims to fill. It establishes a solid theoretical framework for the study, ensuring that the research is grounded in a comprehensive understanding of the topic.

Subsequently, the experimental framework of the study is established, detailing how the research objectives are addressed through systematic investigation and testing. It outlines the methodology used in the study, including the materials used, synthesis route, analytical characterization of the employed nanomaterials to determine their physical and chemical properties. Further, the preparation of nanomaterials-infused drilling fluids, detailing the steps for dispersing nanomaterials and adding necessary additives for uniform and stable formulations. Finally, it covers the performance evaluation of these formulations, including tests for rheology, filtration, lubricity, and thermal aging to assess their suitability for high-temperature drilling conditions. The evaluation of the selected nano additives for HPDF formulation span over the next five chapters, as summarized below.

1. Graphene nanosheets (GNs) synthesized from plastic waste: Through comprehensive characterization and experimental analysis, the chapter demonstrates the efficacy of GNs in enhancing rheological properties, thermal stability, and filtration control of water-based drilling fluids. The findings suggest that plastic-derived GNs can serve as eco-friendly additives, effectively improving drilling fluid performance and offering a sustainable solution to plastic waste while enhancing operations in high-temperature wells.

2. Modified multi-walled carbon nanotubes (mMWCNTs), stabilized for high-

temperature conditions: Through tailored modifications to enhance dispersion and stability, the study comprehensively evaluates the performance of these mMWCNTs using material characterization, rheological analysis, stability assessments, and filtration performance evaluations. Results demonstrate significant improvements in filtration losses and rheological profile, validating the practical applicability of mMWCNTs for enhancing drilling fluid performance in high-temperature drilling operations.

3. Biogenic copper oxide nanomaterials (CuO NPs) synthesized from *Colocasia esculenta* leaf extract: It demonstrates significant improvements in lubricity and filtration, as well as thermal stability under high-temperature conditions, showcasing the potential of these environmentally friendly nanomaterials for efficient and sustainable drilling operations.

4. Influence of morphological variations and dispersion stability of Zinc Oxide (ZnO) nanostructures on the properties of HPDFs: Two different ZnO nanostructures, namely Nano-pencils and Nano-flowers, are selected and their performance evaluated in HPDFs via rheological and filtration tests. The study highlights the significant impact of nanostructure morphology and size distribution on fluid properties. Additionally, it provides insights into optimizing dispersion stability and pH conditions for enhanced HPDF performance.

5. Silane-coated silica nanomaterials for improved aqueous dispersibility: It details the synthesis and coating process of the nanomaterials, followed by rheological and filtration tests at various concentrations. The results show significant improvements in viscosity and reduced degradation after thermal aging, along with a notable reduction in filtrate volume, demonstrating the effectiveness of these nanomaterials for high-temperature drilling applications.

The works wraps up with a crisp conclusion, and offers future recommendations based on the findings and insights gained throughout the investigation. A summary of the key findings and contributions of each study, highlighting the implications for

the field of drilling fluids, are highlighted. Additional suggestions for future research directions and practical applications, aiming to guide further advancements in HPDF technologies for high-temperature drilling environments are also provided.

Contents

List of Figures

List of Tables

Chapter 1

Introduction

This chapter outlines the urgency of drilling high-temperature wells to supplement the ever-increasing global oil and gas demand. The motivation of developing high-performance drilling fluids, and the rationale of exploring nano additives have been touched upon before presenting the problem statement which this thesis aimed to solve by defining the research objectives along with the nanomaterials that can address them. Finally, an outline has been presented to cover the framework of the thesis body.

1.1 Background & Motivation

Global energy demand is a critical aspect of the world's economy, influencing everything from geopolitics to climate change [1]. As of today, the global energy landscape is undergoing significant transformation due to various factors, including technological advancements, environmental concerns, and shifting economic dynamics. It is in a state of flux, with the traditional dominance of fossil fuels gradually giving way to a more diverse and sustainable energy mix [2].

Nevertheless, evident from Figure 1.1, the continued growth in global hydrocarbon demand is compelling the oil and gas industry to push the boundaries of exploration, venturing into new and previously under-explored areas. As exploration delves deeper into the Earth's subsurface, the challenges associated with

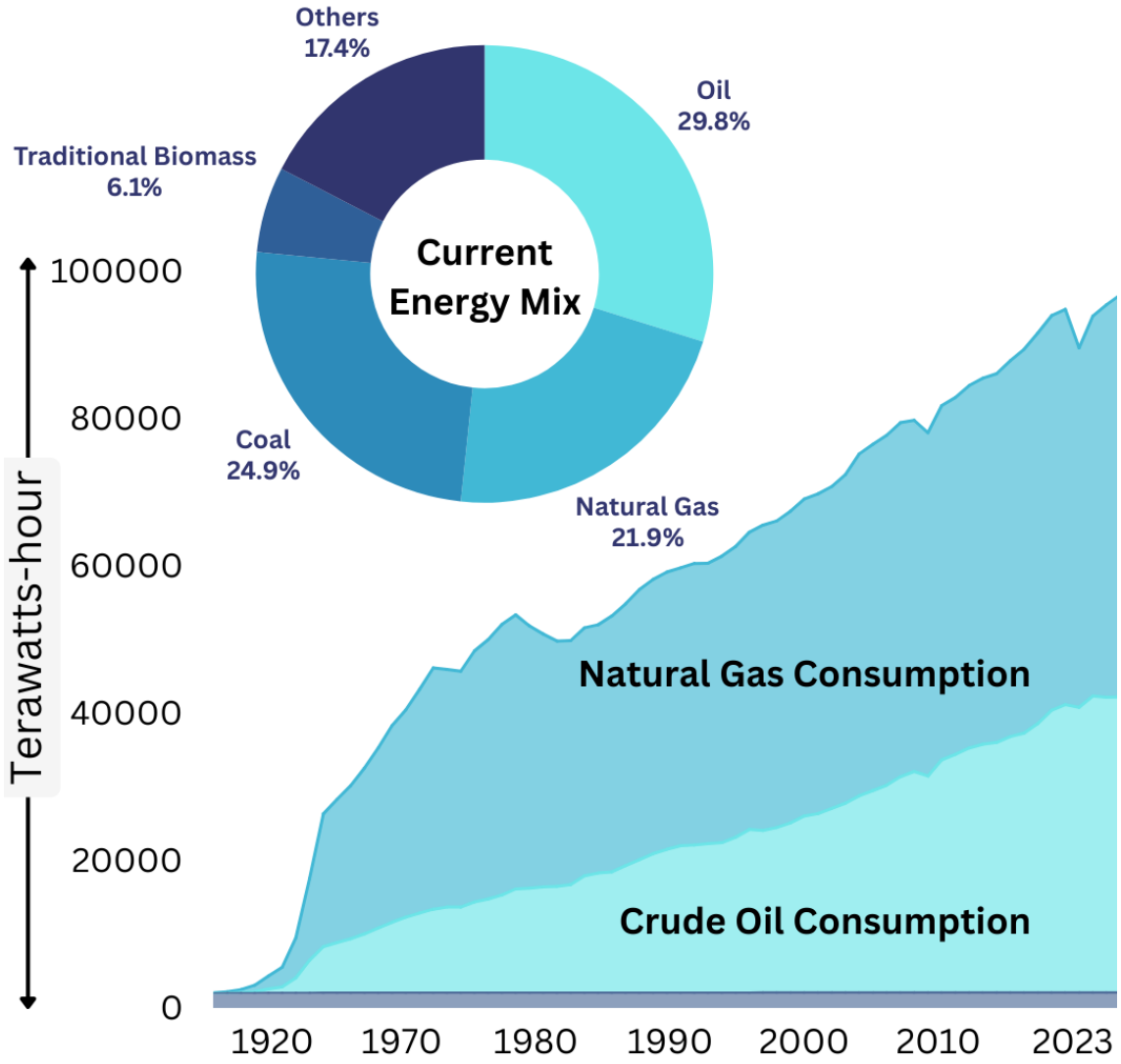

Figure 1.1: Global Energy Consumption through Natural Gas and Crude Oil from the year 1920 to 2023. [inset] The energy mix as of 2024, estimated by Energy Institute - Statistical Review of World Energy (2024).

high-temperature drilling become increasingly significant. The industry has reached a consensus that the era of easily accessible oil fields is over, especially in offshore environments where the complexities of drilling are amplified [3]. Projections indicate that global gasoline and diesel requirements are anticipated to surge from 26.4 million barrels per day in 2019 to 30 million barrels per day as of now, necessitating approximately 109 million barrels of oil daily by 2045 [4]. Global natural gas demand has also increased by over 2.5% in 2024 alone with increase in consumption, and the ratified emphasis of governments on reducing carbon emissions [5]. For instance,

India has intended to become a "gas-based economy" by increasing the share of natural gas in the energy mix up to 15% by 2030 as compared to the current value of 5.7% [6]. Along with market and policy reforms, the supplementation requires access to *more* reserves, again necessitating drilling deeper wells.

Constructing deeper wells, often exceeding 20,000 feet ($\sim$ 6100 m) into the subsurface, present numerous engineering challenges, including sub-salt drilling, narrow drilling windows, and operational hazards such as lost circulation, stuck pipes, and well control issues [7]. These challenges are further exacerbated by the extreme conditions encountered in high-temperature environments, where temperatures soar above 149 °C [8]. Downhole temperatures can be influenced by various natural conditions or external factors. Nearby geothermal hotspots can cause a rapid increase in downhole temperatures during drilling [9]. In contrast, wells drilled in deep and ultra-deep waters often have geothermal gradients lower than the Earth's average, leading to high pressure but temperatures that typically remain below the high-temperature threshold.

Drilling fluids being the *blood of the drilling physiology* is a crucial component when drilling these wells as they may degrade under high-temperature conditions which, in turn, complicates maintaining essential drilling fluid properties, such as equivalent circulation density, filtration, wellbore stability, etc. Insufficiently performing drilling fluid may cause operational failures and also put the drilling personnel at risk. The currently existing formulations has an added concern of ecological hazard as they may involve harsh and toxic additives, which makes their disposal dangerous. Therefore, there's a significant demand for thermally stable and environmental friendly drilling fluids to ensure operational success and safety [10].

1.2 Problem Statement

High-temperature well drilling presents multitude of issues as discussed earlier and involves the utilization of potentially harmful chemicals enhancing the risk of environmental contamination.

Conventional Water-based Drilling Fluids (WBDFs) fail to operate in elevated wellbore temperatures (above 149 °C) due to the degradation of the additives resulting in inconsistent properties. Oil-based Drilling Fluids (OBDFs) deliver technically superior performance in high-temperature conditions but find limited employment due to the higher associated costs and environmental concerns. Novel additives which deliver thermally stable enhanced performance are being explored with utmost urgency. Yet, there is a dearth of additives which are cost-effective, multifunctional, and sustainable.

1.3 Proposed Solution

High-Performance Drilling Fluid (HPDF) formulations, special WBDFs capable of replacing OBDFs, are required to be developed to deliver an environmentally friendly and cheaper solution. The use of nanomaterials as additives in WBDFs offers several potential advantages.

- Firstly, they can significantly enhance the rheological properties of the drilling fluids, leading to better flow behavior and improved control during drilling operations.

- Additionally, the inclusion of nanomaterials can reduce both filtrate and filter cake thickness, which is crucial for minimizing fluid loss and ensuring the integrity of the wellbore.

- Another important benefit is the potential improvement in the heat transfer properties of the drilling fluid, which helps in maintaining optimal temperature conditions and preventing overheating during drilling.

- Furthermore, nanomaterials can contribute to better wellbore stability and an improved lubricity coefficient, reducing the risk of wellbore collapse, and decreasing friction between the drill string and the wellbore.

1.4 Research Objectives

The general aim of the investigation towards this doctoral thesis was to identify and employ multifunctional *nano additives* for HPDFs that can withstand high-temperature (here, 150 °C) well environments with minimal thermal degradation. The comprehensive literature survey conducted on nanomaterials as additives for designing HPDFs, which will be discussed in Chapter 2, helped formulate the research objectives of this thesis.

I. To identify commercially feasible and scalable nanomaterials so that they could be produced and applied on a large scale without prohibitive costs or technical challenges.

II. To formulate thermally tolerant High-Performance Drilling Fluids which can maintain their structural integrity under high-temperature conditions.

III. To employ nanomaterials which possess the potential to enhance at least two properties of the formulated drilling fluids, ensuring multifunctionality.

IV. To investigate the role of different morphologies of the nanomaterials and their size distributions on the performance of the drilling fluid formulations.

V. To ensure the environmental sustainability of nanomaterials reflecting the growing importance of eco-friendly solutions in modern research and development.

VI. To address the aqueous dispersibility of nanomaterials for delivering a consistent performance.

The aforementioned research objectives collectively served as a screening criteria for the selection of five nanomaterials that were studied for application in HPDFs. Table 1.1 gives a precis of the selected nanomaterials and the intended objective(s). As the entire investigation was designed for high-temperature applications, improvement in the thermal stability of the DFs was a common for all the chosen nanomaterials. Cost-related issues have been dealt with proposing sustainable synthesis

routes and low dosage requirements. Aqueous dispersibility was improved by preparing pH-stabilized polymeric nanofluids. But, in some cases surface modifications or functionalizations were done to attain better dispersion stability. The role of morphology in improving the performance of the DFs has also been attempted to be understood.

Table 1.1: Summary of Nanomaterials used in this investigation.

Sl. No.	Product	Objective	Target DF Properties
1	Plastic Waste Upcycled Graphene Nanosheets	Sustainable Additive Development,Low Dosage Assessment	Rheology, Filtration, Thermal Stability
2	Modified Carbon Nanotubes	Improved Aqueous Dispersibility, Low Dosage Assessment	Rheology, Filtration, Thermal Stability
3	Biogenic Copper Oxide Nanoparticles	Sustainable Additive Development, Morphological Assessment	Filtration, Lubricity, Thermal Stability
4	Zinc Oxide Nanostructures	Morphological and Particle Size Distribution Assessment	Rheology, Filtration, Thermal Stability
5	Silane Coated Silica Nanoparticles	Improved Aqueous Dispersibility	Rheology, Filtration, Thermal Stability

1.5 Thesis Organization

The subsequent chapters discuss the overall methodology employed, followed by each nanomaterial's synthesis and performance evaluation towards the development of high-performance drilling fluids for elevated temperatures.

Chapter 1 covered the motivation of evaluating nano-additives for the formulation of high-performance drilling fluids, identification of the problem, proposal of a possible solution, and then laid out research objectives that this thesis work covered.

Chapter 2 covers the fundamentals of the drilling fluids, their functions and properties, before narrowing down to issues with high-temperature drilling and the issues with the existing solutions. A comprehensive review on the nanomaterials of

interest has been presenting, ultimately narrowing down to their limitations which gave way to formulating solution strategies with five nanomaterials which are discussed individually from Chapter 4 to 8.

Chapter 3 discusses the materials utilized in the investigation, generic formulation of nanofluids and drilling fluids, followed by the performance and analytical characterization techniques employed.

Chapter 4 attends to a sustainable method of plastic waste valorization into carbon nanomaterial, here Graphene Nanosheets. Ultra-low dosages were incorporated into a base DF formulation and the effects on the rheology and filtrate loss reduction were studied. The thermally induced decrement in the properties was also investigated.

Chapter 5 discusses stabilizing multiwalled carbon nanotubes through wet base oxidation and then further stabilizing their dispersion in a polymeric media with pH adjustment. This stabilization resulted in improved viscoelastic properties along with enhanced rheological profile in elevated pressure-temperature conditions. The filtration losses were also investigated and showed significant improvement even after exposure to high temperatures for an extended period of time.

Chapter 6 explores green synthesis of Copper Oxide NPs with a leaf extract from a wild plant *Colocasia esculenta* with simultaneous microwave treatment. The optimal size distribution with a plate-like morphology was selected for evaluating its efficacy as a lubricating and filtrate loss-reducing nano additive. The resistance to thermal degradation was also apparent in the case of all the performance parameters like rheology, filtration, and lubrication.

Chapter 7, presents an investigation into the role played by different morphologies and size distribution of a transition metal oxide in the performance of high-performance drilling fluids. In this case, zinc oxide nanomaterials with two distinct morphologies, i.e., nanopencils and nanoflowers were selected and a comparative performance evaluation was presented in terms of rheological and filtration performance, in conjunction with the effects of thermal aging.

Chapter 8 undertakes functionalization of commercially acquired Silica NPs with silane-coating, and dosing them in a base DF at different concentrations. The effectiveness of the Silane-coated Silica NPs was evaluated based on the rheological enhancements, filtration performance improvement and the resistance to thermal degradation.

Chapter 9 finally presents a concise conclusion based on the findings from the investigation around each of the research objectives, and then gives a set of future recommendations.

Chapter 2

Fundamentals and Literature Review

This chapter reviews some of the basic concepts encompassing drilling fluids, their functions, corresponding properties, and classification. It then addresses the challenges associated with high-temperature drilling conditions and highlights the limitations of currently used additives. Recognizing the limitations of conventional additives, the chapter proposes the use of nanomaterials as a potential solution with a three-point screening criteria to evaluate potential candidates through a literature survey of silica, transition metal oxides, and carbonaceous nanomaterials. Followed by identification of the associated limitations, a plan of investigation has been outlined.

2.1 Drilling Fluids: A Crucial Aspect of High-Temperature Drilling

Drilling fluids (DFs) are specially designed formulations that aid in subsurface drilling operations. Traditionally DFs used to be just a simple mixture of clay and water, earning the name - *mud*. Nevertheless, DFs have evolved over a century of fortification in their formulations and associated technologies. Despite of incurring

a minimal share of the drilling expenditure, correctly formulated DFs contribute profoundly in mitigating safety hazards and reduce the operational expenses by a significant margin [11].

Analogous to the blood circulation system in human body, the circulatory system in rotary drilling operations pumps the DF through the drillstring which jets through the drill bit and returns to the surface conditioning setup through annulus via return flowline (Figure 2.1).

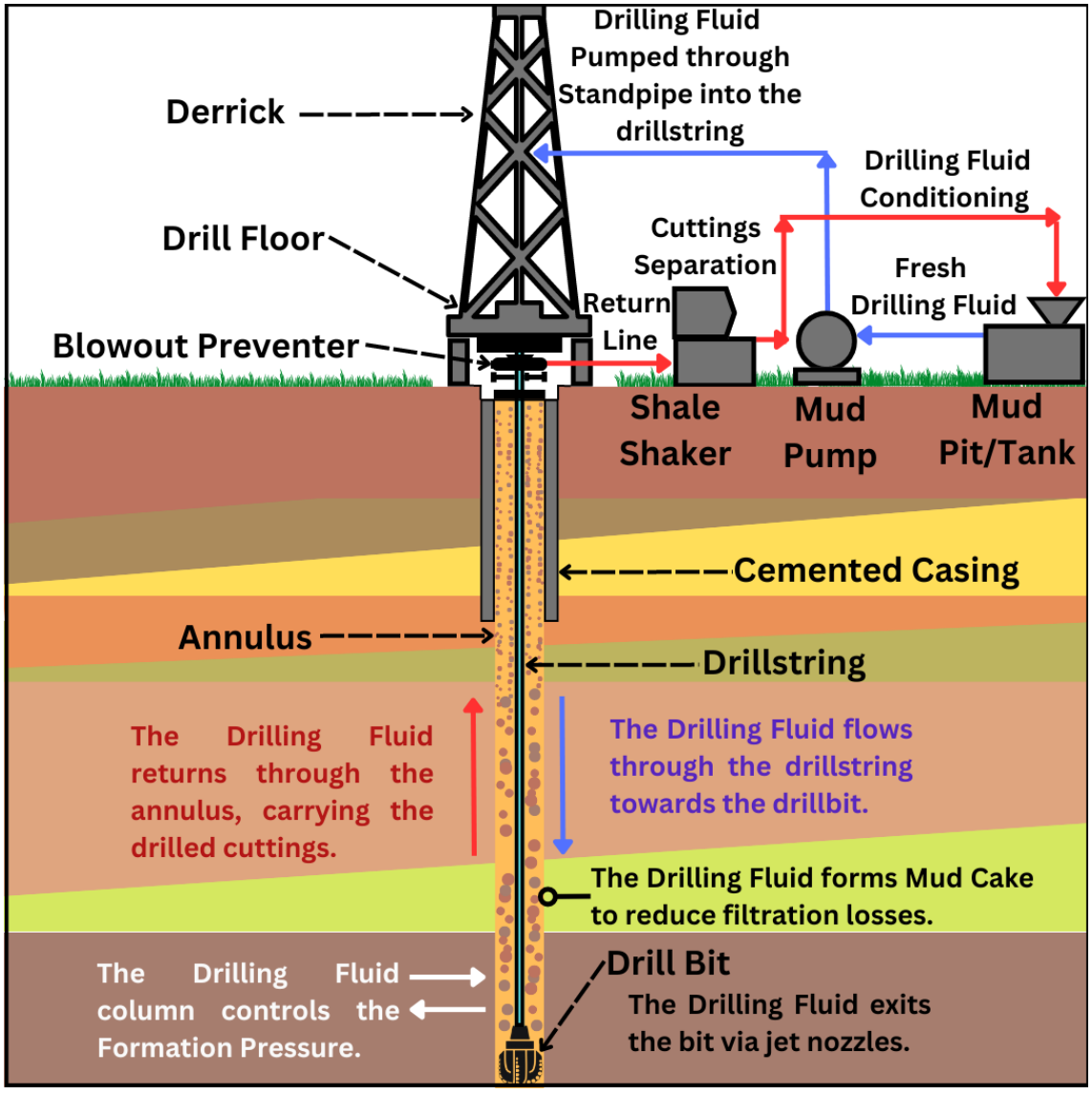

Figure 2.1: Schematic representation of DF circulation while drilling.

The conditioning starts with the separation of cuttings through a vibrating screen, known as the Shale Shaker. Some of these cuttings are collected by the mud loggers for further examination and analysis. The sifted DF then goes for

further solids control via Desander and Desilter, before moving to the mud pit, a storage tank in which the DF is reconditioned (by addition of chemicals or dilution). This reconditioned DF is transported by the Mud Pump through the Standpipe into the drillstring again.

DFs play a critical role in the success of drilling operations by serving multiple functions ensuring optimal wellbore health and efficient performance. Some of the properties which correspond to the essential functions of DFs are discussed henceforth.

2.1.1 Functions and Properties of Drilling Fluids

Some of the primary functions served by the DF during drilling operation are as follows:

1. Transportation of drilled rock cuttings from the bottomhole to the surface through annulus.

2. Maintenance of pressure to prevent influx of formation fluids into the wellbore.

3. Prevention or minimization of fluid losses into the rock formation due to filtration.

4. Reduction of friction between the drillstring and the wellbore wall.

5. Maintenance of wellbore integrity in the uncased region.

Additionally, some other functions of the DFs involve keeping the bit clean and cool, transmitting hydraulic power to the drill bit, providing a buoyant medium to drillstring, facilitating in well logging and mud logging, etc.

In purview of these functions, the some primary properties which are almost crucial for formulating any DF are discussed in the upcoming subsections.

Rheological Properties

The flow properties of the DFs dictate the cuttings transportation, and also influence the pumping efficiency, suspension of high-density solids, rate of penetration, etc. Therefore, it is absolutely critical to identify their *rheological behavior* for optimal performance [12, 13].

When a flowing fluid is in laminar regime, it can be visualized as multiple parallel layer constituents. If a *shear stress* is exerted on one layer and the velocity gradient (*shear rate*) between the layers in response is directly proportional, then that fluid is obeying *Newton's Law of Viscosity*. This *Newtonian fluid* will still oppose the stress exerted (due to the internal friction between the layers) by the virtue of a property called *Viscosity*. Combining this understanding with the illustration in Figure 2.2, the relationship can be mathematically expressed as given in Equation 2.1.

$$\tau = \mu.\gamma \tag{2.1}$$

where, τ is the shear stress, γ is the shear rate, and μ is the viscosity.

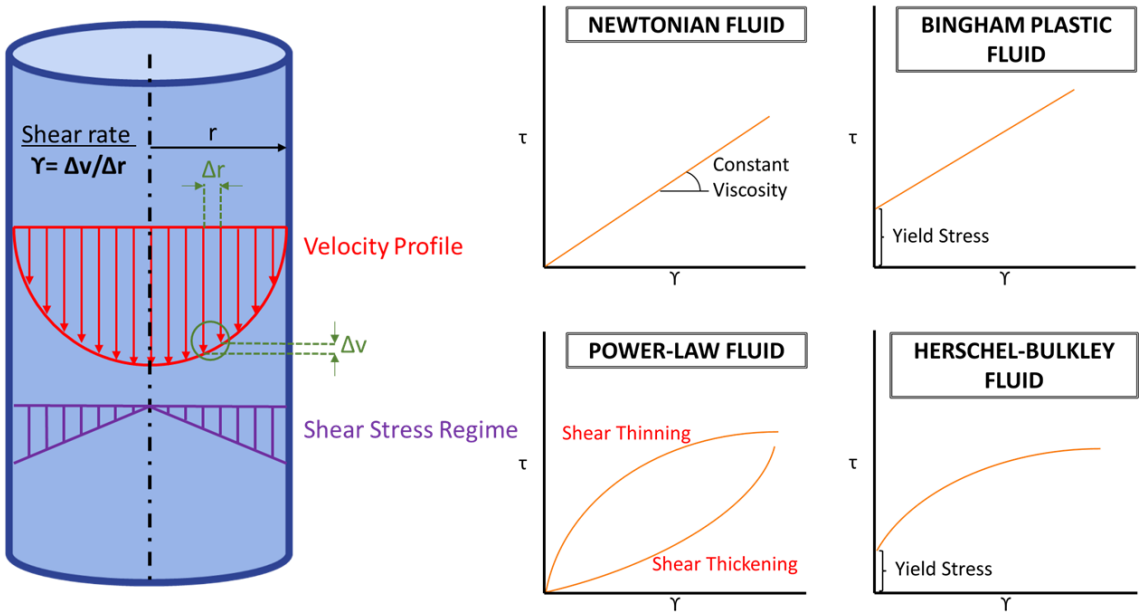

Figure 2.2: Illustration depicting the fundamental basis of DF rheology and the types of fluids.

Therefore, it is clear that in case of the Newtonian fluids, the shear stress varia-

tion corresponding to a varying shear rate will give a straight line from the origin, and shall possess a constant slope depicting the Newtonian viscosity. However, complex fluids like DFs do not obey the Newton's Law of Viscosity, and therefore are classified as *Non-Newtonian Fluids.* The Non-Newtonian rheological models are mathematical representations crucial for predicting DF behavior in diverse drilling conditions. Popular models include the *Bingham Plastic model*, treating fluid as solid below a yield point and Newtonian above it; the *Ostwald-de Waele model*, a Power-Law equation relating shear stress and rate; and the *Herschel-Bulkley model*, an extension of Power-Law model with a yield point from Bingham Plastic model. Equations 2.2-2.4 correspond to these models, and their conformity to the flow characteristics are determined through *Consistency Curves* (Shear rate vs Shear stress plot).

$$\textit{Bingham Plastic:} \qquad \tau = \tau_0 + \mu.\gamma \tag{2.2}$$

$$\textit{Power Law:} \qquad \tau = K\gamma^n \tag{2.3}$$

$$\textit{Herschel-Bulkley:} \qquad \tau = \tau_0 + K\gamma^n \tag{2.4}$$

where, τ is the shear stress ($lb/100ft^2$), γ is the shear rate (s^{-1}),μ is the viscosity (cP), $K$is the consistency index, n is the power law exponent or flow index, and τ_0 is the yield stress.

Bingham Plastic model is widely popular when characterizing DF rheology. Direct-indicating concentric cylinder rotational viscometers provide laminar flow between 1 mm annulus between a stationary bob and a rotating sleeve. The bob, connected to a torsion spring, translates torque into dial readings. The standard equipment utlizes the *Savins-Roper* design and aids in determination of the Bingham Plastic Parameters like Apparent Viscosity, Plastic Viscosity, Yield Point directly from just two rotational speeds: 600 and 300 rpm, as shown in Figure 2.3.

Apparent Viscosity (AV) is generally calculated as the shear stress applied to a fluid divided by the shear rate. For a Newtonian fluid, the AV is constant and equal to the Newtonian viscosity of the fluid. However, for Non-Newtonian fluids,

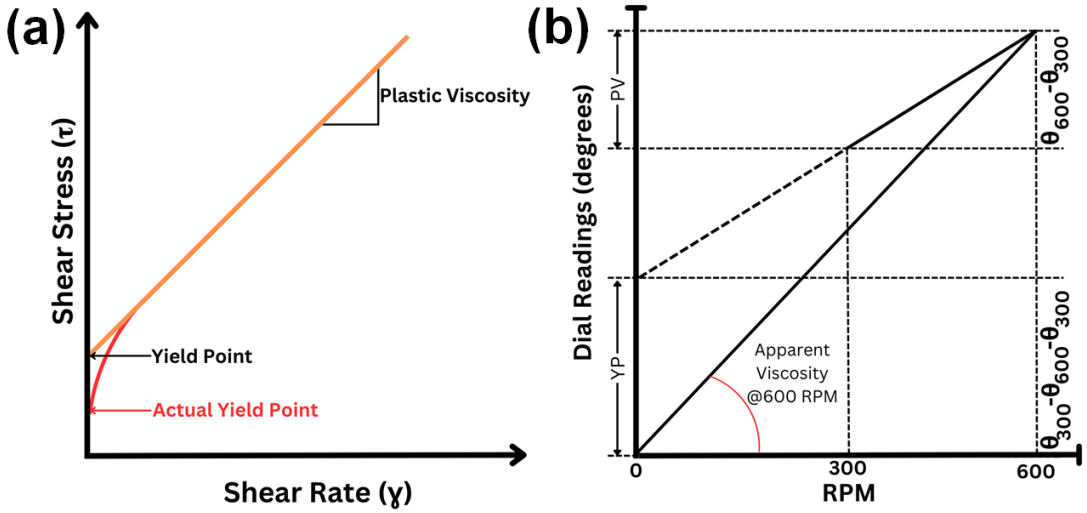

Figure 2.3: Graphical representation of (a) Bingham Plastic Model, and (b) interpretation of parameters from dial readings of a direct-indicating concentric cylinder rotational viscometer.

the AV depends on the shear rate. DFs are usually shear-thinning in nature, which means that as the shear rate increases the resulting effective viscosity reduces. It is measured at a specific shear rate and is affected by the speed and geometry of the instrument used for measurement.

Plastic Viscosity (PV) is a crucial parameter in drilling operations, representing the fluid's resistance to flow. The significance of PV becomes particularly evident in the evaluation of drilling process efficiency, especially concerning the fluid's flow at the drill bit, where high shear rates prevail. The mechanical friction within the DF, contributing to PV, involves the dynamic interaction of various components. Liquids and solids within the fluid experience shear stress, resulting in resistance to flow [14]. So, PV can be controlled by managing the solid content in the liquid phase of the DFs.

As discussed earlier, the Bingham plastic model assumes that a certain amount of stress, known as the yield point or YP, must be exceeded before the fluid starts to flow. Below this YP, the fluid behaves as a solid, resisting deformation. Once the YP is surpassed, the fluid transits to a more liquid-like state, exhibiting flow. This behavior is particularly relevant in drilling operations where the fluid needs to remain stationary when not actively circulated but must readily flow when subjected

to pumping or other shear forces. It is an essential property of DFs because it affects their ability to carry drilled cuttings to the surface and suspend them during drilling operations [15]. YP is generally controlled by manipulating the electrochemical properties through addition of certain chemicals.

A DF possessing a higher YP value may exhibit improved suspension properties, preventing the settling of cuttings. However, it can pose challenges in terms of pumpability. The ratio of yield point to plastic viscosity (YP/PV) emerges as a crucial factor for assessing the flow performance of drilling fluid [16]. Optimizing the pseudo-plastic behavior of the DF involves achieving a lower plastic viscosity and a higher yield point, promoting effective hole-cleaning, good pumpability, and a higher drilling rate [17].

The 2-speed method however has the tendency to overestimate the yield point, whereas in reality at lower shear rates the curve may not be linear. To accommodate this issue, nowadays people use 6-speed or 12-speed variations of the same standard viscometer. Despite of its deviation from the classic Bingham Plastic Model in lower shear rates, the values calculated from 2-speed settings are still indispensable as field indicators for optimizing the DF formulation.

It must be noted that DFs are also *thixotropic* in nature, i.e. they tend to develop higher *sol-gel transition point* when left at rest for extended time period. In DFs, this property is estimated as the *gel strength* at fixed time-intervals of rest, like 10 s, 10 min and 30 min. While it is essential for the DF to have certain gel strength developed immediately after cessation of circulation so that cuttings and high-density solids remain suspended, steep increase in gel strength (*Progressive gel*) over time is considered detrimental. This is because despite the reversible plasticity of the DF, the initial pumping pressure to reinitiate the circulation may rise severely. Furthermore, tripping of drillpipes may incur higher *surge and swab* pressures [18].

Density

As drilling ensues in deeper subsurface strata, the *pore pressure* (the pressure of the formation fluids in the pores of a rock formation) also increases due to the lithological *overburden*. Drilling a wellbore induces a pressure difference, which if not controlled may cause influx of the formation fluids or in severe cases may also result in blowout. Prevention of this problem can be mitigated by exerting an equivalent pressure with the DF. Generally, maintaining the hydrostatic pressure (pressure exerted by a static column of water) should be sufficient. The hydrostatic pressure is calculated using Equation 2.5.

$$P_h = \rho.g.h \tag{2.5}$$

where, P_h is the pressure of a column of fluid possessing density ρ, and g is the acceleration due to gravity.

Yet, there are possibilities of encountering abnormally pressured zones where there is a requirement of higher pressure to be put by the DF column. Evident from the Equation 2.5, density (mass per unit volume) can be enhanced in such cases. Since, the pressure changes with both depth and density, it is a standard practice to translate it into *density gradient*. The density of the DF (also known as *mud weight*) is generally kept slightly higher (by addition of weighting agents) than required to get a overbalanced pressure gradient which offer some benefits like, overcoming the pressure losses due to swabbing while tripping drillpipes (hence called *trip margin*), and formation of the *mud cake* on the wellbore wall (to be discussed in the next subsection). The schematic of the DF density gradient window is represented in Figure 2.4.

It is also imperative to select a suitable window for the DF density gradient as excessive overbalance will result in increased infiltration of the fluid into the formation and build-up the pressure. If this built-up pressure reaches the point of geomechanical stress failure, then it would *fracture* the rock formation. These estimations also aid in casing seat selection planning. Furthermore, excessive overbalance may reduce the rate of penetration and settling of heavy solids in the wellbore (*sagging*).

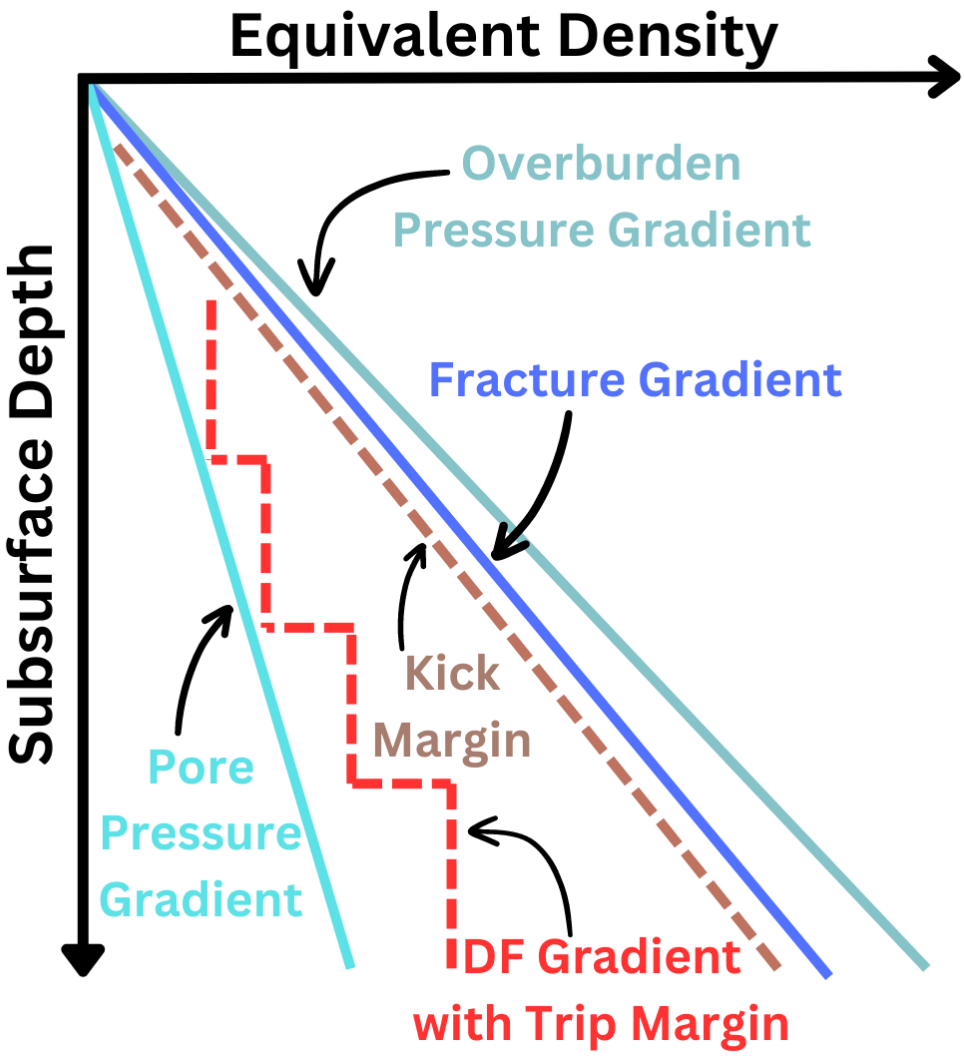

Figure 2.4: Schematic representation of an equivalent density gradient plot showing the DF gradient margin selection.

Filtration Properties

The previous subsection discussed the general preference for overbalanced pressure when drilling. In that case, filtration of the DFs into the formation occurs, leaving solids on the wellbore wall, forming a mud cake (also known as *filter cake*) that stabilizes the wellbore. Over time, this cake buildup reduces the rate of filtration, creating an impermeable barrier between the annulus and the formation as illustrated in Figure 2.5.

The development of a filter cake requires the DF to have particles that are somewhat smaller than the pore openings of the formation. Although smaller particles initially penetrate farther into the formation, these *bridging particles* become

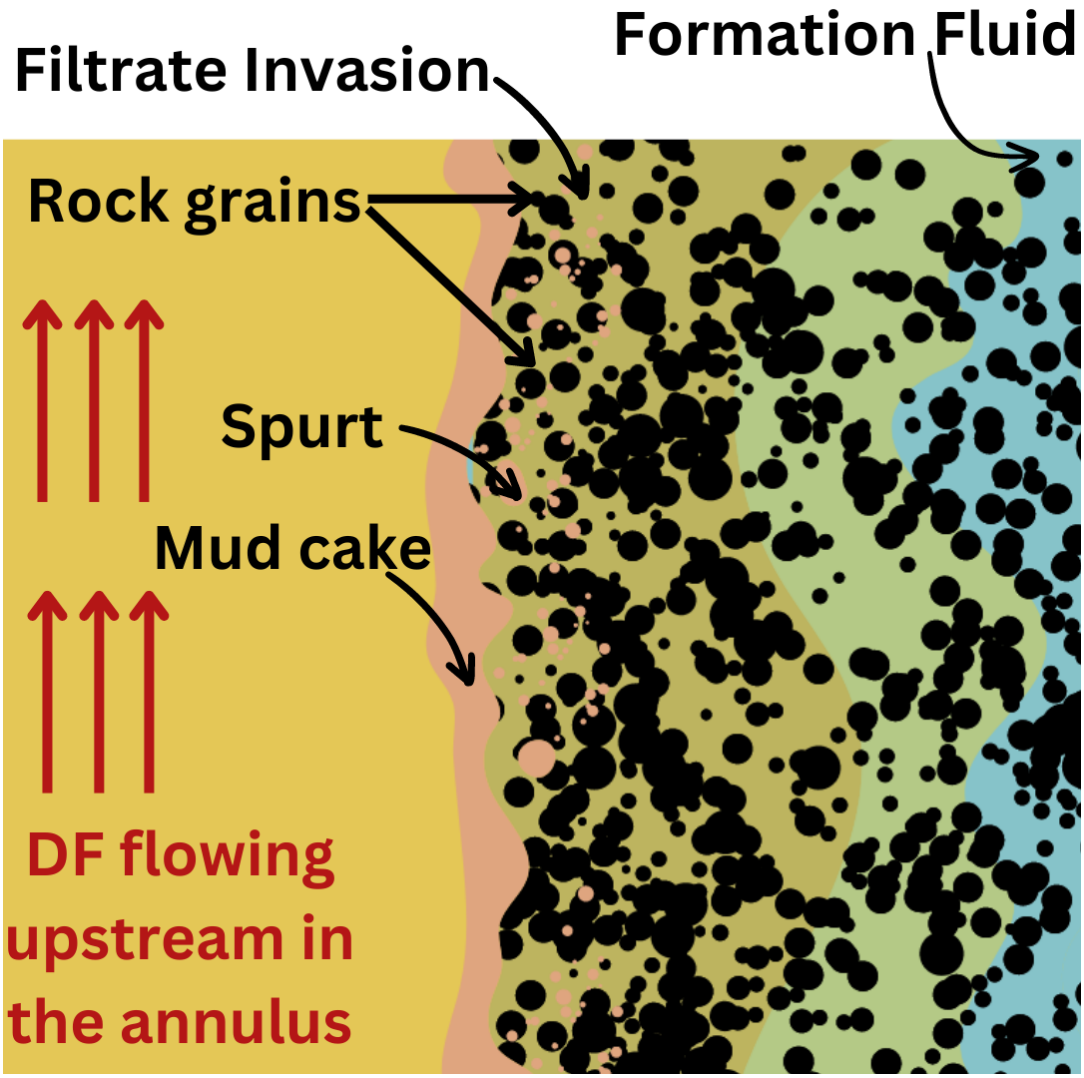

Figure 2.5: Schematic illustration of the DF filtration against the wellbore wall.

trapped in the surface pores. Over time, the bridging particles build up in the surface pores, progressively binding smaller particles and ultimately permitting only liquid to penetrate the formation, as depicted in Figure 2.6.

The first suspension of tiny particles during the development of a filter cake is known as the *mud spurt*, while the subsequent liquid is defined as the *filtrate*. Theoretically, the amount of filtration loss in a static DF pressurized at 100 psi, filtering through a 7 in^2 area, at any given time is calculated using Equation 2.6.

$$V = V_f \times \sqrt{T/T_f} \tag{2.6}$$

where, V is the unknown filtrate volume at time T, while V_f is the known filtrate

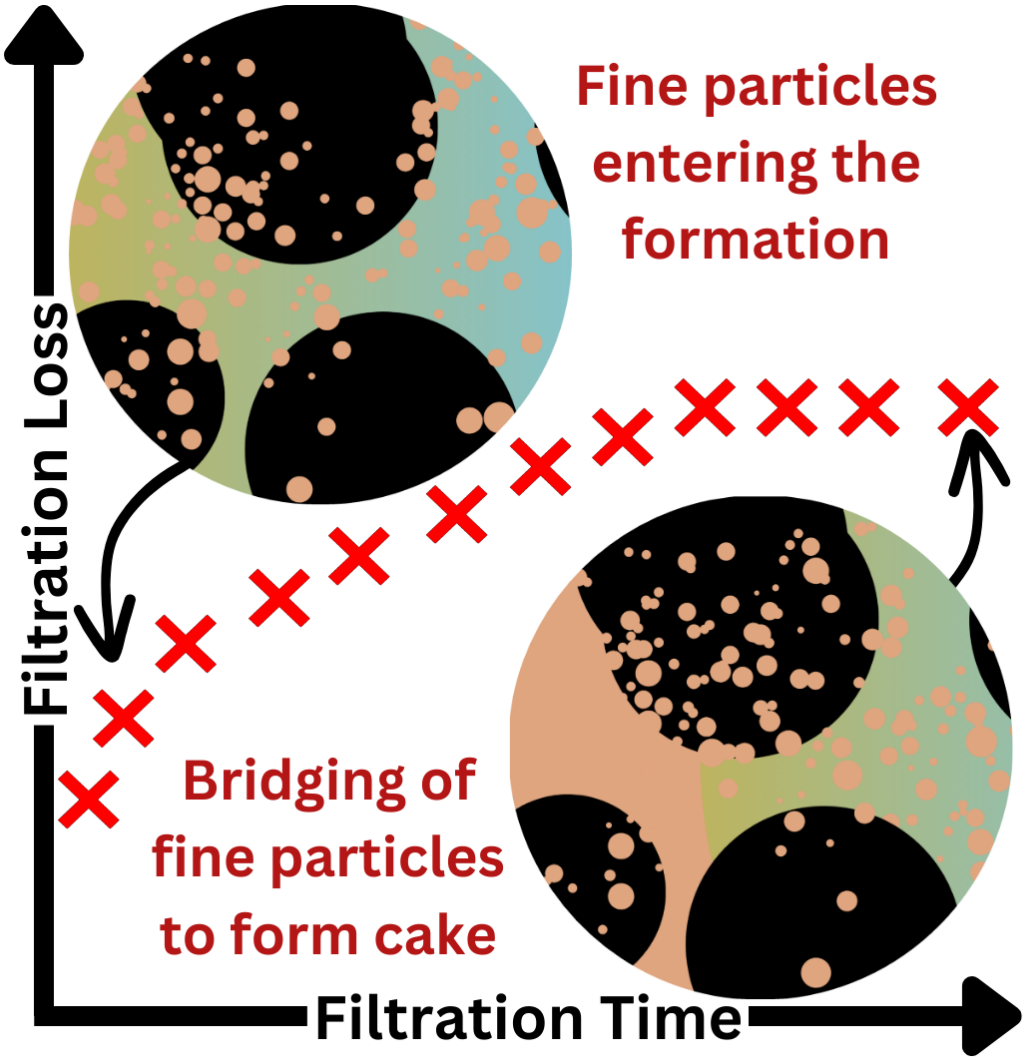

Figure 2.6: A diagrammatic representation of the reducing filtration loss over time due to formation of mud cake.

volume at time T_f.

Build-up of a thick filter cake may reduce the effective diameter of the wellbore which puts the drillstring at a risk of getting stuck. Therefore, the target of the DF formulation is to minimize formation damage while achieving a thin, impermeable cake [19].

Lubricity

Friction is a resulting force of resistance against two surfaces in contact. There are multiple sources of friction while drilling, which can arise in drillstring-casing, drillstring-wellbore (Figure 2.7), and bit-rock contacts. In directional wells the possi-

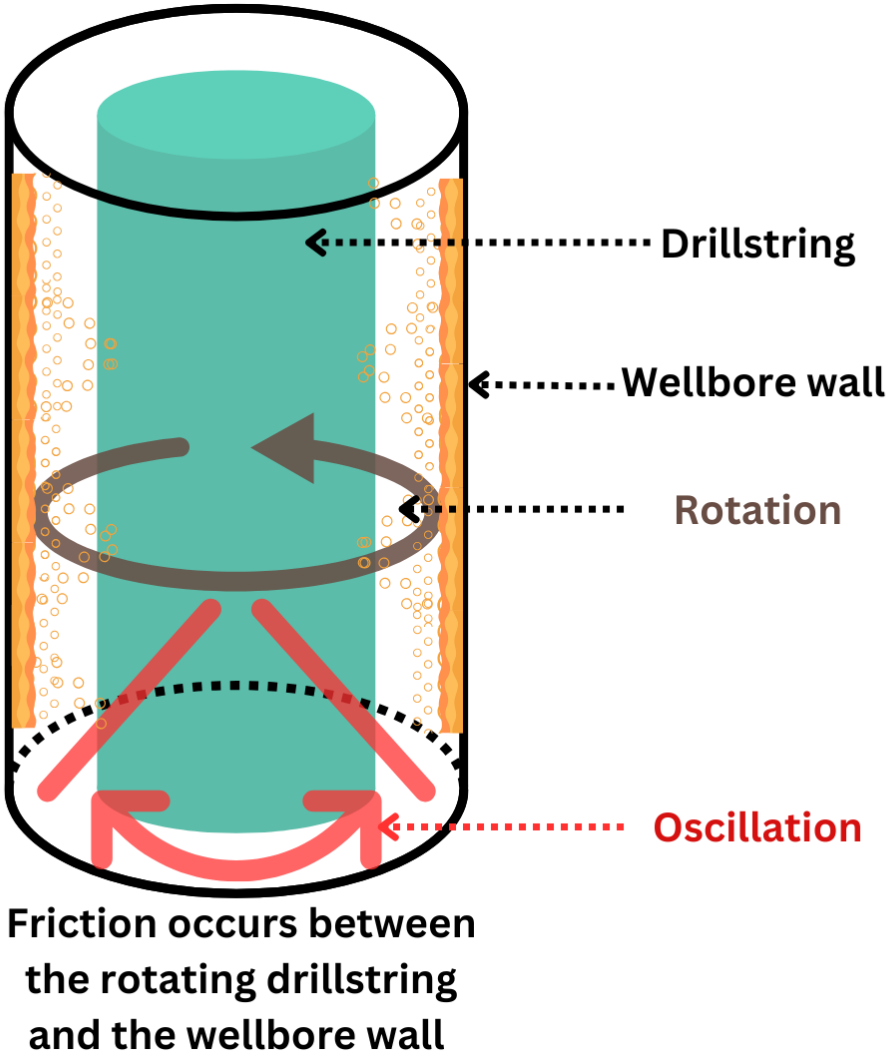

Figure 2.7: Schematic diagram of a rotating drillstring with oscillation causing friction against the wellbore wall.

bility of encountering friction increases due to dog legs, key seats, etc.The interaction between the drill string and the wellbore/casing generates substantial friction and high torque and drag forces. Additionally, the metal-to-metal contact between the drill string and the casing within the wellbore results in accelerated wears. Significant casing wear may also arise in deep and ultra-deep wells, aggravated by the process of tripping in and out of the borehole [20].

Hence, the DF should form a lubricating film at these interfaces to minimize the friction, and delay wearing of the equipment. Higher lubricity of DF also benefits in managing the torque and drag, enhancing rate of penetration, and preventing stuck pipe [21].

Solution pH

pH, an indicator of acidity or alkalinity, is essential while formulating DFs as they may affect other properties if not regulated properly. It is clear from Equation 2.7 that acidic pH is a result of higher hydrogen ionic concentration in a solution, and logarithmically reducing the H+ concentration will make the solution alkaline. In DFs, this alkalinity comes from bicarbonate, hydroxyl and carbonate ions [22].

$$pH = -log_{10}[H^+] \tag{2.7}$$

Generally, alkaline pH ranging between 9 to 11 is preferred for dispersion stability of bentonite and other additives along with ensuring minimal corrosive effects on the tubulars [23, 24].

Other Properties

In addition to the three primary properties discussed, there are several other physical and chemical properties which are often measured and optimized for designing an effective DF system, some of which are listed below.

- Chemical properties: Other than pH, the electrolytic concentrations in the DF introduced due to salts (metal chlorides, carbonates, sulphates, etc.) and polymers are also required to be controlled, in order to ensure consistent properties.

- Cation exchange capacity: It determines the equivalent cations from the clay minerals in DF, indicating the quantity of water-sensitive montmorillonite clay in the system, which should be balanced.

- Swelling: The extended interaction of DFs in a shaly formation would cause *swelling* of the clays, compromising the wellbore integrity. Salts and other swelling inhibitors are optimized in the DF formulations to mitigate such problems.

- Resistivity: It is determined to facilitate the formulation evaluation through wireline logging, which can be affected by the electrolytic and thermal environment of the DF in the wellbore.

2.1.2 Classification of Drilling Fluids

Commonly employed DFs, as shown in Figure 2.8, can be categorized into water-based (WBDFs), oil-based (OBDFs), and pneumatic-based fluids (PDFs), often incorporating additives like polymers and clay. OBDFs like Diesel-based, synthetic oil-based and invert emulsions have good lubricating and stability properties in high-pressure high-temperature zones, but they are expensive, and require treatment before their disposal to a safe place. The WBDFs entail the non-inhibitive, inhibitive and polymer-based fluids which are environmental friendly and cheaper but fail to perform in sensitive clay-bearing rock formations unless complemented with inhibitors or polymers. PDFs include air, foam, mist and aerated fluids for conditions which provide high rate of penetration, low formation damage but assert limited pressure control beyond shallow depths. Hence, it is natural that WBDFs are frequently chosen due to their lower cost, environment-friendly attributes, and fairly good performance [25].

In WBDFs, the base can vary from fresh water to brine depending on the location of drilling and the associated requirements. WBDFs can be subdivided based on the constituents as well. *Non-Inhibitive* WBDFS are generally the classic clay in water dispersions. The clay in these fluids can be of commercial nature (like bentonite) or from the drill cuttings. Additional components like lignosulfonates and phosphates may also be used. On the other hand, *Inhibitive* WBDFs are formulated to inhibit the swelling of water-sensitive clays encountered while drilling, rendering the wellbore stable and asserting more control over the properties of DFs. This inhibition is inculcated by the cations from the base brine or by adding inhibitors like potassium chloride, sodium chloride, etc. There's another way to regulate the electrolytic environment of the WBDFs, and that is through the addition of polymers. *Poly-*

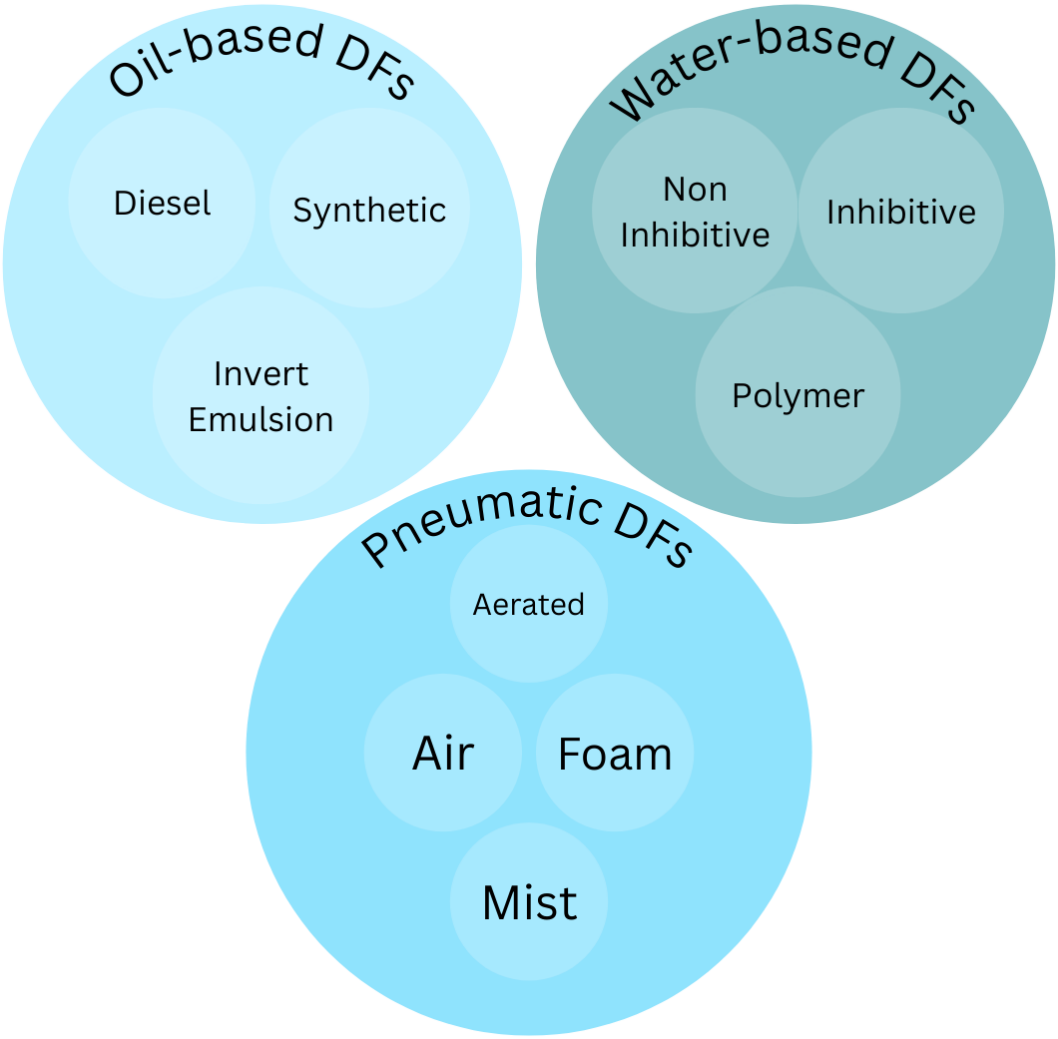

Figure 2.8: Classification of DFs based on the type of continuous phase.

meric WBDFs can be inhibitive or non-inhibitive, and also can funtion with/without clays. The polymeric additives can be polysaccharides, cellulose, acrylamide-based, etc., which are selected based on their specific functions along with their cost and eco-friendliness.

2.1.3 Challenges in High-Temperature Drilling and Opportunities

As discussed in Chapter 1, wells are considered high-temperature when the bottom-hole temperature reaches 149 °C and beyond. The formulation of effective DFs for high-temperature wells presents a substantial challenge, necessitating the incorpo-

ration of various chemicals and polymers as additives to improve DF rheological characteristics, thermal tolerance, lubricity, and filtration [26]. Traditional DF components, such as bentonite and barite, featuring particle diameters ranging in micrometers, prove insufficient in adequately sealing the nano-opening mouths in the wellbore during the simultaneous filtration of the circulating drilling fluid into the rock formations [27]. The utilization of improperly sized bridging materials in DFs, intended to prevent filtrate loss and pore throat plugging in shale formations, can obstruct production channels and diminish hydrocarbon output, resulting in formation damage [28]. Furthermore, achieving the desired rheological and filtration properties requires a significant quantity of bentonite and polymers, prompting the addition of supplements to mitigate undesired consequences [29]. These challenges underscore the importance of well-designed DFs, especially for high-temperature wells. The efficacy of drilling operations is heavily reliant on the optimal performance of these fluids. While WBDFs are conventionally used due to their low manufacturing cost and market availability of the additives, their stability is limited by various factors, including physical, chemical, thermal, and time-dependent considerations [30].

2.2 High-Performance Drilling Fluids

The term "high-performance" is used for the WBDFs offering the same benefits as the OBDFs, which are considered the standard for high-performance drilling. OBDFs offer key advantages, including:

- Keeping shale stable.
- Inhibiting clay and cuttings.
- Increasing the rate of penetration during drilling.
- Reducing bit balling and build-up.
- Lowering torque and drag.
- Maintaining stability at high temperatures.

- Minimizing damage to the formation.

While these benefits are naturally found in OBDFs, high-performance drilling fluids (HPDFs) aim to combine these with better environmental compliance.

2.3 Limitations of Current Additives

The use of potassium chloride (KCl) in WBDFs is widely accepted in the oil and gas industry, particularly for controlling rheological properties, enhancing resistance to hydrates, and inhibiting swelling of active clays in shale formations [31]. Studies have shown that combining KCl with bentonite and polymers can enhance the performance of DFs [32]. However, a high concentration of KCl in WBDFs can lead to the separation of the DF into liquid and sediment phases [33]. To address this, the use of polymers has been expanded to improve the properties of DFs.

Polymers play a crucial role in drilling oil and gas wells under high-pressure, high-temperature (HPHT) conditions [34]. Synthetic polymers are specifically formulated to enhance properties such as viscosity [35], lubricity [36], shale stability [37], filtrate loss reduction [38], and yield value [39]. Although polymers have a wide range of applications, their behavior under increasing thermal gradients with well depth becomes a critical functional characteristic at high temperatures [7]. Field studies have shown that polymers often lose stability at high temperatures, which is essential for performing key operational tasks in challenging drilling environments [40]. This instability arises because polymers lack adequate thermal, mechanical, chemical, and physical properties [41]. Commonly used polymers in WBDFs, such as carboxymethyl cellulose and xanthan gum, are often added to improve viscosity and reduce filtration loss. However, these polymers are costly and not suitable for HPHT conditions. Furthermore, differences with anionic additives limit the application of polymers on a field scale [42]. As a result, the oil and gas industry is actively searching for new, small, multifunctional, environmentally friendly, thermally and chemically stable products to formulate efficient HPDF systems that can be applied

across various drilling operations, especially in high-temperature conditions.

2.4 Incorporation of Nanomaterials in Drilling Fluids

In recent years, advancements in nanomaterials have led to a growing interest in their application within the oil and gas industry, particularly as additives in drilling fluids. Research conducted over the past decade has demonstrated that nanoparticles (NPs) can significantly enhance the properties of DFs (Figure 2.9), making them a valuable addition [22-38]. The mechanical, hydrodynamic, thermal, electrical, and chemical properties of NPs, along with their interaction potential, make them an excellent choice for use in drilling fluids [43]. Due to their extremely fine and thin structure, nanomaterials can reduce frictional resistance between drilling pipes and the wellbore, thereby improving torque and drag performance. Additionally, NPs have proven to be highly effective in HPHT drilling conditions. They can alter the heat transfer capabilities of conventional drilling fluids, improving the cooling of drilling tools and reducing the risk of tool damage in high-temperature environments. The increased surface area of NPs enhances the thermal conductivity of the drilling fluid, thereby improving heat transfer in drilling operations [25,26].

Over time, various types of NPs have been evaluated for HPDFs. Rheological studies have shown that NPs have significant potential for the development of advanced drilling fluids [27]. Moreover, the use of NPs as additives has been shown to enhance borehole stability [28]. By reducing the content of chemicals and solids in drilling fluids, NPs can also help lower overall drilling costs [29-32]. One of the unique features of NPs is their high surface-to-volume ratio, which allows them to effectively plug pore throats in wellbores with a smaller quantity of drilling fluid materials [33]. For optimal plugging, the size of the particles should be about one-third the size of the pore throat [34], making NPs ideal for this purpose. Another key advantage of NPs is their ability to significantly improve the thermal conductiv-

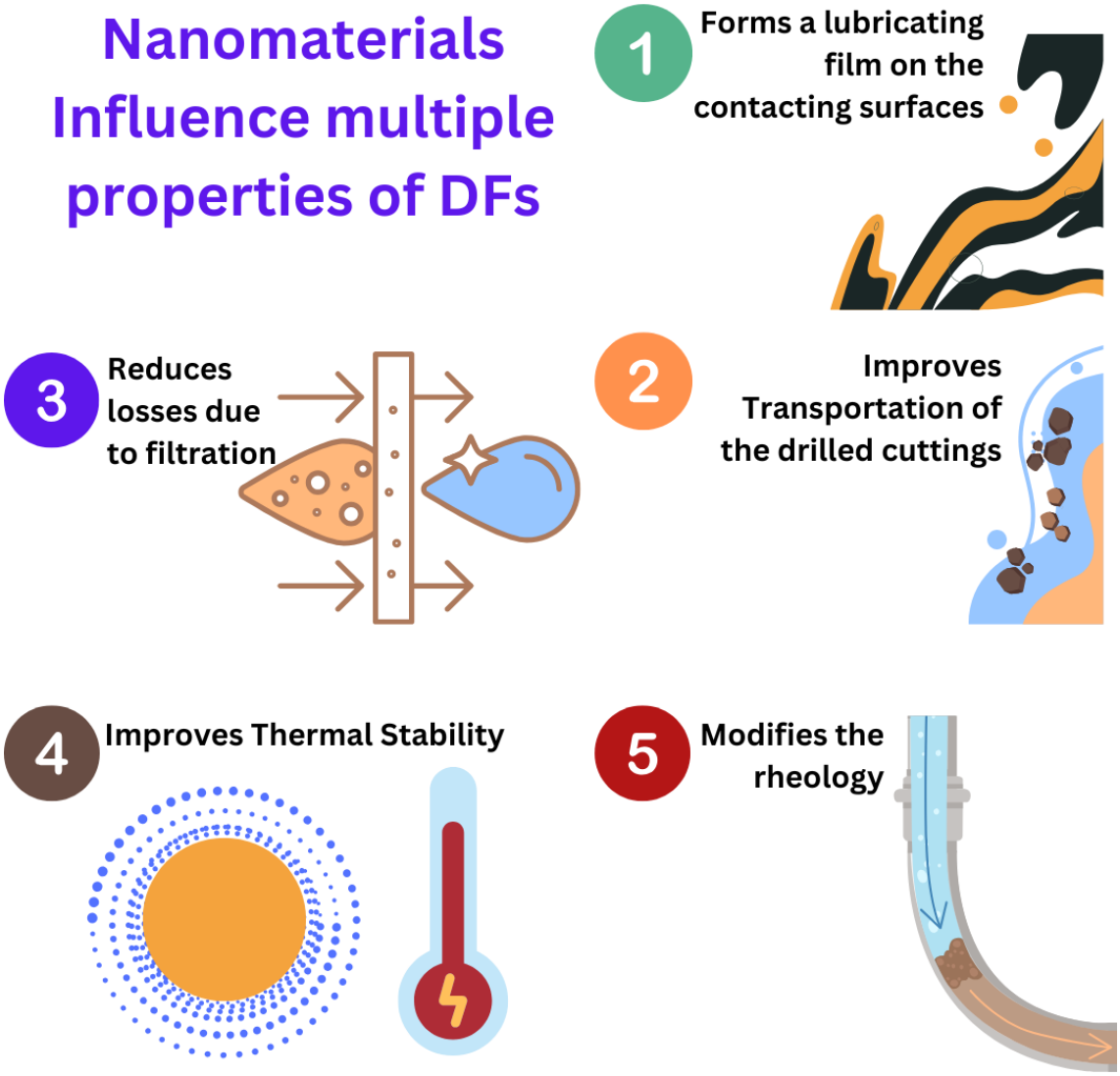

Figure 2.9: Benefits of using Nanomaterials in Drilling Fluids.

ity of drilling fluids, with some NPs increasing heat transfer efficiency by over 20% compared to conventional DFs [35-38]. Throughout the various stages of the drilling process, NPs can also reduce environmental hazards and ecological risks associated with drilling fluids [39].

Nanofluids are a type of engineered fluid that contains nanometer-sized particles suspended within a base fluid. These particles typically range in size from one to a few hundred nanometers and are dispersed uniformly throughout the fluid to enhance its physical and thermal properties. The base fluid can be water or any polymeric media keeping the suspension stable. Nanofluids exhibit superior thermal conductivity compared to traditional fluids like fresh water [44]. For instance, adding

5% by volume of copper oxide NPs can enhance the heat transfer efficiency of a solution by 22.4%. This improvement in thermal conductivity has led researchers to explore the use of nanomaterials in HPHT drilling fluids [45, 46]. The impact of nanomaterials on the physical properties of nanofluids, measuring parameters such as viscosity, gel strength, pH, and filtrate loss volume both with and without the addition of nanomaterials indicated that nanofluids enhanced the rheological properties of DFs [47].

Although, there are several nanomaterials that has been tested for applications in DFs, but there's a dire need for narrowing down to some specifically set criterion in order to objectively understand and explore their applicability as *Nano additives* for high-temperature applications.

2.5 Screening of Nanomaterials for High-Performance Drilling Fluids

The conventional additives are popular because they are widely available and deliver quite often a linear control over the properties of the DFs. The selection criteria for Nano additives for high-temperature drilling therefore settle to three primary considerations:

1. The nanomaterial has to be commercially feasible.

2. The nanomaterial should impart thermal stability to the WBDF system.

3. The nanomaterial should improve the at least two performance parameters of the formulated DF.

Upon a detailed survey of the nanomaterials and their application in DFs utilized to address the aforementioned considerations, three main subdivisions arise (Figure 2.10).

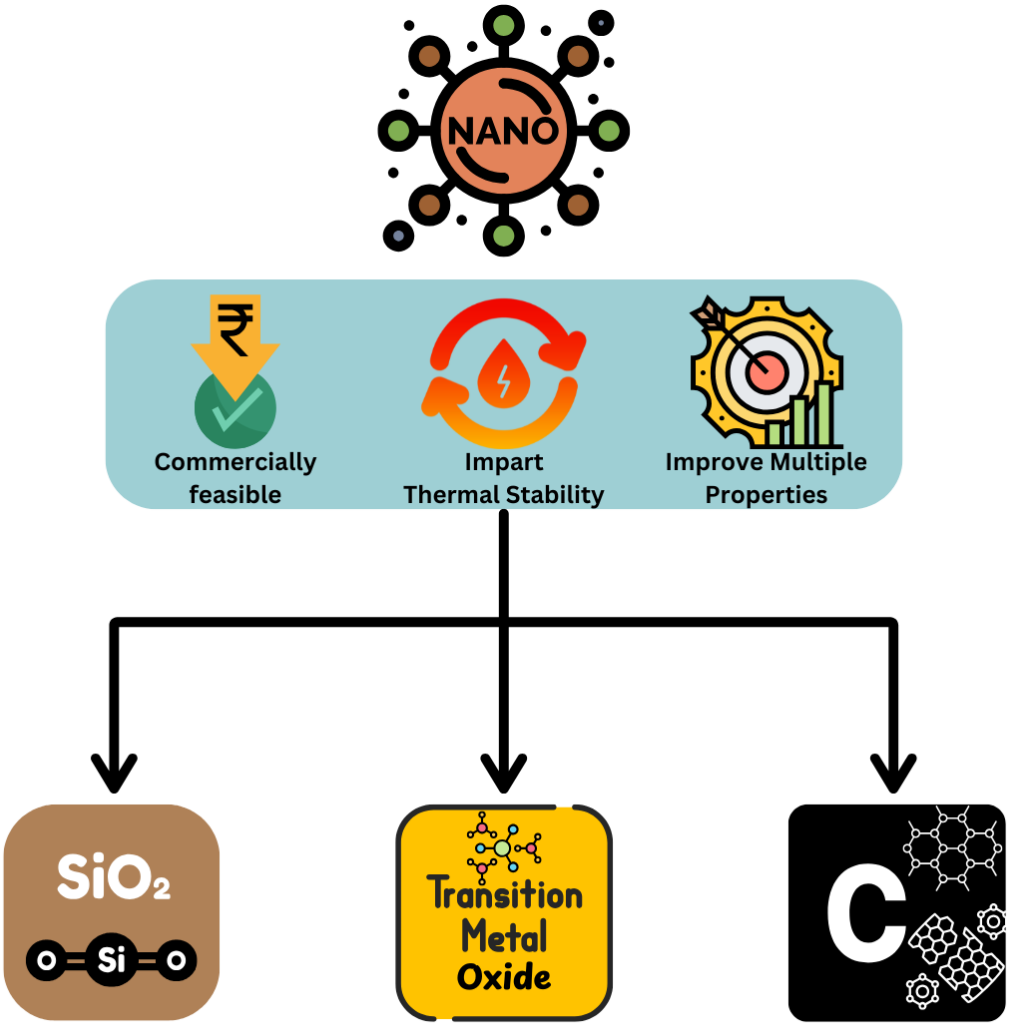

Figure 2.10: Screening of Nanomaterials for HPDFs targeting high-temperature wells.

2.5.1 Silica Nano Additives

Silica NPs have become a focal point in enhancing the rheological properties of drilling fluids, crucial for maintaining wellbore stability, efficient hole cleaning, and cutting-carrying capacity during drilling operations. Table 2.1 demonstrates that Silica NPs have been tested for application in pristine as well as in modified forms.

Various studies have shown that incorporating Silica NPs into WBDFs significantly improves rheological characteristics, such as plastic viscosity (PV), yield point (YP), and gel strength (GS). For instance, Al-Yasiri et al. demonstrated that adding Silica NPs to biopolymer-based WBDF increased viscosity due to the formation of Silica-xanthan composites [55]. This composite structure resulted in enhanced gel

Table 2.1: Silica nanomaterials used to formulate WBDFs for high-temperature applications.

Product	**Influence on WBDFs**	**Ref**
Silica NPs	Improved rheological properties, cuttings suspension, pumpability, reduced filtration loss	[45, 48–52]
PEG-nanosilica composite	Excellent plugging, reduced shale permeability	[53]
HPEI-grafter Silica NPs	Improved shale stability, improved cuttings recovery	[37]
Cationic surfactant-modified Silica NPs	Improved rheological properties, enhanced flocculation, reduced filtration loss, and cake thickness	[54]
Silica-Xanthan Composite	Enhanced gel strength, reduced filtration loss	[55]
Silica NPs and Graphene nanoplatelets	Improved Pumpability and overall performance, reduced filtration loss	[56]
Surface-modified Silica NPs	Prevent polymer degradation at high-temperature	[49]
Polymer-based nanosilica composite	Maintained structural integrity, improve wellbore stability	[57]
Polypropylene-nanosilica	Reduced friction	[58]
Mesoporous nanosilica	Improved rheological properties, reduced filtration loss, enhanced shale inhibition	[59]

strength, essential for suspending drill cuttings, as confirmed by the gel strength increase in Silica NPs' addition. Similarly, Cheraghian et al. reported that incorporating Silica NPs into WBDFs improved PV and YP by 38% and 53%, respectively, at elevated temperatures, thus ensuring better DF stability and hole cleaning under extreme conditions [45]. The studies also showed that different nanoparticle concentrations affect the drilling fluids' properties. For example, Bayat and Shams found that a 0.01 wt% Silica NPs concentration optimized PV and YP, enhancing the fluid's cutting suspension capability [48]. Moreover, advanced formulations such as those developed by Vargas et al. using surface-modified Silica NPs showed that they could prevent polymer degradation at high temperatures, further stabilizing the WBDFs' rheological properties after thermal aging [49].

The interaction between Silica NPs and other additives has also been studied extensively. For example, Oseh et al. compared the performance of polypropylene-nanosilica composites with traditional drag-reducing agents and found that the nanosilica-based fluids offered improved thermal stability and lower friction, which are vital for deep well drilling [58]. The use of Silica NPs in combination with graphene nanoplatelets, as investigated by Aramendiz and Imqam, showed that NPs maintained their dispersion even with graphitic additives, enhancing the drilling fluid's pumpability and overall performance [56].

Research has also explored the effects of modifying the surface of Silica NPs to further improve drilling fluid properties. For example, studies by Elochukwu et al. showed that cationic surfactant-modified Silica NPs significantly improved YP and PV compared to unmodified NPs, due to enhanced flocculation and electrostatic interactions within the fluid [54]. Additionally, novel polymer-based nanosilica composites, such as those developed by Mao et al., demonstrated that these materials could maintain their structural integrity under ultra-high temperature and pressure conditions, making them suitable for ultra-deep well drilling applications [57]. Furthermore, the use of Silica NPs has proven effective in maintaining the stability of drilling fluids under varying temperature and pressure conditions, as seen in the work by Moraveji et al [52]. This study highlighted the Silica NPs' role in enhancing the thermal stability and cutting recovery of glycol-based DFs, while also reducing fluid loss. These properties are crucial for minimizing wellbore instability and ensuring efficient drilling operations.

The integration of Silica NPs into WBDFs has also demonstrated significant improvements in filtration loss control and the mitigation of formation damage, particularly in challenging environments like HPHT conditions. Various studies have shown the effectiveness of these NPs in enhancing the performance of WBDFs through their interaction with polymers and other additives, leading to a reduction in fluid loss, formation of thinner and denser filter cakes, and improved wellbore stability. Al-Yasiri et al. found that combining Silica NPs with xanthan gum resulted

in a more substantial reduction in filtration loss compared to their individual use, highlighting the synergistic effect between the NPs and polymers [55]. Similarly, Aramendiz and Imqam reported that a mixture of graphite and Silica NPs, along with other additives like polyanionic cellulose and bentonite, reduced filtrate loss by 20.93%, demonstrating the potential of these combinations in minimizing fluid invasion and maintaining pore pressure in unconventional shale formations [56]. Further investigations by Gbadamosi et al. revealed a decrease in filtrate loss volume when Silica NPs were added to conventional WBDFss, which was attributed to the formation of an interconnected network due to electrostatic attractions between the NPs and bentonite [50]. Elochukwu et al. supported these findings, showing that modified Silica NPs could decrease filtrate loss and reduce filter cake thickness by 33.3%, making them more effective for filtration control compared to unmodified Silica NPs [54].

The use of silica NPs has also been shown to enhance wellbore stability, particularly in shale formations. Zhong et al. observed that Silica NPs grafted with hyperbranched polyethylenimine (HPEI) significantly improved shale stability by reducing swelling and enhancing cuttings recovery, thanks to the electrostatic interactions and hydrogen bonding between the NPs and clay particles in the shale [37]. This effect was further demonstrated by the reduction in shale permeability by 85.50% and a decrease in water imbibition rates, indicating the NPs' ability to effectively stabilize shale formations. Predictive models developed by Afolabi et al. to estimate fluid loss in Silica NPs-based WBDFs showed a significant reduction in fluid loss due to the structural changes in the filter cake, which resulted in a low permeability medium [51]. Xu et al. also reported that nanosilica composites (PEG-NS) exhibited excellent plugging properties in shale, reducing pore pressure transmission and shale permeability, thus enhancing the stability of the wellbore [53]. Studies by Minakov et al. demonstrated that Silica NP-modified DFs could reduce filtration loss while forming dense, homogeneous mud cakes with excellent adhesion properties [60]. This effect was further supported by the work of Bardhan et al.,

who found that mesoporous nanosilica (MNS) improved the thermal properties of WBDFs, resulting in better rheological characteristics, reduced filtration loss, and enhanced inhibitive properties [59].

However, the problem with aqueous dispersibility remains even after multiple attempts to functionalize the commercially available Silica NPs. Their stability is in fact influenced by the concentration, pH, and electrolytic environment of the dispersing media. Therefore, a surface treatment is required to improve their stability in water-based dispersions [61].

On the basis of the literature survey, the efficacy of Silica nanomaterials as additives in improving the DF properties is illustrated in Figure 2.11.

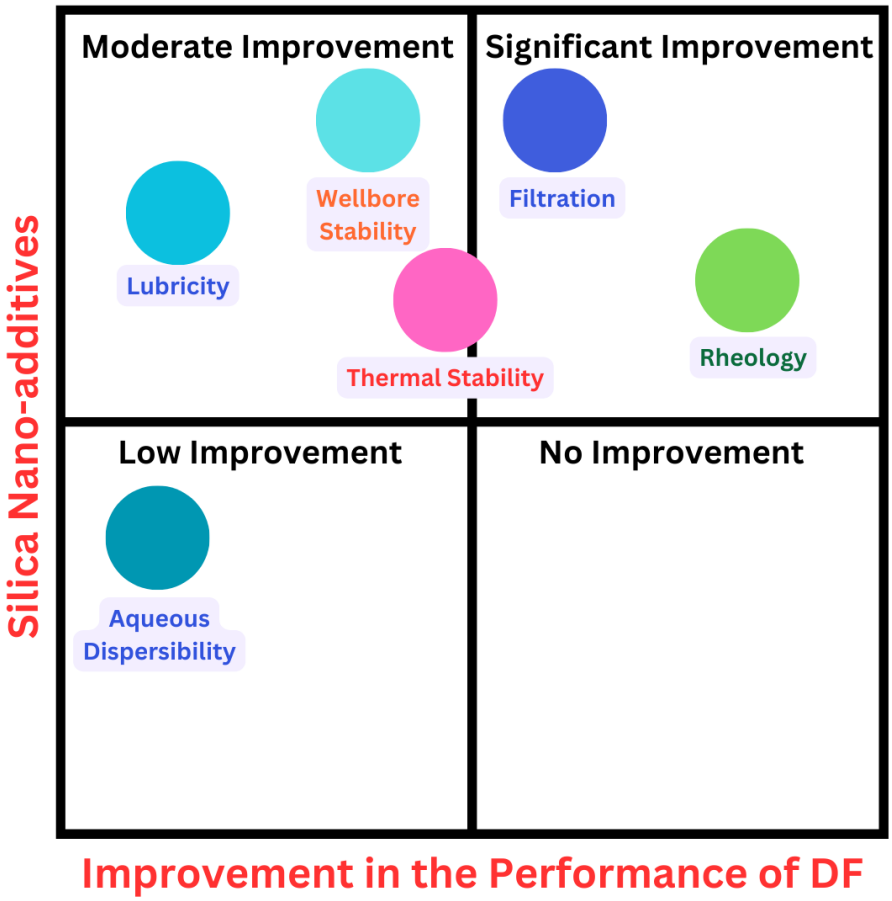

Figure 2.11: The degree of improvement introduced by Silica Nano Additives in the performance of DFs based on literature survey.

2.5.2 Transition Metal Oxide Nano Additives

Transition Metal oxide (TMO) NPs have emerged as effective additives in drilling fluids, significantly enhancing their performance in various ways. Various studies have explored the applicability of TMO NPs, some of which are listed in Tables **??** and 2.3, using Titanium Oxide, Zinc Oxide, Copper Oxide, Iron Oxide, Bimetallic Oxides, Zirconium Oxide, Manganese Oxide, Tin Oxide, and more in pure form, combinations, as well as in form of nanocomposites.

Research by Beg et al. revealed that titanium dioxide NPs improve the AV of WBDFs containing polyanionic cellulose (PAC) and hydroxyethyl cellulose (HEC) [73]. Before hot rolling, the AV for PAC was notably higher than for HEC. However, after 16 h of hot rolling at 110°C, AV decreased in both systems, more so in PAC than HEC. The PV also decreased with increasing concentration of NPs, with a temperature-dependent behavior differing between PAC and HEC. YP values decreased significantly after hot rolling, especially in PAC, where the reduction was about 50%. GS increased with both concentration and temperature, with PAC-based fluids showing a much more substantial increase than HEC-based fluids. Perween et al. focused on bismuth ferrite NPs in WBDFs, finding that increasing nanoparticle concentration led to a rise in AV before and after hot rolling [72]. Although post-hot rolling, AV values decreased, the DF remained thermally stable. PV slightly decreased with higher nanoparticle concentration, while YP initially increased but then declined slightly after hot rolling. GS increased significantly with nanoparticle concentration, indicating enhanced stability. In another study, Aftab et al. explored zinc oxide-acrylamide (ZnO-Am) composites in WBDFs, reporting higher AV and YP compared to conventional fluids [46]. The addition of these nanocomposites also significantly improved gel strength, suggesting better cutting suspension capacity, a critical factor in drilling efficiency. Further research by Vryzas et al. into iron oxide NPs demonstrated that custom-made iron oxide NPs offered better dispersion and higher yield stress (YS) compared to commercial variants, enhancing the fluid's ability to carry drill cuttings [67]. Similarly, Smith et al. showed that aluminum

Table 2.2: TMO nanomaterials used to formulate WBDFs for high-temperature applications.

Product	**Influence on WBDFs**	**Ref**
Magnesium Oxide	Improved rheological properties and cuttings suspension, high filtration loss	[62]
Tin Dioxide NPs	Increased thixotropy, reduced filtration loss, high filter cake permeability	[63]
Aluminum Oxide NPs	Improved Pumpability	[64]
Zirconium Dioxide NPs	Improved rheological and viscoelastic properties	[65]
Gilsonite NPs	Reduced filtration loss and mud cake thickness	[66]
Iron Oxide NPs	Improved cuttings suspension, high filtration loss and mud cake thickness	[67,68]
Iron(III) oxide NPs	Reduced filtration loss	[69]
Iron Oxide NPs/ Poly (sodium p-styrene sulfonate)	Improved shear thinning, reduced filtration loss, improved plugging	[70]
Magnetic NPs	Enhanced mud cake stabiltiy	[71]
Bismuth Ferrite	Improved rheological properties, reduced filtration loss	[72]
Titanium Dioxide	Improved rheological properties, reduced filtration loss	[73]
Titanium Dioxide/ Bentonite nanocomposite	Increased mud cake thickness, high viscosity, improved plugging, reduced shale swelling	[74]
Titanium dioxide NPs/ Polyacrylamide nanocomposite	Improved rheological properties	[41]
Copper Oxide NPs	High filtration loss	[75]
Copper Oxide and Aluminium NPs	Reduced filtration loss	[62]
Zinc Oxide and Titanium Dioxide NPs	Decreased rheological properties	[48]
Zinc Titanate NPs	Improved rheological properties and cuttings suspension, reduced filtration loss	[76]
Zinc Oxide and Copper Oxide	Improved overall performance, reduced filtration loss	[77]

Table 2.3: TMO nanomaterials used to formulate WBDFs for high-temperature applications (contd.)

Product	**Influence on WBDFs**	**Ref**
Zinc Oxide NPs/ Acrylamide composite	Improved cuttings suspension, reduced shale swelling, reduced filtration loss	[46]
Graphene Oxide-Zinc Oxide nanocomposites	Improved rheological properties and cuttings suspension, reduced filtration loss	[78]
Copper Oxide/ polyacrylamide nanocomposite	Improved rheological properties and thermal conductivity, reduced filtration loss and mud cake thickness	[79]

oxide NPs reduce shear stress at higher concentrations, especially under elevated temperatures, improving fluid stability in harsh drilling conditions [64]. Medhi et al. examined zirconium dioxide NPs, finding substantial increases in viscosity and shear stress across various shear rates, along with improved viscoelastic properties, making the drilling fluid more resilient to deformation [65]. Studies by Al-saba et al. on magnesium oxide NPs indicated significant improvements in PV, YP, and GS, along with a substantial impact on YP [62]. This enhancement in rheological properties is crucial for maintaining wellbore stability and optimizing drilling operations. Wang et al. highlighted the benefits of iron oxide NPs modified with Poly (sodium p-styrene sulfonate, noting improved shear thinning behavior and maintained rheological properties at specific concentrations [70]. This suggests a balanced enhancement in fluid performance without excessive viscosity, which could hinder fluid circulation. Parizad and Shahbazi investigated tin dioxide NPs, which increased the thixotropy and gel strength of WBDFs, albeit with some challenges in recirculation due to higher viscosity [63].

Ghayedi and Khosravi's research on graphene oxide-zinc oxide nanocomposites showed a notable increase in PV and YP, improving the drilling fluid's ability to carry cuttings, while also enhancing gel strength, ensuring better suspension of drill cuttings [78]. In another study, Perween et al. synthesized zinc titanate NPs, observing that higher concentrations of these NPs significantly increased AV and GS,

particularly when using electrospun NPs, which provided better surface area and interaction with the fluid [76]. Dejtaradon et al. examined zinc oxide and copper oxide NPs, finding that these additives reduced shear stress and PV at lower concentrations, with NP-modified fluids showing better overall performance in maintaining fluid stability and reducing mechanical friction [77]. Saboori et al. synthesized copper oxide/polyacrylamide nanocomposites, finding significant improvements in viscosity and thermal conductivity with increasing nanocomposite concentration, which is crucial for maintaining fluid performance at elevated temperatures [79]. Sadeghalvaad and Sabbaghi's study on titanium dioxide/polyacrylamide nanocomposites also highlighted increased PV and YP, with the fluids maintaining stability even after prolonged exposure to drilling conditions [41]. Furthermore, Bayat and Shams reported that both zinc oxide and titanium dioxide NPs could decrease PV at specific concentrations, particularly at elevated temperatures, which is beneficial for reducing mechanical friction and improving fluid flow efficiency [48].

Faisal et al. explored the influence of magnetic NPs on the pore-plugging mechanism in mud cakes via X-ray computed tomography. Their findings revealed that higher CT numbers in filter cakes containing 2 wt% magnetic NPs (MNPs), compared to those with 0.92 wt%, indicated a denser and more stable structure, underscoring the vital role of MNPs in enhancing mud cake stability [71]. The study illustrated that MNPs at a concentration of 0.5 wt% effectively eliminate cracks and reduce pore spaces, resulting in a higher quality mud cake. However, an increase in MNP concentration to 2 wt% led to the reappearance of cracks, possibly due to nanoparticle agglomeration, suggesting that MNPs improve mud cake quality up to an optimal concentration, beyond which the structural integrity is compromised. Additional studies presented by Beg et al., who examined the filtrate loss properties of DF formulations with TiO2 NPs, revealed that titanium oxide NPs reduced fluid loss and effectively plugged microfractures in filter cakes [73]. Similarly, Perween et al. observed that the inclusion of bismuth ferrite NPs significantly reduced API filtrate loss after hot rolling tests, further confirmed by Field Emission Scan-

ning Electron Microscopy (FESEM) [72]. Aftab et al. noted that the introduction of ZnO-Am nanocomposite in drilling fluids reduced shale swelling and improved fluid loss control, demonstrating superior nanopore-plugging abilities [80]. Meanwhile, Vryzas et al. reported that metal oxide NPs effectively reduced fluid loss and enhanced the surface area of drilling fluids, with better pore plugging due to smaller nanopores [67]. Furthermore, Al-saba et al. found that low concentrations of copper oxide and aluminium NPs improved fluid loss control, while higher concentrations led to adverse effects, particularly with MgO NPs [62]. Parizad and Shahbazi showed that tin oxide NPs reduced filtration volume and improved filter cake permeability [63]. Ghayedi and Khosravi demonstrated that the GO-ZnO nanocomposite significantly reduced filtration volume, attributed to the small size of the NPs filling pore spaces in the filter cake [78]. Wang et al.'s investigation into iron oxide/PSSS NPs revealed that an optimal concentration of 0.1 wt% provided the best fluid loss control. This was supported by X-ray diffraction (XRD) and FESEM analyses, which confirmed the effective sealing properties and nanopore-plugging ability of the NPs [70]. Additionally, Perween et al. found that smaller particle sizes led to better fluid loss reduction and thinner, more impermeable filter cakes with their study on synthesized zinc titanate NPs [76].

Dejtaradon et al. examined the effects of ZnO and CuO NPs at varying temperatures, finding that these NPs effectively decreased fluid loss, particularly at concentrations of 0.8 wt%, with CuO exhibiting superior pore plugging efficiency [77]. Saboori et al. studied CuO/PAM nanocomposites, showing that increased nanocomposite concentrations reduced fluid loss and mud cake thickness, with better performance in freshwater than in brine [81]. Mahmoud et al. utilized iron oxide NPs in calcium bentonite-based drilling fluids, reporting significant reductions in filtrate volume and enhancements in filter cake thickness [68]. However, higher NP concentrations led to increased filtration loss and mud cake thickness due to NP agglomeration. Medhi et al. investigated CuO NPs in polyamine-based and conventional drilling fluids, finding that moderate concentrations improved filtration properties,

while higher concentrations led to increased fluid loss due to agglomeration [75]. Aftab et al. synthesized a titanium dioxide-bentonite nanocomposite, noting that it increased mud cake thickness and reduced shale and clay swelling, attributed to enhanced viscosity and efficient pore plugging [74]. Hassanzadeh et al. reported that alumina NPs improved shale stability and pore-plugging efficiency. Pakdaman et al. introduced hydrophilic Gilsonite NPs, which reduced filtration loss and mud cake thickness [66], while Alam et al. incorporated iron(III) oxide NPs into DF, finding that an optimal concentration of 0.5 wt% significantly improved filtration properties [69].

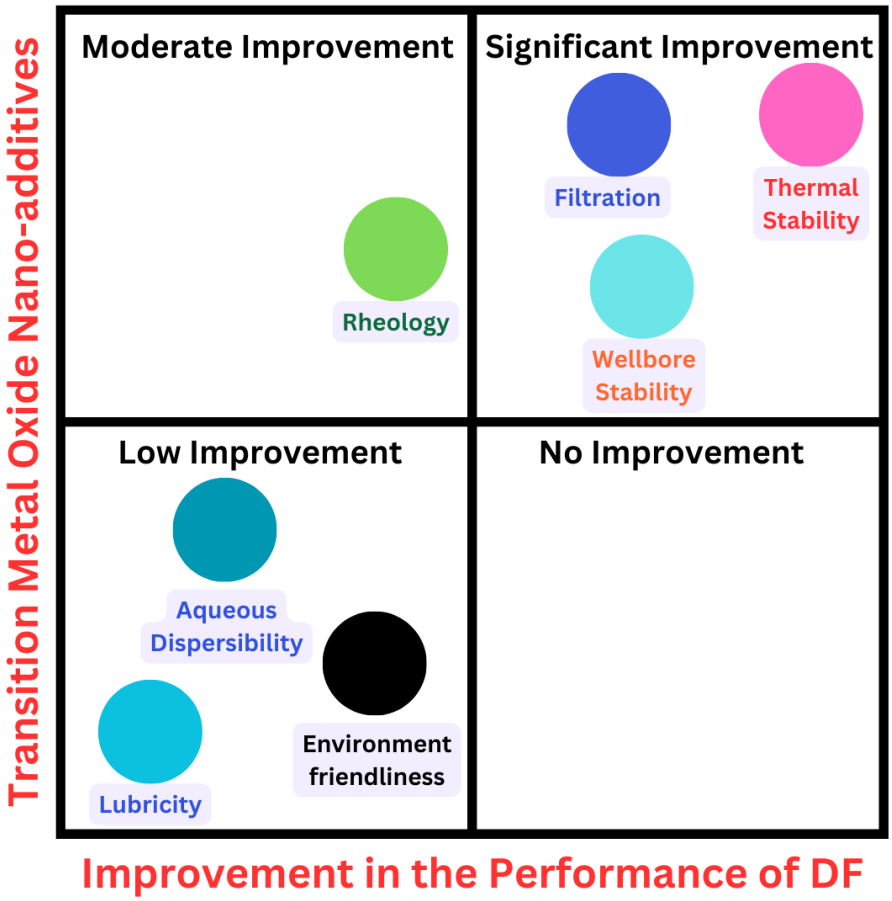

Figure 2.12: The degree of improvement introduced by Transition Metal Oxide Nano Additives in the performance of DFs based on literature survey.

Nonetheless, two critical uncertainties remain. First, the commercial viability and environmental sustainability of producing and deploying transition metal oxide NPs are yet to be fully established. Second, there is a fundamental gap in understanding how the morphology of these NPs influences the performance of HPDFs.

On the basis of the literature survey, the efficacy of Transition Metal Oxide nanomaterials as additives in improving the DF properties is illustrated in Figure 2.12.

2.5.3 Carbonaceous Nano Additives

Carbon-based nanomaterials, recognized for their versatility and remarkable properties, have found widespread applications in various industrial sectors, including the oil and gas industry. These nanomaterials include several allotropes and forms of carbon, such as graphite, diamond, fullerene, carbon nanotubes, and graphene. Their unique physical and chemical properties make them ideal candidates for enhancing the performance of drilling fluids, which are essential in drilling operations to maintain wellbore stability, control formation pressure, and facilitate the removal of cuttings. Table 2.4 encapsulates the different carbonaceous nanomaterials applied for the formulation of high-temperature WBDFs.

Table 2.4: Carbonaceous nanomaterials used to formulate WBDFs for high-temperature applications.

Product	**Influence on WBDFs**	**Ref**
Graphite NPs	Improved rheological properties, reduced filtration loss	[82]
Nanographite Oxide	Optimized rheological properties, Improved wellbore stability, reduced friction	[83]
Carbon Nanotubes	Improved cuttings suspension, and rheology, reduced filtration loss	[84–86]
Carbon Nanotubes-filled poly (vinylidene fluoride)	Improved rheological properties, reduced filtration loss	[87]
Multiwalled Carbon Nanotubes	Reduced filtration loss	[88]
Graphene Nanomaterials	Improved rheological properties and thermal conductivity, reduced filtration loss and mud cake thickness	[89, 90]

The use of graphite NPs in drilling fluids has been explored extensively. Studies have shown that incorporating graphite NPs into WBDFs can significantly improve rheological properties such as viscosity and filtration loss (FL). For instance, Nasser

et al. found that adding 40 nm graphite nanoparticles enhanced the shear-thinning behavior of WBDF and reduced FL by 50% [82]. Additionally, other nanomaterials like nanographite oxide have been shown to improve wellbore stability, reduce friction coefficients, and optimize other rheological properties [83].

Carbon nanotubes (CNTs) have gained significant attention for their role in improving the rheological and filtration behavior of drilling fluids. These nanomaterials can be single-walled (SWCNTs) or multi-walled (MWCNTs) depending on the number of graphene layers. Several studies have demonstrated the benefits of CNTs in drilling fluids. For instance, research by Fazelabdolabadi et al. demonstrated that adding functionalized CNTs to WBDF increased shear stress, particularly at higher rotational speeds, and improved CNT dispersion at high shear rates (around 600 rpm [84]). This led to greater pressure losses in laminar flow regimes within the wellbore, attributed to the increased yield stress when compared to conventional DFs. Similar trends were observed in oil-based DFs, where the PV decreased by 14%, enhancing the suitability of CNT-containing fluids for drilling operations. This reduction in PV can be beneficial in reducing the frictional pressure losses during drilling, thereby optimizing drilling efficiency. Further studies by Ma et al. indicated that the addition of CNTs to suspending mediums increases base viscosity, although this effect diminishes as shear rates increase, a phenomenon known as "shear thinning". [85] This shear-thinning effect is more pronounced in CNT suspensions compared to traditional fiber or glass suspensions, making processing more challenging but also potentially more effective in certain drilling conditions. Liu et al. investigated the effects of dosing CNTs into bentonite drilling fluids under high-temperature and high-salinity conditions [86]. They found that CNTs adsorbed on bentonite particles, preventing coalescence and maintaining the DF's structure even in harsh environments. This resulted in a significant improvement in the drilling fluid's ability to carry rock cuttings, increasing by 85.1%. Additionally, the resulting dense mud cake reduced the filtrate loss by 30.2%, enhancing wellbore stability. Wu et al. studied the rheological behavior of CNT-filled poly(vinylidene fluoride)

(PVDF) composites, finding that CNTs have a flow-impeding effect, increasing AV at low shear rates [87]. At higher CNT loadings, the nanotubes were more likely to form entangled bundles, further increasing viscosity and complicating flow. However, this increased viscosity can be advantageous in stabilizing the drilling fluid and controlling fluid loss, particularly in challenging drilling environments.

Studies by Özkan et al. showed that even small concentrations of MWCNTs could significantly enhance the stability and filtration properties of water-based drilling fluids, with predicted improvements in gel structure stability and reduced filtration rates based on DLVO theory [88]. Moreover, Ismail et al. demonstrated that MWCNTs, when combined with nanosilica, could improve both the PV and YP of drilling fluids, making them more effective under high-temperature conditions [91]. The impact of MWCNTs on fluid loss control and wellbore stability has also been well documented. For example, MWCNTs have been shown to reduce water loss in drilling fluids and improve mud cake formation, which is crucial for preventing formation damage and maintaining wellbore integrity. The use of MWCNTs in combination with other additives, such as durian rind or synthetic-based fluids, has further enhanced the performance of drilling fluids, particularly in terms of reducing filtrate loss and improving the stability of the DF under high-pressure, high-temperature conditions.

Graphene's remarkable physical and chemical properties, including high thermal conductivity, mechanical strength, and surface area, make it an excellent additive for enhancing drilling fluid performance. Graphene oxide, a derivative of graphene with oxygen-containing functional groups, has also been extensively studied for its ability to improve the properties of drilling fluids. Recent studies have shown that graphene and graphene oxide can significantly reduce filtration loss, improve emulsion stability, and enhance thermal stability in drilling fluids. For instance, Kosynkin et al. demonstrated that adding graphene oxide to WBDF reduced filtration loss by up to 0.2 wt% of the original content while maintaining stability at high temperatures [89]. Similarly, Taha et al. reported that combining a proprietary engineered

surfactant with graphene nanoparticles improved various properties of drilling fluids, such as FL, lubricity, and thermal stability under HPHT conditions [90]. Graphene nanoplates, another derivative of graphene, have been used to stabilize rheological and thermal properties in drilling fluids. These nanoplates have been shown to outperform other nanomaterials, such as nanosilica and glass beads, in enhancing drilling fluid performance under low-pressure, low-temperature (LPLT) conditions.

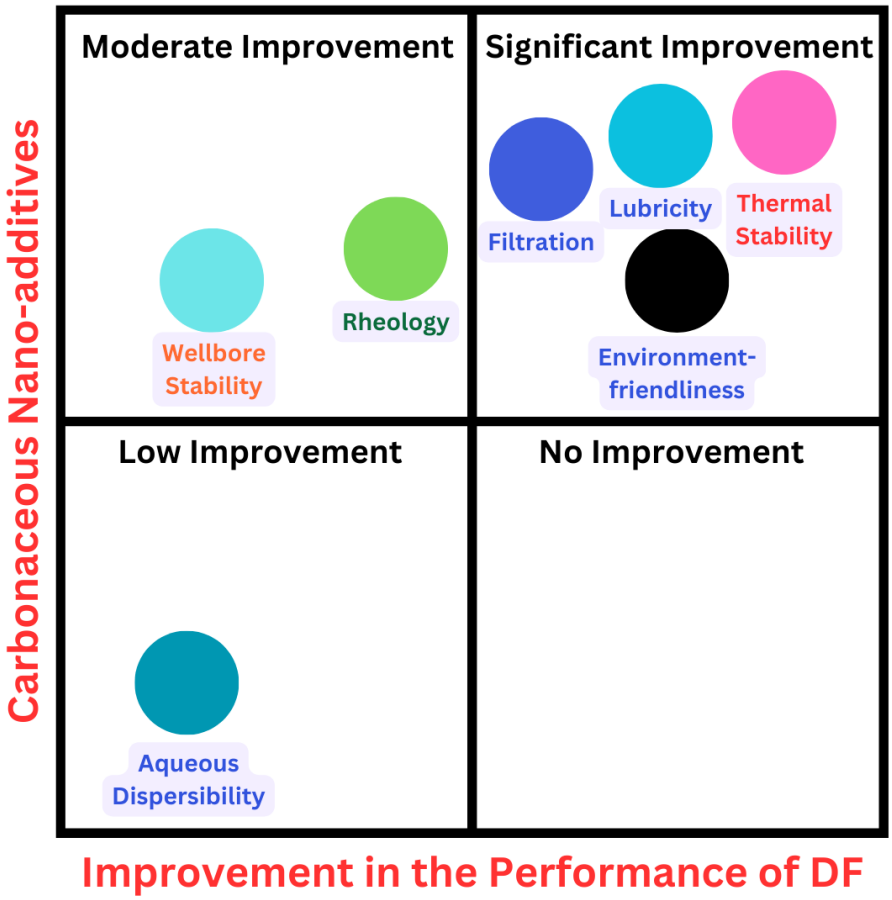

Figure 2.13: The degree of improvement introduced by Carbonaceous Nano Additives in the performance of DFs based on literature survey.

However, there are ongoing concerns that warrant attention related to the application of carbonaceous nanomaterials in WBDFs. One major issue is the need for the development of durable, cost-effective, and environmentally friendly nanomaterials. Eco-friendly methods for scaling up the production of carbon nanomaterials are essential to make their use more economically viable. Over the past decade, functionalized nanoparticles have seen widespread application in the drilling industry, which

highlights the need for further development of carbon nanomaterials. This development should prioritize several key features: improving thermal conductivity under high-temperature conditions, ensuring a high surface-area-to-volume ratio, requiring minimal amounts to significantly enhance fluid performance, and maintaining high dispersion stability when mixed with water, polymers, surfactants, alcohols, and esters.

On the basis of the literature survey, the efficacy of Carbonaceous nanomaterials as additives in improving the DF properties is illustrated in Figure 2.13.

2.6 Identification of Potential Nano Additives

While significant advancements have been made in the development of WBDFs incorporating nanomaterials, challenges persist, especially in high-temperature drilling applications. The literature survey from each of the group of nanomaterials discussed in the previous section presents the following limitations:

- **Silica Nano Additives:** Despite functionalization efforts, the stability of silica nanoparticles in aqueous dispersions remains a significant issue, influenced by factors such as concentration, pH, and electrolyte concentration. Surface treatments are necessary to enhance their stability.
- **Transition Metal Oxide Nano Additives:** The commercial viability and environmental sustainability of producing and deploying transition metal oxide nanoparticles are still uncertain. Also, the role of morphology in influencing the performance of the DFs is less understood.
- **Carbonaceous Nano Additives:** While carbon nanomaterials have shown potential, there is a need to develop durable, cost-effective, and environmentally friendly materials. Eco-friendly scaling-up methods are essential for their widespread adoption.

Since performance improvement capabilities and thermal stability are sacrosanct criteria, the other requirements for the selection of nanomaterials were mapped in

a quadrant chart and five were selected with appropriate synthesis techniques as illustrated in Figure 2.14.

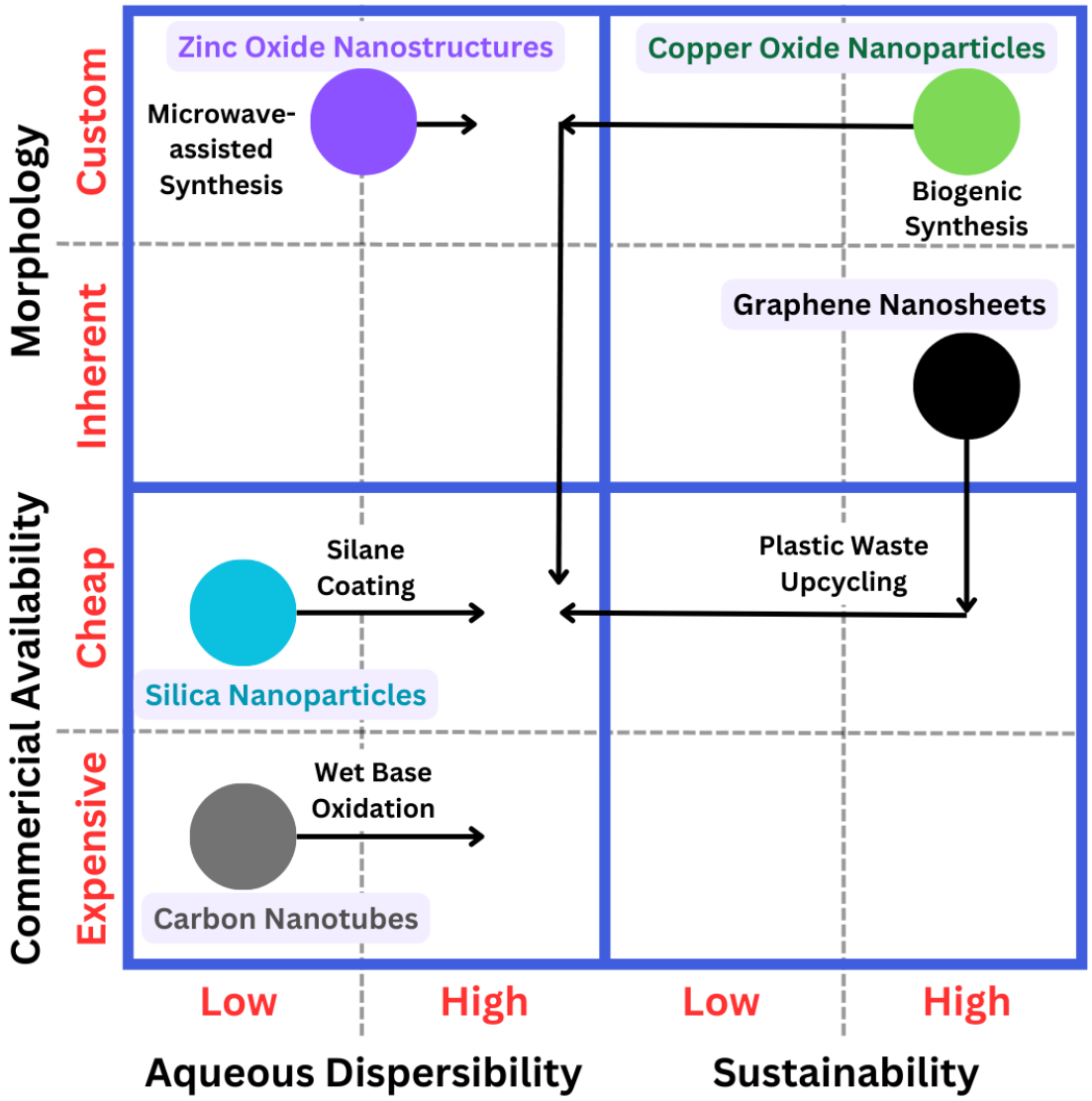

Figure 2.14: Selection Map of the Nanomaterials. The key considerations are put in the axes. The arrows signify the objectives of each synthesis.

The following nanomaterials were carefully selected for suitability as HPDF nano additives to address the research objectives defined in **Chapter 1**:

1. Graphene Nanosheets

    - Plastic Waste Valorization for cheap and sustainable production.
    - Sheet-like morphology for higher surface area (facilitating higher interaction with the additives), and low dosage requirements.

2. Carbon Nanotubes

    - Surface-modified for higher dispersibility in aqueous media.
    - Mechanistic insights for long term stability in polymeric nanofluid and viscoelastic behavior.

3. Copper Oxide Nanoparticles

    - Green synthesis for cheap and sustainable production.
    - Plate-like morphology (through microwave-assisted synthesis) aimed to enhance lubricity and filtration performance.

4. Zinc Oxide Nanostructures

    - Different size distribution and morphology through microwave-assisted synthesis.
    - Comparative insights on the stability and performance due to Nanopencil and Nanoflower morphology.

5. Silica Nanoparticles

    - Coated with [3-(2-Aminoethylamino) propyl] trimethoxy silane for improved thermal stability and higher dispersibility in aqueous media.
    - Insights into the performance improvement capabilities.

2.7 Conclusion

This chapter discussed the fundamentals of DFs and their functional properties. The urgency of developing nano additives for HPDFs for sustainable high-temperature drilling operations is clear, and the literature review worked to highlight the present limitations and opportunities for further research in this domain. The five potential nano additives identified here will be discussed for their multifunctionality and thermal stability in WBDFs in the subsequent chapters (4 to 8). The next chapter will discuss the experimental framework of the entire investigation.

Chapter 3

Experimental Methodology and Characterization Techniques

This chapter presents the synthesis route of nanomaterials in brief, methodologies employed in the analysis of the synthesized nanomaterials, as well as their integration into nanofluids and DF formulations. Figure 3.1 outlines the generic sequence of the key steps involved in the investigation.

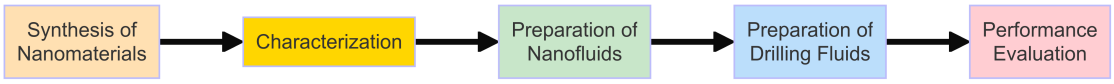

Figure 3.1: Sequence diagram of the investigation

The first section summarizes the general synthesis routes for the nanomaterials based on the objectives described in Chapter 1. The next section defines the techniques used for confirmation of synthesis and the characteristics of the synthesized nanomaterials, with some of them serving as the screening steps before further testing. The following sections demonstrates how nanofluids are prepared with the nanomaterials and used as an additive to prepare DFs. Followed by the preparation, the performance of the DFs are evaluated to determine the efficacy of the nanomaterials as *nano additives*, the methodology of which is described in the successive section. In this body of work, the characterization of the nanomaterials and the performance parameters tested vary based on the requirements set by each of the

research objective listed in the previous chapter.

The synthesis technique and the compositional information of the DFs specific to each nanomaterial employed will be described in the subsequent chapters.

3.1 Synthesis of Nanomaterials

3.1.1 Materials

Silica nanoparticles of average particle size 15 nm and specific surface area of 650 m^2/g with a purity of 99.5% were procured from Sisco Research Laboratories Private Limited, India. AEAPTS ([3-(2-Aminoethylamino) propyl] trimethoxy silane) of purity 97% was acquired from TCI, Japan. Sodium hydroxide (97% pure), ammonium hydroxide (95% pure), and methanol (99% pure) were purchased from SD-Fine Chem Limited, India. The raw materials required for synthesis of Graphene nanosheets, i.e. the plastic wastes, were collected from flea markets and the local municipality, and then categorized into PP, PE, and PS. Zinc nitrate hexahydrate and Cupric nitrate trihydrate were purchased from Molychem, India. Pristine multiwalled carbon nanotubes (MWCNT) of >95% purity was purchased from Plasma Chem Gmbh.

3.1.2 Synthesis Route and Purpose

In line with the proposed solution discussed previously, for a nanomaterial to be effectively utilized as an additive in the development of HPDFs for high-temperature drilling applications, it must be both sustainable and economically viable. Additionally, the nanomaterial should maintain stable dispersion in aqueous media and exhibit desirable morphology with a narrow size distribution. The research objectives were formulated based on these criteria, and five different nanomaterials were subsequently synthesized, each tailored to exhibit one or more of the aforementioned key characteristics, as evident from Table 3.1.

Graphene Nanosheets used plastic waste as a precursor, while Copper Oxide

(CuO) NPs had a green reducing-cum-capping agent, both supporting cheaper and sustainable product development. Microwave-assisted synthesis of CuO NPs and Zinc Oxide (ZnO) NPs helped ensure control over the morphology whilst offering narrow particle size distribution. Additionally, surface modification of Silica NPs and multi-walled carbon nanotubes (MWCNTs) was carried out to enhance their dispersibility in aqueous media, a critical factor for ensuring stable performance.

Table 3.1: Nanomaterials and their synthesis for application in this investigation.

Sl. No.	**Product**	**Objective**	**Source/ Precursor**	**Synthesis Route**	**Target DF Properties**
1	Graphene Nanosheets	Sustainable Additive Development,Low Dosage Assessment	Plastic Waste	Two-Step Pyrolysis	Rheology, Filtration
2	Modified Carbon Nanotubes	Improved Aqueous Dispersibility, Low Dosage Assessment	Pristine Multiwalled Carbon Nanotubes	Wet Base Oxidation	Rheology, Filtration
3	Biogenic Copper Oxide NPs	Sustainable Additive Development, Morphological Assessment	Copper (II) Nitrate Trihydrate	Plant Leaf Extract mediated Sol-gel + Microwave Treatment	Filtration, Lubricity
4	Zinc Oxide Nanostructures	Morphological and Particle Size Distribution Assessment	Zinc Nitrate Hexahydrate	Sol-gel + Microwave Treatment	Rheology, Filtration
5	Silane Coated Silica NPs	Improved Aqueous Dispersibility	Commercial Silicon Dioxide NPs	Surface Silanization	Rheology, Filtration

Microwave Setup for Synthesis

Microwave synthesis is a rapid and efficient method used to produce nanomaterials by utilizing microwave radiation to heat reaction mixtures. This technique offers several advantages over conventional heating methods, such as faster reaction times, enhanced reaction rates, and improved product yields [92]. The microwave radiation

interacts with polar molecules and ions in the reaction mixture, causing them to rotate and collide, which generates heat and accelerates chemical reactions. This localized heating leads to uniform nucleation and growth of nanomaterials, resulting in better control over their size, shape, and distribution.

The synthesis of the metal oxide nanomaterials like ZnO and CuO were performed in a microwave digester/synthesis setup (NuWav-Pro, NutechAnalytical) in Power-Time mode with constant sonication at 20kHz. The schematic of the setup is illustrated in Figure 3.2.

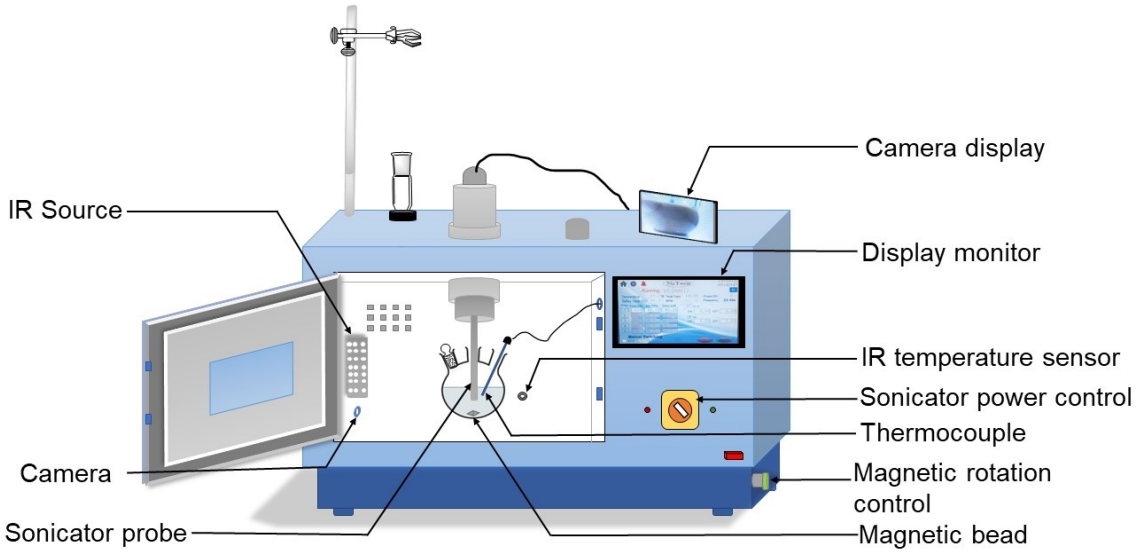

Figure 3.2: The schematic of the microwave setup (adapted from Prajapati et. al.)

3.2 Characterization of Nanomaterials

The key factors analyzed while characterizing nanomaterials are their size and morphology. The assessment may include size distribution, surface properties, structural features, attached functional groups, etc. So, accurate measurement techniques for nanomaterials are essential for their commercial application and regulatory compliance. The techniques employed are presented henceforth.

3.2.1 Photon Correlation Spectroscopy

Photon Correlation Spectroscopy, also known as Dynamic Light Scattering (DLS), is a technique used to measure the size distribution of small particles and macromolecules in suspension [93]. DLS works by analyzing the fluctuations in the intensity of scattered light caused by the Brownian motion of particles. These fluctuations are correlated over time to determine the diffusion coefficients of the particles, which can then be used to calculate their hydrodynamic radii using the Stokes-Einstein equation [94].

Electrophoretic Light Scattering (ELS) is a technique used to measure the zeta potential of particles in a colloidal suspension [95]. ELS works by applying an electric field to the suspension, causing the charged particles to move. As a laser is passed through the suspension, the movement of these particles scatters the light, and the Doppler shift in the frequency of the scattered light is measured to determine the velocity of the particles. This velocity, or electrophoretic mobility, is used to calculate the zeta potential, which provides information about the surface charge and stability of the particles in suspension.

A photon correlation spectroscope (Zetasizer Nano ZS, Malvern) was used to measure the particle size distribution and zeta potential. Each test was conducted three times. Samples were equilibrated for 120 s at 25 °C before each measurement.

3.2.2 Electron Microscopy

Scanning Electron Microscopy (SEM) is utilized for high-resolution imaging and characterization of surfaces, including nanomaterials. Field Emission SEM (FE-SEM) employs a field emission electron source, which provides a narrower electron beam and higher electron brightness compared to the thermionic sources used in traditional SEM. On the other hand, High-Resolution Transmission Electron Microscopy (HRTEM) uses phase contrast to produce images with atomic resolution. This allows for direct imaging of the atomic lattice structure of a material. It works by transmitting a beam of electrons through an ultra-thin specimen [96]. Electrons

interact with the sample as they pass through it, and an image is formed based on these interactions. The transmitted electrons are focused by electromagnetic lenses to form an image, which is magnified and projected onto a screen or detector. Both these techniques offer morphological visualization of the nanomaterials.

A high-resolution transmission electron microscope (G2 20, Tecnai) and a field-emission scanning electron microscope (JSM 7900F, JEOL) were used in this study.

3.2.3 X-ray Diffraction Analysis

X-ray Diffraction (XRD) is an analytical technique used to determine the crystalline structure of materials. It operates by directing X-rays at a sample and measuring the intensity and angles of the rays that are diffracted by the atomic planes within the crystal. This diffraction pattern provides information about the spacing between the planes, enabling the identification of the crystal structure, phase composition, and other structural parameters. The average crystallite size of the nanomaterials can be calculated with the diffraction parameters employing Scherrer's Equation [97] as given in equation 3.1.

$$D = K\lambda/\beta\cos\theta \tag{3.1}$$

Where D denotes the crystallite size in nm, and K is the Scherrer shape factor, which was assumed to be 0.9 for this calculation. λ, the incident X-ray wavelength, was fixed at 0.15406 nm. β represents the full-width at half-maxima value (FWHM) of the peaks, expressed in radians, while θ is the Bragg's scattering angle.

An powder X-ray diffractometer (X'Pert Pro, PANalytical) was used for the crystal structure identification utilizing a Cu K source.

3.2.4 Fourier Transform Infrared Spectroscopy (FTIR)

Fourier Transform Infrared Spectroscopy (FTIR) is an analytical technique used to obtain the infrared spectrum of absorption or emission of a sample. It works by

passing infrared radiation through the sample and measuring the wavelengths that are absorbed, which correspond to the vibrational frequencies of the chemical bonds in the molecules. The resulting spectrum provides a molecular fingerprint that can be used to identify the different functional groups within the sample.

An infrared spectrometer (PerkinElmer) was used for identifying the functional groups.

3.2.5 Micro Raman Spectroscopy

Micro-Raman spectroscopy is a technique used to study the vibrational modes of molecules with high spatial resolution, typically on the micrometer scale [98]. It involves illuminating a small area of a sample with a laser beam and analyzing the scattered light to detect shifts in energy that correspond to specific vibrational modes of the molecules in the sample. These shifts, known as Raman shifts, provide a unique spectral fingerprint that can be used to identify and characterize materials.

Samples were characterized by a Micro Raman Spectrometer (Renishaw) and the excitation was carried out at 785 nm with an Argon laser.

3.2.6 X-ray Photoelectron Spectroscopy

X-ray Photoelectron Spectroscopy (XPS) is a surface-sensitive analytical technique used to study the elemental composition and chemical state of materials. It works by irradiating a sample with X-rays, which causes the emission of core-level electrons. The kinetic energy of these emitted electrons is measured to determine the binding energies, providing information about the elements present, their concentrations, and their chemical states.

An X-ray photoelectron spectrometer (K-Alpha, ThermoFisher Scientific) with an Al Kα source was utilized for the surface characterization.

3.2.7 BET Specific Surface Area Analysis

The Brunauer-Emmett-Teller (BET) method is used to measure the specific surface area of materials, particularly porous solids [99]. It is based on the physical adsorption of gas molecules on a solid surface and the analysis of adsorption isotherms. In a BET analysis, the amount of gas adsorbed at different pressures is measured, allowing for the calculation of the surface area by applying the BET equation, which extends the Langmuir theory to multilayer adsorption.

Nitrogen adsorption isotherms were measured at 77 K using an adsorption analyzer (ASAP 2020, Micromeritics) to determine the Brunauer-Emmett-Teller (BET) specific surface area.

3.3 Preparation of Nanofluids

Nanomaterials aggregate in water due to several interrelated factors that influence their stability and interactions with the surrounding medium. The primary reasons may be due to the fact that the repulsive forces between the particles are weaker than the attractive (i.e. van der Waal) forces between them. Other factors can be can be mediated by the medium, like ionic screening, pH alterations, etc. or dosing issues like high polydispersity and concentration [100]. This aggregation of the nanomaterials in the drilling fluids may hinder the intended efficacy and may also prove detrimental in attaining the desired property enhancements. Therefore, a simple fix would be to prepare stabilized nanofluids of the nanomaterials before subjecting them to the drilling fluids to test their effectiveness.

A stock solution of 0.25 wt% Xanthan gum (XG) was mixed in deionized water using a homogenizer (HG-15D, Daihan) at 1000 rpm. This XG stock solution was poured into different beakers (100 mL in each). Subsequently, the nanomaterial powder were added in base solutions at different concentrations, and put under ultrasonic treatment using a UNIGENETICS probe sonicator model SKL- 1200 (at a 20kHz frequency) in an ultrasonic cell crusher noise-isolating chamber for 4 cycles

of 15 min (1 h) while maintaining the temperature below 45 ℃. Hence the prepared nanofluids and the base XG solution were further used to prepare the drilling fluid samples. The nanofluid preparation methodology is graphically illustrated in Figure 3.3.

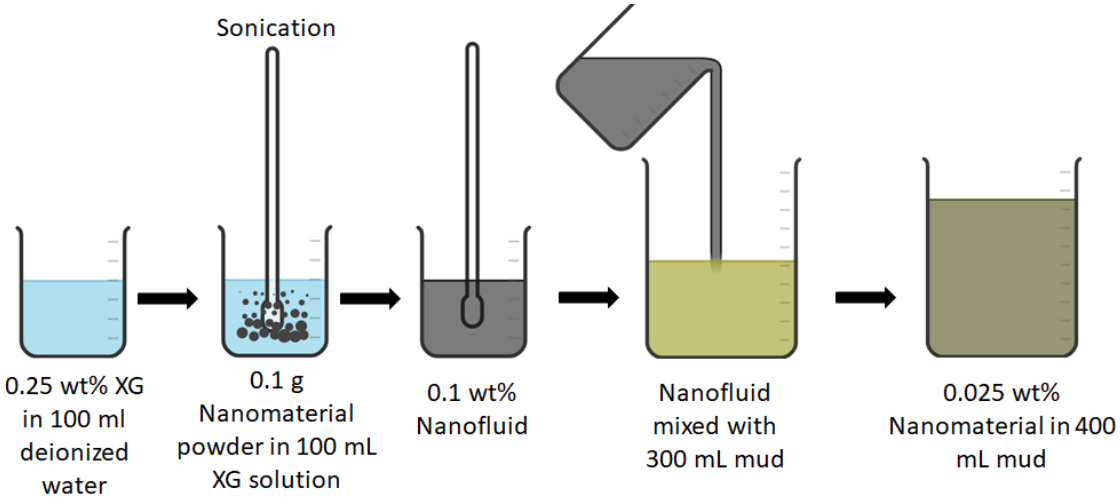

Figure 3.3: Mixing protocol for nanofluid preparation.

3.4 Drilling Fluid Formulation

3.4.1 Materials

Aluminium Silicate Hydrate (Bentonite) pure and Sodium Silicate Metahydrate and were acquired from SRL Pvt Ltd. 1-Octanol (99.5% pure) was bought from CDH Pvt Ltd, India. Potassium hydroxide LR grade (KOH, >85%), Potassium chloride (KCl, >99% pure) and Xanthan gum pure (Food grade) were purchased from Molychem, India. Polyanionic cellulose regular grade (PAC-R) was provided by Oil India Limited, India. Deionized water was used throughout the investigation.

3.4.2 Composition and Preparation

A prehydrated bentonite slurry (PHBS) was prepared by dispersing 3 wt% bentonite in deionized water using a Hamilton Beach Mixer for 20 min followed by keeping the slurry at rest for 16 h to ensure proper exfoliation of the clay in water. This

PHBS was then sheared in the mixer for 15 min before the addition of the additives in sequence reported in Table 3.2. The nanofluids were then added to the base formulation and their effects were studied through a comprehensive performance evaluation.

Table 3.2: General Composition of the DFs.

Seq.	Chemicals	Function	Mix Time (min)
1	Deionized water	Major phase	-
2	Bentonite	Viscosifier, Fluid loss controller	10
3	KOH	pH controller (adjust to 9 pH)	2
4	Xanthan Gum	Viscosifier	5
5	PAC-R	Fluid loss controller	5
6	KCl	Shale inhibitor	8
7	1-Octanol	Defoamer	2
8	Nanofluid	Rheology modifier, Fluid loss controller, Lubricity improver	10

3.5 Performance Evaluation of the Drilling Fluids

The performance studies on the drilling fluids for different properties were carried out in accordance to the API Recommended Practices 13-1 [101]. A brief description of the testing performed on the samples are presented in the subsequent sections.

3.5.1 Dynamic Thermal Conditioning

In order to understand the in-situ effects while the DF is in the wellbore, dynamic hot rolling tests were also carried out on the DF samples and compared with the fresh ones.

The samples were poured into stainless steel aging cells and sealed. A nitrogen pressure of 100psi was applied to each cell and was put in a roller oven (ARIES Engineering Works) at a temperature of 150℃ for 16 h while rolling at 30 rpm., as illustrated in Figure 3.4. After hot rolling, the cells were taken out, cooled, and then mixed in the Hamilton Beach Mixer for 15 min before further studies.

Figure 3.4: Schematic of aging cell and roller oven.

3.5.2 Rheological Measurement

The flow properties of the drilling fluids are required to be measured as the transportation of the drilled cuttings through the annulus out on the surface are one of the primary functions that they serve. The water-based drilling fluids are therefore designed to be shear thinning and thixotropic in nature.

A direct-indicating concentric cylinder viscometer (35SA, FANN), as shown in Figure 3.5 (a), was used in this study to quantify the aforementioned nature of the formulated drilling fluids. A bob suspended by a spring is positioned concentrically inside an outer cylinder. The entire assembly is lowered to a specific level in a container of DF, and the outer cylinder is then rotated at a constant speed. The viscous resistance of the DF causes the bob to rotate until the torque from the spring counteracts the viscous drag. The angle of deflection is measured using a calibrated dial on top of the device, providing an indication of the shear stress at the bob's surface. The viscometer features a range of rotational speeds, ranging from 3 to 600 rpm, and provides detailed rheological data, essential for characterizing various fluid types and conditions. The dial readings, denoted by θ were used to obtain the Bingham Plastic Parameters [102] as given in equations below:

$$AV(cp) = \theta_{600}/2 \tag{3.2}$$

$$PV(cp) = \theta_{600} - \theta_{300} \tag{3.3}$$

$$YP(lbf/100ft^2) = \theta_{300} - PV \tag{3.4}$$

where, AV is the apparent viscosity, PV is the plastic viscosity, YP is the yield point, θ_{600} and θ_{300} are the dial readings at 600 and 300 rpm rotor speeds respectively. The initial gel strength (Gel0) and the final gel strength (Gel10) were obtained in terms of lb/100 ft^2 by arresting the flow of the sample for 10 s and 10 min respectively, followed by deformation at 3 rpm.

The flow curves were plotted by converting the motor speed to shear rates (denoted by γ) and the dial readings to shear stress values, (denoted by τ) as shown in the equations below:

$$\gamma(s^{-1}) = \ N \times 1.703 \tag{3.5}$$

$$\tau(lb/100\ ft^2) = \theta_N \times 1.067 \tag{3.6}$$

where, N is the rotor speed and θ_N is the corresponding dial reading.

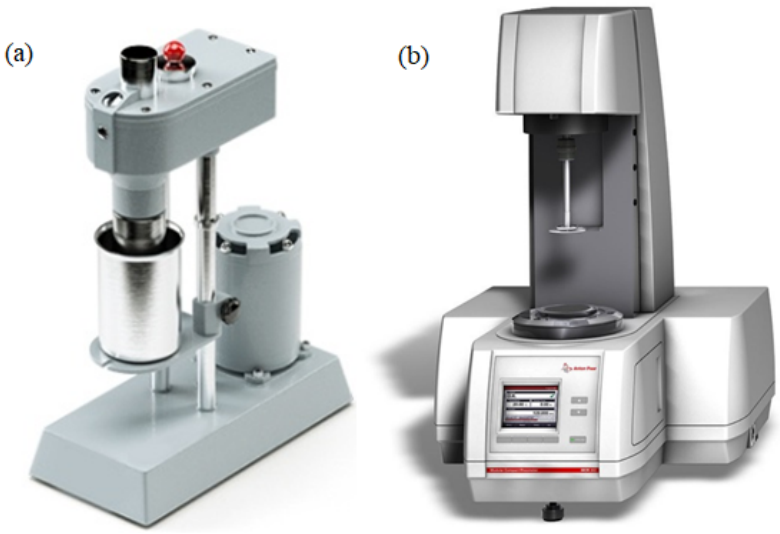

Figure 3.5: (a) Direct-indicating Viscometer (Credit: FANN Instrument Company); (b) Stress-controlled Rheometer (Credit: Anton Paar GmbH).

In order to accurately determine the behavior of the formulations at ambient as well as different pressure-temperature conditions, the shear rheology analysis for the samples before and after hot rolling was performed utilizing a stress-controlled rheometer (MCR 302e, Anton Paar), as in Figure 3.5 (b), equipped with a pressure cell unit and a double gap geometry. Prior to measurements at elevated tempera-

tures, a conditioning step (pre-shearing) was performed for all samples at a rate of 400 s^{-1} for 120 s using the pressure cell unit. Rheological studies with shear rate sweep from 1 to 1000 s^{-1} and oscillatory amplitude sweep at 10 rad/s frequency were then performed at 500 psi with temperature variations of 20 and 80 °C.

3.5.3 Filtration Loss Measurement

While drilling, the DF is pumped into the drill string which comes out from the drill bit's nozzles and then circulates through the annulus to the surface, while carrying the rock cuttings. The DF is in contact with the annular wall and the pressure exerted may be greater than that of the formation. This results in the invasion of the drilling fluid into the formation due to the differential pressure. The solids bigger than the pore size of the formation rock in the suspension tend to stay behind on the w wellbore wall, only allowing water to shift into the formation. This phenomenon is called filtration and it may cause formation damage. However, there is another aspect to this that must be considered. The particles which have accumulated on the wall get compacted under pressure and form 'mud cake'. This ensures good wellbore stability while limiting further fluid loss from the drilling fluid system [103]. Hence, the objective of designing a drilling fluid from the filtration loss point of view is to have minimal formation damage with very thin and impermeable mud cake.

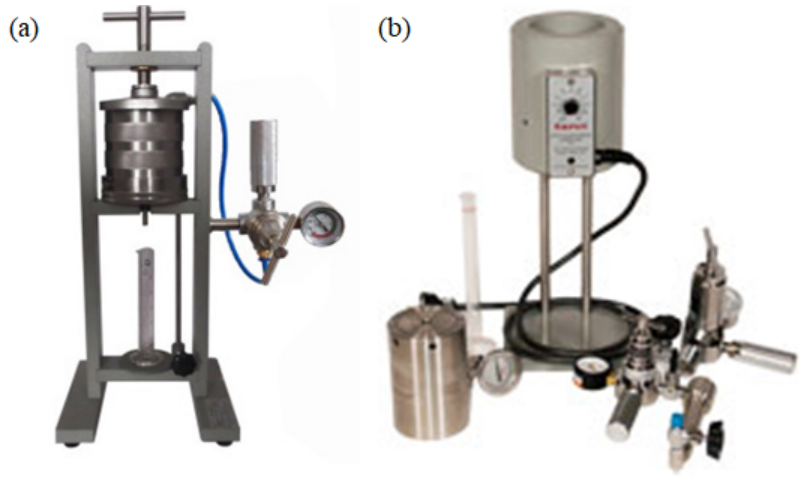

Figure 3.6: The filter presses: (a) LPLT and (b) HPHT (Credit: FANN Instrument Company)

Low-pressure low temperature (LPLT) or API filtration was executed using an API Filter Press (Series 3000, FANN) under 100 psi pressure for 30 minutes. HPHT filtration loss was assessed utilizing an HPHT Filter Press (Series 387, FANN) at 150 °C temperature and 500 psi differential pressure. The mud cake thickness were measure in 1/32" using a FANN ruler.

3.5.4 Lubricity Measurement

The lubricity of DF plays a significant role in reducing friction between the drill string and the wellbore, thereby minimizing equipment wear, extending drill bit lifespan, and decreasing the likelihood of issues such as a stuck pipe. Additionally, good lubricity ensures smoother drilling operations, leading to faster penetration rates and reduced torque and drag, which is particularly beneficial in difficult scenarios like deviated or horizontal wells [104].

Figure 3.7: EP/lubricity tester.

The evaluation of drilling fluid lubricity was conducted using a Lubricity Tester (Model 212, FANN). This test assesses the fluid's film strength by measuring the coefficient of friction (CoF) under specified conditions. The standard lubricity coefficient test involves applying a force of 150 in-lb (equivalent to approximately 600 psi or 4137 kPa pressure) to two hardened steel surfaces – a rotating ring and a stationary block – at 60 rpm. The CoF, representing the frictional force between interacting solids, is determined by the force required to slide the block and ring surfaces across each other at a specified rate, measured by the power needed to turn

the test ring shaft. The instrument was calibrated using deionized water at a speed of 60 rpm with 150 in-lb of force applied for 5 min, which generally gives a torque reading of 34 ± 2. The CoF was then calculated by dividing the torque reading (or meter reading) by 100 for each sample. A correction factor (in this case 0.94) was then applied to the CoF to compensate for the mechanical wear and tear in the block.

3.6 Conclusion

This chapter provided an overview of the synthesis of nanomaterials and the methodologies used for their analysis, the preparation of stabilized nanofluids and their incorporation into DF formulations to evaluate their performance as nano additives. The description of the entire methodological framework serves as the foundation for discussing the findings of the investigation with each nanomaterial in the next chapters.

Chapter 4

Plastic Waste Upcycled Graphene Nanosheets

The global plastic waste predicament constitutes a monumental environmental threat as substantial volumes of plastics amass in landfills and permeate terrestrial and marine ecosystems. Over the preceding thirty years, plastic production has escalated by over fourfold, reaching a volumetric output of 460 million tonnes. Presently, plastic waste accumulation stands at an alarming 353 million tonnes, with a mere 9% undergoing effective recycling processes as per OECD data from 2022 [105]. The predominant fraction of this waste as can be seen in Figure 4.1, comprising 50%, is relegated to landfills, while an additional 19% is subjected to incineration or inadvertent environmental dispersion. Notably, 22% of the waste evades structured disposal mechanisms, infiltrating aquatic and terrestrial ecosystems, and thereby exacerbating environmental contamination trends. Predominantly, plastics such as Polystyrene (PS), Polypropylene (PP), Polyethylene Terephthalate (PET), Polyvinyl Chloride (PVC), as well as High-Density Polyethylene (HDPE), and Low-Density Polyethylene (LDPE), constitute the bulk of global plastic waste generation [106]. The persistent non-degradable attributes of these plastics pose substantial ecological threats, catalyzing heightened awareness and research endeavors to counteract plastic pollution hazards. The valorization of plastic waste into value-added

materials presents an avenue for cost mitigation in production processes. Contemporary research has explored the utilization of these economically viable plastic waste substrates for the synthesis of carbonaceous nanomaterials, inclusive of carbon nanotubes and graphene nanostructures [107].

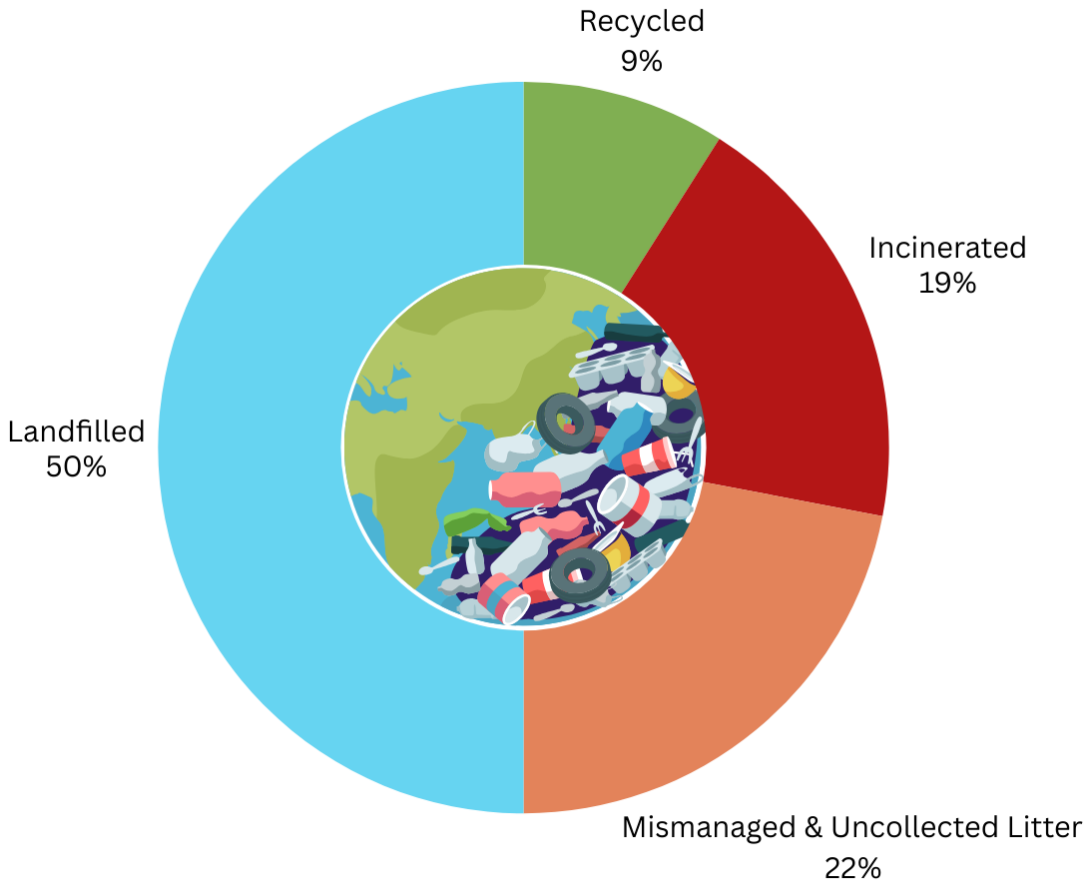

Figure 4.1: Global Plastic Waste Management Scenario (OECD 2022).

Graphene, characterized by its monolayer two-dimensional graphite configuration, has demonstrated commendable efficacy in Oil-Based Drilling Fluids and invert-emulsion drilling fluids. [108–112]. However, the inherent instability of pristine graphene in aqueous dispersions, attributable to particle flocculation [83], has spurred the development and deployment of derivatives such as Graphene Oxide and graphene-derived nanocomposites, which have found application in Water-Based Drilling Flu-

ids [89, 113–117]. Graphene derivatives such as graphene oxide have exhibited effectiveness in WBDF systems [108]. Harnessing plastic-derived GNs as WBDF additives can mitigate environmental plastic accumulation and cost concerns affiliated with nanomaterial additives. Graphene nanoparticles in WBDFs can help form very thin and impermeable filter-cake while efficiently maintaining the rheological performance at higher temperatures [59, 118–121]. However, graphene nanosheets have not yet been used in KCl/Silicate/polymer DF to study the synergistic effect of the complex composition on the flow and filtration behavior. Also, its effectivity at a very low concentration like 0.05% w/v in WBDFs is yet to be investigated. If the performance of the DF is enhanced with such quantity, the requirement of expensive graphene would be reduced and its feasibility at the field scale is likely to be increased. But synthesis and utilization of graphene at a commercial scale have been a challenge for decades now. However, Pandey et al. have recently devised a synthesis technique aimed at the mass production of graphene nanosheets from plastic wastes like polypropylene, polyethylene, and polystyrene using nano-clay [122]. This zero-waste approach for bulk synthesis of nanomaterials like graphene nanosheets opens up a gateway to many applications [123]. The environmental concerns in connection to the intensifying threat from the accumulating non-degradable plastics, as well as reluctance to use nano-additives for WBDFs owing to the upsurge in the cost, can be mitigated now. This approach may make it possible to move towards cleaner production and utilization, gradually reducing the evident carbon footprint by ensuring a sustainable solution to the existing problems.

This experimental investigation, as summarized in Figure 4.2, is inspired to provide a highly effective additive, Graphene Nanosheets (GNs) synthesized from plastic waste for WBDFs. It was aimed to experimentally evaluate the rheological and filtration performance of GNs-enhanced WBDFs for prospective high-temperature oil well drilling utility. Plastic wastes were chopped into minute fragments to synthesize graphene nanosheets, followed by washing, drying, and mixing with bentonite. Subsequent pyrolysis and heating of the mixture under a nitrogen environment pro-

duced GNs. Various analytical techniques characterized the synthesized GNs regarding surface morphology, specific surface area, crystallite dimensions, and elemental distribution. GNs-infused WBDFs were prepared and evaluated under different conditions imitating field drilling operations.

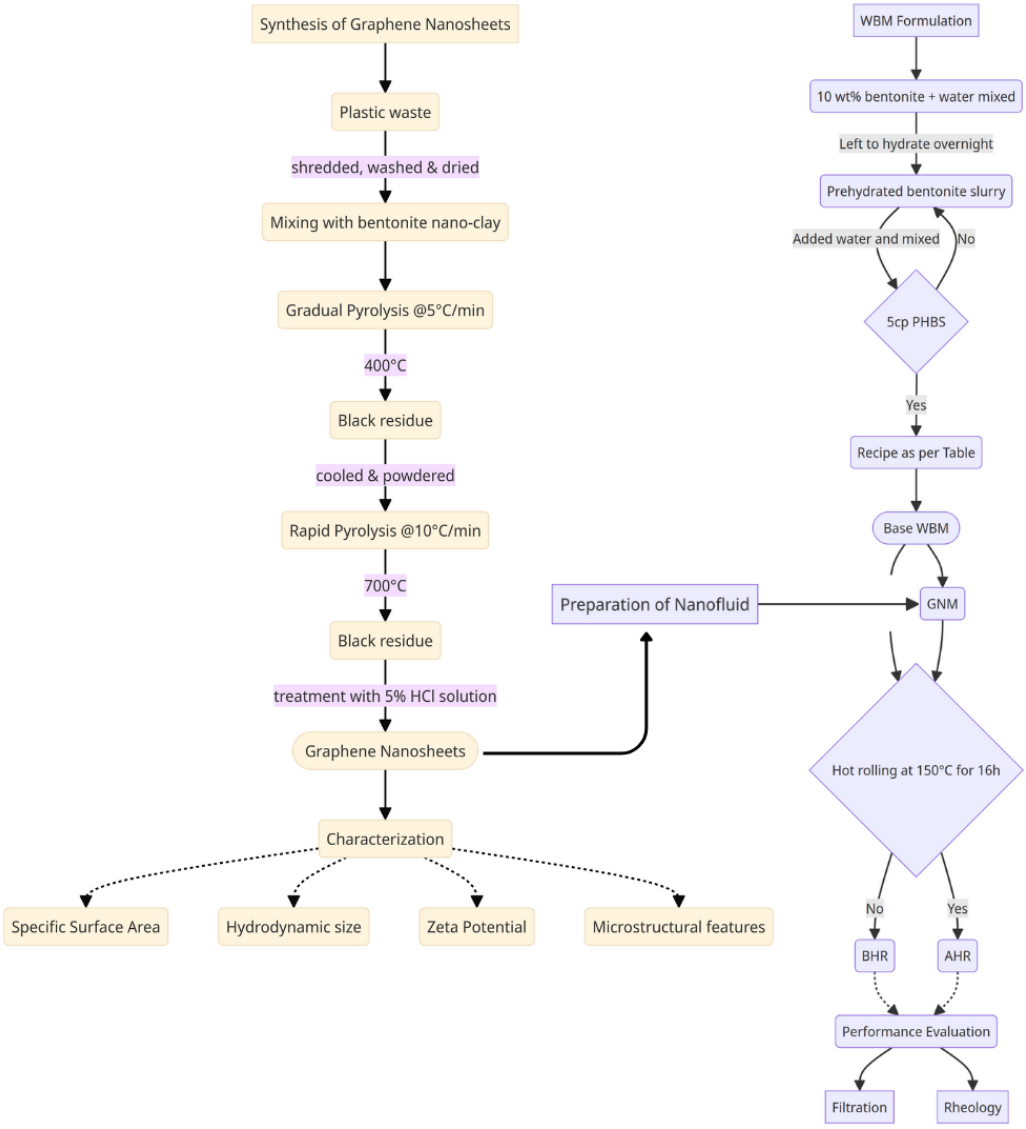

Figure 4.2: Flowchart for the experimental methodology

4.1 Synthesis of Graphene Nanosheets from Plastic Waste

The GNs were synthesized following the previously reported method by Sahoo et al. (2016) [124]. The gathered plastics underwent a shredding process to achieve a flake-like morphology. Following this, the shredded plastics were subjected to washing and subsequent drying, after which they were thoroughly mixed with bentonite nano-clay. This composite sample was then subjected to a gradual pyrolysis process (utilizing a stainless steel horizontal hollow cylindrical feeder unit with a volume of 0.41 m^3) under a N_2 inert atmosphere at a temperature of 400 °C. The controlled pyrolytic decomposition, with a heating gradient of 5 °C/min up to 400 °C, effectively eliminated oil-based hydrocarbons and gaseous components within the sample mixture. Upon completion of the pyrolysis, a residual black amorphous carbon matrix was obtained. This residual material was subsequently processed in a ball milling apparatus to achieve a finely powdered state in preparation for a secondary thermal treatment, aimed at enhancing GNs yield. The finely milled carbonaceous powder was then subjected to rapid thermal treatment in a secondary reactor (comprising a vertical cylindrical feeder unit with a capacity of 0.06 m^3), maintaining a temperature of 750 °C and a heating gradient of 10 °C/min, again under a N_2 gas atmosphere (flow rate: 20 mL/min). This procedure yielded black-colored GNs. To ensure product purity, residual nanoclays were eliminated through a combination of distilled water rinsing and a mild acidic treatment using 5% hydrochloric acid.

4.2 Characterization of the GNs

The characterization of the plastic waste upcycled GNs is depicted in Figure 4.3.

The X-ray diffractogram can be seen in Figure 4.3 (a). The XRD data suggested a sharp peak around 27°, corresponding to the (002) crystal plane with a d-spacing of 3.39 Å according to JCPDS (Joint Committee on Powder Diffraction Standards) card number 75-2078. The mean crystallite size was estimated as 34 nm,

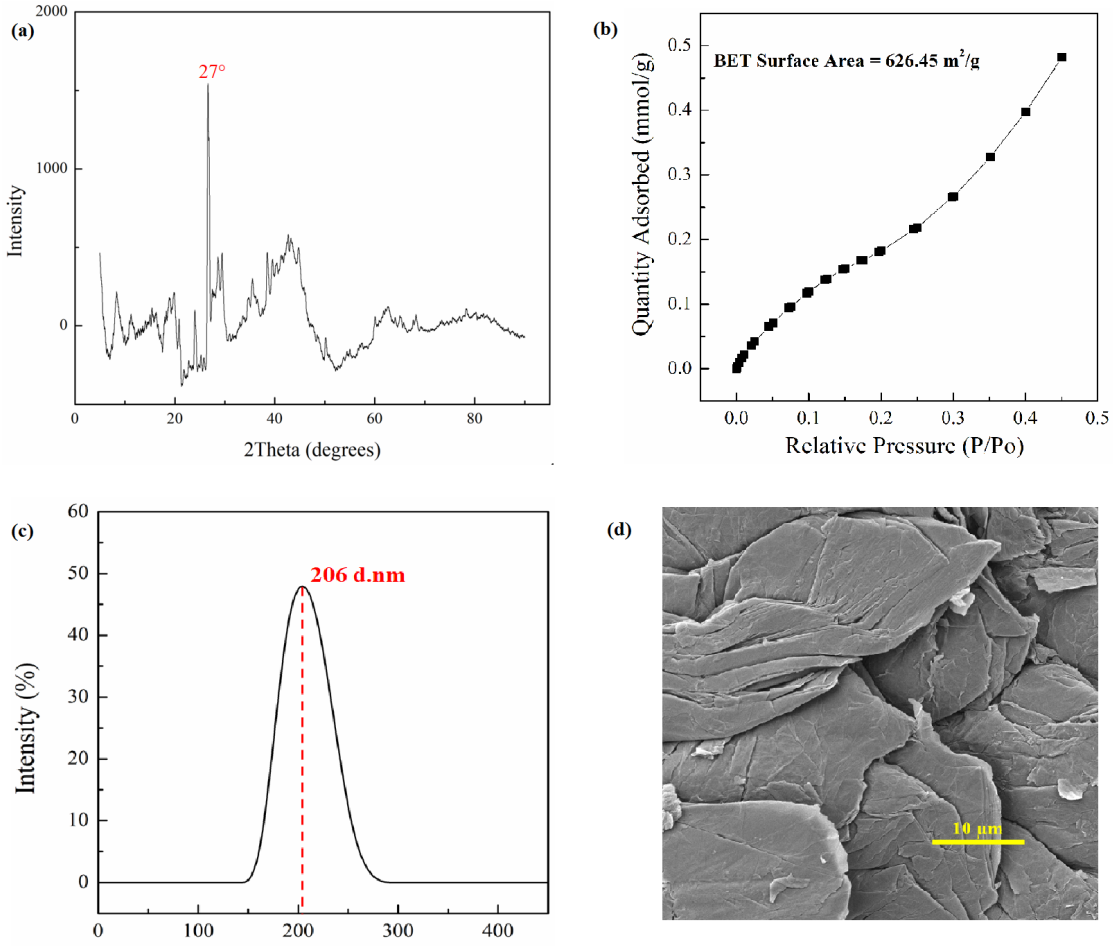

Figure 4.3: Characterization data of the GNs: (a) X-ray Diffraction plot of the GNs. (b) N_2 Adsorption for BET isotherm of GNs. (c) Average Particle Size distribution of GNs by DLS. (d) FE-SEM image of GNs (at 20,000X magnification)

characteristic of graphene nanosheets [110].

Figure 4.3(b) depicts the adsorption isotherm of the GNs. The specific surface area of the GNs was calculated through the Brunauer–Emmett–Teller or BET method at relative pressure points for the quantity of nitrogen adsorption. Notably, the BET surface area came out to be 626.45 m^2/g. The estimated surface area is 76% less than the theoretical value of approximately 2630 m^2/g due to probable aggregation [125]. However, the surface area of GNs is 14 times that of graphite and is adequate for application as a nano-additive.

The size vs. intensity plot from DLS for GNs is given in Figure 4.3 (c). The determined average particle size was 206 nm with a polydispersity index (PDI) of 0.365. The PDI value of 0.1 or above shows the widening particle size distribution

(PSD) range in a colloidal dispersion [126]. The electrophoretic stability parameter or the zeta potential was found to be -29.1 mV when GNs were dispersed in deionized water, rendering them relatively stable for further application.

As shown in Figure 4.3 (d), it was discovered by FESEM analysis that the GNs had wrinkled morphology with arching boundaries caused by chemical interaction between carbon layers; nonetheless, the signature array of stacked sheets was also observed. The EDX data quantified carbon and oxygen values as 82.3 and 17.7 wt% respectively. These values correspond to the functionalization of the GNs during the synthesis in the previous studies [122, 123, 127].

4.3 Performance of Drilling Fluids with GNs

The composition of the base and the GNs-infused DFs to be discussed hereinafter is shown in Table 4.1.

Table 4.1: Composition of the WBDFs with GNs.

Sequence	**Constituents**	**Concentration (wt%)**
1	Deionized water	-
2	Bentonite	3.00
3	KOH	0.07
4	Xanthan Gum	0.25
5	PAC-R	0.50
6	KCl	3.00
7	Sodium Silicate	1.50
8	1-Octanol	2-3 drops
9	Graphene Nanosheets	0-0.44

The samples were named corresponding to the GNs concentration as given below:

- BASE: WBDF with 0wt% GNs.
- GNM-0.5: WBDF with 0.05wt% GNs.
- GNM-1: WBDF with 0.11wt% GNs.
- GNM-2: WBDF with 0.22wt% GNs.
- GNM-4: WBDF with 0.44wt% GNs.

4.3.1 Rheological Performance

The rheological attributes of drilling fluids considerably impact functionality during drilling processes. Multiple fundamental parameters exhibited marked improvements with the incorporation of GNs in the DFs. Effective dispersion of the two-dimensional GNs facilitates optimal heat distribution attributed to their high intrinsic thermal conductivity, thereby preserving uniform additive allocation and polymer hydration even with salts and silicates present [27]. This heat transfer capacity likely contributed to thermal stability enhancements observed in this chapter.

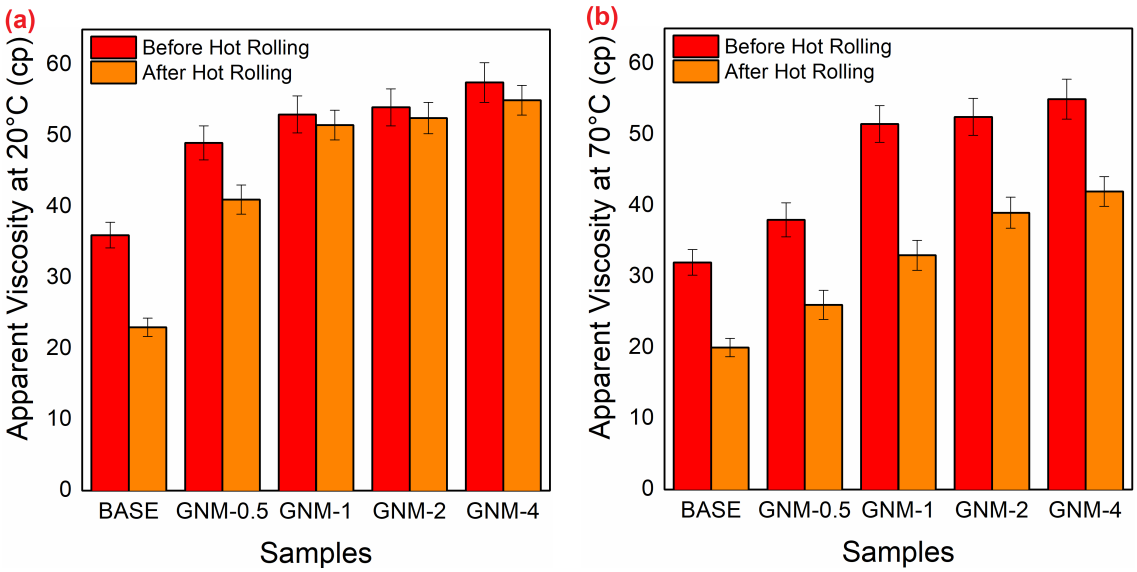

Figure 4.4: (a) AV of the WBDFs at 20 ℃, (b) AV of the WBDFs at 70℃.

Figure 4.4 (a) and (b) illustrate the apparent viscosities for various concentrations of GNs in the WBDFs. At a temperature of 20°C, the AV values exhibited a steady increased with increasing GNs dosage in the DF, both before and after subjecting the DF to thermal aging. As expected, the impact of thermal degradation was comparatively less pronounced in the DF samples containing GNs. This observation suggests that proper dispersion of GNs results in enhanced heat dissipation and, consequently improved thermal stability of the entire fluid system [128]. A similar incremental trend in AV was observed at 70°C for all the WBDF samples. However, the samples subjected to thermal aging exhibited noticeable degradation in AV values when compared to their counterparts before hot rolling. Upon visual

inspection, it was evident that some particles were floating and forming aggregates on the surface of the sample. This behavior is primarily attributed to the degradation of the polymeric dispersant, xanthan gum, within the nanofluid at elevated temperatures. Additionally, electrostatic and van der Waals forces govern interactions between the layered GNs and the clay-based rheology modifier bentonite. This interaction manifests as an augmentation of yield point and apparent viscosity. Microscopic evidence reveals nanofluid particles can adsorb onto clay surfaces, restricting mobility and inertial flow. The tendency for face-to-face stacking between adjacent graphene sheets would hinder rotational and translational motion. Analogous phenomena have been reported for analogous nanocarbons in silicate solutions [27]. Nevertheless, increasing the concentration of well-dispersed GNs showed relatively better thermal stability.

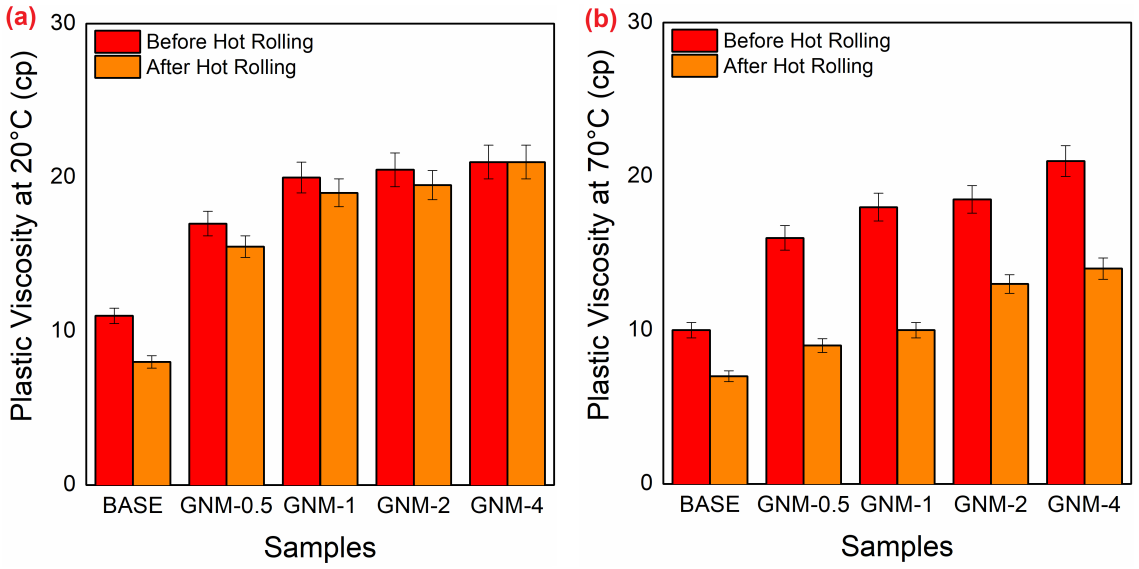

Figure 4.5: (a) PV of the WBDFs at 20 ℃, (b) PV of the WBDFs at 70℃,

As evident in Figure 4.5 (a) and (b), the PV of drilling fluids increased with the concentration of graphene nanosheets (GNs) at 20 °C. This was likely due to the higher solid content and frictional interactions, as shown in Figure 4.6 between GNs and other additives [84]. An initial 0.05 wt% GNs increased PV by 54.5% after which there were slight increments with increasing concentrations of GNs. However, as the temperature increased to 70 °C, it led to the aggregation of GNs and the

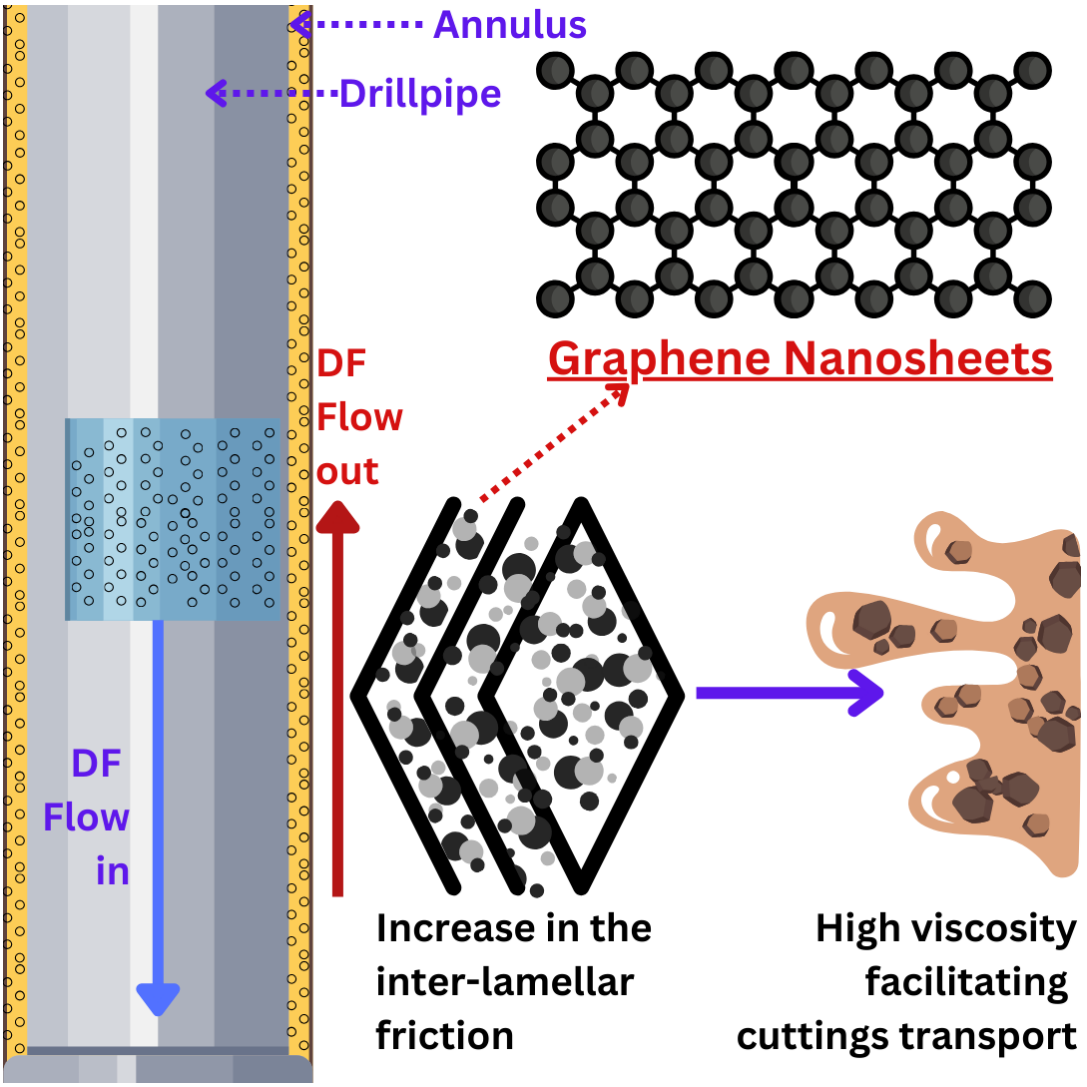

Figure 4.6: Schematic Diagram of viscosity enhancement in WBDFs due to GNs.

destabilization of their dispersion after hot rolling. Consequently, the gap in the values of PV between the measurements taken before and after hot rolling expanded at higher temperatures. Following thermal aging, PV exhibited a similar pattern, with the sample containing 0.44 wt% GNs showing nearly identical PV values before and after aging. In contrast, the base DF exhibited a substantial decline in PV after aging.

Upon examination of Figure 4.7(a) and (b)), the yield point (YP) to plastic viscosity (PV) ratios of the GNMs increase after thermal aging, especially at higher temperatures. This enhancement of YP/PV values suggests improved cuttings carrying capacity and hole cleaning potential within the annulus. Although the plastic

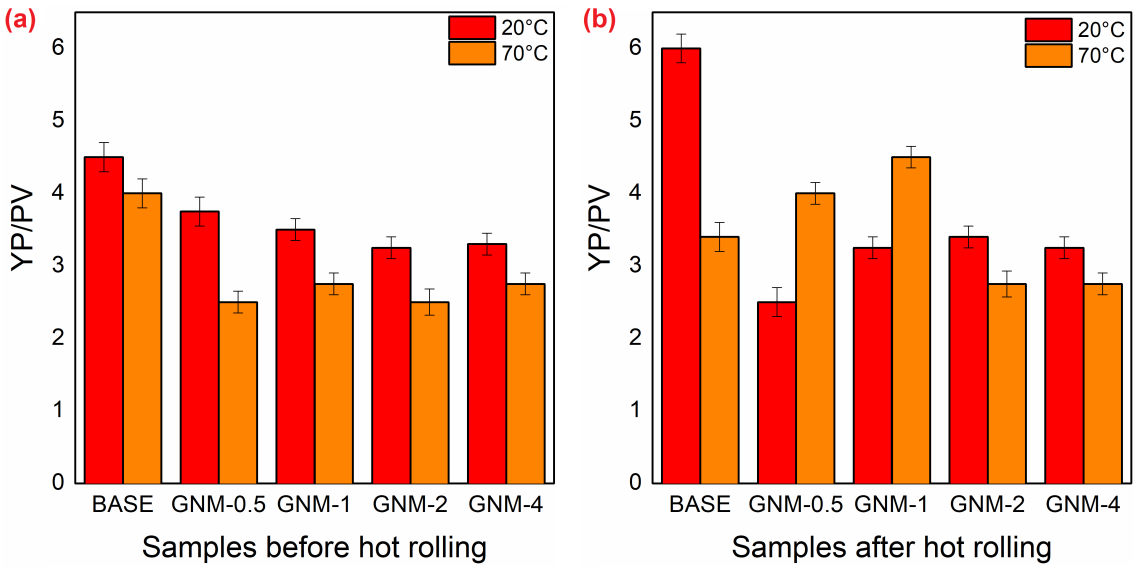

Figure 4.7: (a) YP/PV ratio of the WBDFs before thermal aging, and (b) YP/PV ratio of the WBDFs after thermal aging.

viscosity rises with greater GNM concentrations, definitive trends between incremental nanoparticle loading and resulting yield point differentials are absent. This indicates that factors beyond solely GNM quantity are governing rheological response.

The gel strength values of different WBDF formulations can be seen in Figure 4.8 (a)-(d). Initial gel strength (Gel 0) is measured after 10-seconds after circulation stops, while 10-minute gel strength (Gel 10) is measured after 10 seconds of rest following shearing. Gel 0 values increased with higher graphene nanosheet (GN) concentrations, likely due to interactions between GNs and clay platelets. However, at elevated temperatures (70°C), the 10-second gel strength decreased, a pattern also seen when comparing systems before and after hot rolling.The 10-minute gel strength (Gel 10) is determined after 10 minutes of static conditions post-shearing. This allows clay platelets to reorder and minimize free energy, creating a stronger gel network and higher Gel 10 values [76]. The Gel 10 variations followed a similar pattern to the initial gel strength. Increasing GN concentration improved Gel 10, but elevated temperatures decreased it. Comparing pre- and post-hot rolling systems also showed declining Gel 10 at higher temperatures.

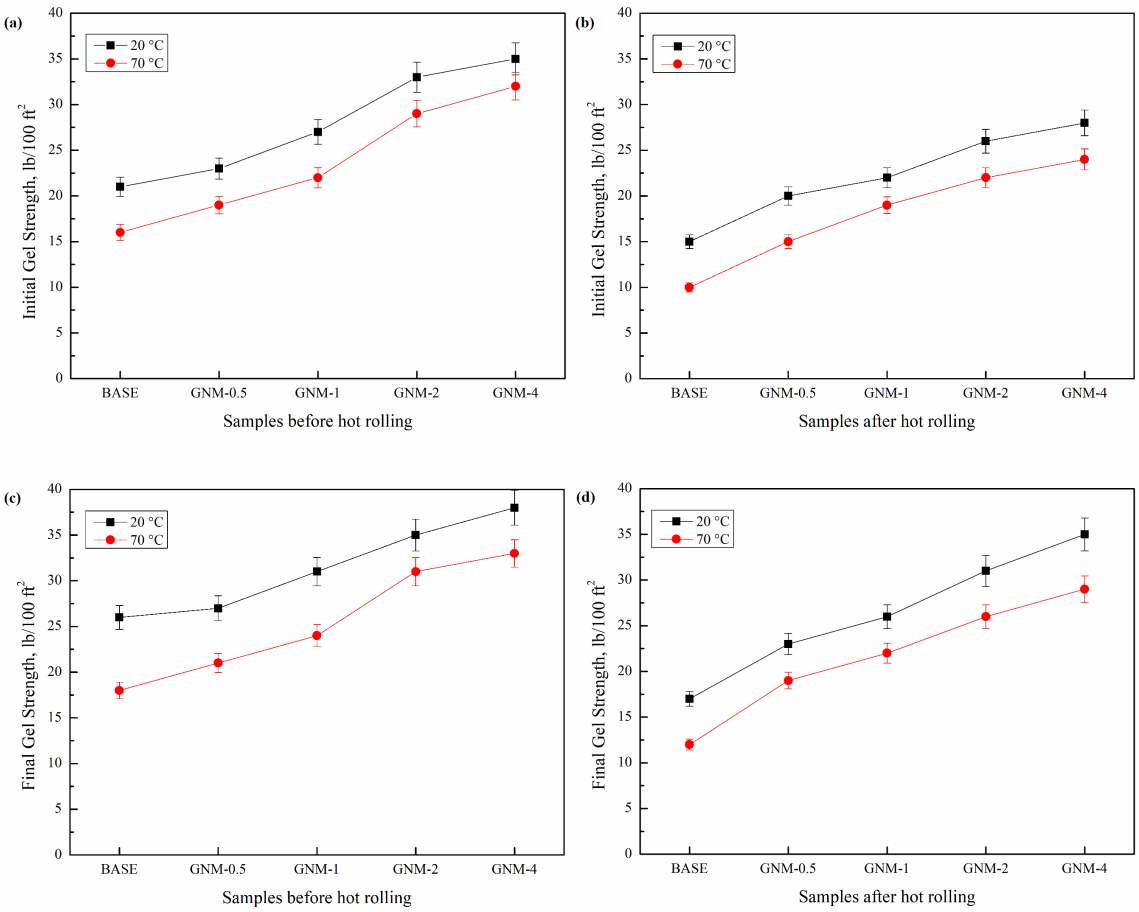

Figure 4.8: (a) Gel 0 of the WBDFs before thermal aging, (b)) Gel 0 of the WBDFs after thermal aging, (c) Gel 10 of the WBDFs before thermal aging, and (d) Gel 10 of the WBDFs after thermal aging.

4.3.2 Filtration Performance

Excessive filtration can severely damage potential hydrocarbon bearing formations. At the same time, some degree of fluid loss is inevitable and essential to facilitate formation of a thin, low-permeability mud cake. This deposited filter cake serves the vital function of stabilizing the wellbore while minimizing further infiltration losses. Therefore, an optimized drilling fluid system will enable sufficient solids build up to generate a stable mud cake, while restricting total filtrate volumes to mitigate formation damage risks. This balanced formulation allows taking advantage of the filtration mechanism's constructive effects while controlling its most deleterious impacts. Careful DF engineering ensures both wellbore stability via an impervious cake, as well as preserved formation productivity for subsequent operations [103].

Figure 4.9 depicts this filtrate loss over time, with all GNM formulations exhibit-

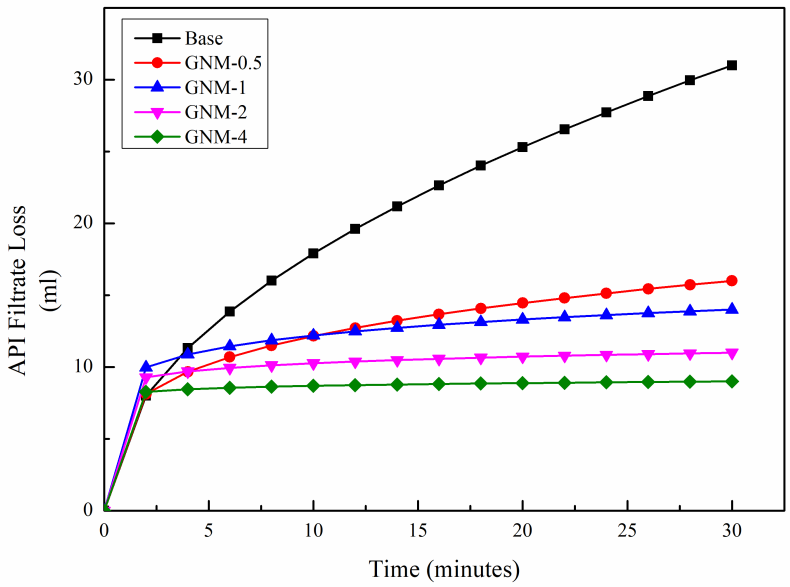

Figure 4.9: API Filtration loss of the base DF and GNMs.

ing a similar spurt loss around 7-10 mL.

After thermal aging, the addition of just 0.5% graphene nanomaterials (GNM-0.5) drastically reduced the filtrate volume by 48.38% compared to the base fluid. As the GNs concentration was incrementally increased up to 0.44% w/v (GNM-4), the API filtrate loss continued declining, reaching an over 70% reduction. However, with ongoing filtration, accumulating clay particles and other loss circulation materials within the developing mud cake act as a sealant layer. This prevents further infiltration, though excessive thickening can also hamper drilling.

Under high pressure, high temperature (HPHT) conditions, evident from Figure 4.10, infusion of GNs again significantly improved filtration control, cutting losses by 54.54% before hot rolling. Further elevating GNs loading only marginally enhanced performance. The combination of bentonite and GNs proved resilient even as temperatures rose, effectively stabilizing the wellbore and mitigating formation damage. Size of the nanomaterials plays a key role in infiltrating and sealing porous zones. Enhanced heat transfer properties also preserve stability at higher temperatures when polymeric additives degrade. Visual examination revealed smooth, compact filter cakes.

Thus GNs in DFs can maintain wellbore integrity and limit productivity impair-

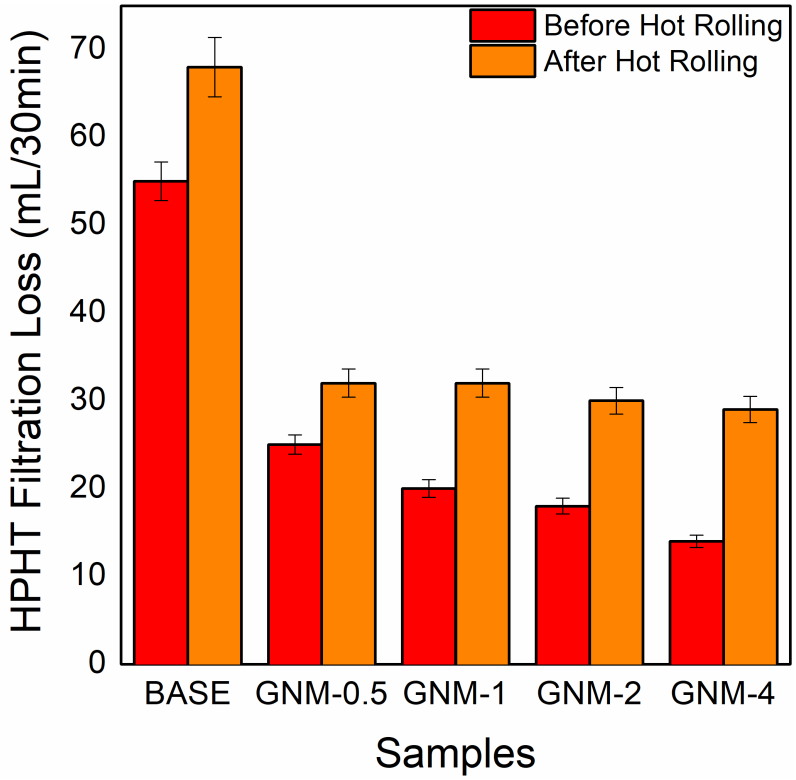

Figure 4.10: HPHT Filtration loss of the base DF and GNMs.

ment under HPHT extremes where conventional options falter. Potential thermal degradation and ensuing fluid losses are curtailed. According to Darcy's Law, the nanoparticle sizes dominate plugging efficiency. Their presence in the external filter cake significantly reduces permeability and water loss. This stems from nanoparticles filling nanoscale pores within the mud cake. In real dynamic wellbore conditions with various forces acting on particles, lower filtration shrinks normal drag on cake particles. The resulting tangential force allows the generation of thinner filter cake.

Figure 4.11 depicts the FESEM visualization of the GNs in filter cake. The filter cake quality and build-up characteristics are also critical in preventing drilling and completion issues. The filter cake is formed when the insoluble solid section of a fluid slurry is deposited on a permeable material when the slurry comes into contact with it under pressure. Because of the increased torque and drag on the drill string when fluid losses are substantial, thick filter cakes and excessive filtration enhance the risk of narrow hole occurrences while drilling which may possibly cause pipe sticking, lost circulation, poor-quality well log data, and formation damage [28].

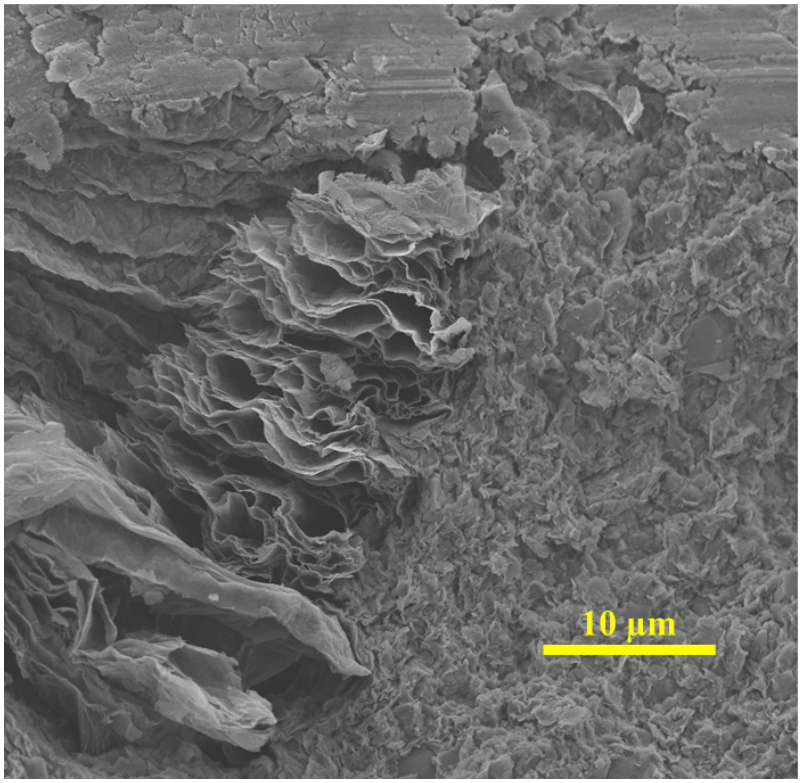

Figure 4.11: FE-SEM images of the filter cake of the WBDF with GNs (at 20,000X magnification)

The mud cake thickness was observed after the initial dosage of just 0.05%w/v of GNs reduced immensely after the initial dosage. The later increments were very low, and that too because of the increasing solids content in the fluid system. However, the cake thickness increased in the case of hot-rolled samples as the polymeric fluid loss additives had degraded. Yet the difference was not much as the GNs could still act excellently as filtration loss additive by sealing the nanopores due to their size and plate-like morphology. When visualized through FESEM stacks of GNs between clay platelets could be seen to some extent. Most of the GNs may have been encapsulated.

4.4 Conclusion

This study demonstrates the significant potential for graphene nanosheets (GNs) derived from plastic waste to serve as effective and eco-friendly drilling fluid additives, especially for challenging high pressure, high temperature (HPHT) well environ-

ments. The experimental results reveal that incorporating even small concentrations of plastic-derived GNs, from 0.05 to 0.44 wt%, can considerably enhance the performance of water-based drilling fluids (WBDFs). As GN content increased, substantial improvements occurred across key DF properties including rheology, thermal stability, and most critically, filtration control. Rheological parameters exhibited marked upgrades with GNs supplementation, indicating benefits for hole cleaning, cuttings suspension, and pump startup capacity. GNs also enabled better preservation of these DF attributes under thermal aging compared to the base fluid. However, the most significant GN impacts came in filtration loss mitigation, where most conventional loss circulation materials falter, especially under HPHT extremes. Here, GNs delivered exceptional filtration control, cutting API fluid losses by up to 70% and HPHT losses by over 50% at maximum concentrations. The nanoparticle sizes and morphologies provide superior pore sealing. Resulting filter cakes were thinner yet more impermeable. Therefore, repurposing plastic waste as value-added GNs creates environmental and economic value. Reduced GNs loading generates outsized enhancements in WBDF stability and performance at elevated temperatures. Their effectiveness at ultra-low concentrations improves operational feasibility and cost savings. With increased global vigilance over environmental conservation, it is imperative to go for net zero waste solutions. Keeping this in view, a dual-pronged approach of comparatively safer WBDF enhanced with plastic waste-progenerated graphene nanosheets is presented.

Chapter 5

Modified Carbon Nanotubes

Carbonaceous nanoparticles, especially carbon nanotubes (CNTs) have a significant impact on the properties of drilling fluids [129]. CNTs are sp2 nanocarbon materials featuring tubular structures created by the rolling of graphene sheets. Alongside their distinctive nanostructures, these materials demonstrate remarkable properties, some stemming from the analogous characteristics of graphite and others from their one-dimensional aspects. CNTs boast a mechanical tensile strength significantly surpassing that of steel, and their thermal conductivity outperforms even diamond [130]. The unique tubular structures with small diameters contribute to CNTs having an exceptionally high aspect ratio, occasionally exceeding 1000, and a substantial surface area exceeding 1300 m^2/g [131, 132]. Due to their composition of carbon atoms, CNTs exhibit remarkable lightweight properties, with a density of merely one-sixth that of steel. Additionally, CNTs demonstrate high chemical stability, resisting nearly all chemical impacts unless subjected to both high temperatures and oxygen simultaneously [133]. CNTs are present in two forms: single-walled CNTs and multi-walled CNTs [134]. The addition of CNTs to WBDFs can enhance thermal conductivity, which is beneficial for drilling in HPHT environments [84]. Moreover, CNTs improve the rheological properties of the fluids, such as yield point

---

This chapter is based on :

A. Bardhan, S. Kumar, S. Basu, A. Pandey, H. Kesarwani, A. Saxena, J. Sarkar, S. Sharma, and S. Kumar, "Mechanistic Performance of Modified Carbon Nanotubes Stabilized in Water-Based Drilling Fluids for High-Temperature Applications." *Energy & Fuels*, 2024, 38 (17): 16066-16078. doi: https://doi.org/10.1021/acs.energyfuels.4c02548

and filtration properties, without adversely affecting other characteristics [135]. The use of CNTs in oil-based DF systems has also been explored, with findings indicating that CNTs can improve the flow properties of the DF, resulting in fluids that behave as pseudo-plastic, which is desirable for optimal hole cleaning [136]. However, the study's relevance to water-based fluids is indirect, as it focuses on oil-based systems.

Furthermore, the concentration of CNTs is critical for achieving the desired effects without negative consequences. Concentrations up to 0.5 wt% have been found to enhance the rheological and filtration characteristics of WBDFs [18]. In addition to the concentration, the shape, size, and surface charge of the CNTs, as well as their functionalization, can influence the viscous properties of the drilling fluid. Functionalization with specific groups can modify the interaction between the CNTs and the base fluid, thus affecting the fluid's rheological behavior [137]. The literature review reveals the importance of nanoparticles in enhancing drilling fluid stability, reducing fluid loss, and improving rheological characteristics [40, 43, 138]. Recently, Lysakova et al. suggested lower bentonite concentration as conducive for CNTs' inclusion in water-based drilling fluids but also found a relatively less significant effect on the filtration performance [139]. While prior studies have primarily focused on low-pressure and low-temperature conditions, this research endeavors to bridge the gap by scrutinizing MWCNT nanoparticle-infused water-based drilling fluids under elevated temperature and pressure scenarios. Detailed examinations of pressure and temperature effects, coupled with varying concentrations, offer a nuanced perspective on the interplay of these parameters. The choice of MWCNT in this study aligns with their recognized benefits and widespread applicability.

This chapter focuses on modifying MWCNTs to enhance their dispersibility in aqueous medium. The stability was further ensured by optimizing the pH and viscosifying the dispersing media with Xanthan gum. Different characterization techniques like X-ray diffraction, Raman spectroscopy, infrared spectroscopy, scanning and transmission electron microscopy, as well as photon correlation spectroscopy,

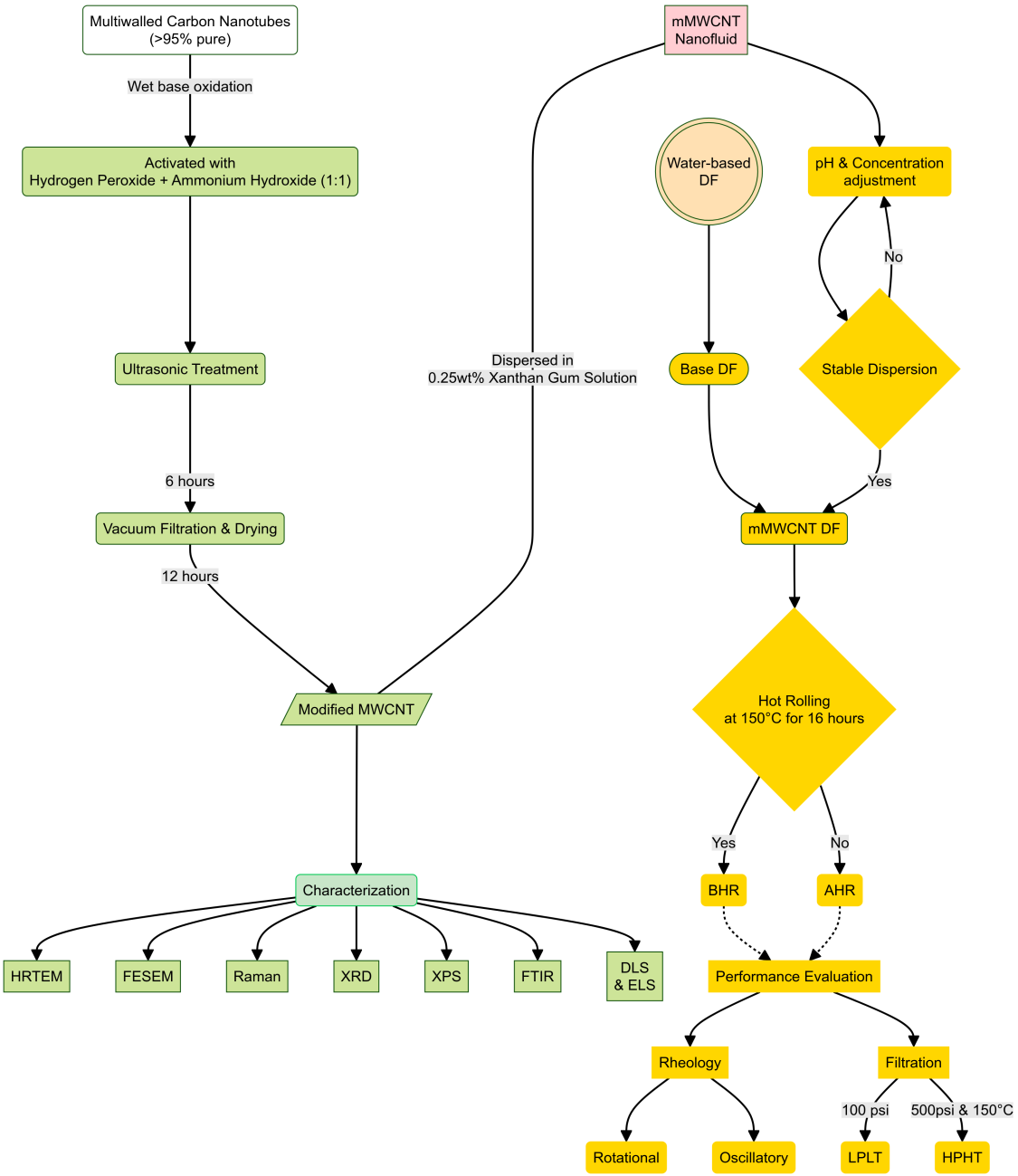

Figure 5.1: Flowchart of the experimental methodology

were utilized to confirm the modification and stabilization. The current work seeks to contribute to the existing body of knowledge by providing a comprehensive understanding of the filtration and rheological dynamics exhibited by drilling fluids containing MWCNTs under conditions mirroring subsurface drilling environments. Therefore, filtration and rheological tests were performed at different temperatures and an elevated pressure of 500 psi. In order to understand the microstructural deformation of the drilling fluids under low shear an oscillatory test was also performed. This analysis sheds light on the dynamic mechanism of the drilling fluid performance by the presence of nanoparticles (in this case mMWCNT). The methodology carried out throughout the entire study is illustrated in Figure 5.1.

5.1 Surface Modification of Pristine CNTs

MWCNT was functionalized through wet base oxidation by thoroughly mixing with Ammonium Hydroxide and Hydrogen Peroxide in equal proportions, followed by ultrasonic treatment lasting 6 h [140]. Subsequently, they underwent vacuum filtration and were dried under vacuum for 12 h. The MWCNT was modified with surface functionalization (henceforth mMWCNT) to improve the dispersibility and stability in aqueous medium [98, 141].

5.2 Characterization of the mMWCNT

The morphological, structural, and hydrodynamic stability of the MWCNT after modification are discussed herein.

The field-emission scanning electron microscopy (FESEM) and high-resolution transmission electron microscopy (HRTEM) images of mMWCNTs provided valuable insights into their morphology and structure. Both the FESEM and HRTEM images as depicted in Figures 5.2 and 5.3 confirm the distinct tube-like morphology of carbon nanotubes with an approximate outer diameter of 34 nm. There is a high degree of entanglement and aggregation into bundles between the tubes [142].

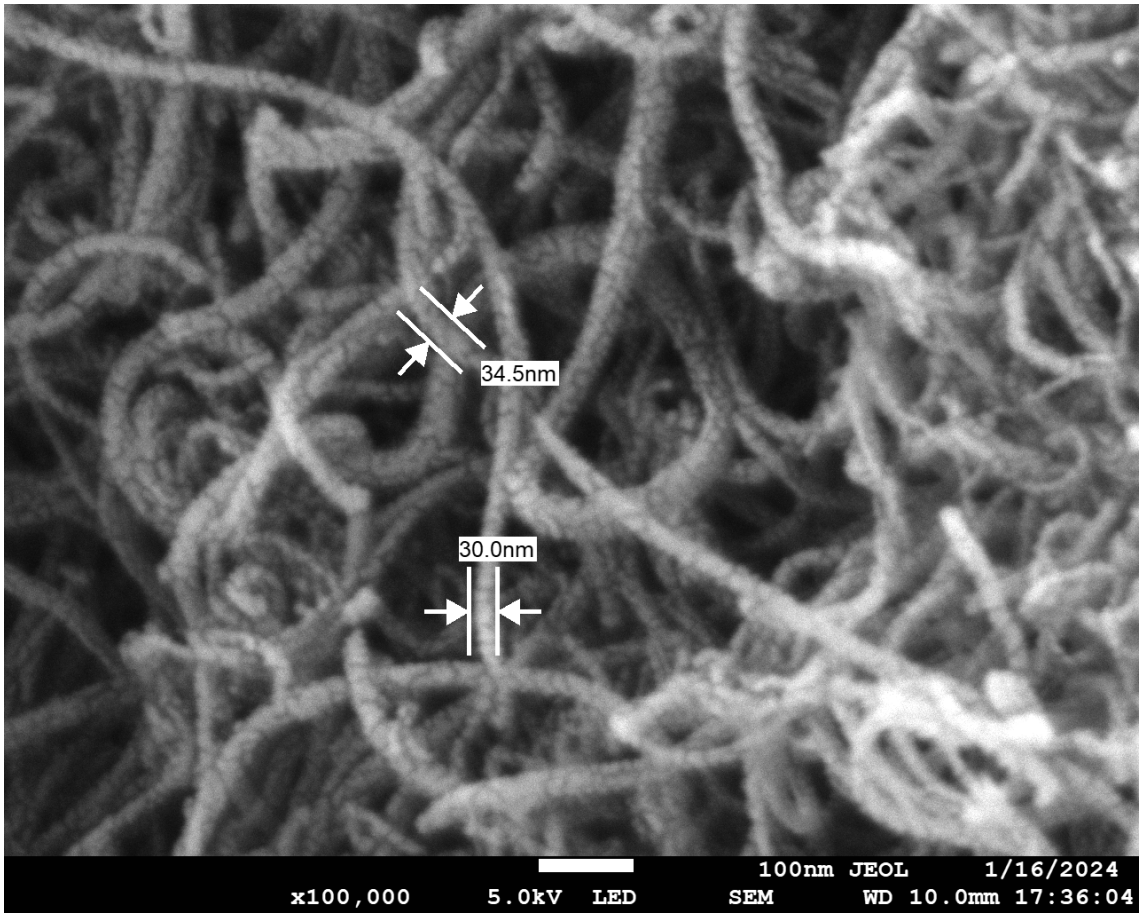

Figure 5.2: FESEM image of the modified MWCNT.

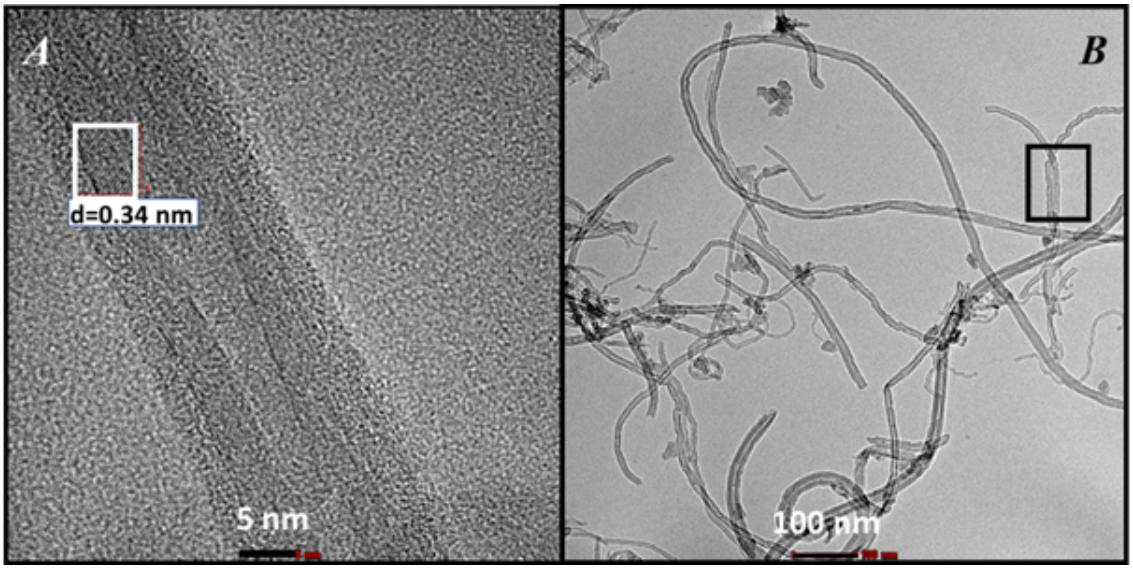

Figure 5.3: HRTEM images of the modified MWCNT.

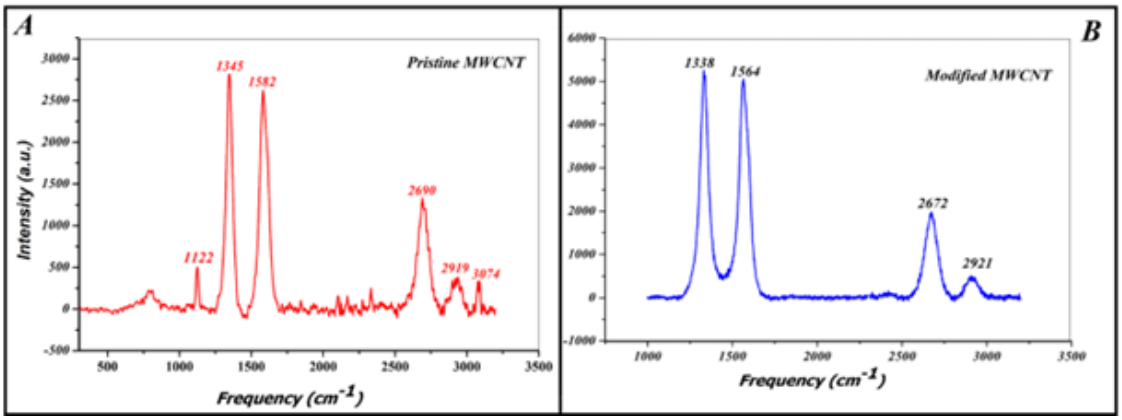

Figure 5.4: Raman Spectra of (A) Pristine MWCNT vs (B) Modified MWCNT

The Raman spectroscopic characterization of the pristine and modified MWCNT was analyzed based on the spectra shown in Figure 5.4 (a) and (b). In the examination of pristine MWCNT, the Raman spectrum revealed a prominent G band, indicative of the stretching mode of the graphitic plane, at approximately 1582 cm^{-1} [143]. However, this characteristic G band is notably influenced by any strain or modifications present. Consequently, a discernible shift in this band was observed following surface modification, resulting in a blue shift with the G band peak now situated at 1564 cm^{-1}. Additionally, both the pristine and modified MWCNT exhibited a second-order dispersive Raman feature known as the G' or 2D band, typically appearing around 2600 cm^{-1} [144]. The D-band, associated with defect activation in Raman modes, was also detected at approximately 1350 cm^{-1} in both instances. Furthermore, the presence of bands corresponding to D+D', indicative of disorder, was evident in both pristine and modified MWCNT samples [141]. Particularly noteworthy was the increased intensity of these bands in the modified MWCNT, serving as confirmation of modifications and the attachment of functional groups to the MWCNT surface.

The X-ray diffractogram of the mMWCNT is displayed in Figure 5.5. There were two prominent peaks representing (002) and (100) planes similar to graphite at 25.99° and 43.27° respectively. These reflections comply with card no. 01-0646 by the Joint Committee of Powder Diffraction studies and have been similarly reported in the literature [142,145–148]. CNTs can structurally be identified with stacks of graphene

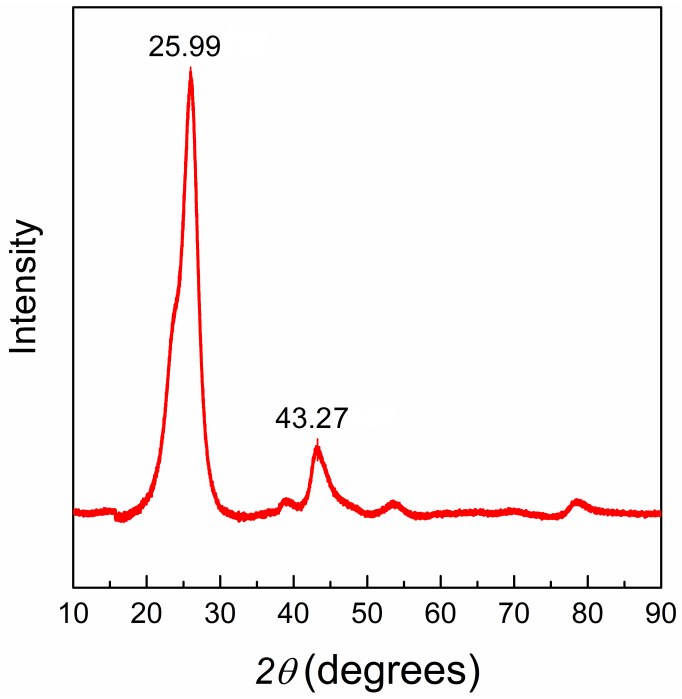

Figure 5.5: X-ray diffractogram of the modified MWCNT.

Table 5.1: X-ray diffraction crystallographic parameters for calculation of the average crystallite size of mMWCNT.

2θ	Planes (h k l)	$\theta(deg)$	$\beta(rad)$	$1/\beta$	$\cos\theta$	$\lambda(nm)$	K	D (nm)
25.99	(0 0 2)	12.99	0.065	15.418	0.974	0.15406	0.9	21.939
43.27	(1 0 0)	21.64	0.053	18.975	0.929	0.15406	0.9	28.303

rolled into tubes, and their inter-layer d spacing (002 plane) in the radial direction equivalent to 3.44 Å in comparison to graphite's 3.25 Å [149]. Moreover, the average crystallite size of the mMWCNT was calculated with the diffraction parameters (Table 5.1) employing Scherrer's Equation and was found to be approximately 25.12 nm.

The Fourier Transform Infrared Spectra of the mMWCNT is depicted in Figure 5.6. The transmittance peaks observed at wavenumbers 3600 and 3150 cm^{-1} are attributed to the stretching vibrations of O-H and C-H bonds, respectively. Notably, the peak centered around 1550 cm^{-1} signifies the stretching vibration of C=O bonds, indicative of carboxylic groups resulting from oxidative treatments. Additionally, minor peaks within this spectral range are associated with oxygen-containing functional groups present at attachment sites along the surfaces of the MWCNT, including both walls and caps [150]. The heightened susceptibility of ter-

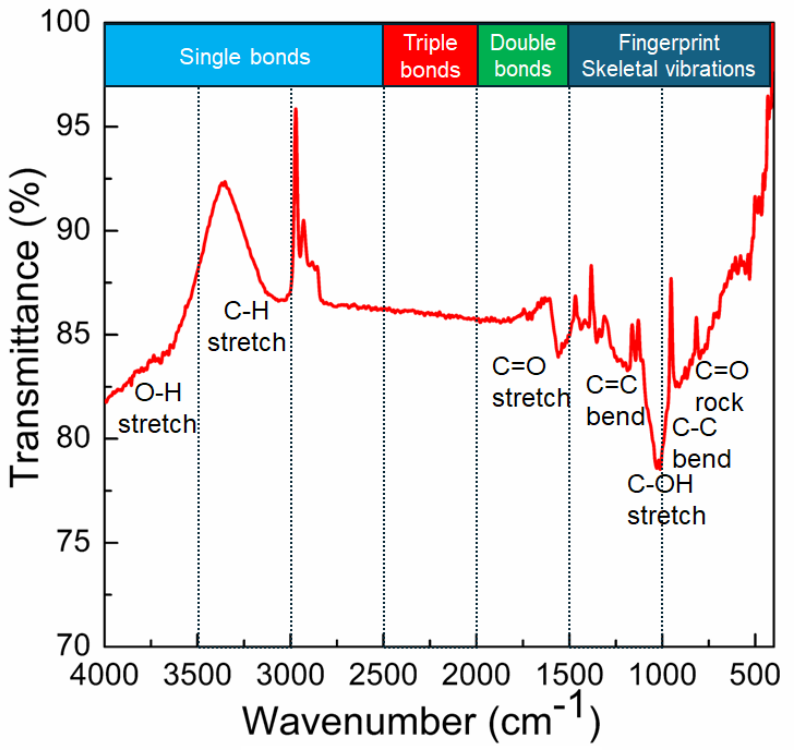

Figure 5.6: Infrared Spectra of the modified MWCNT.

minal C active sites at open ends to oxidation facilitates the formation of carboxylic groups, owing to their heightened reactivity [151]. Analysis of the fingerprint region reveals characteristic peaks at wavenumbers 1050, 900, and 760 cm^{-1}, corresponding to C-OH stretching, C-C bending, and C=O rocking vibrations, respectively. These spectral features indicate the presence of structural defects and confirm the intended functionalization [152].

The X-ray photoelectron spectroscopy (XPS) analysis of the mMWCNT is presented in Figure 5.7. Analysis of C1 in Figure 5.7 (a) shows a prominent peak at 284.8 eV attributed to the graphitic structure of the MWCNTs [153]. Additionally, a peak at 285.8 eV was identified, indicating defects within the CNT structure. The presence of peaks at 286.2 and and 291.1 eV was linked to carbon atoms bonded to various oxygen-containing functional groups [154]. Furthermore, the π–π^* transition loss peak was observed at 291.5 eV. Analysis of the O1s peak, depicted in Figure 5.7 (b), corroborated the existence of certain carboxylic and hydroxyl groups on the surface of the carbon nanotubes. These groups were detected at binding energies of 532.4 eV and 534.9 eV respectively [151].The oxygen functionalities are influenced

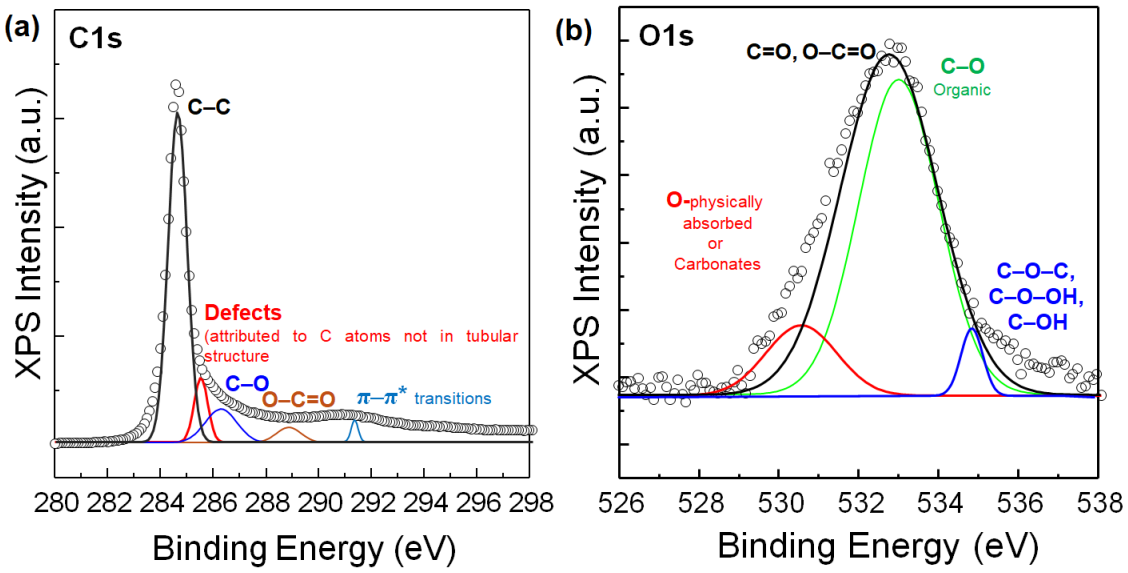

Figure 5.7: XPS Spectra of the modified MWCNT: (a) C1 scan and (b) O1 scan.

by the oxidation conditions, with the overall oxygen content increasing as the power of the oxidizing agents is increased [155].

5.3 Hydrodynamic size and stability adjustment of mMWCNT

The photon correlation spectroscopy, popularly known as dynamic light scattering, translates the Brownian motion of particles in a dispersing media to hydrodynamic diameter [94]. Since the quantification is highly temperature-dependent, all the samples were equilibrated at 25 °C before testing. As the hydrodynamics takes into account the effect of the solvent (in this case, water), this analysis is crucial before applying the mMWCNT in water-based drilling fluids. Another factor considered was the electrophoretic stability or the zeta potential as it plays a dominant role in determining how stable would the dispersion remain without rapidly aggregating. As evident from Figure 5.8, the functional group modification of MWCNT resulted in changing the zeta potential from -8.34 mV (highly unstable) to -21.2 mV (moderately stable) which is apparent from the calculated average hydrodynamic

size reducing from 162 nm to 139 nm. Alterations in surface properties via different ionic mechanisms precipitated changes in the zeta potential and subsequent stability. Consequently, the modification engenders enhanced stability characteristics within the MWCNT, augmenting its dispersibility [140].

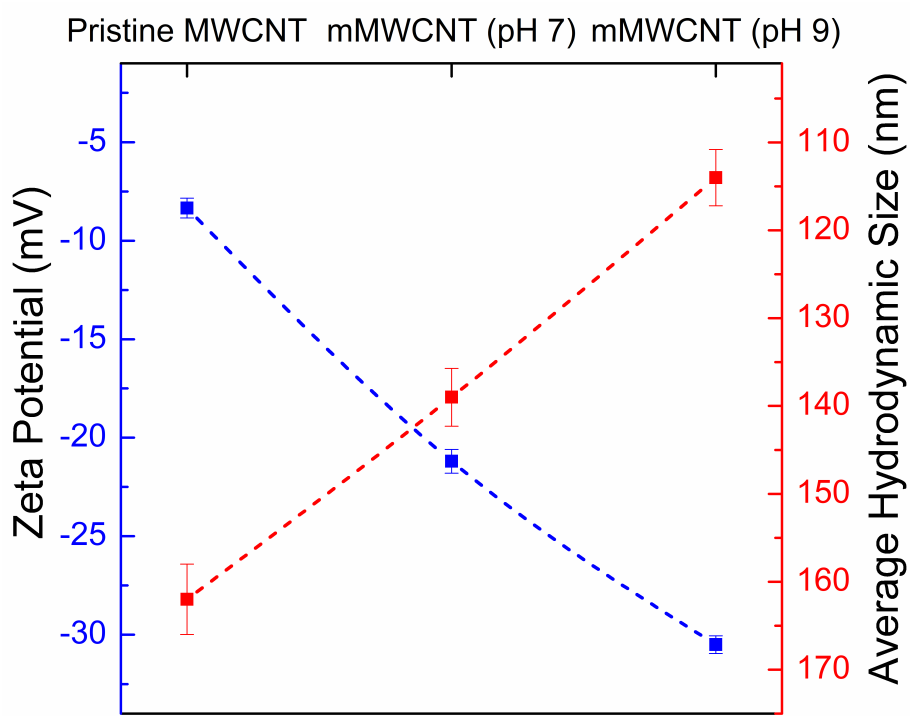

Figure 5.8: Zeta potential (in blue) and the average hydrodynamic sizes (in red) of pristine and modified MWCNT in aqueous medium.

A dispersion is considered stable in the range of greater than +25 mV to less than -25 mV [156]. However, the requirement pertaining to the performance of drilling fluids is for higher stability and a different operating pH (moderately alkaline). Therefore, the dispersing medium's pH was adjusted to a 9 using KOH, and then the mMWCNTs were dispersed in it. Interestingly, the resulting zeta potential and average hydrodynamic size were -30.5 mV and 114 nm respectively. A well-dispersed suspension can be achieved through a high surface charge density, which facilitates strong repulsive forces. As the pH increases, both the zeta potential of the particle surface and its absorbency experience an augmentation. Consequently, the electrostatic repulsion force between particles becomes sufficient to counteract the attraction and collision-induced by Brownian motion. Increased electrostatic force further promotes particle dispersion by augmenting the particle-particle distance

beyond the range of hydrogen bonding between particles, thereby diminishing the likelihood of particle aggregation and settling, thereby enhancing dispersion stability [93, 157].

Time-dependent stability analysis of mMWCNT nanofluids

The stability of nanofluids is imperative when considering their applicability in drilling fluids. Stability, in this context, refers to the ability of a nanofluid to resist the settling of suspended mMWCNT, a characteristic known as dispersion stability. However, since mMWCNT are solid particulates, gravitational forces inevitably lead to their sedimentation. Hence, a nanofluid exhibiting prolonged dispersion stability is deemed more stable compared to one experiencing rapid settling [158]. A visual examination was employed to assess the dispersion stability of the nanofluids. Immediately after preparation, nanofluids were transferred to transparent vessels and left undisturbed to monitor changes in appearance over time. Although all prepared nanofluids initially appeared black, they exhibited gradual settlement as time progressed as shown in Figure 5.9.

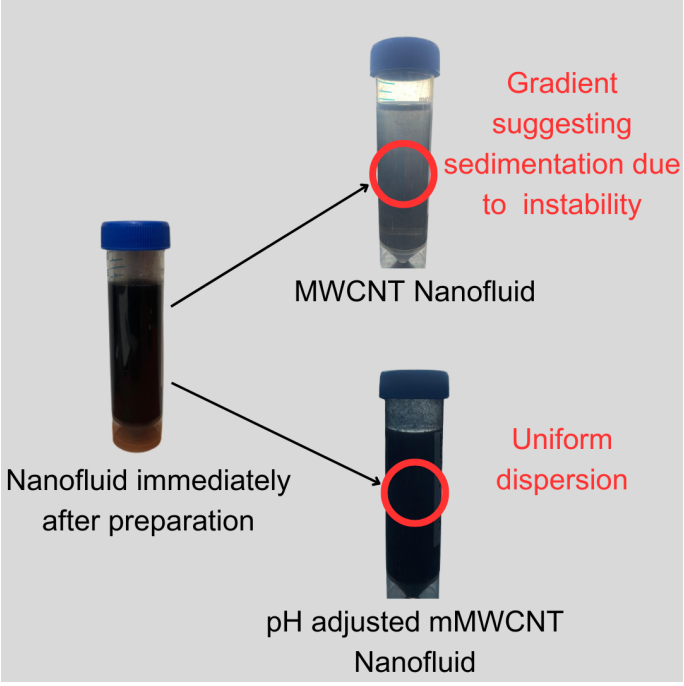

Figure 5.9: Visual representation of the nanofluid dispersions of MWCNT vs mMWCNT for time-dependent stability analysis.

Notably, a nanofluid prepared with 0.1 wt% mMWCNT and Deionized water began to show signs of settlement within two hours, whereas those prepared with 0.25 wt% XG solutions showed no settlement for ten days. It was also observed that increasing the concentration of mMWCNT beyond 0.1 wt% showed faster settling. Hence, it can be inferred that a higher population led to aggregation resulting in bigger cluster size and eventual settlement [159]. Zeta potential measurements were performed to cross-validate the visual findings. The zeta potential of the nanofluid with 0.1 wt% mMWCNT in XG solution showed a value of -33.4 mV which changed to -32.6 mV after 16 h and then -29 mV after 10 days. While zeta potential in nanofluids may change with time due to various physical, chemical, and environmental factors, the observed changes may be attributed to aggregation of the mMWCNTs due to van der Waals forces and gravity, eventually leading to a change in the surface area (and charge distribution) [160].As a result, four effective concentrations of mMWCNT in the DF were identified for the performance evaluation: 0.025, 0.050, 0.075, and 0.1 wt%.

5.4 Performance of DFs with mMWCNT

The composition of the base and the mMWCNT-infused DFs to be discussed hereinafter is shown in Table 5.2.

Table 5.2: Composition of the DFs with mMWCNT.

Sequence	**Constituents**	**Concentration (wt%)**
1	Deionized water	-
2	Bentonite	3
3	KOH	0.07
4	Xanthan Gum	0.25
5	PAC-R	0.5
6	KCl	3
7	1-Octanol	2-3 drops
8	mMWCNT	0-0.1

5.4.1 Rheological Performance

As discussed before, DFs undergo increasing pressure-temperature conditions as the depth while drilling increases. Therefore, the behavior of the DFs was studied across varying temperatures and pressures to identify mMWCNT's effect on the formulation.

Figure 5.10 (a-d) displays the relationship between viscosity and shear rate for the base and mMWCNT-infused samples at 20°C temperature before and after hot rolling.

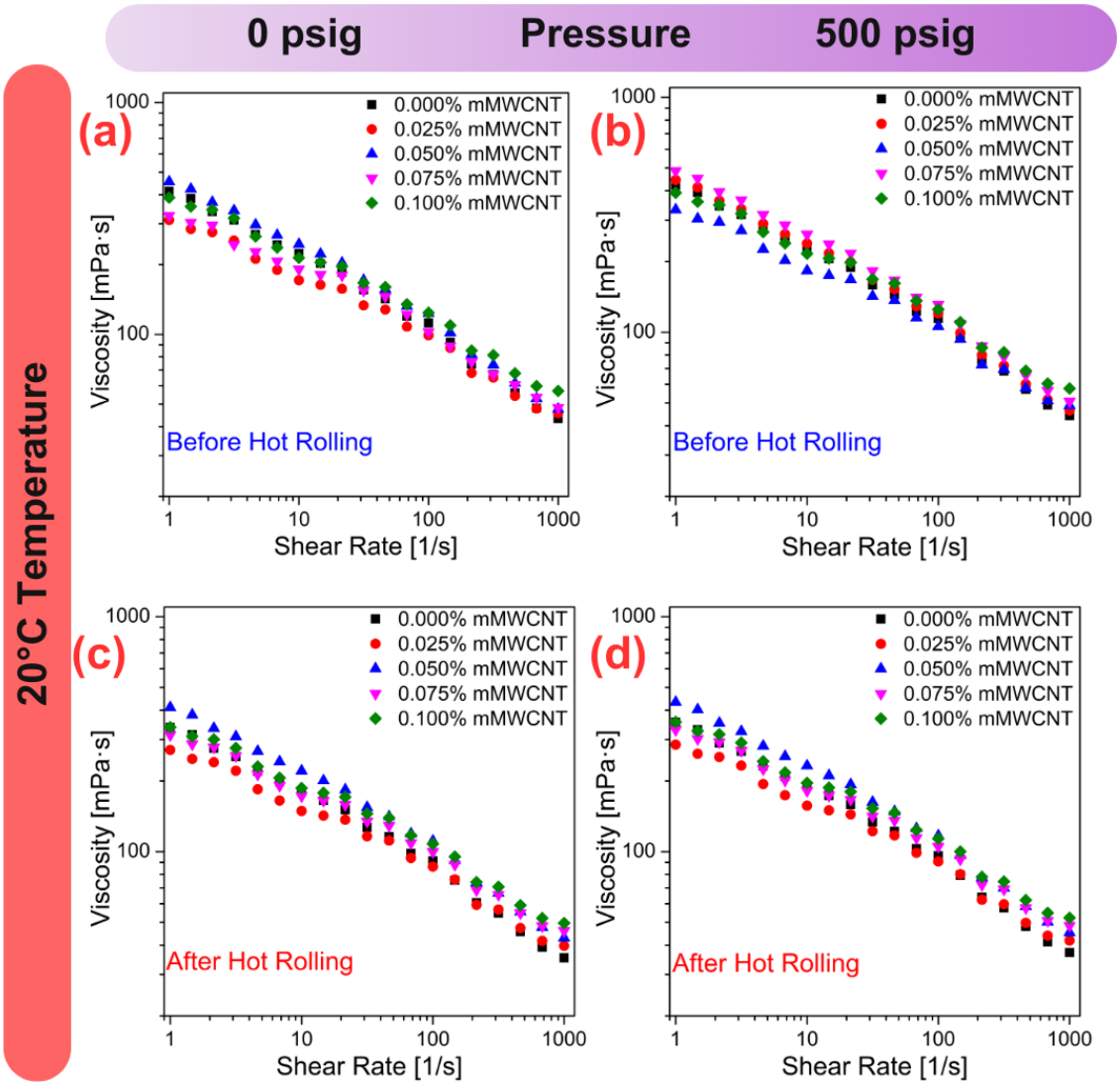

Figure 5.10: Viscosity profiles of the DFs at 20 °C: before hot rolling at (a) ambient pressure and (b) 500 psi; after hot rolling at (c) ambient pressure and (d) 500 psi.

At 0 psig, the incorporation of mMWCNT in the DF led to a notable increase

in viscosity across various shear rates. Specifically, compared to the base DF, the addition of 0.1 wt% mMWCNT resulted in a viscosity increment of 10.68% at intermediate shear rates (100 s^{-1}). Similarly, at higher shear rates (1000 s^{-1}), viscosity augmentation of approximately 6%, 10%, 12%, and 32% was noted for the 0.025, 0.05, 0.075, and 0.1 wt% mMWCNT concentrations respectively. Conversely, after hot rolling, the overall viscosity of all the DF sampled diminished in comparison to the fresh DF samples (BHR). Notably, the most significant reduction, amounting to a 19% decrease, was observed for the base DF at 1000 s^{-1}, whereas the mMWCNT-infused DF samples showed lesser degradation apparent from a marginal decrement of 10% at 0.1wt% mMWCNT concentration. When the pressure was increased to 500 psig, all the samples showed slightly higher viscosities both in the case of before and after hot rolling. At 1000 s^{-1}, 0.1 wt% of mMWCNT dosage enhanced the viscosity by 31% (BHR) and 40% (AHR) as compared to the base DF counterparts under the same pressure condition.

At 80°C, a sharp decline in viscosity is observed for the base as evident from Figure 5.11 (a-d). In contrast, the 0.1% mMWCNT exhibited the highest retention in viscosity at 0.1 wt% mMWCNT concentration surpassing the base DF which had a viscosity degradation by 52%. Similarly, after hot rolling results display the lowest viscosity profiles at elevated temperatures with mMWCNT-infused DFs showing resilience to thermal degradation. Then again when the pressure was ramped to 500 psig, the viscosities increased slightly for all the samples.

These findings suggest that at 20°C, the incorporation of mMWCNT fosters a shear-thinning behavior in the fluid, whereas at elevated temperatures, viscosity retention improves with mMWCNT in DF, particularly evident at 0.1 wt% concentration. In the formulation of DFs, augmenting viscosity commonly involves the addition of polymers, such as cellulose and polysaccharides, in the continuous phase (here, water). However, variations in polymer entanglement result in viscosity alterations under different shear rates. Particularly, the interconnection of polymer within the fluid-structure weakens under high shear rates, commonly encountered

in confined geometries like nozzles or slim open-hole annular regions. Despite the decreased viscosity in such regions, pressure losses compensate for the velocity, aiding in cuttings removal. Conversely, in larger hole sections characterized by lower velocities, the rheological properties of a drilling fluid dictate its ability to transport cuttings. Notably, the consistently superior viscosities observed for 0.1 wt% mMWCNT at low and intermediate shear rates imply enhanced cutting carrying capacity compared to other concentrations.

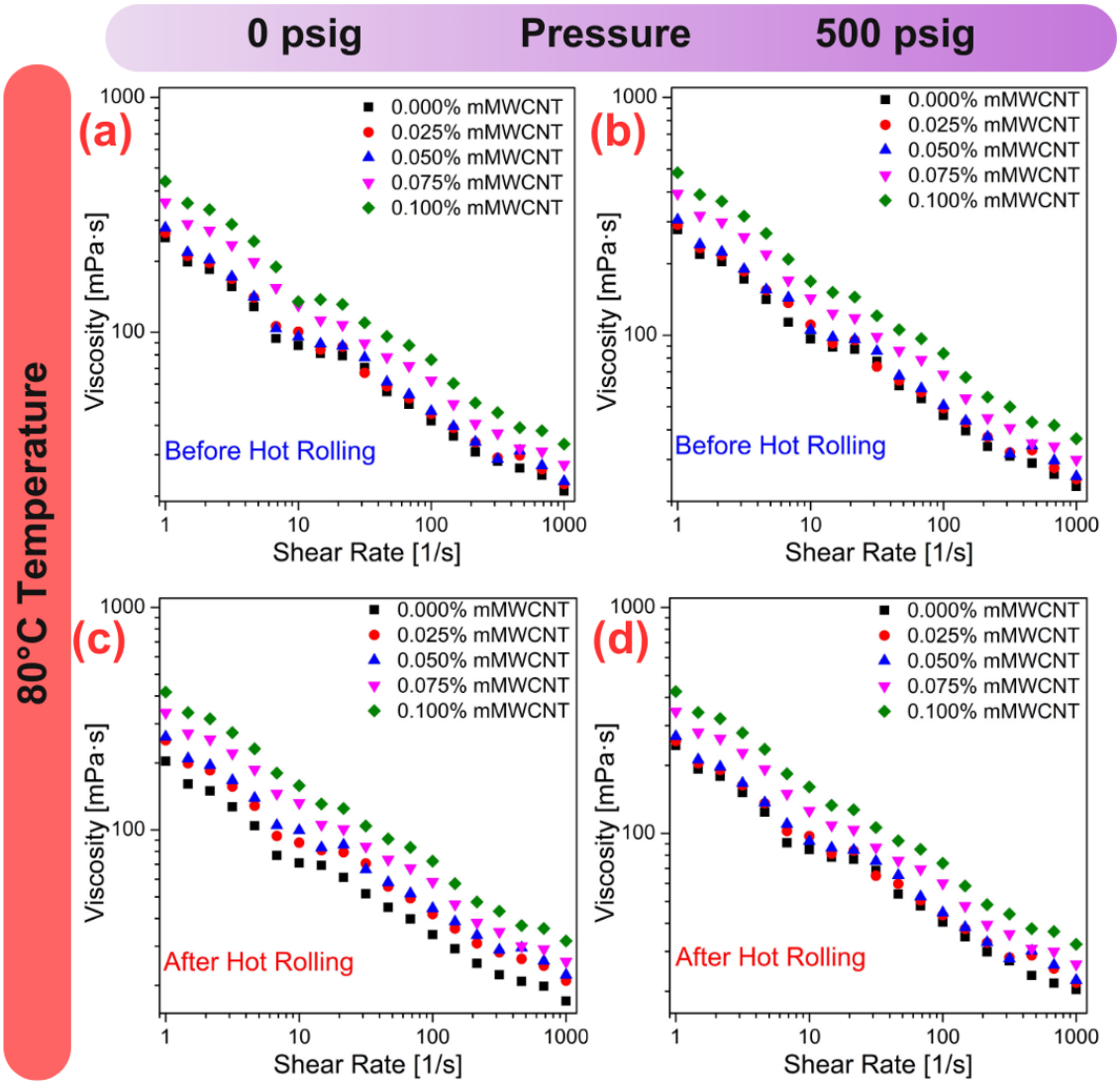

Figure 5.11: Viscosity profiles of the DFs at 80 °C: before hot rolling at (a) ambient pressure and (b) 500 psi; after hot rolling at (c) ambient pressure and (d) 500 psi.

5.4.2 Viscoelastic Characterization

DFs being a mixture of clay and polymers displays a combination of elastic and viscous behavior under stress. This viscoelastic nature dictates the yield and cutting suspension ability of a particular formulation and therefore requires to be characterized [161]. The oscillatory amplitude sweep test describes the structural deformation of a viscoelastic sample by quantizing the quasi-elastic behavior with the storage modulus (G′) and the viscous behavior with the loss modulus (G″) corresponding to different shear strains. The viscosity of a substance emerges from the friction occurring among its constituent molecules and particles as it flows. This friction generates heat, converting deformation energy into thermal energy. Consequently, this energy is absorbed by the substance, utilized in internal friction processes, and becomes unavailable for further material behavior—a phenomenon termed energy dissipation. Conversely, the elastic component of energy becomes stored within the deformed material, achieved by extending and stretching its internal structures without causing damage. Upon release, this stored energy acts as a driving force for the material to revert to its original shape. The storage modulus G′ quantifies the stored deformation energy, while G″ measures the energy dissipated through internal friction during flow.

Figure 5.12 (a-d) illustrates the loss factor in the DF samples at 500 psig and temperatures of 20 and 80 °C. The loss factor is defined as the ratio between G″ and G′ indicating the transition of the sample to the flowing phase (G′=G″) at a particular strain. At 20 °C, the transition point was attained at a strain of 4.5% for the fresh base DF whereas with the increasing mMWCNT concentration, the point was subsequently delayed up to 70% strain. After hot rolling, the breakdown of the polymeric network and flocculation of the suspended clay in the base reduced the strain required to reach the loss factor of 1 to 0.4%. However, the mMWCNT-infused DFs displayed resilience to the degradation and displayed higher strain values at the transition point. At 80 °C, both BHR and AHR samples showed relatively lower transition points relative to their 20 °C counterparts. Yet again in all the cases,

mMWCNT-laden samples showed a stronger viscoelastic nature as compared to the base samples. This can be attributed to the even distribution of the mMWCNTs in the media promoting higher resistance to the bentonite-polymer network in the system [162, 163]. Additionally, the repulsive forces between the nanostructures also account for their higher dispersion stability even after hot rolling keeping the network's rigidity intact [164]. Therefore, mMWCNT can be utilized for preserving the structural integrity (gel) of the DF at elevated pressure-temperature conditions to maintain the cutting transport efficiency [17].

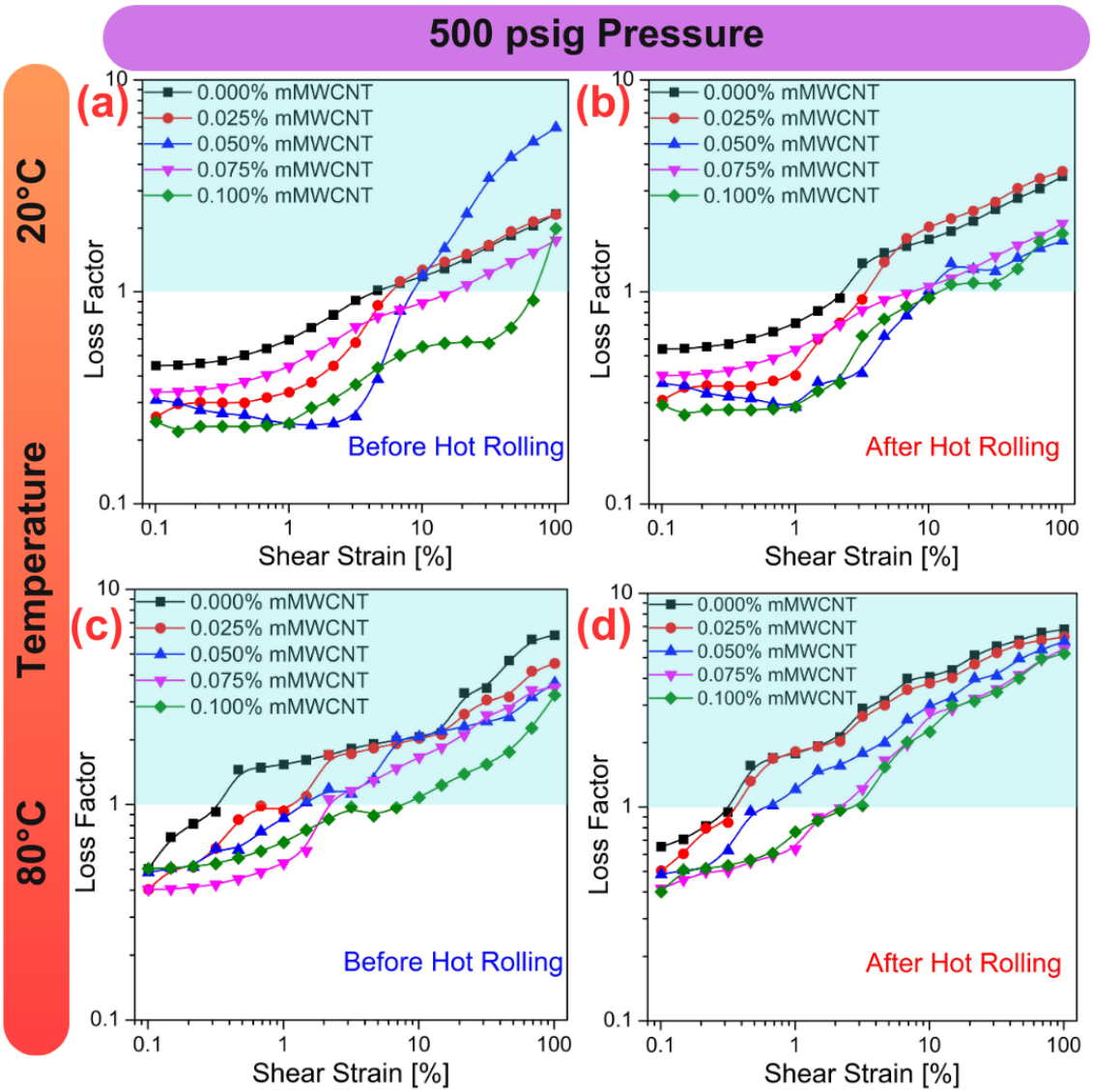

Figure 5.12: Loss Factor of the DFs at 500 psi: (a) before hot rolling, at 20 °C; (b) after hot rolling, at 20 °C; (c) before hot rolling, at 80 °C; (d) after hot rolling, at 80 °C. The blue region indicates the flow zone when the viscous behavior becomes dominant over the elastic behavior.

5.4.3 Filtration Performance

In this comparative evaluation, the influence of the mMWCNT on filtrate loss in formulated DF samples was investigated, aiming to address the critical issue of excessive fluid loss due to filtration during high-temperature drilling operations. Figure 5.13 presents the LPLT FL before and after hot rolling.

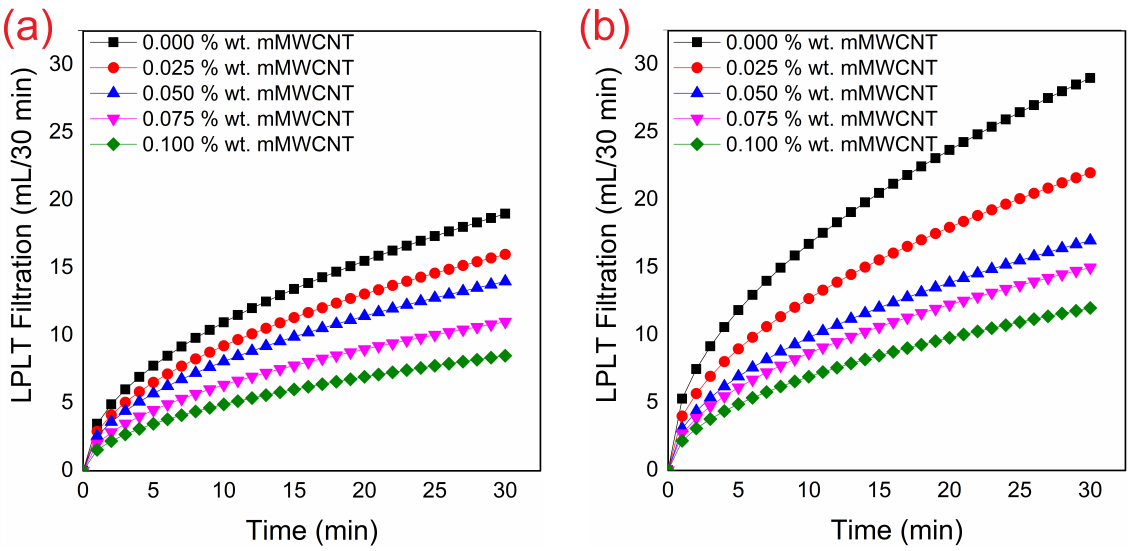

Figure 5.13: Filtration performance of the DFs at 100 psi differential pressure (a) before hot rolling and (b) after hot rolling.

As shown in Figure 5.13 (a), in the first phase (BHR), fresh DF samples containing 0.025 wt% mMWCNT demonstrated a 16% decrease in fluid loss compared to the base sample. This reduction in fluid loss persisted with increasing concentrations of mMWCNT, reaching a substantial 55% reduction at 0.1 wt% mMWCNT concentration relative to the base. However, thermal aging at elevated temperatures led to the degradation of polymeric fluid loss additives and subsequent increased fluid loss for the DF samples which can be seen in Figure 5.13 (b). Despite this, the inclusion of mMWCNT continued to exhibit a considerable impact on filtrate volume reduction. Even after thermal aging (AHR), DF samples containing mMWCNT maintained a reduction in fluid loss compared to the base sample. For instance, at 0.025 wt% mMWCNT concentration, a 24% decrease in filtrate volume was observed relative to the base fluid. Subsequently, the FL volume ultimately showed a noteworthy decrement by 58% at a mMWCNT concentration of 0.1 wt% even after

hot rolling.

It is crucial to emphasize that the improved performance of these mMWCNT is specifically required for wellbores subjected to elevated temperatures and pressures, conditions that the standard LPLT FL test may not adequately capture. Relying solely on standard API filtrate loss tests may overestimate the true efficacy of the mMWCNT. To address this limitation, all drilling fluid samples underwent HPHT FL tests at a differential pressure of 500 psi and a temperature of 150 °C. Significantly, the addition of mMWCNT proved highly effective in mitigating fluid loss in the DFs even in the HPHT FL scenario, as illustrated in Figure 5.14.

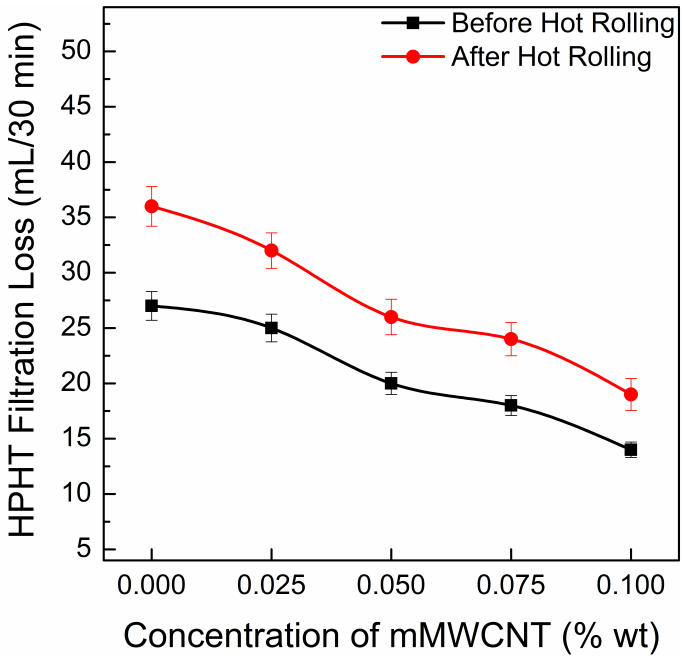

Figure 5.14: Filtration losses of the DFs at 150 °C and 500 psi differential pressure before and after hot rolling.

Before hot rolling, the initial filtrate volume of 27 mL from the base, exhibited a reduction of approximately 7.5% with the infusion of mMWCNT at 0.025 wt%. The reduction in filtration loss became more pronounced with concentrations of 0.05 and 0.075 wt%, resulting in reductions of 26% and 33%, respectively. A substantial total percentage reduction of 48% was achieved when comparing the base sample without mMWCNT (0 wt%) to the sample containing 0.1 wt% mMWCNT. Even after subjecting the base fluid to hot rolling, which resulted in an HPHT fluid loss of 36 mL, approximately 37% more than the base sample subjected to HPHT tests

before hot rolling (BHR), the trend of fluid loss reduction remained intact as the concentration of mMWCNT increased. This demonstrated a remarkable net reduction of 48%. These results underscore the notable efficacy of mMWCNT as a filtrate-reducing nano-additive, particularly under high temperatures and pressures. Therefore, it can be inferred that mMWCNT effectively interacted with clay particles, preventing their aggregation and enhanced nanopore clogging, leading to reduced filtration losses. This interaction was substantiated by previous research [165]. Additionally, mMWCNT exhibits efficient heat-dissipating properties within the system, contributing to maintaining the consistency of clay dispersion in the water-based drilling fluid system, as highlighted in previous work [84].

5.5 Conclusion

This study presented compelling evidence of the reinforcing potential of modified multi-walled nanotubes (mMWCNT) in water-based drilling fluid systems for high-temperature applications. The MWCNT was not only functionally modified but also stabilized in a polymeric nanofluid system mitigating settling tendencies and ensuring sustained performance over time. The rendered hydrodynamic stability was confirmed with zeta potential and visual sedimentation analyses over several days. Importantly, this also helped set an upper limit of the mMWCNT concentration at 0.1 wt% for application in DFs. Upon evaluating the performance of the DFs substantial reductions in filtration loss were observed with mMWCNT, even under simulated downhole conditions.

- Fresh DF samples with 0.1 wt% mMWCNT showed 55% reduction in filtration loss compared to base samples.
- After thermal aging, mMWCNT-infused samples maintained up to 58% reduction in filtration loss.

Furthermore, the investigation into the rheological performance of mMWCNT-infused DF samples revealed intriguing findings.

- mMWCNT-infused DFs displayed greater resilience to viscosity degradation after thermal aging compared to base DFs.
- At elevated pressures, mMWCNT significantly enhanced viscosity.

Viscoelastic characteristics were also greatly enhanced with mMWCNT, showing thermally tolerant microstructural integrity.

- Higher strains were required for flow in mMWCNT-infused DFs.

These findings contribute to high-temperature drilling applications, paving the way for the development of eco-friendly water-based drilling fluid formulations with improved fluid loss control, rheological behavior, and structural integrity preservation.

Chapter 6

Biogenic Copper Oxide Nanoparticles

The use of metal oxide NPs, owing to their high surface area-to-volume ratio, has gained prominence in the oil and gas industry [59, 166, 167]. Copper oxide (CuO) NPs, in particular, have demonstrated the ability to enhance DF properties like rheology, filtration, and thermal conductivity. Liu et al demonstrated that the thermal conductivity of polyethylene glycol can be amplified when CuO NPs are introduced into it [44]. William et. al. reported that CuO nanofluids enhanced the thermoelectrical properties by 35% while showing a considerably stable rheological profile [167]. Ponmani et. al. varied the base for CuO nanofluids and reported consistently superior performance of WBDFs when compared with similar micro fluids [47]. Saboori et. al. confirmed similar findings by reporting that the thermal conductivity of the DF increased by 29% with the introduction of CuO nanofluid [79]. Dejtaradon et. al. further advanced the study by identifying that CuO NPs below 1 wt% concentration could reduce the filtration losses by approximately 30% at 500 psi differential pressure and 100 °C [77]. Beg et. al. also suggested that CuO

This chapter is based on :

A. Bardhan , A. Singh, H. Nishanta, S. Sharma, A. K. Choubey, and S. Kumar, "Biogenic Copper Oxide Nanoparticles for Improved Lubricity and Filtration Control in Water-Based Drilling Mud." *Energy & Fuels*, 2024, 38(10):8564-8578. doi: https://doi.org/10.1021/acs.energyfuels.4c00635

can improve the HPHT filtration performance of WBDF formulation even after hot rolling [73]. CuO NPs are gaining prominence among various metal and metal oxide NPs as they exhibit a wide direct band gap of 1.2–2.1 eV with monoclinic structures. They have also emerged as promising candidates for environmental applications due to their low toxicity, high chemical and thermal stability, compatibility, easy synthesis route, variable morphology at the nanoscale, high specific surface area, and cost-effectiveness [168]. Recent advancements have witnessed the synthesis of well-defined CuO nanostructures, including nanospheres, nanoflowers, micromachines, nano leaves, nanorods, nanotubes, nanosheets, and nanorings, aimed at enhancing surface reactivity and nanoparticle properties [169].

Frictional resistance between the drill string and the wellbore wall in the presence of DF in dynamic conditions is another challenge that needs particular attention. The reduction in torque and drag force while drilling is significantly influenced by lubricity. In addition, lubricity plays a crucial role in cooling both the bit and downhole equipment. As a result, lubricity stands out as a key property of an ideal drilling fluid. The lubricating additives have high surface activity, enhance surface adhesion, and therefore impart lubricity [170]. NPs can contribute to this property by forming a continuous and thin lubricating film at the DF-drill string interface, substantially diminishing the frictional resistance between the pipe and the wall [104]. Although various nanomaterials have been explored for improving the lubrication in WBDFs, CuO NPs are yet to be investigated.

While CuO NPs can be synthesized using various chemical and physical methods, these techniques often entail high costs, long-term growth, multi-step procedures, and a lack of environmental friendliness. In response, researchers are actively pursuing the development of clean, non-toxic, and cost-effective methods that can eliminate the need for hazardous chemicals. Biosynthesis methods of CuO NPs have been explored using various plants, such as Punica granatum peel, Cedrus deodara, Ailanthus altissima leaf, Bougainvillea flower, Cucumis sativus (cucumber), and Brassica oleracea [171]. This method offers the benefit of facilitating large-scale production

of NPs while also ensuring a natural supply of phytochemicals that serve as both reducing and capping agents for nanoparticle stabilization [172]. Importantly, this approach eliminates the necessity for toxins and avoids extreme temperature and pressure conditions. The leaves of taro (*Colocasia esculenta*) contain a variety of sugars (such as sucrose, glucose, fructose, etc.), vitamins (including Niacin, Thiamin, Riboflavin, etc.), and minerals (such as calcium, iron, copper, potassium, etc.) [173]. These leaves exhibit rapid oxidation, enhancing their potential as effective reducing agents. Previous research has documented the successful synthesis of ZnO NPs and ZnO/Ag nanocomposites using *Colocasia esculenta* extract [173].

Leveraging the pronounced reducing and capping capabilities of *Colocasia esculenta*, the current study investigates the novel synthesis of CuO NPs using an eco-friendly *Colocasia esculenta* extract base, and its application in WBDF to enhance the lubrication, filtration, and rheological characteristics. The synthesized CuO NPs were characterized for size distribution, zeta potential, crystalline structure, morphological features, and functional group identification. The NPs were then added to the DF at various concentrations followed by thermal aging at 150 ℃ to identify the thermal degradation in the properties of the DFs. Three popular models for non-Newtonian fluids were used to fit the rheological data, namely Bingham Plastic, Power Law, and Herschel-Buckley models. The filtration experiments were performed at both low-pressure low-temperature (LPLT) and high-pressure high-temperature (HPHT) conditions. The lubricity characteristics imparted by the CuO NPs in WBDFs have been investigated for the first time. This comprehensive research investigation contributes to the ongoing efforts to develop advanced drilling fluid formulations that address environmental concerns and economic considerations. By exploring the potential of NPs as additives, the study aims to pave the way for more sustainable and efficient drilling operations in the oil and gas industry.The methodology carried out throughout the entire study is illustrated in Figure 6.1.

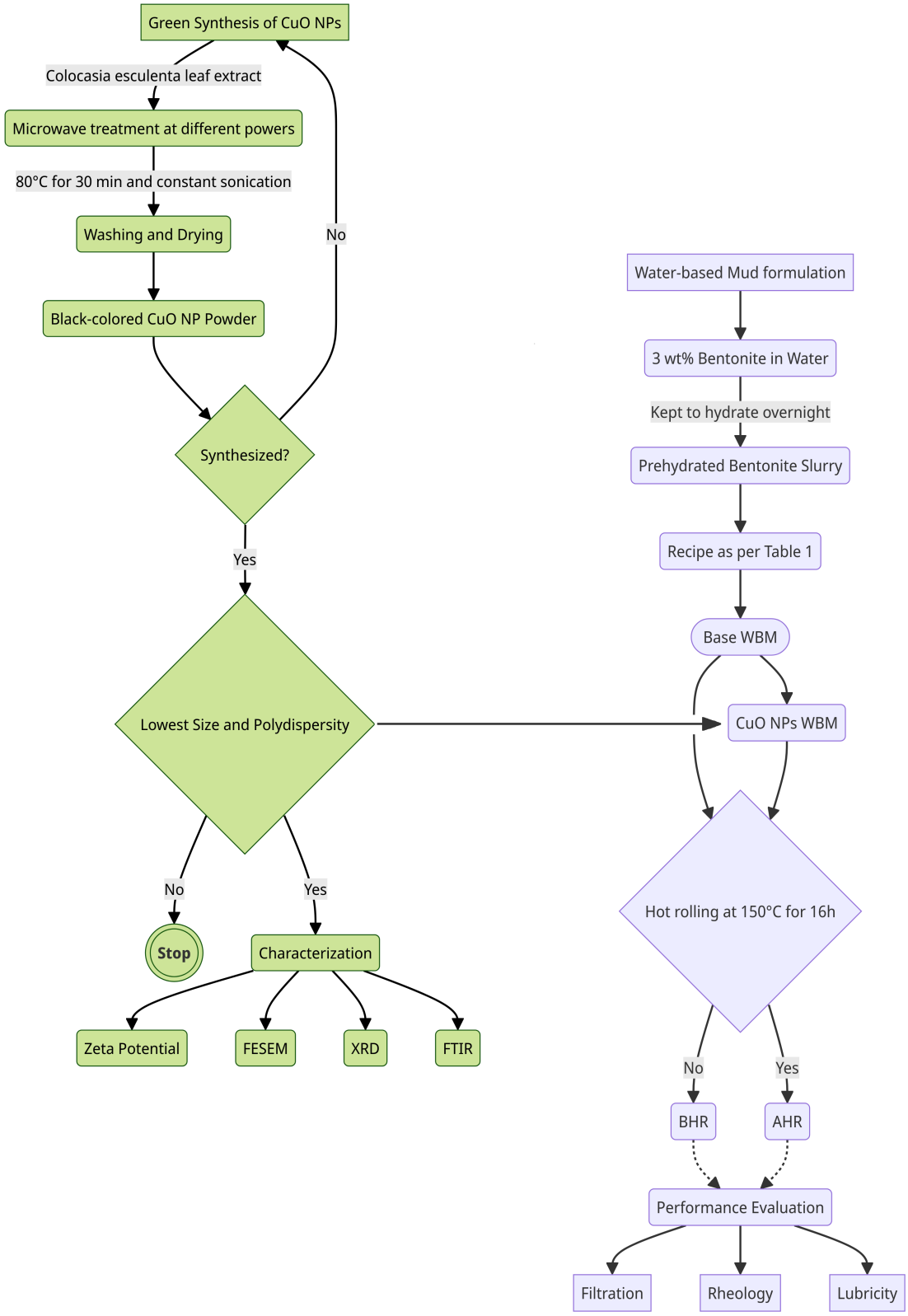

Figure 6.1: Flowchart of the NP synthesis, DF preparation, and performance evaluation.

6.1 Synthesis of Copper Oxide NPs

The synthesis scheme of the biogenic CuO NPs is presented in Figure 6.2. A solution of 6 wt% dry Colocasia esculenta leaf powder in deionized water was prepared at 50 °C. The solution was cooled and filtered twice to collect the extract. Separately, a 4 wt% aqueous solution of cupric nitrate was prepared, obtaining a royal blue-colored precursor solution. Now, seven sets each having 200 mL of the extract base and 60 mL of the precursor solution were mixed at 600 rpm on a magnetic stirrer for 1 h. The obtained solutions were treated with microwave at different power settings: 150, 200, 400, 600, 800, 900, and 1000 W. Simultaneously, constant sonication at 24 kHz for 30 min was ensured with a safety temperature set at 80 °C. The seven sets of the product obtained post-treatment were centrifuged, washed with methanol, vacuum filtered, and dried to receive black-colored CuO NP powder. Each of the set was synthesized thrice following the same procedure to test for the method's reproducibility. The seven sets of CuO NPs were screened for their hydrodynamic sizes when dispersed in deionized water (post ultrasonic treatment of 30 min) at 25 °C. Only the set having a low polydispersity and the smallest average hydrodynamic size was selected for further characterization and application.

Mechanism behind the Green Synthesis

Many metal oxide NPs have been synthesized with biomaterials, yet the precise mechanism remains unknown. The presence of compound groups in plants such as flavonoids, alkaloids, tannins, steroids/terpenoids, phenylpropanoids, and amides as metabolite compounds exhibit potential for serving as both reducing agents and capping/stabilizing agents in the synthesis of NPs [172]. A similar phenomenon occurred in the biogenic synthesis of the CuO NPs in this study. The reduction of the precursor began after adding the *Colocasia esculenta* extract, and the formation of CuO NPs is demonstrated by the changing of color from blue to black. The phytochemicals in the plant leaf extract aid in reducing, stabilizing, and capping the CuO NPs. The utilized *Colocasia esculenta* leaf extract possesses two key phytochemicals

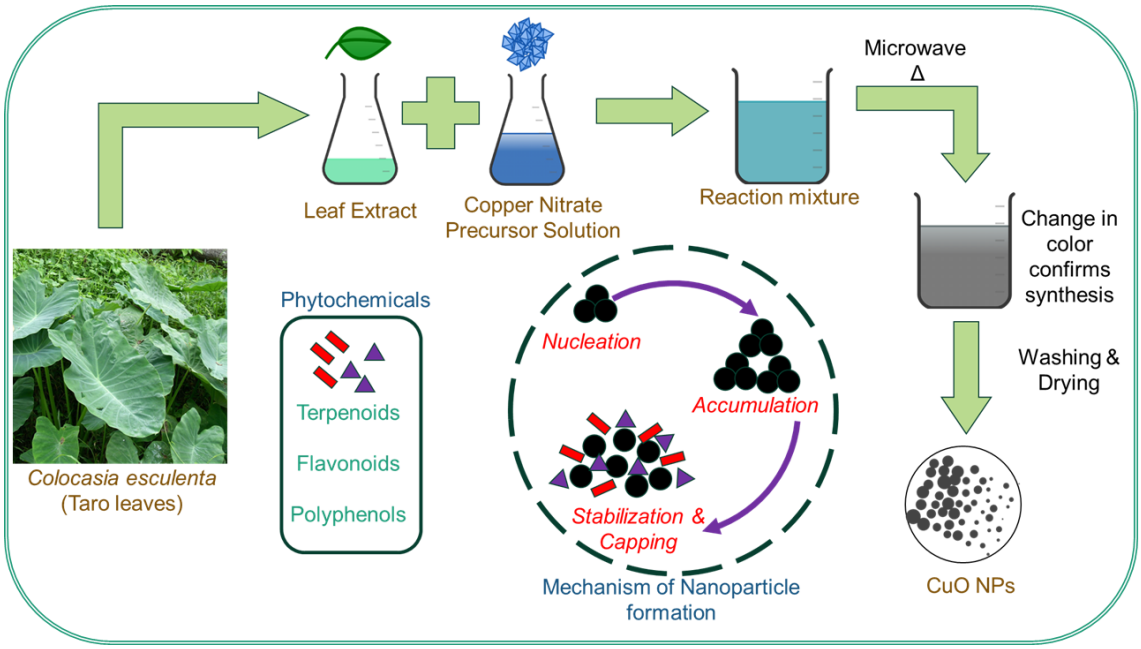

Figure 6.2: Schematic representation of the copper oxide nanoparticle synthesis with C. esculenta leaf extract.

which may have interacted with the copper nitrate precursor: Caffeic acid and Luteolin. The evolution of hydrogen atoms during interaction with flavonoids (in this case majorly luteolin) in the *Colocasia esculenta* involves tautomeric conversion of the enol into keto forms causing the reduction of the metal ions, while the oxidized polyphenolic groups (here caffeic acid) cap the NPs [174–176]. Additionally, caffeic acid has been reported in the literature as a strong bioreducing agent due to the delocalization of electrons from the propanoic groups [177]. The binding of the CuO due to electrostatic attractions results in stabilized NPs. It can be predicted that the role of bio-extracts in the synthesis of NPs opens a pathway for cost-effective and ecologically non-toxic manufacturing in the future.

6.2 Characterization and Screening of the Biogenic CuO NPs

The hydrodynamic diameter represents the effective size of the particle in the context of its motion through the dispersing fluid. This diameter takes into account the

size of the particle as well as its interaction with the surrounding solvent molecules, considering factors such as shape and surface properties. The Stokes-Einstein equation [94] considers the Brownian motion of the particles resulting in light scattering at different intensities over time and converts the measured diffusion coefficient into information about the size of particles in the sample.

Accurate knowledge of the size distribution of CuO NPs in drilling fluids is crucial for predicting their behavior during drilling processes. It aids in understanding how these NPs may affect the rheological properties, stability, and overall performance of the drilling fluid. The Polydispersity Index or PDI is a dimensionless value that quantifies the width of the particle size distribution. The PDI provides information about the uniformity or heterogeneity of the particle sizes in a sample. A PDI close to 0 indicates a monodisperse (narrow) size distribution, where the particles are relatively uniform in size. Conversely, a higher PDI suggests a broader (polydisperse) size distribution, indicating the presence of particles with a range of sizes [178, 179]. DLS gives a fairly accurate measurement of a monodisperse sample. However, as polydispersity increases, there is a subsequent rise in NP aggregation over time, resulting in larger hydrodynamic sizes. In polydisperse samples, DLS analysis may sometimes fail to track smaller-sized NPs because of higher light scattering by larger aggregates in the system leading to skewing of average size calculations. Consequently, achieving a smaller PDI, coupled with a lower average particle size, is crucial for selecting suitable NPs. Table 6.1 shows the average hydrodynamic size distribution for synthesis trials at different microwave irradiation power obtained by DLS.

As evident from Table 6.1, the set of biogenic CuO NPs synthesized at 800 W microwave power (trial no. 5) has the lowest average size of 115.4 nm with a fairly good PDI of 0.263. However, the lowest PDI was achieved at 400 W power, but the average size was larger. The utilization of microwave synthesis methodology has been leveraged in nanoparticle synthesis due to its amalgamation of rapidity and uniform thermal distribution across precursor materials. Microwave irradia-

Table 6.1: Average size and corresponding polydispersity index for trials at different microwave irradiation power.

Trial	Microwave Power (W)	Average Size (nm)	PDI
1	150	183.9	0.530
2	200	174.9	0.285
3	400	163.4	0.216
4	600	157.2	0.259
5	800	115.4	0.263
6	9000	157.2	0.259
7	1000	296.0	0.358

tion possesses a penetration attribute, facilitating homogeneous heating of the reaction solution. This engenders consistent nucleation and expeditious crystal growth, thereby fostering the development of crystallites characterized by a narrow size distribution [180,181]. Therefore, CuO NPs synthesized in trial no. 5 were selected for further characterization and utilized to formulate WBDF samples. The repeatability of the size was checked at 800 W microwave irradiation power and found to be approximately ±15 nm. The DLS distribution curve of this CuO NP is shown in Figure 6.3.

Zeta potential provides information about the stability of colloidal dispersions since particles with higher absolute Zeta potential values typically exhibit greater electrostatic repulsion and are less prone to aggregation [178, 182]. The zeta potential of the biogenic CuO NPs in a neutral pH aqueous medium was -4.46 mV. However, the zeta potential drastically changed to -33.4 mV when the pH was adjusted to 9. NPs with higher electrophoretic mobility and more negative or positive Zeta potential values generally experience greater repulsion or attraction, affecting their dispersion, stability, and behavior in a given medium [183].In accordance with Derjaguin–Landau–Verwey–Overbeek (DLVO) theory, the stability between two particles is assessed as the combination of the electrical double-layer repulsion energy and the van der Waals attraction energy. The aggregation and stability of particle suspensions are governed predominantly by the repulsive interaction energy. Consequently, an energy barrier arises from the repulsive forces, hindering particles from

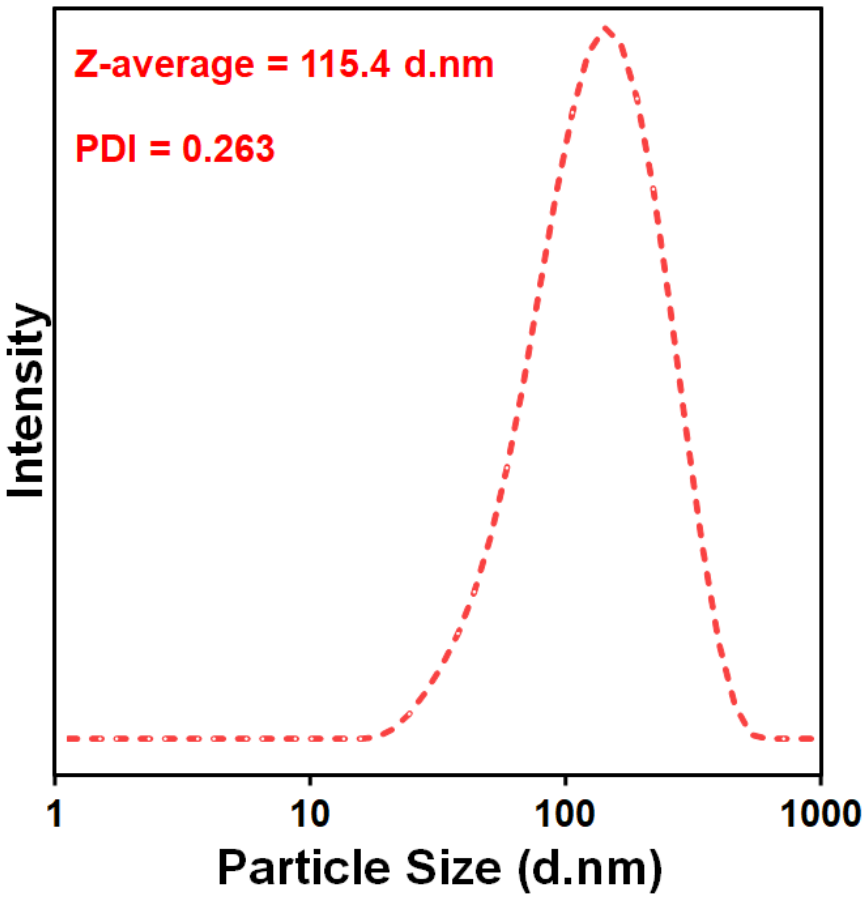

Figure 6.3: The size distribution curve of the biogenic CuO NPs.

approaching and aggregating, thereby ensuring suspension stability. Conversely, should the energy barrier be surpassed, attractive forces draw particles towards each other, promoting aggregation and leading to suspension instability [184].Hence, it can be inferred that the electrophoretic mobility increased upon the introduction of alkalizing ions in the system rendering stability to the dispersed CuO NPs. NPs in a solution are prevented from aggregating through mechanisms such as electrostatic repulsion, steric hindrance, or a combination of both [96].Electrostatic repulsion is a result of the surface charge on the NPs. Analyzing the surface charge of colloidal particles poses challenges, and the commonly employed method is measuring the zeta potential, representing the charge at the surface of the electrical double layer. Typically, NPs remain stable in a solution when the zeta potential values fall within a specific range, considering factors like particle size, concentration, and others. NPs are usually considered stable in the range of greater than +25 mV to less than -25

mV [156].

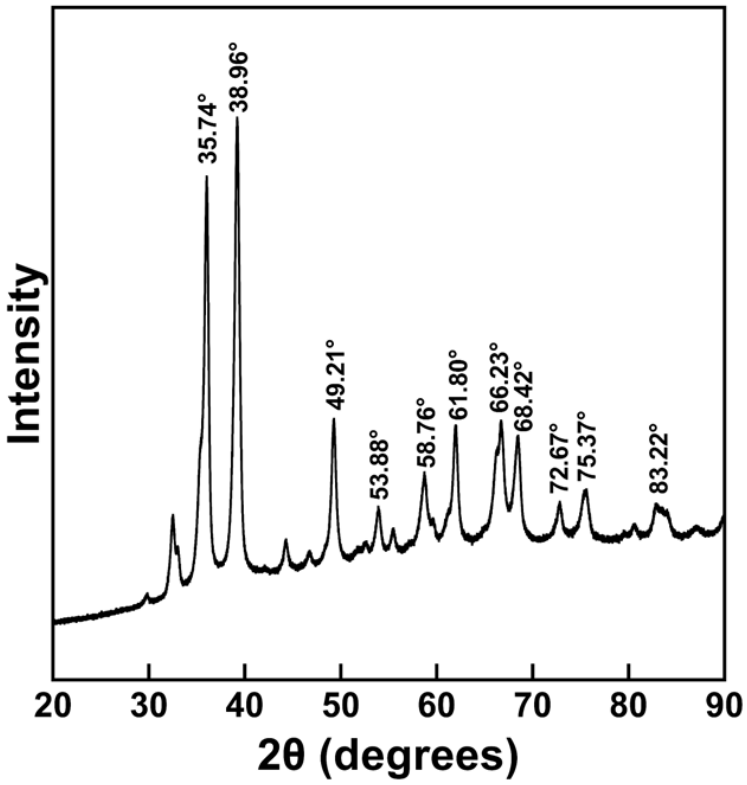

Figure 6.4: The X-ray diffractogram of the synthesized CuO NPs.

Figure 6.4 depicts the diffraction pattern obtained for the biogenic CuO NPs. This pattern revealed that the NPs are monoclinic crystalline and correspond to JCPDS Card no. 01-001-1117 [174]. The structure was also identified through the two most intense peaks at 35.74° and 38.96°. The crystallite size of the biogenic CuO NPs was determined employing the widely popular Scherrer Equation [97]. The calculated parameters are given in Table 6.2, and the resulting average crystallite size was approximately 95.04 nm.

Field Emission Scanning Electron Microscopy (FESEM) is usually performed to visualize the microstructural features of any material. The FESEM analysis of the synthesized CuO NPs revealed majorly disc-like morphology with a small number of filamentous outgrowths as illustrated in Figure 6.5. While the lateral dimensions of the discs fall beyond 100 nm, their thicknesses are confined to the nano-scale. Similarly, the filaments exhibit dimensions ranging from 1 to 100 nm. An intriguing

Table 6.2: The crystallographic phases and the parameters for the size determination of the biogenic CuO NPs.

2θ	Planes (h k l)	$\theta(deg)$	FWHM or $\beta(rad)$	$1/\beta$	$\cos\theta$	$\lambda(nm)$	K	D (nm)
35.74	(-1 1 1)	17.87	0.014	0.951	71.677	0.15406	0.9	104.421
38.96	(1 1 1)	19.48	0.012	0.942	83.316	0.15406	0.9	122.535
49.21	(-2 0 2)	24.605	0.009	0.909	102.36	0.15406	0.9	156.105
53.88	(2 0 2)	26.94	0.841	0.891	1.188	0.15406	0.9	1.848
58.76	(0 0 2)	29.38	0.018	0.871	55.786	0.15406	0.9	88.7673
61.8	(-1 1 3)	30.9	0.013	0.858	74.692	0.15406	0.9	120.694
66.23	(0 2 2)	33.115	0.023	0.837	43.539	0.15406	0.9	72.075
68.42	(2 2 0)	34.21	0.014	0.826	69.181	0.15406	0.9	115.992
72.67	(3 1 1)	36.335	0.012	0.805	82.620	0.15406	0.9	142.206
75.37	(0 0 4)	37.685	0.014	0.791	67.635	0.15406	0.9	118.499
83.22	(-3 1 3)	41.61	0.798	0.747	1.252	0.15406	0.9	2.321

observation is the minimal occurrence of agglomeration or clusters, a characteristic that proves advantageous, particularly when considering dispersion in drilling fluids. Furthermore, the unique structural attributes of these discs open the possibility of them arranging on a surface, coating it entirely. This arrangement has the potential to foster the creation of a protective film around the surface, thereby mitigating wear and tear. Such a protective film could play a crucial role in enhancing the durability of the underlying surface and improving the lubricity of the entire system.

FTIR was conducted to analyze the role of underlying bio-phytochemicals or functional groups responsible for initiating the formation of CuO NPs. As shown in Figure 6.6, the peaks observed in this spectrum act as fingerprints, aiding in the identification of surface functional groups or bio-phytochemicals orchestrating the processes of bio-reduction and stabilization of CuO NPs. The *Colocasia esculenta* leaf extract, with its rich repertoire of functional groups, emerges as a remarkable agent, not only guiding the reduction of copper ions but also playing a pivotal role in maintaining the stability of the resulting NPs. The discerned peaks at 510 and 590 cm^{-1} are indicative of the distinctive stretching vibrations characteristic of the Cu-O bonds in CuO. Notably, the sharp peak observed at 510 cm^{-1} further solidifies the evidence of Cu-O bond formation in the CuO NPs. Additionally, the absence of any other IR active mode within the range of 610 to 660 cm^{-1} unequivocally dismisses the presence of another phase, specifically Cu_2O [185]. A broad absorption peak at approximately 3424 cm^{-1} is attributed to the presence of adsorbed water

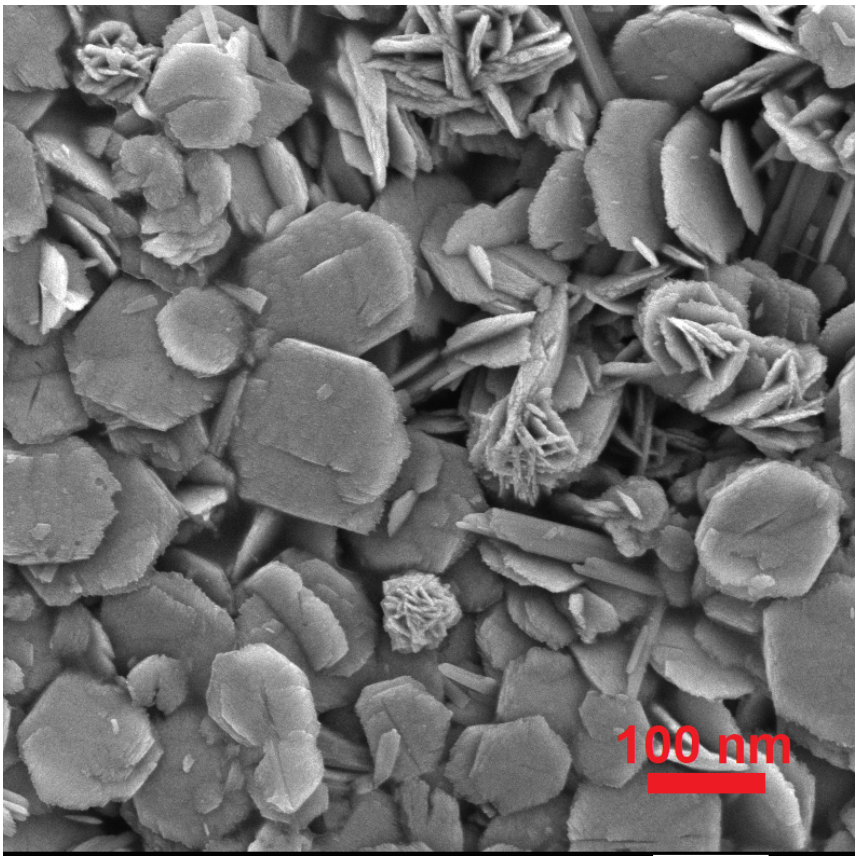

Figure 6.5: FESEM image of the biogenic CuO nanostructures (synthesized with 800W Microwave power).

molecules. This phenomenon is common in nanocrystalline materials due to their high surface-to-volume ratio, leading them to absorb moisture. Consequently, the FTIR analysis reaffirms the presence of pure-phase CuO with a monoclinic structure. Dual functionality is exhibited by biological functional groups within the taro leaf extract – they act both as reducers and stabilizers in the synthesis of pure CuO NPs. These functional groups, encompassing aromatic, phenolic, amino groups, and hydroxyl, contribute significantly to the reduction of copper ions, facilitating the transformation into copper oxide NPs. This reduction is made possible primarily through the synergistic effects of hydroxyl and carbonyl linkages present in the plant leaf extract.

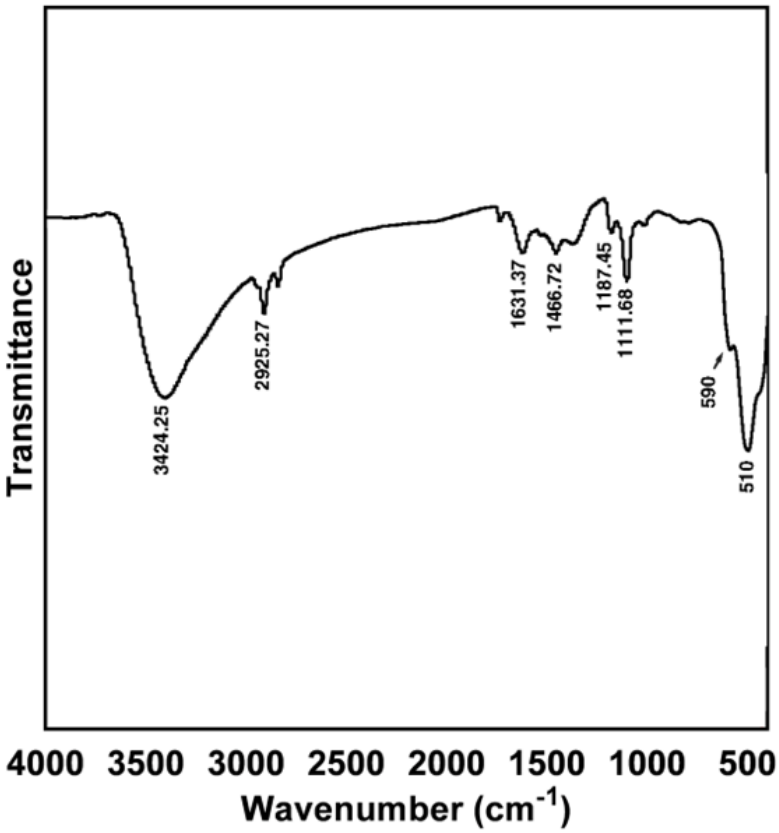

Figure 6.6: Infrared Spectra of the biogenic CuO NPs.

6.3 Performance of Drilling Fluids with the biogenic CuO NPs

The composition of the base and the NP-infused DFs to be discussed hereinafter is shown in Table 6.3.

Table 6.3: Composition of the WBDFs with Biogenic CuO NPs.

Sequence	Constituents	Concentration (wt%)
1	Deionized water	-
2	Bentonite	3
3	KOH	0.07
4	Xanthan Gum	0.25
5	PAC-R	0.5
6	KCl	3
7	1-Octanol	2-3 drops
8	Biogenic CuO NPs	0-1.0

The incorporation of CuO NPs can bring potential enhancements to the performance of WBDFs. CuO NPs, when properly dispersed in DFs, can influence the

rheological properties of the fluid. This includes alterations in the viscosity and yield point. The controlled addition of CuO NPs may contribute to improved fluid stability and flow characteristics, enhancing the fluid's ability to carry cuttings to the surface. The NPs contribute to reducing friction between the fluid and the drill string, facilitating the efficient removal of cuttings from the wellbore. When introduced into drilling fluids, CuO NPs can enhance the fluid's thermal stability. This is particularly advantageous in high-temperature drilling environments, where maintaining fluid integrity and preventing thermal degradation are critical for operational success. Moreover, CuO NPs may assist in improving filtration control, influencing the fluid's filter cake formation on the wellbore walls. This can lead to reduced fluid loss, enhanced wellbore stability, and improved overall drilling fluid performance. The controlled release of copper ions from the NPs can have biocidal effects as well, reducing bio-degradation of the additives. Lastly, the use of biogenic CuO NPs in drilling fluids may offer environmentally friendly alternatives for certain chemical additives in drilling fluid formulations. In addition, the morphology of the biogenic CuO NPs may positively influence the performance of the DF. The plate-shaped NPs may offer unique advantages due to their large surface area-to-volume ratio and anisotropic properties [175]. They can enhance lubrication by forming a boundary layer between the drill bit and the borehole wall, reducing friction and minimizing torque and drag during drilling operations. Their flat geometry allows them to slide more easily along surfaces, thereby improving fluid rheology and reducing viscosity fluctuations. Furthermore, nanoplates can act as reinforcement agents, enhancing the structural integrity of the drilling fluid matrix and preventing sagging or settling of solids [186].This helps maintain wellbore stability and prevents issues like differential sticking. Additionally, nanoplates can serve as effective additives for controlling fluid loss and improving filtration control. Their ability to form a network structure within the fluid can help seal porous formations and prevent fluid invasion, reducing formation damage and improving well productivity [187].

Therefore, three primary indicators, namely rheological, filtration, and lubricity

performance of the base and CuO NPs infused WBDFs are investigated henceforth.

6.3.1 Rheological Performance

The AV values at different concentrations of the biogenic CuO NPs in the WBDF are shown in Figure 6.7 (a). Interestingly, there was only a slight increase of approximately 3 to 4% in the AV for both the fresh and aged WBDF samples across the entire range from 0 to 1 wt% CuO NP concentrations. The apparent viscosity of drilling fluids can remain constant even when NPs are added due to the unique properties and effects of NPs on the fluid [168, 188]. NPs can effectively disperse within the WBDF, leading to a more uniform distribution of the particles which may contribute to maintaining the AV of the fluid.

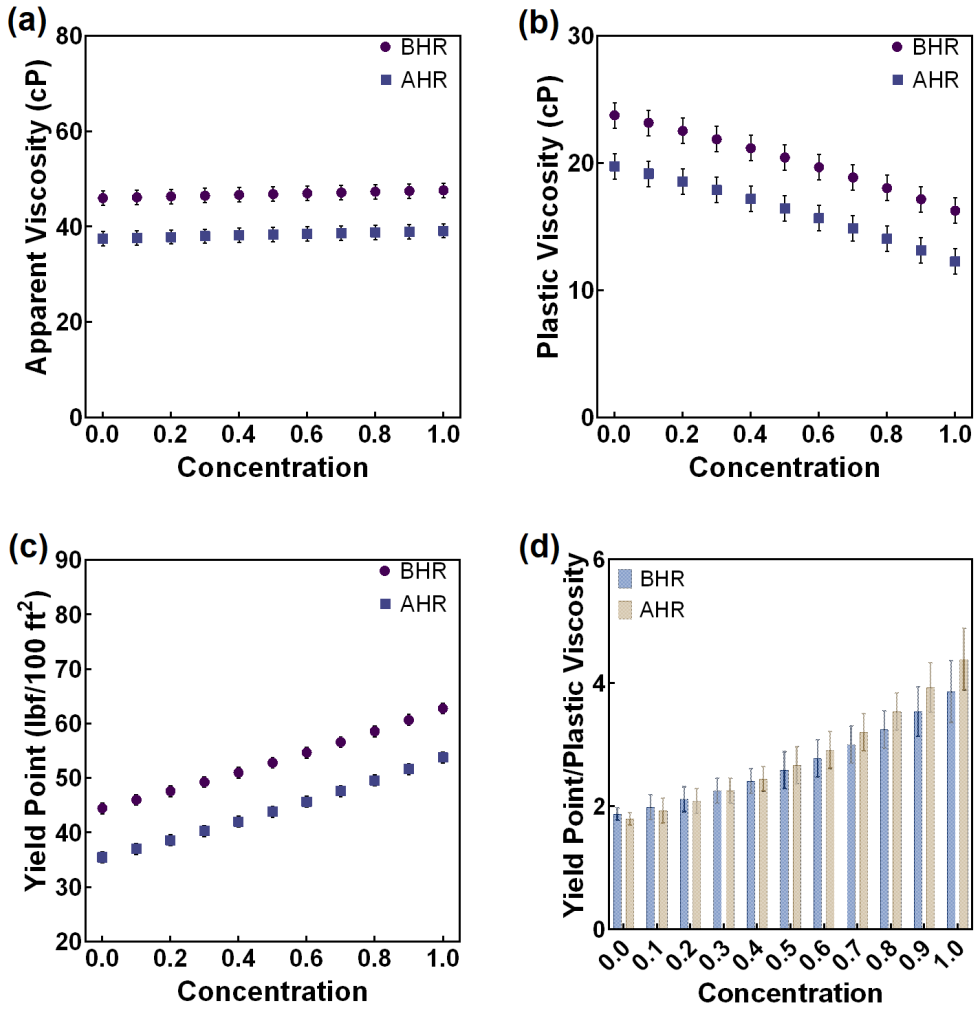

Figure 6.7: Bingham Plastic rheological parameters for the WBDF formulations with increasing concentrations of the biogenic CuO NPs.

As depicted in Figure 6.7 (b), the PV values for both the BHR and AHR WBDF samples gradually reduced with increasing concentrations of the biogenic CuO NPs in the system. When compared to the base WBDFs, the ultimate decrement for the BHR samples was 31.5% whereas for AHR samples it was 38%. NPs exhibit a substantial surface area-to-volume ratio, resulting in heightened interactions between these NPs and both the surrounding WBDF and the matrix. This increased surface area provides sites for potential bonding with functional groups, which can profoundly impact chain entanglement and, consequently, bestow a diverse array of properties upon the matrix. Consequently, the NPs may establish direct or intermediary chemical linkages with the base fluid, thereby enhancing the PV of the WBDFs [19, 72] . It is worth noting, however, that the presence of CuO NPs induces a repulsive force with water molecules. This phenomenon led to a reduction in the PV as NP concentration escalated, primarily due to the intensified repulsive forces [189, 190]. In addition, Dejtaradon et. al. and Liu et. al. supplemented a similar observation of decreasing PV with an explanation of the reduced mechanical friction due to the presence of NPs in the drilling fluid system [77, 191]. This effect is particularly crucial in the context of drilling fluids, where it plays a vital role in preserving fluid viscosity under conditions of elevated pressure and temperature.

Figure 6.7 (c) shows the YP variation at different concentrations of the biogenic CuO NPs at BHR and AHR conditions. In both cases, the trend of YP was incremental with the concentration of CuO NPs in the WBDF. From 0 to 1 wt% CuO NP concentration, the YP increased by approximately 41% for the BHR samples, and by 52% for the AHR samples. This is in contrast to the flat line-like viscosity profiles displayed by the samples. The effect of thermal degradation was prominent in the base WBDF where the YP was reduced by 20%. However, with the inclusion of CuO NPs in the WBDF, the degradation in the YP was nearly 16% at 1 wt% concentration. The results indicate that drilling fluid formulations incorporating the biogenic CuO NPs exhibit improved thermal stability in terms of yield point variations. This enhanced stability is likely due to the small size of the particles and

their significant effective surface area at a specific concentration [64].

Evident from Figure 6.7 (d), the YP/PV ratio of the fresh and aged samples observed a steady increase with the increasing concentration of the biogenic CuO NPs. From 0 to 1 wt% CuO NP concentration, the YP/PV increased by 2 times for the BHR samples, and by approximately 2.5 times for the AHR samples. This tremendous increase may be attributed to the increasing YP and decreasing PV in the picture. This may prove conducive for the drilling fluid performance if the concentration of CuO NPs is optimized with the existing WBDF formulation as per the requirement of the operation. However, no definitive trend could be established when the thermal degradation was compared for the CuO NP-infused WBDFs and the base WBDF.

Rheological Model Fitting

The rheological models were fitted on the obtained shear stress vs strain data as given in Figure 6.8. In the context of drilling fluid rheological models or any statistical modeling related to fluid behavior, R^2 could be used to assess how well the chosen model captures and explains the observed variability in the rheological properties of the fluid. It is a statistical measure that represents the proportion of the variance in the dependent variable that is explained by the independent variables in a regression model. It is also known as the *coefficient of determination*. The values of this coefficient range from 0 to 1. A value of 0 indicates that the independent variables do not explain any of the variability in the dependent variable, while a value of 1 suggests that the independent variables explain all the variability. Hence, a higher R^2 would suggest a better fit between the model and the actual data, indicating that the chosen model is effective in explaining the variation in the rheological behavior of the drilling fluid under specific conditions. The coefficient of determination for each model across all the concentrations of the biogenic CuO NPs in WBDF can be found summarized in Table 6.4:

Evident from the model fitting, the Bingham plastic model exhibited limitations

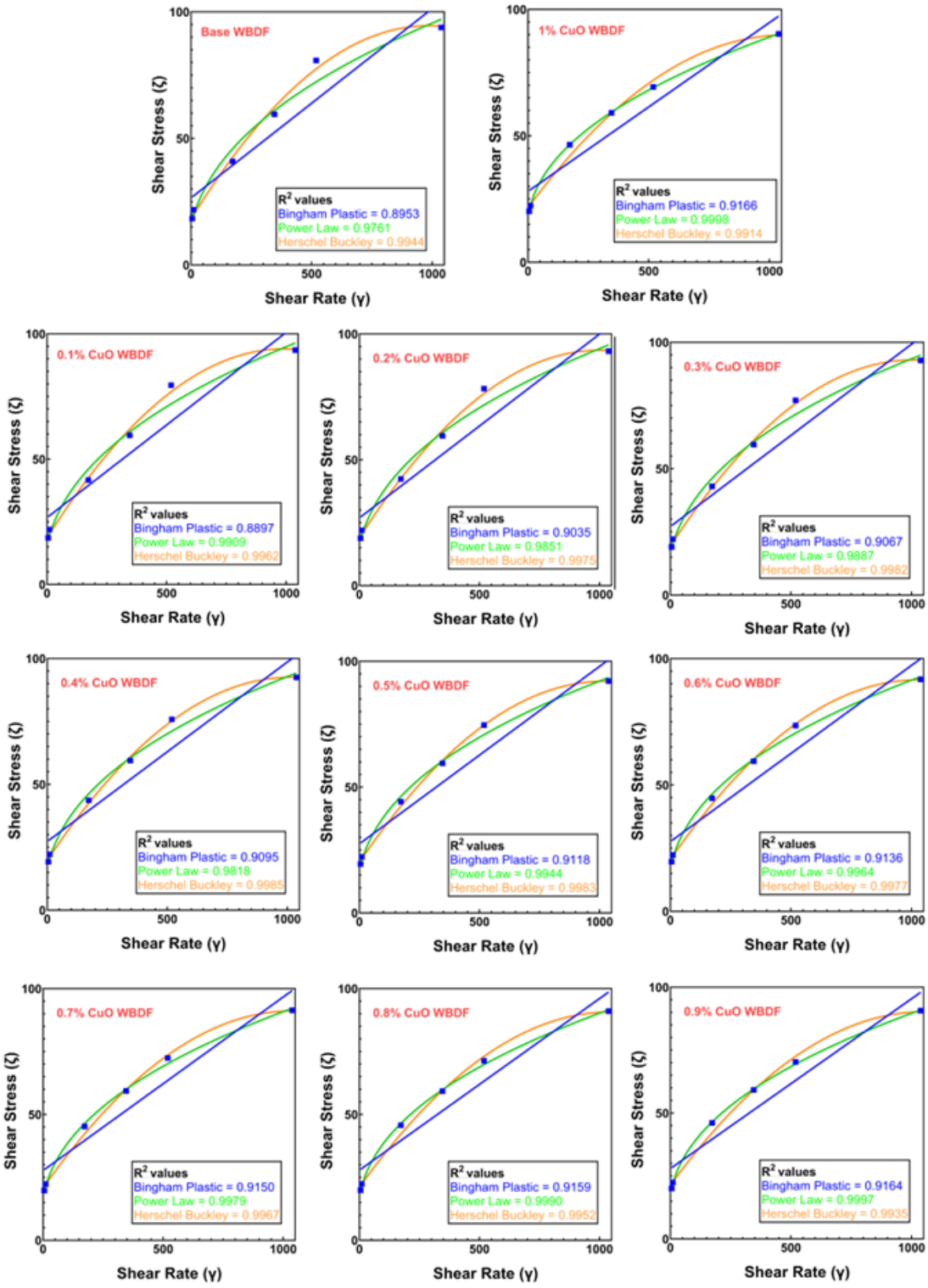

Figure 6.8: The shear stress vs rate plots for WBDF formulations at different biogenic CuO NP concentrations, fitted with Bingham plastic (blue), Power law (green) and Herschel-Buckley (orange) rheological models.

Table 6.4: Fitting evaluation of different rheological models for the WBDF formulations at different biogenic CuO NP concentrations.

Models	0	0.1	0.2	0.3	0.4	0.5	0.6	0.7	0.8	0.9	1.0
Bingham Plastic	0.8953	0.8897	0.9035	0.9067	0.9095	0.9118	0.9136	0.9150	0.9159	0.9164	0.9166
Power Law	0.9761	0.9906	0.9851	0.9887	0.9818	0.9944	0.9964	0.9979	0.9990	0.9997	0.9998
Herschel-Buckley	0.9944	0.9962	0.9975	0.9982	0.9985	0.9983	0.9977	0.99967	0.9952	0.9935	0.9914

in adequately capturing the rheological characteristics of the WBDF formulations, as indicated by R^2 values less than 0.92. In this instance, the lack of goodness of fit suggests that the Bingham plastic model's assumptions and parameters may not sufficiently align with the complex rheological properties exhibited by the WBDF formulations. As a result, relying on this model for predictive purposes may introduce inconsistencies and inaccuracies in anticipating the performance of the drilling fluid under different operational conditions. Conversely, the Herschel-Buckley model demonstrated promising results with R^2 values exceeding 0.99. The higher value of R^2 indicates a robust fit of the Herschel-Buckley model to the observed rheological data of the WBDF formulations. This suggests that the Herschel-Buckley model provides a more accurate representation of the fluid's rheological behavior, offering a reliable framework for predicting how the WBDF with the biogenic CuO NPs will respond to various stress and shear rate conditions. Therefore, the observed discrepancy in values underscores the importance of selecting an appropriate rheological model for accurately characterizing drilling fluid behavior.

6.3.2 Filtration Performance

The filtration performance at both LPLT and HPHT conditions for the fresh DF/BHR samples is shown in Figure 6.9 (a). Notably, the HPHT filtration loss (FL) was reduced by approximately 48% at 1.0 wt% CuO concentration as compared to the base WBDF, which was 29 ± 1 mL initially. On the other hand, the API/LPLT FL also went down from 16 ± 1 to 9 ± 1 mL which accounts for approximately 43% reduction when the concentration of the biogenic CuO NPs increased from 0 to 1 wt%. However, the trend of FL reduction in both cases should also be observed. In HPHT, the decremental trend of the FL was smoother as compared to LPLT where

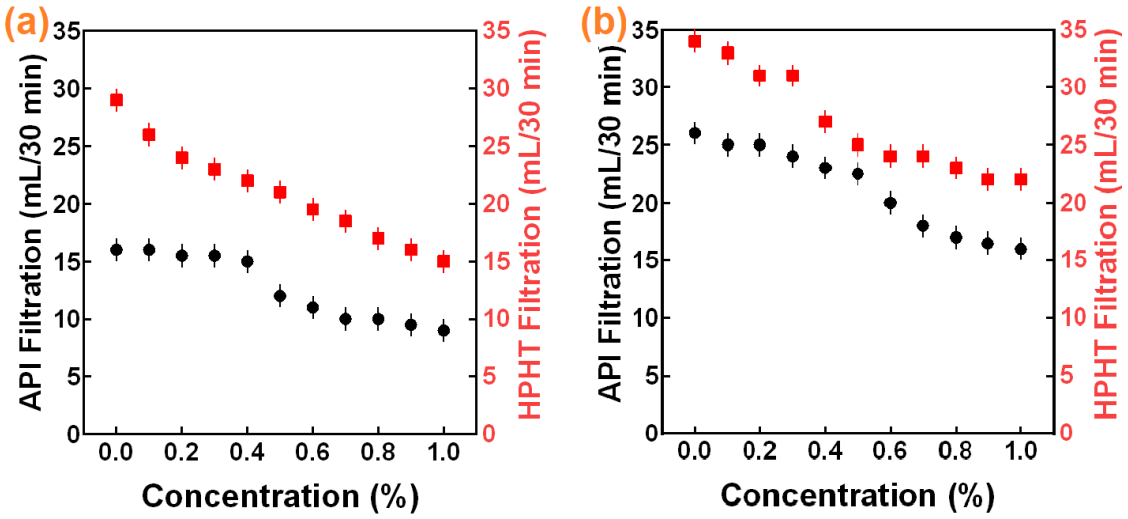

Figure 6.9: LPLT/API and HPHT Filtration performance of the WBDF samples at (a) BHR, and (b) AHR conditions.

the first noticeable change occurred at 0.5 wt% concentration.

The LPLT and HPHT FL for the hot rolled samples (AHR) are depicted in Figure 6.9 (b) and notably showed lesser degradation. The FL in HPHT was reduced by approximately 35% when the WBDF with 0.9 wt% CuO NPs was compared with the base WBDF. The HPHT FL remained unchanged even at 1 wt% concentration. Similarly, the LPLT FL also saw an ultimate reduction of 38.5% when the concentration of the biogenic CuO NPs increased from 0 to 1 wt%. Subsequently, the effect of thermal degradation should also be taken into account. The FL in the base WBDF increased from 16 $\pm$ 1 to 26 $\pm$ 1 mL at the LPLT condition, whereas in the HPHT condition, the increment was from 29 $\pm$ 1 to 34 $\pm$ 1 mL. This degradation in the FL reduction performance was significantly reduced by 44% and 32% at LPLT and HPHT conditions respectively, rendering CuO NPs effective as a thermally stable additive in WBDF formulations.

The reduction of filtration loss in water-based drilling fluids through the incorporation of copper oxide (CuO) NPs involves multiple mechanisms that collectively contribute to improving the fluid's filtration control. CuO NPs possess the ability to accumulate and form a thin, impermeable NP cake with bentonite on the wellbore wall during filtration. This cake acts as a barrier, limiting the passage of fluid and solids into the formation. Being of nanoscale dimensions, the NPs can also

bridge and plug the pore spaces in the wellbore wall. This bridging effect hinders the movement of larger solid particles, preventing them from entering the formation and reducing the overall filtration rate. Following Darcy's law, the presence of NPs in the external filter cake can instigate a decrease in cake permeability, thereby impacting fluid filtration or water loss. This effect is ascribed to the infiltration of NPs into the nanopores within the mud cake [135]. In the context of practical drilling operations, where diverse forces come into play on particles at the cake surface, a reduced filtration rate results in a diminished normal drag force acting on these surface particles. This, in turn, facilitates the formation of a thinner cake due to the tangential force applied to the surface particles of the cake [192].

6.3.3 Lubricity Performance

Lubricity is the property of a substance that aids in reducing friction, while the coefficient of friction quantifies the level of friction between two surfaces. Effective lubrication results in a lower coefficient of friction (CoF), promoting smoother movement and minimizing wear between interacting surfaces.

As shown in Figure 6.10, the fresh samples (BHR) as compared to the aged samples (AHR) showed overall higher CoF values throughout the varying concentrations of the biogenic CuO NPs. The base BHR WBDF had a CoF value of 0.30 ± 0.03. The CoF started decreasing when 0.2 wt% CuO NPs were added to the WBDF system. The ultimate decrease was approximately 27% at 1 wt% CuO concentration as compared to the base. In the case of the AHR samples, the CoF of the base WBDF was 0.33 ± 0.03. The AHR samples also showed a decremental trend reducing the CoF by approximately 27% at 0.8 wt% CuO NP concentration after which the CoF remained the same till 1 wt% concentration. In order to understand, the effect of thermal aging in the degradation of the lubricity properties, the BHR and AHR values of the same composition require to be compared. In the base formulation of WBDF, the CoF increased from 0.30 to 0.33, accounting for approximately

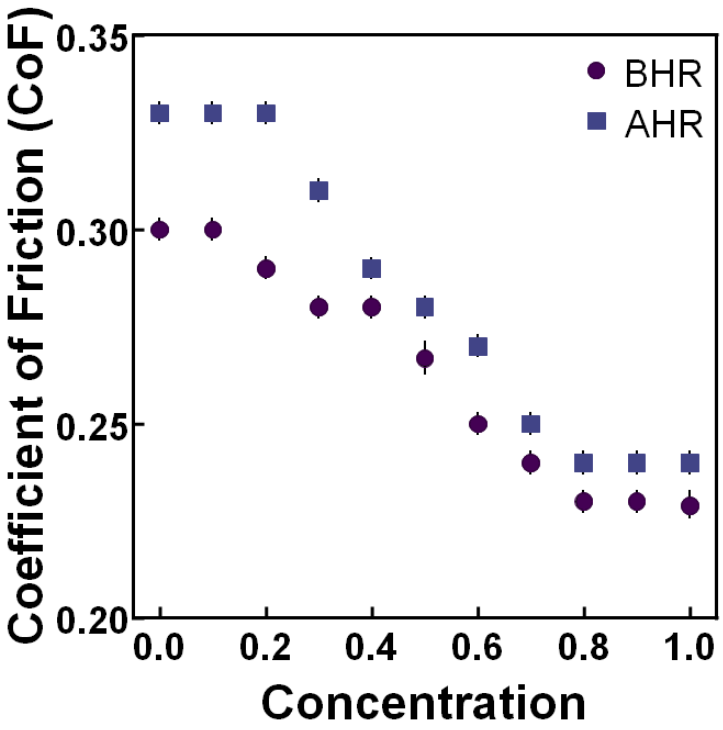

Figure 6.10: CoF variation in the WBDF samples with concentrations of CuO NPs.

10% increase. However, this degradation reduced when CuO NPs were infused in the WBDF. This is evident from the fact that at 0.8 wt% concentration of the CuO NPs in WBDF, the degradation reduced to only 4%. A low CoF value indicates that the force required for sliding against the surface is less. The coefficient of friction is a crucial parameter influencing the efficiency and performance of drilling fluids in wellbore operations. NPs, owing to their unique properties, play a significant role in mitigating frictional forces and improving the overall performance of drilling fluids [193]. NPs of graphene, titanium dioxide, silicon dioxide, or other solid lubricants, are known for their exceptional lubricating properties [104, 128, 170, 194]. When dispersed in drilling fluids, these NPs act as lubricating agents, reducing the friction between the drill string and the wellbore surfaces. This leads to smoother drilling operations and a decrease in the coefficient of friction. In addition, NPs can modify the surface characteristics of drilling components. By forming a protective layer on metal surfaces, NPs mitigate direct metal-to-metal contact, reducing friction and wear. This protective layer contributes to enhanced tool longevity and

improved drilling efficiency. Certain NPs, like CuO exhibit excellent thermal conductivity. In drilling operations, where elevated temperatures are common, the addition of these NPs enhances the fluid's ability to dissipate heat [47].This thermal conductivity helps minimize frictional heating, maintaining fluid viscosity, and reducing the coefficient of friction.

The standalone performance of the biogenic CuO NPs in improving the lubricity of WBDF is noteworthy and can be attributed to any of the four distinct mechanisms as illustrated in Figure 6.11: (a) NPs can form a boundary layer on the surfaces in contact, creating a protective film that prevents direct metal-to-metal contact [195].This boundary lubrication involves the adsorption of NPs at the surface, reducing friction and wear. (b) NPs can act like miniature ball bearings generating a rolling effect. When dispersed in a lubricant, these NPs can roll between surfaces, reducing friction by creating a rolling mechanism. (c) NPs can actively work to fill in surface irregularities, smooth out rough areas, and provide a mending effect. (d) NPs can also sometimes smooth and polish the surfaces in contact.

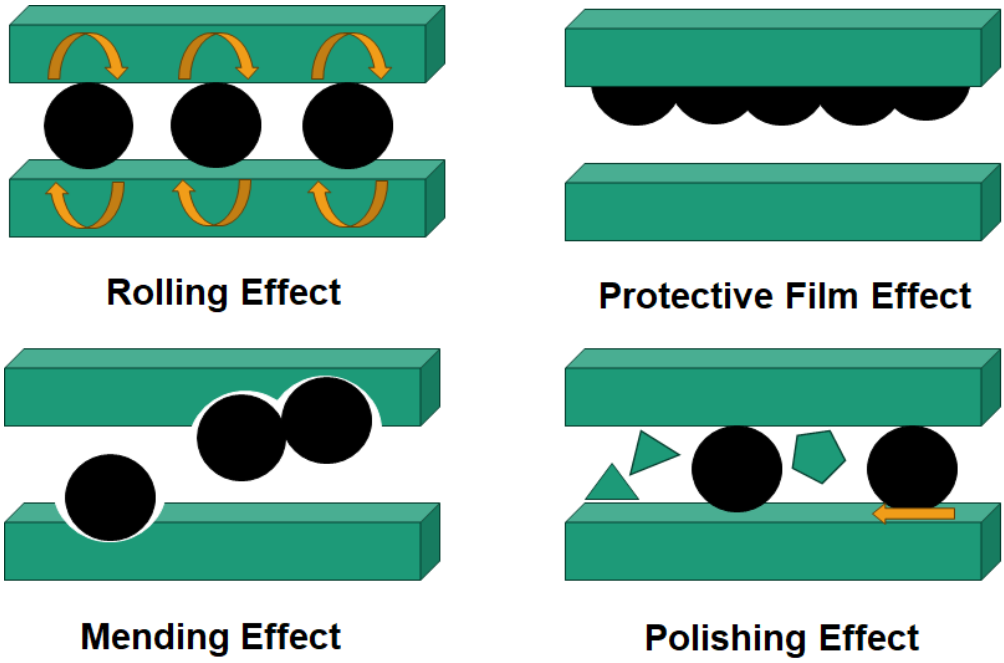

Figure 6.11: CoF variation in the WBDF samples with concentrations of CuO NPs.

This is particularly beneficial in cases where surface asperities and roughness contribute to increased friction. The presence of NPs helps fill in surface irregular-

ities, resulting in a smoother interface. It can be inferred from the microstructure visualized through FE-SEM and the decreasing trend of CoF values with increasing concentrations of CuO NPs that the dominant mechanism of lubrication should be the formation of a protective film on the surface.

6.4 Conclusion

This study successfully demonstrated the green synthesis of copper oxide NPs using Colocasia esculenta leaf extract as a bifunctional reducing and capping agent with the aid of microwave treatment and continuous sonication. The analytical characterization has confirmed the formation of well-defined crystalline disc-like nanostructures. Integration of these biogenic CuO NPs into WBDF formulations has led to significant enhancements in lubricity and filtration performance, alongside a reduction in thermally induced degradation. Notably, a 27% increase in lubricity has been observed, indicating improved friction reduction and smoother drilling operations facilitated by the infusion of biogenic copper oxide NPs, with the optimal concentration identified at 0.5 wt%. This enhancement suggests potential efficiency gains and reduced wear on drilling equipment, thereby enhancing operational effectiveness. Moreover, the substantial 48% enhancement in filtration performance highlights promising implications for maintaining wellbore stability and minimizing formation damage during drilling, underscoring the positive impact of NPs on filtration efficiency in practical drilling applications. The rheological analysis, utilizing three established models, has identified the Herschel-Bulkley model as the superior fit for the WBDF formulations containing biogenic CuO NPs. While the potential benefits of incorporating CuO NPs into drilling fluids are promising, it is crucial to meticulously consider factors such as nanoparticle shape, size, concentration, and overall impact on fluid properties.

Chapter 7

Zinc Oxide Nanostructures

Among numerous nanostructured materials, zinc oxide (ZnO) has emerged as a promising candidate owing to its unique properties, such as high thermal conductivity, chemical stability, and low toxicity [196]. Several researchers have investigated the effect of ZnO NPs on the rheological properties of water-based drilling fluids. For instance, a study by Dejtaradon et al. revealed that the addition of ZnO NPs to bentonite-based drilling fluids enhanced their rheological properties [77]. These improvements were attributed to the strong interactions between the NPs and the drilling fluid components, leading to better cuttings transport and hole cleaning. In addition to rheological properties, ZnO nanostructures have also demonstrated promising results in improving the filtration capabilities of water-based drilling fluids [47, 167, 197]. Dejtaradon et al. also reported that the incorporation of ZnO NPs into water-based drilling fluids significantly reduced fluid loss and enhanced the formation of a thin, impermeable filter cake, which is crucial for maintaining wellbore stability [198]. In the same line, Bayat and Shams identified similar results when tested at different temperatures [48]. Furthermore, the lubrication properties of water-based drilling fluids have been shown to improve with the addition of

---

This chapter is based on:

A. Bardhan, S. Sharma, S. Kumar, "Influence of Morphology and Dispersion Stability on the Properties of High-Performance Water-based Drilling Fluids: A Comparative Study on Zinc Oxide Nanostructures". Paper presented at the 17th *International Conference on Nanostructured Materials (ICNM-NANO)*, Abu Dhabi, United Arab Emirates, November 2024.

ZnO nanostructures. A study by Aftab et al. showed that ZnO NPs/acrylamide composites improved the yield point, gel strength, and apparent viscosity along with lubricity and filtration performance as well [46]. Abdo et al. modified bentonite and attapulgite with nano-ZnO and demonstrated improved rheology at high temperature-pressure conditions [199]. Ahasan et al. commented that in the absence of KCl, ZnO NPs can effectively form thinner mud cakes and highly improve the rheological properties of DFs [200]. While most studies have focused on the application of ZnO NPs, some researchers have explored the potential of other ZnO nanostructures, such as nanorods. For instance, Haneef et al. investigated the use of ZnO nanorods grown in clay matrix for application in water-based drilling fluids and observed enhanced rheological properties, filtration control, and thermal stability compared to conventional drilling fluids [201]. Recently, Prajapati et al. illustrated the synthesis of ZnO nanoflowers with controlled microwave irradiation and their application in HPDFs for improved for improved filtration properties [175].

Despite the promising results reported in the literature, there are still challenges and knowledge gaps that need to be addressed. It is important to note that the morphology and dispersion stability of ZnO nanostructures are critical factors that can profoundly impact the rheological, and filtration properties of water-based drilling fluids [201]. ZnO nanostructures have also shown the potential to prevent the hydration and swelling of shale in a few studies [48, 200]. Morphology, which refers to the shape, size, and structural configuration of the nanostructures, plays a pivotal role in determining their surface area-to-volume ratio and surface energy [202]. These characteristics can significantly influence the interaction between the nanostructures and the drilling fluid components, thereby affecting the overall fluid properties. Additionally, the dispersion stability of the nanostructures within the fluid matrix is crucial for maintaining homogeneity and preventing agglomeration or sedimentation, which can lead to performance degradation [95].

This study aims to conduct a comprehensive comparative analysis of the influence of morphology and dispersion stability on the properties of high-performance water-

based drilling fluids incorporating 2 different types of ZnO nanostructures, namely *Nanopencils* and *Nanoflowers*. Through a systematic investigation evaluation of ZnO nanostructures with different morphologies, this study seeks to elucidate the underlying mechanisms governing the performance of water-based drilling fluids. The experimental flowchart of the investigation is illustrated in Figure 7.1.

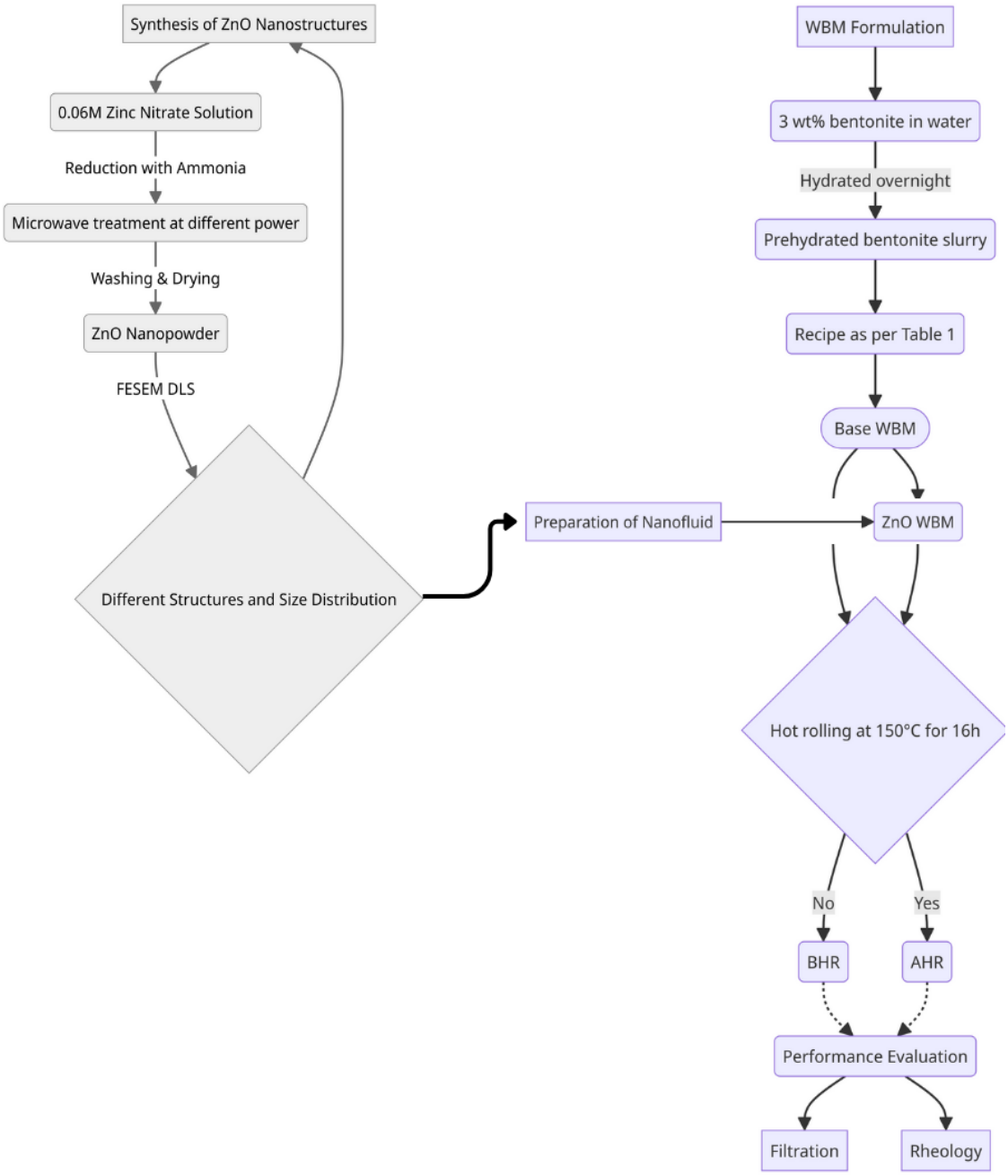

Figure 7.1: Flowchart of the experimental methodology.

7.1 Synthesis of ZnO Nanostructures

A solution was prepared by dissolving zinc nitrate in 400 mL deionized water at a concentration of 0.06 M. This solution was stirred using a magnetic stirrer at 600 rpm for 30 min. Ammonia was then incrementally added dropwise until the pH reached 11.5. The resultant mixture was divided into two 100 mL aliquots, each subjected to microwave irradiation in a digester (NuWav-Pro, Nutech Analytical Technologies) for 20 min at varying power levels of 520 and 680 W. Simultaneously, each aliquot underwent ultrasonication at 24 kHz and stirring at 250 rpm. The reaction temperature was maintained at 80 ℃ throughout the process. The precipitate was collected by centrifugation for 10 min. The resulting white powder was washed twice with deionized water and methanol. The ZnO nanopowders obtained from different power levels were dried in a vacuum oven at 80 ℃ for 10 h and subsequently stored in sealed culture tubes.

7.2 Characterization of the ZnO Nanostructures

7.2.1 Morphological and Size Distribution Analysis

Figure 7.2 illustrates the morphology and size distribution of the ZnO nanostructures obtained by varying the power conditions for microwave synthesis. Figure 7.2 (a) depicts elongated pencil-shaped rod structures (synthesized at 520 W) with a broad particle size distribution as illustrated in Figure 7.2 (c) and will be henceforth referred to as Nanopencils. Figure 7.2 (b) shows smaller rods, (synthesized at 680 W) emerging from common nuclei to form flower-like structures. These structures, henceforth referred to as Nanoflowers, have a sharp particle size distribution lying well below 100 nm, as illustrated in Figure 7.2 (d). The average hydrodynamic size

The synthesis and the morphological characterization in this chapter was performed in an early work :

D. K. Prajapati, A. Bardhan , S. Sharma, "Microwave-assisted Synthesis of Zinc Oxide Nanoflowers for Improving the Rheological and Filtration Performance of High-Temperature Water-based Drilling Fluids." *Journal of Dispersion Science and Technology*, 2023, 1-13. doi: https://doi.org/10.1080/01932691.2023.2294303

of the Nanopencils was 226.89 nm while Nanoflowers had a very low average value of 26.89 nm.

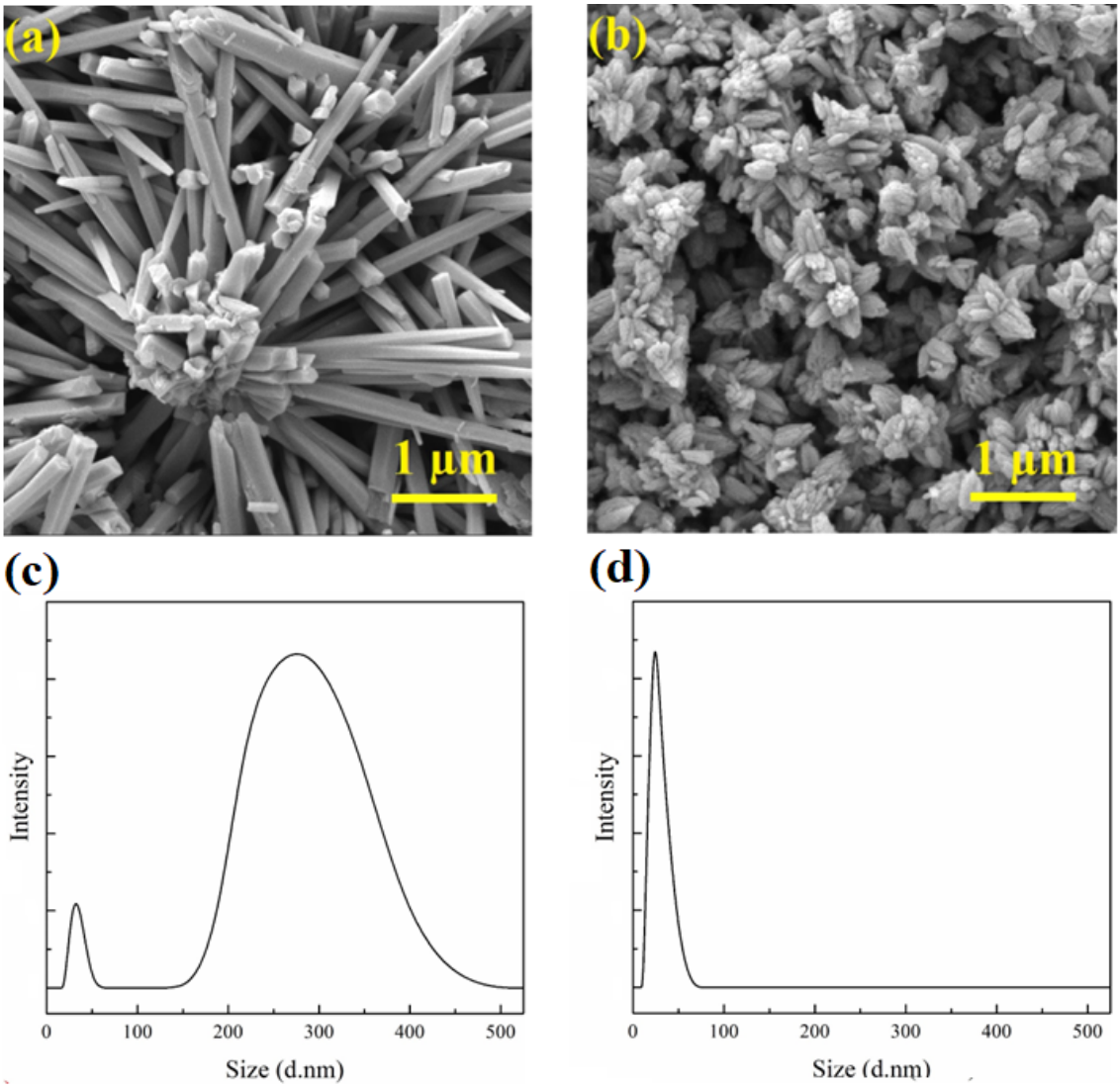

Figure 7.2: (a) FESEM image of ZnO Nanopencils synthesized at 520 W; (b) FESEM image of ZnO Nanoflowers synthesized at 680 W; (c) Particle Size Distribution of ZnO Nanopencils synthesized at 520 W; (d) Particle Size Distribution of of ZnO Nanoflowers synthesized at 680 W.

Mechanism behind Different Morphologies

The formation of different ZnO nanostructures, such as nanorods, nanopencils, and nanoflowers, is a complex process influenced by chemical interactions and crystal growth dynamics, as shown in Figure 7.3. ZnO formation typically initiates with the reaction between zinc ions and hydroxide ions in aqueous solution, resulting

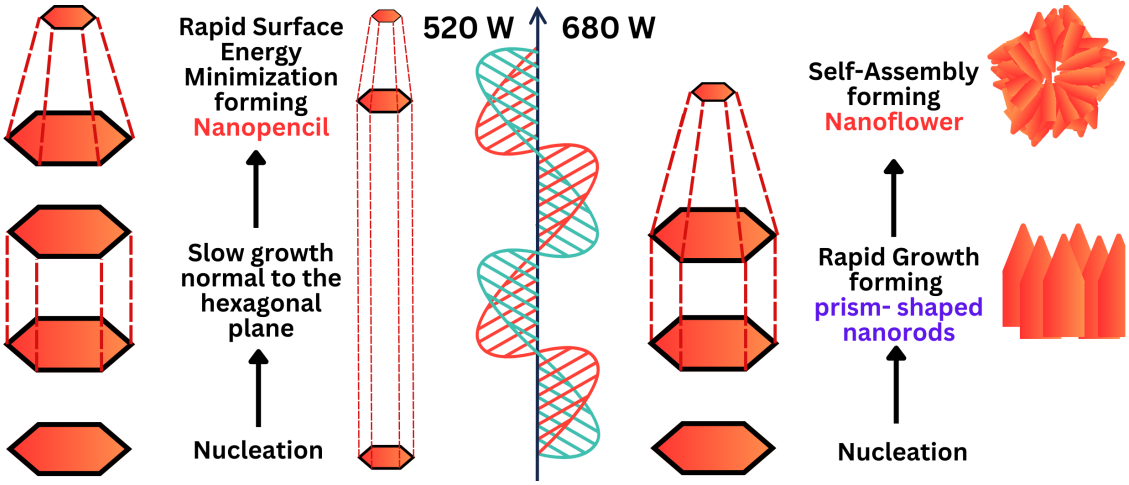

Figure 7.3: Schematic diagram showing the growth and formation of different ZnO Nanostructures.

in the formation of zinc hydroxide. This intermediate compound is unstable and readily dehydrates, leading to the nucleation of ZnO. ZnO crystals, particularly in their wurtzite hexagonal phase, exhibit distinct polar and non-polar faces that significantly influence their growth patterns [203]. Polar faces, such as the Zn-terminated faces, tend to grow faster than non-polar O-terminated faces faces. The latter contribute to the characteristic hexagonal shape of ZnO nanorods. At lower temperatures, growth along the polar face dominates, leading to the formation of nanorods with a hexagonal cross-section. These nanorods typically exhibit polar Zn-terminated top and O-terminated bottom surfaces, bounded by six non-polar planes [203, 204].

As the reaction temperature increases, surface mobility enhances, enabling ZnO species to migrate from the base and sides towards the tip. This migration, coupled with electrostatic interactions, favors the development of lower surface energy planes. These planes grow more rapidly, resulting in pencil-like structures with a tapering tip. Insufficient surface mobility can lead to the formation of prism-shaped nanorods [205].

However, if the energy is sufficient to activate nucleation and prolong growth then Nanoflowers emerge from the self-assembly of numerous prism-shaped nanorods structures arranged radially. A seeding layer often provides nucleation sites for

this assembly process. The density of nanorods within the flower-like structure is influenced by the initial nucleation sites [206].

7.2.2 Electrophoretic Stability Analysis with Variation in pH

Figure 7.4 reports the changes in zeta potential values of the ZnO nanostructures dispersed in aqueous media at different pH values. While the isoelectric points of both the nanostructures were between 5 to 6 pH, the Nanoflowers showed better stability as compared to the Nanopencils at a neutral pH of 7. The increasing alkalinity of the media resulted in negative zeta potential values with nanoflowers with higher stability again. This observation can be attributed to the smaller size distribution and higher repulsive forces coming into play [95]. It is also interesting to note that both the nanostructures had zeta potential beyond -30 mV at 9 pH making them suitably stable in the formulated DF [207].

7.3 Performance of Drilling Fluids with ZnO Nanostructures

The composition of the DFs to be discussed hereinafter is shown in Table 7.1.

Table 7.1: Composition of the DFs with ZnO Nanostructures.

Sequence	**Constituents**	**Concentration (wt%)**
1	Deionized water	-
2	Bentonite	3.00
3	KOH	0.07
4	Xanthan Gum	0.25
5	PAC-R	0.50
6	KCl	3.00
7	1-Octanol	2-3 drops
8	ZnO Nanostructures	0-1.0

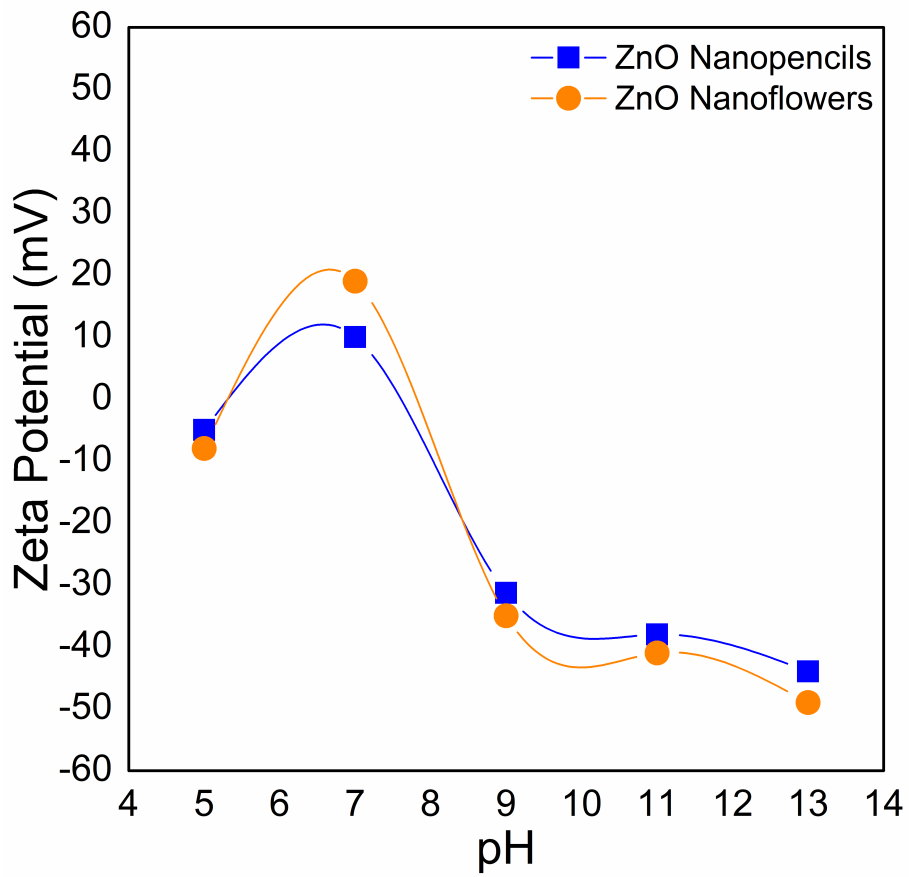

Figure 7.4: Variation of aqueous zeta potential of the ZnO Nanostructures with pH.

7.3.1 Rheological Performance

The viscometric analysis of the DF samples was performed with calculated Bingham Plastic parameters from the recorded viscosity data following API recommended practices 13-B [101].

The AV of the DF samples are plotted in Figure 7.5 (a-b). Both the ZnO nanostructures increased the AV of the DF samples with their increase in dosages. The Nanoflowers showed a steeper increment in AV as compared to the Nanopencils. Upon comparing the samples before hot rolling (BHR), it was observed that while the Nanopencils increased the AV of the base DF by 19%, the Nanoflowers increased the AV by 29% at 1 wt% concentration. This increment in AV values can be attributed to the intensifying interaction between the DF and the nanostructures. This enhanced interaction forms a network structure within the fluid, leading to greater flow resistance [46]. The effect of thermal degradation was also minimized

with the ZnO nanostructures in DF, as evident from a 10.2% decrease in AV for Nanopencils and a 3.92% decrease in AV for Nanoflowers at 1 wt%, compared to a 16.42% decrease in the base DF after hot rolling (AHR). The higher thermal conductivity of the ZnO nanostructures can be credited for the effective viscosity retention capability at higher temperatures [167].

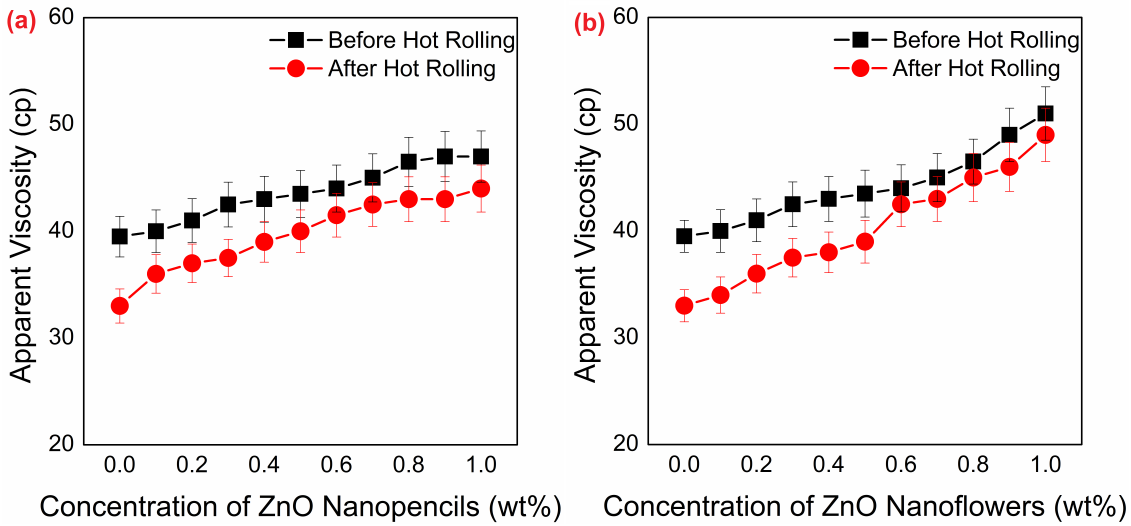

Figure 7.5: Apparent viscosity of the DF samples with (a) ZnO Nanopencils and (b) ZnO Nanoflowers.

Figure 7.6 (a-b) displays the PV of the DF samples. Both the nanostructures enhanced the PV with increasing concentrations in the DF. The BHR DF samples demonstrated a 55.5% increase in PV with Nanopencils and a 61% increase with Nanoflowers at a 1 wt% concentration compared to the base DF. While the Nanopencils showed better viscosity retention after hot rolling at lower concentrations, the Nanopencils showed comparable performance at higher concentrations. The base DF AHR had a PV degradation of 39%, which was minimized by Nanopencils to 10.6% and by Nanoflowers to 7% at 1 wt% concentration. The dispersion of ZnO nanostructures increases PV by elevating the friction between fluid layers. This heightened friction leads to greater flow resistance under stress, which is essential for ensuring wellbore stability during drilling operations [208].

The YP variation with increasing concentrations of the ZnO nanostructures in DF samples is shown in Figure 7.7 (a-b). Interestingly the YP at 1 wt% increased

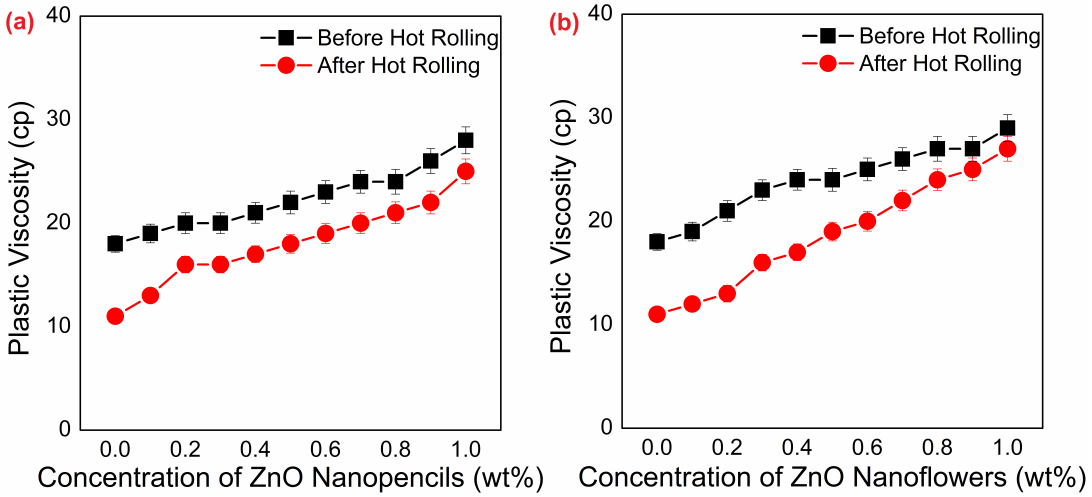

Figure 7.6: Plastic viscosity of the DF samples with (a) ZnO Nanopencils and (b) ZnO Nanoflowers.

by 25% for both the nanostructures when compared to the base DF which can be attributed to the enhanced cohesive forces in the DF system [209]. However, the Nanoflowers enhanced the YP greatly at a concentration of 0.1 wt% whereas the Nanopencils showed the same enhancement only after 0.5 wt%. The effect of thermal degradation ranged for both the nanostructures similarly around 7 to 8

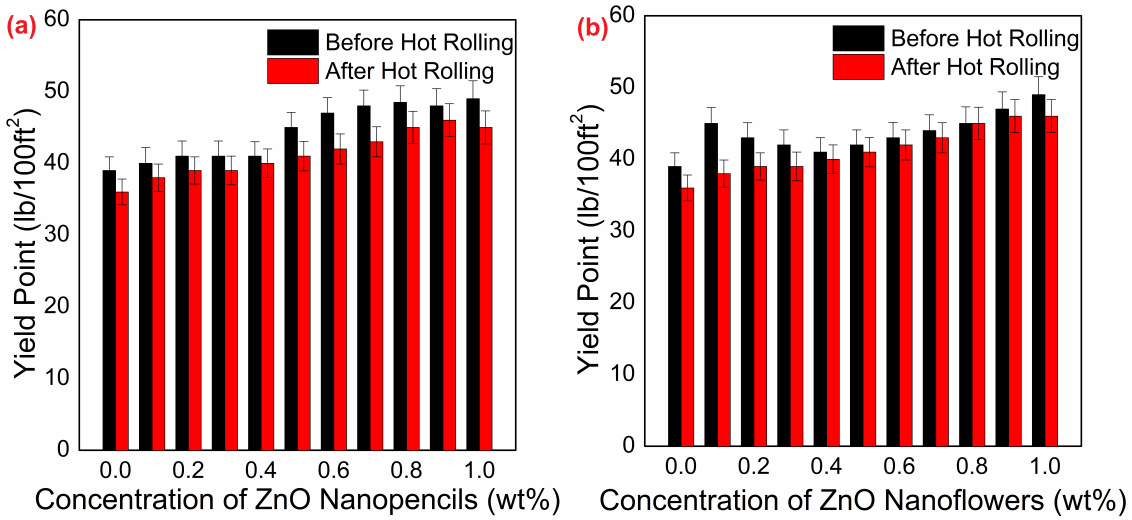

Figure 7.7: The yield points of the DF samples with (a) ZnO Nanopencils and (b) ZnO Nanoflowers.

7.3.2 Filtration Performance

Figure 7.8 (a-b) depicts the filtration performance at ambient temperature and 100 psi pressure of the DFs with varying concentrations of the ZnO Nanostructures. The ultimate reduction in filtration losses (FL) was 37.5% and 50% for the Nanopencils and Nanoflowers respectively at 1 wt% concentration when compared to the base DF. However, at lower dosages (below 0.5 wt%) the Nanopencils outperformed the Nanoflowers in terms of reducing the FL. The Nanopencils can create a more extensive network within the filter cake due to their elongated shape. This enhances the bridging effect between particles, leading to a denser filter cake that significantly reduces filtration loss. However, at higher concentrations, the shorter rods of the Nanoflowers may have contributed to the effective sealing of nanopores in the mud cake. The effect of thermal degradation was prominent with an increase in FL by 62.5% for the base DF which was minimized to 33% by the Nanoflowers at 0.5 wt% concentration, which can be attributed to the better viscosity retention abilities as discussed in the previous section.

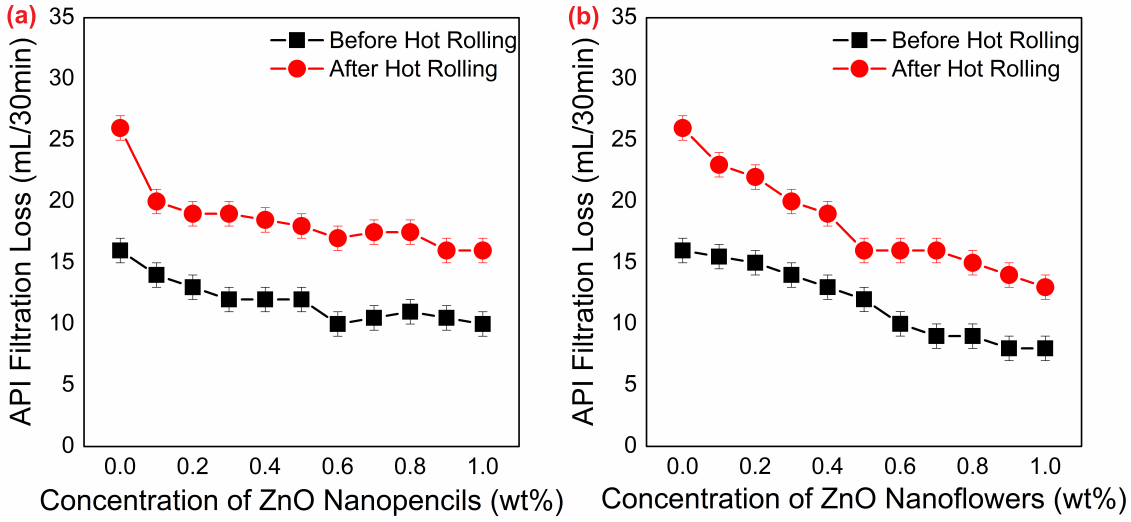

Figure 7.8: The API filtration losses of the DF samples with (a) ZnO Nanopencils and (b) ZnO Nanoflowers.

The HPHT FL obtained after 30 min of filtration at 150 °C and 500 psi differential pressure for the DFs with ZnO nanostructures is given in Figure 7.9 (a-b). The reduction in FL BHR in comparison to the base DF was 41.38% for the Nanopencils

and 48.28% for the Nanoflowers at 1 wt% concentration. Here, Nanoflowers could influence the FL properties of DF at lower dosages as compared to the Nanopencils. The AHR samples showed an increase in FL between 17 to 28%. This gap was closed by the Nanoflowers at 0.1% concentration where the FL increase AHR was only 11%. At elevated pressure-temperature conditions, the properties of other additives degrade and the prominence of smaller-sized nanostructures in mud cake buildup is observed through the Nanoflowers' superior performance.

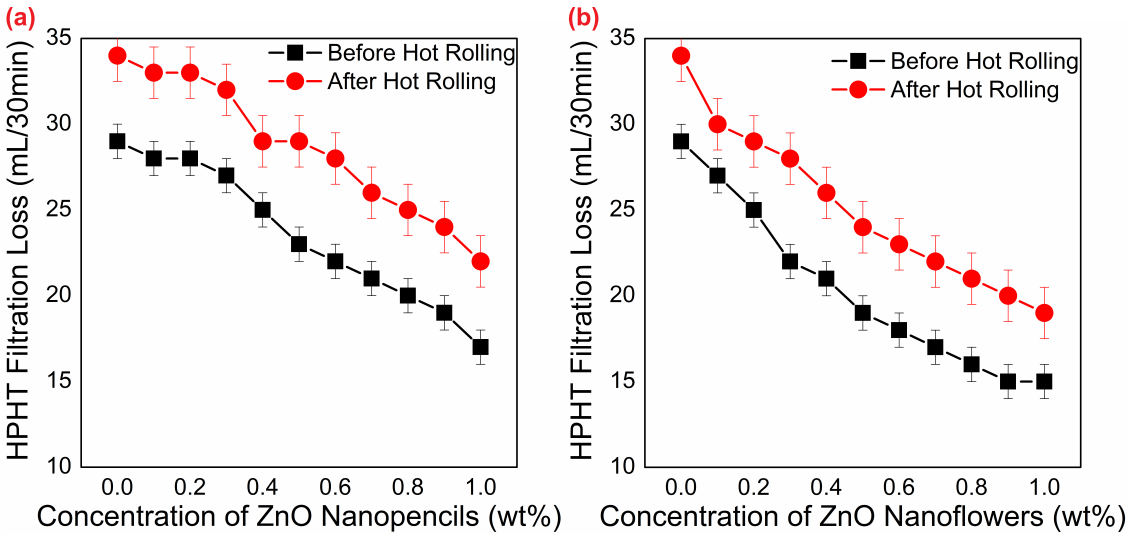

Figure 7.9: The HPHT filtration losses of the DF samples with (a) ZnO Nanopencils and (b) ZnO Nanoflowers.

7.4 Conclusion

This study compared two distinct morphologies of ZnO nanostructures namely Nanopencils and Nanoflowers in their ability to influence the properties of a WBDF for thermally tolerant performance in high-temperature wells. The findings can be summarized to identify the role of morphology and stability of nanostructures in HPDF formulations:

- The hydrodynamic size distribution of the Nanopencils was broader with a higher average size as compared to the Nanoflowers which had a narrower distribution and a very small average size. This impacted their polydispersity

and their stability in aqueous medium, due to different surface charge densities and zeta potential values, giving different performances when infused in DFs.

- The Nanoflowers had a higher incremental impact on the viscosity of the DF as compared to the Nanopencils.
- However, the thermal tolerance of the DFs were roughly similar for both the nanostructures.
- The Nanoflowers outperformed the Nanopencils in filtration performance by approximately 20% at higher concentrations possibly due to better sealing of the nanopores in the mud cake. At lower concentrations, the bridging mechanism by the Nanopencils was more prominent as compared to the Nanoflowers.

These results emphasize the importance of selecting nanostructures with specific morphological characteristics determining their effectiveness in improving viscosity, filtration control, and thermal stability.

Chapter 8

Silane Coated Silica Nanoparticles

Silica NPs have garnered significant attention for their potential to improve the performance of WBDFs in high-temperature environments [59]. Silica NPs play a crucial role in reducing water infiltration in shale formations while also managing the rheological and filtration characteristics of drilling fluids [210]. Research has demonstrated that these NPs can improve the thermal stability of drilling fluids, enhancing their performance under high-temperature conditions [68]. Additionally, they are instrumental in maintaining the stability of the wellbore [211]. In WBDF systems, such as those containing potassium chloride (KCl), silica NPs have been shown to significantly decrease fluid loss and improve the rheological properties of the DF [212]. However, it is important to note that the NPs' tendency to aggregate, especially when dispersed or in colloidal sol form, can affect their effectiveness and alter their properties [213]. The incorporation of Silica NPs may lead to weaker structural formations and reduced yield stress compared to the base fluid alone [214].

To maximize the benefits of silica NPs, it is crucial to address their aqueous dispersibility and compatibility with other drilling fluid components. Silane coating has emerged as a viable solution to enhance the stability and performance of

---

This chapter is based on :

A. Bardhan , F. Khan, H. Kesarwani, S. Vats, S. Sharma, and S. Kumar, "Performance Evaluation of Novel Silane Coated Nanoparticles as an Additive for High-Performance Drilling Fluid Applications." Paper presented at the *International Petroleum Technology Conference*, Bangkok, Thailand, March 2023. Online on *OnePetro*. doi: https://doi.org/10.2523/IPTC-22878-MS

silica NPs in WBDFs. The silane coating improves the hydrophilicity of the NPs, allowing them to disperse more effectively in aqueous environments and interact synergistically with other fluid components [215]. This modification also enhances the thermal stability of the NPs, enabling them to withstand the extreme temperatures encountered in deep drilling operations.

In the present study, commercially procured silica NPs were coated with [3-(2-Aminoethylamino) propyl] trimethoxy silane (AEAPTS), and the product was confirmed by FTIR (Fourier transform infrared spectra) spectra. A base DF was prepared with bentonite, xanthan gum, polyanionic cellulose, KCl, etc. The concentration of the silane-coated nanoparticle was varied from 0.2 to 0.4 wt% to investigate the effect of the nanoparticle on the rheological and filtration properties of the WBDFs. The DF was kept for aging at 150 °C for 16 h in the roller oven. Rheology of the Nano DF both before and after aging was analyzed using Fann VG meter and the filtration properties were analyzed by using API Filter Press (LPLT).

The methodology carried out throughout the entire study is illustrated in Figure 8.1.

8.1 Silane Coating of Silica NPs

The coating of AEAPTS on the silica NPs was done in two steps. In the first step 2.5 wt% of silica NPs was added to the 20 mL aqueous solution of the 0.5 M sodium hydroxide. The mixture was continuously stirred at 600 rpm for 24 h in a magnetic stirrer at ambient conditions. This results in the addition of hydroxyl groups on the surface of the silica NPs [216]. After stirring, the product was centrifuged at 12000 rpm for 20 min and then washed thrice with deionized water. Then the product obtained was dried out for 24 h in a desiccator. In the second step, the coating of AEAPTS on hydroxyl groups attached to the silica NPs was done. The 200 mg of Si-OH (product of the first step) NPs were dispersed in an aqueous medium containing 80 mL of water + 2 mL of ammonium hydroxide + 20 mL of methanol + 1 mL of AEAPTS. The resulting mixture was stirred at 600 rpm for 2 h at ambient

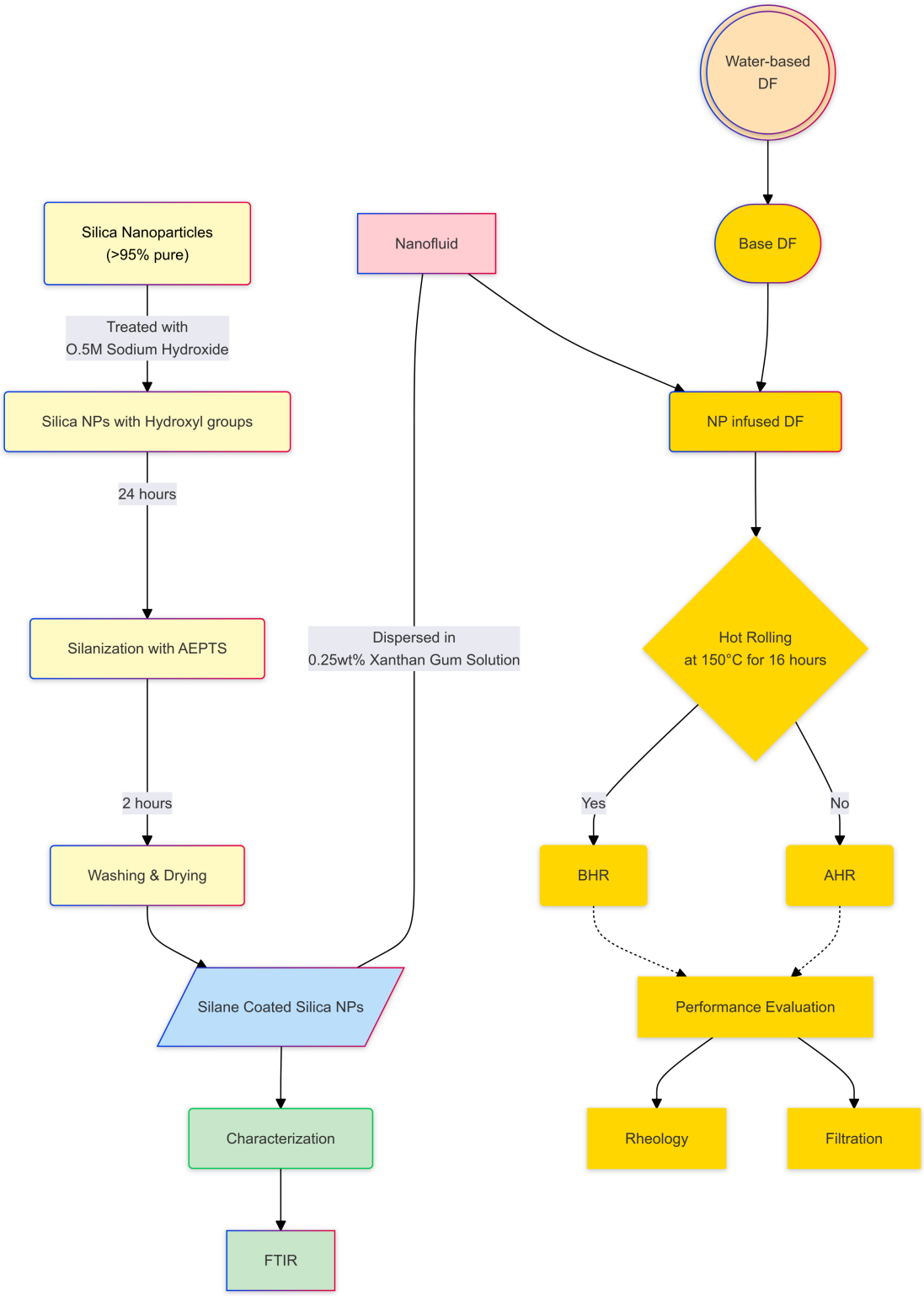

Figure 8.1: Flowchart of the experimental methodology

conditions, and then the temperature was increased to 70°C and was maintained for 24 h followed by centrifugation at 13000 rpm for 25 min. The product thus obtained was washed with the isopropyl alcohol (33% dilution) in a centrifuge three times at 12000 rpm for 15 min each and the resultant solution was dried for 24 h in a desiccator. The schematic of the process is given in Figure 8.2.

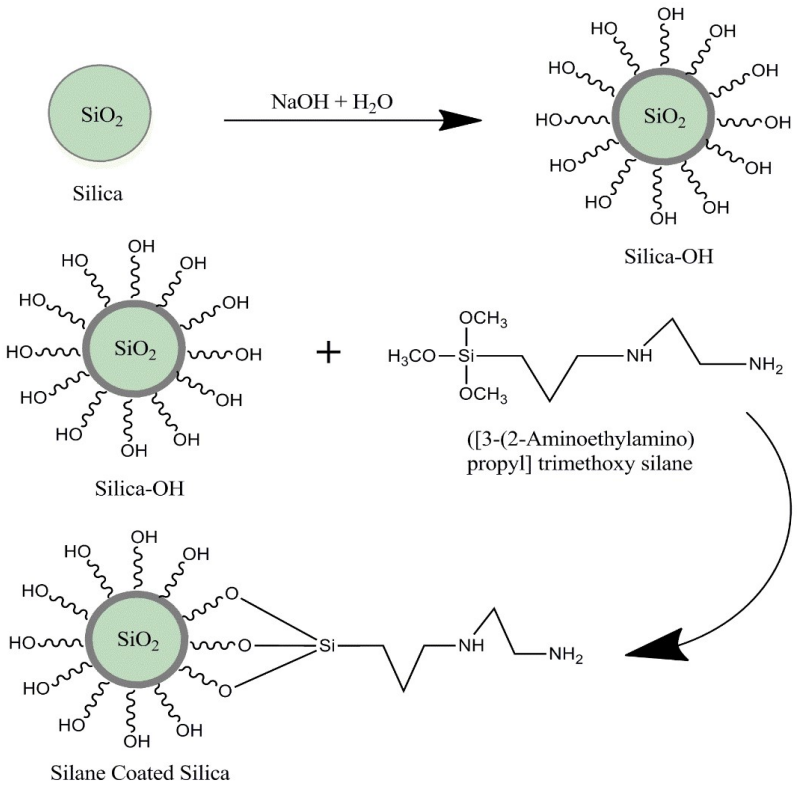

Figure 8.2: Reaction Schematic of the coating of silica NPs

8.2 Characterization of the Silane Coated Silica NPs

The silane coating on the NPs was characterized by the FT-IR absorption spectra which is shown in Figure 8.3. The peaks corresponding to 990-1050 cm^{-1} are attributed to the alkyl-substituted ether whereas the peaks at 1080 cm^{-1} and 880 cm^{-1} are attributed to the Si-O-Si and Si-OH absorption. The absorption spectra in the range of 3200-3400 cm^{-1} correspond to the OH functional group. The peaks from 813-981 cm^{-1} are due to the C-C stretching whereas 2877-2967 cm^{-1} are attributed

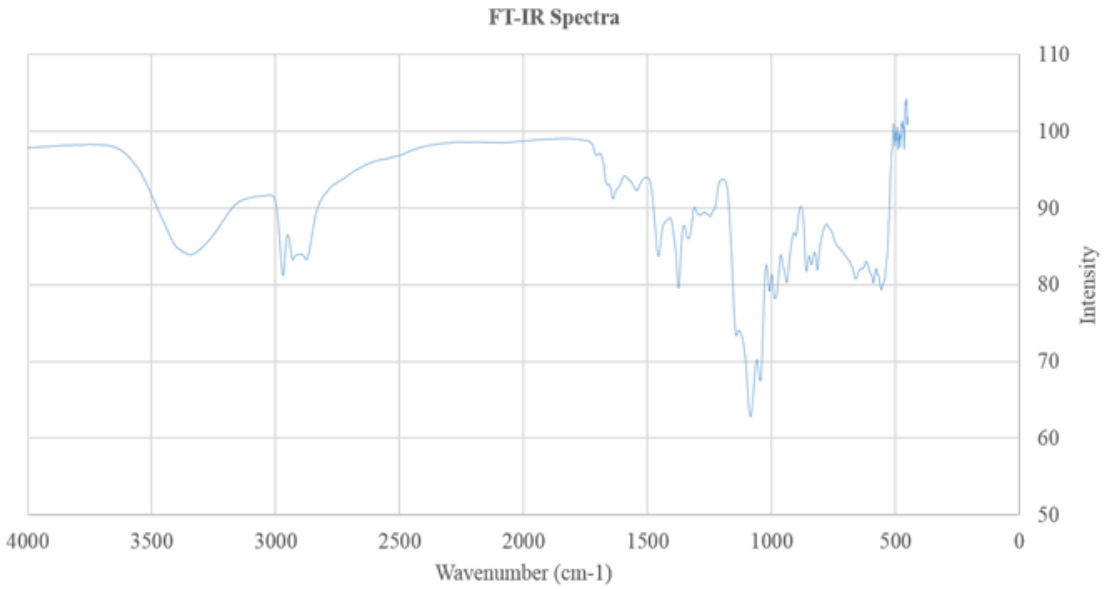

Figure 8.3: FTIR Spectra of silane-coated silica NPs

to the C-H stretching. The absorption peak at 1642 cm^{-1} is due to the presence of NH_2 as a functional group in the compound whereas the wide spectra at 3300-3500 cm^{-1} are attributed to the N-H stretching. All these peaks manifest the successful coating of silane on the silica NPs.

8.3 Performance of Drilling Fluids with Silane Coated Silica NPs

The composition of the base and the NP-infused DFs to be discussed hereinafter is shown in Table 8.1.

Table 8.1: Composition of the DFs with mMWCNT.

Sequence	Constituents	Concentration (wt%)
1	Deionized water	-
2	Bentonite	3
3	KOH	0.07
4	Xanthan Gum	0.25
5	PAC-R	0.5
6	KCl	3
7	1-Octanol	2-3 drops
8	Silane Coated Silica NPs	0-0.4

8.3.1 Rheological Performance

The rheological parameter of the DF samples was measured both before and after hot rolling at 150 °C for 16 h and the data obtained are presented in Figure 8.4(a-f). The rheology of all the DF samples was measured at two different temperatures i.e., at 30 °C and 60 °C. The apparent viscosity of the DF was improved by approximately 46% with the concentration of 0.4 wt% of the silane-coated silica NPs. The plastic viscosity increased with a minimum dosage of 0.2 wt% of the NPs after which the increment continued directly with the increase in concentrations. The yield point also showed a considerable enhancement of 47% in the case of 0.4 wt% concentration. Hence, the data obtained clearly shows the improvement in the rheological parameters on the addition of the silane-coated silica NPs. The degradation in the DF rheology was reduced up to 19% after aging, although the effect of the addition of NPs was significantly observed when it was added in lesser concentrations.

Thermal stability is one of the most important properties that a drilling fluid must possess. Since the drilling fluid is used in the wellbore that has a significantly high temperature as compared to the surface temperature so it becomes necessary to design the fluid that can sustain at subsurface temperature. The general trend of the viscosity follows an inverse relationship with temperature and hence the drilling fluid must be designed keeping in mind the subsurface temperature. Although the decrease in the viscosity of the DF with increasing temperature cannot be avoided but it can be decreased with the addition of proper DF additives that can thermally stabilize the DF. In the experiment, the rheological parameters of the base DF were found to be reduced up to 56% of their original value after aging whereas after addition of only 0.2 wt% silane-coated silica NPs the changes in the rheological parameters were quite significant. The trend remained similar with 0.3 wt% and 0.4 wt%. The thermal degradation in the rheological beaviour, which can be seen in Figure 8.5, was reduced in the silane-coated silica NPs-enhanced DF, considerably as compared to the base DF. After hot rolling these parameters were around 80% of their respective before hot rolling values. This clearly reflects that the addition

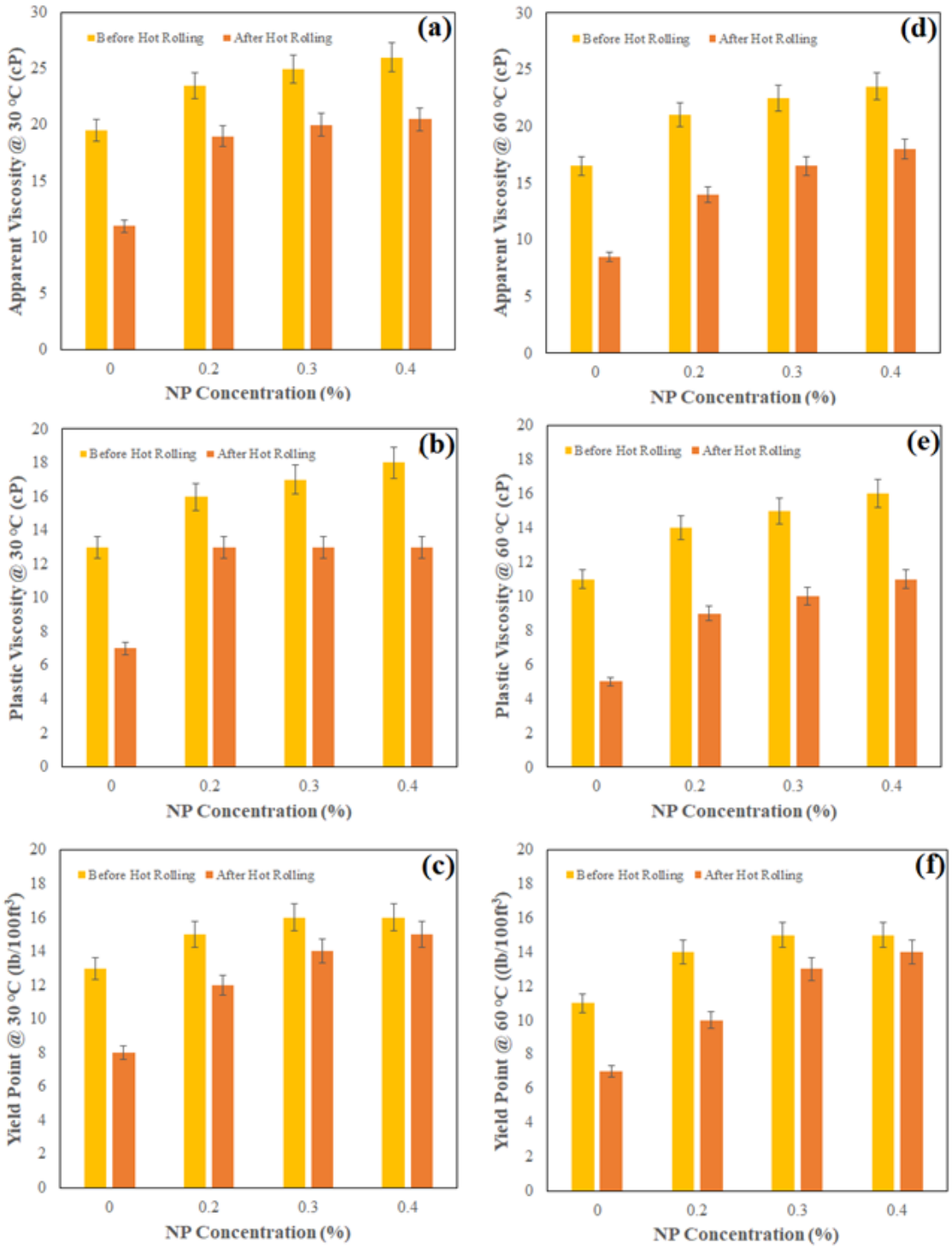

Figure 8.4: Bingham Plastic Rheological Parameters of the DF samples with increasing concentration of silane-coated silica NPs at 30 ℃ (a, b, c) and at 60 ℃ (d, e, f) before and after hot rolling.

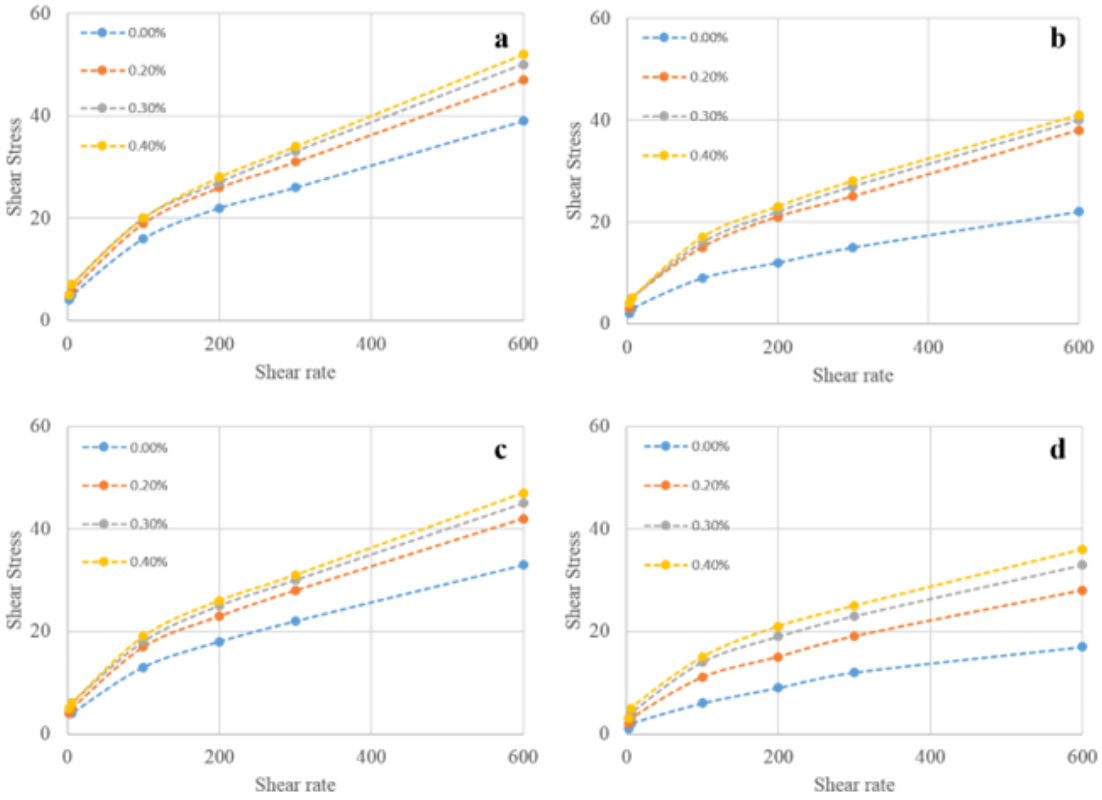

Figure 8.5: Shear rheology of the DF with the increase in the concentration of silane-coated silica NPs, a) BHR at 30 °C; b) AHR at 30 °C; c) BHR at 60 °C; d) AHR at 60 °C

of silane-coated silica NPs thermally stabilized the WBDF system.

8.3.2 Filtration Performance

Figure 8.6 shows the API filtrate loss in the formulated DF samples with the silane-coated silica NP concentrations ranging from 0 wt% to 0.4 wt%, under a pressure of 100 psi at room temperature, after hot rolling. The API FL (mL/30min) in the case of base DF was found to be 32.3 ml which decreased to 16 mL with the introduction of the NPs at the concentration of 0.2 wt%. This accounts for a remarkable reduction of around 50%. It can be inferred that the majority of the filtrate volume can be controlled with a minimum amount of NPs in a bentonite/polymer WBDF even when the polymers in the system tend to disintegrate after exposure to higher temperatures for a prolonged duration along with the tendency of the bentonite clay to flocculate. The subsequent reduction at 0.3 wt% NPs was 12.5% in comparison

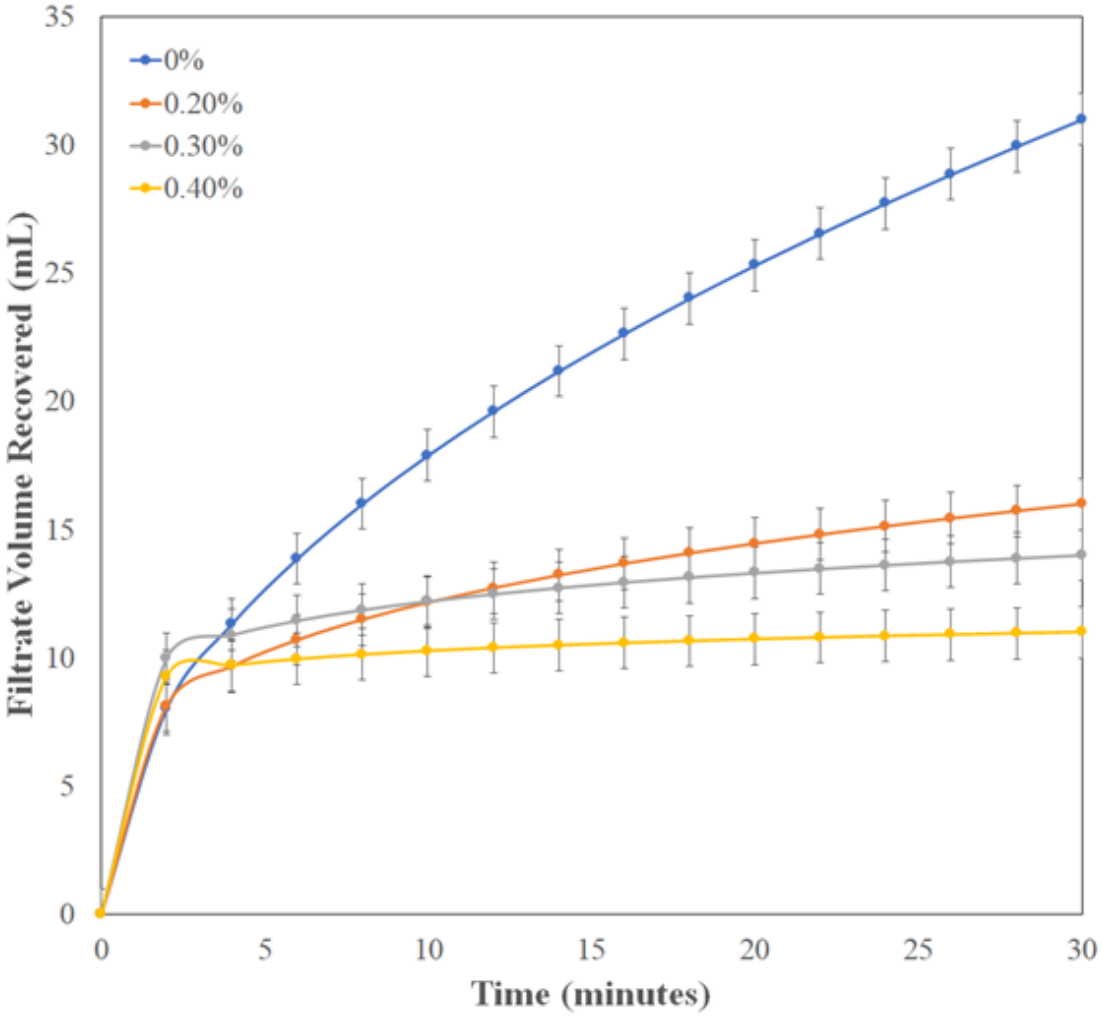

Figure 8.6: API Filtrate Loss of the DFs for different concentrations of silane-coated silica NPs (with an error of ±1 mL).

to fluid loss at 0.2 wt% concentration. Furthermore, the FL was reduced to 11.2 ml with an addition of 0.4 wt% NPs in the DF sample. This stands at a 64% percent decrement in the fluid loss as compared to the base DF (0 wt%). The recovered filter cakes of the nanoparticle-infused DF samples were smooth in texture and all below 1/32 inch.

8.4 Conclusion

Silane-coated silica NPs can work as a rheological as well as a fluid loss control agent in WBDFs. They thermally stabilize the DFs and helps in keeping the rheological property of the DFs intact even at subsurface temperature. The degradation in

rheological parameters of the base DF was found to be around 55% which was reduced up to a value of 20% as well as the fluid loss was reduced by 64% upon adding the silane-coated silica nanoparticle which clearly shows that this additive can be used as a potential candidate for the high-performance rheology and fluid loss control in WBDF systems.

Chapter 9

Conclusion and Future Recommendations

This body of work comprehensively advocated for the application of Nanomaterials as additives for formulating High-Performance Drilling Fluids. Five different types of nanomaterials were used to conclusively support their multifunctionality in terms of improving the rheological, filtration, and lubrication properties by imparting high degree of thermal stability to the conventional drilling fluids systems. Therefore, following statements can be made based on the findings of the investigation:

- Plastic Waste is a matter of concern and therefore various approaches have been taken to mitigate plastic pollution for a sustainable future. The conducted work accomodated valorization of these wastes into graphene nanonsheets and their applications in high-performance drilling fluids. The results indicate that even extremely low dosages of the synthesized graphene nanosheets could sufficiently impart thermal tolerance to the drilling fluid alongside improved rheological and filtration properties.

- Carbonaceous nanoparticles are very interesting nanomaterials that has been proved effective in non-aqueous drilling fluids. However, high-performance drilling fluid formulation requires greater degree of dispersion stability of these nanomaterials in aqueous medium to attain similar efficiency. This work dealt

with modified carbon nanotubes through wet base oxidation method and adjusted the pH of the dispersing media to ensure optimal dispersion stability. The mechanistic insights on the viscoelastic superiority of a carbon nanotubes infused drilling fluid system, enhanced rheological profile and ultra low filtration losses were explored in high temperature and high pressure conditions.

- Metal oxide nanoparticles are very good candidates for application as nanoadditives. In this work, green synthesis of copper oxide nanoparticles were performed by using *Colocasia esculenta* leaf extract alongwith microwave treatment. This resulted in uniform size distribution and plate-like morphology which contributed to improved lubricating properties of the formulated drilling fluid. In addition, the fitration losses reduced, thermal tolerance enhanced and the rheological profile was unaffected.

- Although the candidacy of the metal oxide NPs has been justified time and again, the role of morphology and the size distribution have been seldom discussed. In this research, zinc oxide nanostructures with pencil-like and flower-like morphologies were infused in drilling fluids and their efficacy in improving the rheological and filtration performance in high-temperature well situation were explored. The resultant mechanism revealed the higher charge distribution, smaller size and lower polydispersity contributed more in selection of high-performance nano-additives.

- Commercial silica nanoparticles are one of the most feasible nanomaterials that can readily be applied to drilling fluids for improved performance. However, their aqueous dispersibility is limited and hence require functionalization to address this problem. In this study, the silica nanoparticles' surface was coated with [3-(2-Aminoethylamino)propyl]trimethoxysilane and incorporated in water-based drilling fluid system. The filtration and rheological properties improved as the dosage of the silance coated silica nanoparticles increased and the thermal degradation was minimized.

Table 9.1 summarizes the findings of the investigation conducted to verify the viability of the employed nanomaterials as *nano-additives* for the formulation of high-performance drilling fluids. While the nanomaterials are indeed multifunctional, they require to be stable in aqueous dispersions to prove their efficacy in inhibited bentonite/polymer water-based systems. The role of morphology plays a key role in advocating the efficacy of nano-additives for different purposes. Green synthesis as well as upcycling of wastes into viable nanomaterials are effective in addressing production cost-related issues.

Table 9.1: Multifunctionality of the employed nanomaterials.

Sl. No.	**Nanomaterial**	**Conc. (wt%)**	**Efficacy as Nano Additive**			
			Filtrate Loss Reducer	**Rheology Modifier**	**Thermal Stabilizer**	**Lubricity Improver**
1	Plastic Upcycled Graphene Nanosheets	0.050-0.440	Yes	Yes	Yes	-
2	Modified Carbon Nanotubes	0.025-0.100	Yes	Yes	Yes	-
3	Biogenic Copper Oxide NPs	0.100-1.000	Yes	No	Yes	Yes
4	Zinc Oxide Nanostructures	0.100-1.000	Yes	Yes	Yes	-
5	Silane Coated Silica NPs	0.200-0.400	Yes	Yes	Yes	-

Directions for Future Research

While this research investigation was experimentally based on some specific set conditions to synthesize and identify the viability of nano-additives for the formulation of high-performance drilling fluids, the scope of this work can be developed further with the following recommendations:

- The nanomaterials may be utilized to further verify the mechanism of filtration control as size distribution and the effective charge plays a crucial role.
- The role of dispersion stability may be addressed by synthesizing polymeric or clay-based nanocomposites which can be readily deployed in the field scale scenario.
- The surface modification of commercially viable nanoparticles could be further explored for various applications.
- It is also evident that morphology plays a dominant role in controlling properties like lubricity. Therefore, further investigation can be performed to employ techniques to derive desirable morphologies through advance nanomaterial synthesis techniques.
- Molecular dynamics simulation of the existing nanoparticle-clay/polymer interaction in aqueous dispersions with varying salinity and temperature conditions may reveal some fundamental basis for selecting nano-additives.
- Computational fluid dynamics simulations shall shed some light on the efficacy of these nano-additives in various well geometries under different pressure-temperature conditions.

Bibliography

[1] Ł. Lach. Oil Usage, Gas Consumption and Economic Growth: Evidence from Poland. *Energy Sources, Part B: Economics, Planning, and Policy*, 10(3):223–232, jul 2015.

[2] International Energy Agency. International Energy Agency (IEA) World Energy Outlook 2022. *International Information Administration*, page 524, 2022.

[3] Y Wang, J-C Feng, X-S Li, L Zhan, and X-Y Li. Pilot-scale experimental evaluation of gas recovery from methane hydrate using cycling-depressurization scheme. *Energy*, 160:835–844, oct 2018.

[4] N Sonnichsen. Global Distribution of Crude Oil Production, 2022.

[5] International Energy Agency. Global Gas Security Review 2024. Technical report, nov 2024.

[6] Anne-Sophie Corbeau, Shahid Hasan, and Swati Dsouza. The Challenges Facing India on its Road to a Gas-Based Economy. Technical report, King Abdullah Petroleum Studies and Research Center, Riyadh, Saudi Arabia, oct 2018.

[7] Hui Mao, Yan Yang, Hao Zhang, Jiang Zhang, and Yan Huang. A critical review of the possible effects of physical and chemical properties of subcritical water on the performance of water-based drilling fluids designed for ultra-high temperature and ultra-high pressure drilling applications. *Journal of Petroleum Science and Engineering*, 187:106795, 2020.

[8] Allan Katende, Natalie V. Boyou, Issham Ismail, Derek Z. Chung, Farad Sagala, Norhafizuddin Hussein, and Muhamad S. Ismail. Improving the performance of oil based mud and water based mud in a high temperature hole using nanosilica nanoparticles, sep 2019.

[9] Fred Dupriest and Sam Noynaert. Drilling Practices and Workflows for Geothermal Operations. *SPE - International Association of Drilling Contractors Drilling Conference Proceedings*, 2022-March, 2022.

[10] Sidharth Gautam. Rheological Investigation and Development of High-Pressure and High-Temperature Drilling Fluid. 2022.

[11] Johannes Karl Fink. *Water-Based Chemicals and Technology for Drilling, Completion, and Workover Fluids*. Elsevier, 2015.

[12] A. T. Bourgoyne Jr, K. K Millheim, M. E. Chenevert, and F.S. Young Jr. *Applied Drilling Engineering*, volume 2. Society of Petroleum Engineers, Richardson, 1991.

[13] Sidharth Gautam, Chandan Guria, and Vinay K. Rajak. A state of the art review on the performance of high-pressure and high-temperature drilling fluids: Towards understanding the structure-property relationship of drilling fluid additives. *Journal of Petroleum Science and Engineering*, 213:110318, jun 2022.

[14] Ian A. Frigaard, Kristofer G. Paso, and Paulo R. de Souza Mendes. Bingham's model in the oil and gas industry. *Rheologica Acta*, 56(3):259–282, 2017.

[15] Mohammad Mojammel Huque, Stephen Butt, Sohrab Zendehboudi, and Syed Imtiaz. Systematic sensitivity analysis of cuttings transport in drilling operation using computational fluid dynamics approach. *Journal of Natural Gas Science and Engineering*, 81:103386, sep 2020.

[16] Slavomir S. Okrajni and J. J. Azar. The Effects of Mud Rheology on Annular Hole Cleaning in Directional Wells. *SPE Drilling Engineering*, 1(04):297–308, aug 1986.

[17] Sidharth Gautam and Chandan Guria. Optimal Synthesis, Characterization, and Performance Evaluation of High-Pressure High-Temperature Polymer-Based Drilling Fluid: The Effect of Viscoelasticity on Cutting Transport, Filtration Loss, and Lubricity. *SPE Journal*, 25(03):1333–1350, jun 2020.

[18] Majid Sajjadian, Vali Ahmad Sajjadian, and Alimorad Rashidi. Experimental evaluation of nanomaterials to improve drilling fluid properties of water-based muds HP/HT applications. *Journal of Petroleum Science and Engineering*, 190, jul 2020.

[19] Anirudh Bardhan, Fahad Khan, Himanshu Kesarwani, Sushipra Vats, Shivanjali Sharma, Shailesh Kumar, and Petroleum Technology. Performance Evaluation of Novel Silane Coated Nanoparticles as an Additive for High-Performance Drilling Fluid Applications. 2023.

[20] Dina Kania, Robiah Yunus, Rozita Omar, Suraya Abdul Rashid, Badrul Mohamed Jan, and Akmal Aulia. Lubricity performance of non-ionic surfactants in high-solid drilling fluids: A perspective from quantum chemical calculations and filtration properties. *Journal of Petroleum Science and Engineering*, 207(June):109162, 2021.

[21] W. E. Foxenberg, S. A. Ali, T. P. Long, and J. Vian. Field experience shows that new lubricant reduces friction and improves formation compatibility and environmental impact. *Proceedings - SPE International Symposium on Formation Damage Control*, 2:842–854, 2008.

[22] Ebikapaye Peretomode and Obiajulu Peretomode. Temperature Effects on the pH of Water Based Drilling Mud and Mud Ph Concerns on the Environment. *FUPRE Journal of Scientific and Industrial Research*, 5(2):2021, 2021.

[23] Hany Gamal, Salaheldin Elkatatny, Salem Basfar, and Abdulaziz Al-Majed. Effect of pH on rheological and filtration properties of water-based drilling fluid based on bentonite. *Sustainability (Switzerland)*, 11(23):1–13, 2019.

[24] Abdelazim Abbas Ahmed, Ismail Mohd Saaid, Nur Asyraf Md Akhir, and Meysam Rashedi. Influence of various cation valence, salinity, pH and temperature on bentonite swelling behaviour. *AIP Conference Proceedings*, 1774(August 2023), 2016.

[25] Ryen Caenn and George V. Chillingar. Drilling fluids: State of the art. *Journal of Petroleum Science and Engineering*, 14(3-4):221–230, may 1996.

[26] Shu He, Lixi Liang, Yinjin Zeng, Yi Ding, Yongxue Lin, and Xiangjun Liu. The influence of water-based drilling fluid on mechanical property of shale and the wellbore stability. *Petroleum*, 2(1):61–66, mar 2016.

[27] Jose Aramendiz and Abdulmohsin Imqam. Silica and graphene oxide nanoparticle formulation to improve thermal stability and inhibition capabilities of water-based drilling fluid applied to Woodford shale. *SPE Drilling and Completion*, 35(2):164–179, jun 2020.

[28] A. Aftab, A. R. Ismail, Z. H. Ibupoto, H. Akeiber, and M. G.K. Malghani. Nanoparticles based drilling muds a solution to drill elevated temperature wells: A review, 2017.

[29] Mei Chun Li, Qinglin Wu, Kunlin Song, Sunyoung Lee, Chunde Jin, Suxia Ren, and Tingzhou Lei. Soy Protein Isolate As Fluid Loss Additive in Bentonite-Water-Based Drilling Fluids. *ACS Applied Materials and Interfaces*, 7(44):24799–24809, nov 2015.

[30] Himanshu Kesarwani, Amit Saxena, and Shivanjali Sharma. Novel Jatropha Oil Based Emulsion Drilling Mud Out performs Conventional Drilling Mud : A comparative study. *Energy Sources, Part A: Recovery, Utilization and Environmental Effects*, 2020.

[31] Mohamed Khodja, Jean Paul Canselier, Faiza Bergaya, Karim Fourar, Malika Khodja, Nathalie Cohaut, and Abdelbaki Benmounah. Shale problems and

water-based drilling fluid optimisation in the Hassi Messaoud Algerian oil field. *Applied Clay Science*, 49(4):383–393, 2010.

[32] R K Clark, R F Scheuerman, H Rath, and H G Van Laar. Polyacrylamide / Potassium-Chloride Mud for Drilling Water-Sensitive Shales. *Journal of Petroleum Technology*, pages 719–727, 1976.

[33] Wei-Zhong Chang and Yee-Kwong Leong. Ageing and collapse of bentonite gels—effects of Li, Na, K and Cs ions. *Rheologica Acta*, 53(2):109–122, feb 2014.

[34] Lili Yan, Chengbiao Wang, Bo Xu, Jinsheng Sun, Wen Yue, and Zexing Yang. Preparation of a novel amphiphilic comb-like terpolymer as viscosifying additive in low-solid drilling fluid. *Materials Letters*, 105:232–235, 2013.

[35] Binqiang Xie, Zhengsong Qiu, Weian Huang, Jie Cao, and Hanyi Zhong. Characterization and Aqueous Solution Behavior of Novel Thermo-associating Polymers. *Journal of Macromolecular Science, Part A*, 50(2):230–237, jan 2013.

[36] Dina Kania, Robiah Yunus, Rozita Omar, Suraya Abdul Rashid, and Badrul Mohamad Jan. A review of biolubricants in drilling fluids: Recent research, performance, and applications. *Journal of Petroleum Science and Engineering*, 135:177–184, nov 2015.

[37] H. Y. Zhong, Z. S. Qiu, W. A. Huang, J. Cao, F. W. Wang, and X. B. Zhang. An inhibition properties comparison of potassium chloride and polyoxypropylene diamine in water-based drilling fluid. *Petroleum Science and Technology*, 31(20):2127–2133, 2013.

[38] Qi Chu, Pingya Luo, Qingfeng Zhao, Junxiong Feng, Xubing Kuang, and Delong Wang. Application of a new family of organosilicon quadripolymer as a fluid loss additive for drilling fluid at high temperature. *Journal of Applied Polymer Science*, 128(1):28–40, apr 2013.

[39] Imtiaz Ali, Maqsood Ahmad, and Tarek Ganat. Experimental study of bentonite-free water based mud reinforced with carboxymethylated tapioca starch: Rheological modeling and optimization using response surface methodology (RSM). *Polymers*, 13(19), oct 2021.

[40] Camilo A. Franco, Carlos A. Franco, Richard D. Zabala, Ítalo Bahamón, Ángela Forero, and Farid B. Cortés. Field Applications of Nanotechnology in the Oil and Gas Industry: Recent Advances and Perspectives, dec 2021.

[41] Mehran Sadeghalvaad and Samad Sabbaghi. The effect of the TiO2/polyacrylamide nanocomposite on water-based drilling fluid properties. *Powder Technology*, 272:113–119, 2015.

[42] B. G. Chesser. Design Considerations for an Inhibitive, Stable Water-Based Mud System. *SPE Drilling Engineering*, 2(4):331–336, 1987.

[43] Goshtasp Cheraghian. Nanoparticles in drilling fluid: A review of the state-of-the-art. *Journal of Materials Research and Technology*, 13:737–753, jul 2021.

[44] M.-S. Liu, M. C.-C. Lin, I.-T. Huang, and C.-C. Wang. Enhancement of Thermal Conductivity with CuO for Nanofluids. *Chemical Engineering & Technology*, 29(1):72–77, jan 2006.

[45] Goshtasp Cheraghian, Qinglin Wu, Masood Mostofi, Mei Chun Li, Masoud Afrand, and Jitendra Shital Sangwai. Effect of a novel clay/silica nanocomposite on water-based drilling fluids: Improvements in rheological and filtration properties. *Colloids and Surfaces A: Physicochemical and Engineering Aspects*, 555:339–350, oct 2018.

[46] A. Aftab, A. R. Ismail, S. Khokhar, and Z. H. Ibupoto. Novel zinc oxide nanoparticles deposited acrylamide composite used for enhancing the performance of water-based drilling fluids at elevated temperature conditions. *Journal of Petroleum Science and Engineering*, 146:1142–1157, 2016.

[47] Swaminathan Ponmani, Jay Karen Maria William, Robello Samuel, R. Nagarajan, and Jitendra S. Sangwai. Formation and characterization of thermal and electrical properties of CuO and ZnO nanofluids in xanthan gum. *Colloids and Surfaces A: Physicochemical and Engineering Aspects*, 443:37–43, feb 2014.

[48] Ali Esfandyari Bayat and Reza Shams. Appraising the impacts of SiO2, ZnO and TiO2 nanoparticles on rheological properties and shale inhibition of water-based drilling muds. *Colloids and Surfaces A: Physicochemical and Engineering Aspects*, 581, nov 2019.

[49] Johanna Vargas, Leidy Johanna Roldán, Sergio Hernando Lopera, José Carlo Cardenas, Richard Disney Zabala, Camilo Andrés Franco, and Farid Bernardo Cortés. Effect of silica nanoparticles on thermal stability in bentonite free water-based drilling fluids to improve its rheological and filtration properties after aging process. *Offshore Technology Conference Brasil 2019, OTCB 2019*, 2020.

[50] Afeez O. Gbadamosi, Radzuan Junin, Yassir Abdalla, Augustine Agi, and Jeffrey O. Oseh. Experimental investigation of the effects of silica nanoparticle on hole cleaning efficiency of water-based drilling mud. *Journal of Petroleum Science and Engineering*, 172(June 2018):1226–1234, 2019.

[51] Richard O. Afolabi, Peter Paseda, Sedogan Hunjenukon, and Esther A. Oyeniyi. Model prediction of the impact of zinc oxide nanoparticles on the fluid loss of water-based drilling mud. *Cogent Engineering*, 5(1):1–14, 2018.

[52] Mostafa Keshavarz Moraveji, Ahmadreza Ghaffarkhah, Farough Agin, Mohsen Talebkeikhah, Amirhosein Jahanshahi, Alireza Kalantar, Saman Fazel Amirhosseini, Mohsen Karimifard, Seyed Iman Mortazavipour, Ali Akbari Sehat, and Mohammad Arjmand. Application of amorphous silica nanoparticles in improving the rheological properties, filtration and shale stability of

glycol-based drilling fluids. *International Communications in Heat and Mass Transfer*, 115:104625, jun 2020.

[53] Jianhang Xu, Aaron Wlaschin, and Robert M. Enick. Thickening Carbon Dioxide With the Fluoroacrylate-Styrene Copolymer. *SPE Journal*, 8(02):85–91, jun 2003.

[54] Henry Elochukwu, Raoof Gholami, and Sharul Sham Dol. An approach to improve the cuttings carrying capacity of nanosilica based muds. *Journal of Petroleum Science and Engineering*, 152(September 2016):309–316, 2017.

[55] Mortatha Al-Yasiri, Afrah Awad, Shahid Pervaiz, and Dongsheng Wen. Influence of silica nanoparticles on the functionality of water-based drilling fluids. *Journal of Petroleum Science and Engineering*, 179:504–512, aug 2019.

[56] Jose Aramendiz and Abdulmohsin Imqam. Water-based drilling fluid formulation using silica and graphene nanoparticles for unconventional shale applications. *Journal of Petroleum Science and Engineering*, 179:742–749, aug 2019.

[57] Hui Mao, Yan Yang, Hao Zhang, Jiang Zhang, and Yan Huang. A critical review of the possible effects of physical and chemical properties of subcritical water on the performance of water-based drilling fluids designed for ultra-high temperature and ultra-high pressure drilling applications. *Journal of Petroleum Science and Engineering*, 187(1):106795, 2020.

[58] Jeffrey O. Oseh, Norddin M.N.A. Mohd, Afeez O. Gbadamosi, Augustine Agi, Shafeeg O. Blkoor, Issham Ismail, Kevin C. Igwilo, and Anselm I. Igbafe. Polymer nanocomposites application in drilling fluids: A review. *Geoenergy Science and Engineering*, 222(November 2022):211416, 2023.

[59] Anirudh Bardhan, Sushipra Vats, Deepak Kumar Prajapati, Darshan Halari, Shivanjali Sharma, and Amit Saxena. Utilization of mesoporous nano-silica as high-temperature water-based drilling fluids additive: Insights into the fluid

loss reduction and shale stabilization potential. *Geoenergy Science and Engineering*, 232(Part A):212436, jan 2024.

[60] A. V. Minakov, E. I. Mikhienkova, Y. O. Voronenkova, A. L. Neverov, G. M. Zeer, and S. M. Zharkov. Systematic experimental investigation of filtration losses of drilling fluids containing silicon oxide nanoparticles. *Journal of Natural Gas Science and Engineering*, 71(May):102984, 2019.

[61] Johanna Vargas Clavijo, Ivan Moncayo-Riascos, Maen Husein, Sergio H. Lopera, Camilo A. Franco, and Farid B. Cortés. Theoretical and Experimental Approach for Understanding the Interactions among SiO2Nanoparticles, CaCO3, and Xanthan Gum Components of Water-Based Mud. *Energy and Fuels*, 35(6):4803–4814, mar 2021.

[62] M. T. Al-Saba, A. Al Fadhli, A. Marafi, A. Hussain, F. Bander, and M. F. Al Dushaishi. Application of nanoparticles in improving rheological properties of water based drilling fluids. *Society of Petroleum Engineers - SPE Kingdom of Saudi Arabia Annual Technical Symposium and Exhibition 2018, SATS 2018*, pages 1–10, 2018.

[63] Amirhossein Parizad and Khalil Shahbazi. Experimental investigation of the effects of SnO2 nanoparticles and KCl salt on a water base drilling fluid properties. *Canadian Journal of Chemical Engineering*, 94(10):1924–1938, 2016.

[64] Sean Robert Smith, Roozbeh Rafati, Amin Sharifi Haddad, Ashleigh Cooper, and Hossein Hamidi. Application of aluminium oxide nanoparticles to enhance rheological and filtration properties of water based muds at HPHT conditions. *Colloids and Surfaces A: Physicochemical and Engineering Aspects*, 537:361–371, jan 2018.

[65] Srawanti Medhi, Satyajit Chowdhury, Amit Kumar, Dharmender Kumar Gupta, Zenitha Aswal, and Jitendra S. Sangwai. Zirconium oxide nanoparticle as an effective additive for non-damaging drilling fluid: A study through rhe-

ology and computational fluid dynamics investigation. *Journal of Petroleum Science and Engineering*, 187, apr 2020.

[66] Ehsan Pakdaman, Shahriar Osfouri, Reza Azin, Khodabakhsh Niknam, and Abbas Roohi. Synthesis and characterization of hydrophilic gilsonite fine particles for improving water-based drilling mud properties. *Journal of Dispersion Science and Technology*, 41(11):1633–1642, sep 2020.

[67] Vryzas, Zisis, Arkoudeas, P., Mahmoud, O., Nasr-El-Din, H., and Kelessidis, V. Utilization of Iron Oxide Nanoparticles in Drilling Fluids Improves Fluid Loss and Formation Damage Characteristics. In *First EAGE Workshop on Well Injectivity & Productivity in Carbonates*, Doha, Qatar, 2015. European Association of Geoscientists and Engineers.

[68] Omar Mahmoud, Hisham A. Nasr-El-Din, Zisis Vryzas, and Vassilios C. Kelessidis. Nanoparticle-Based Drilling Fluids for Minimizing Formation Damage in HP/HT Applications. In *Day 1 Wed, February 24, 2016*. SPE, feb 2016.

[69] Md. Saiful Alam, Nayem Ahmed, and M.A. Salam. Study on rheology and filtration properties of field used mud using iron (III) oxide nanoparticles. *Upstream Oil and Gas Technology*, 7:100038, sep 2021.

[70] Zhihao Wang, Yuanpeng Wu, Pingya Luo, Yingpei Tian, Yuanhua Lin, and Qipeng Guo. Poly (sodium p-styrene sulfonate) modified Fe3O4 nanoparticles as effective additives in water-based drilling fluids. *Journal of Petroleum Science and Engineering*, 165:786–797, jun 2018.

[71] Rasan Faisal, Ibtisam Kamal, Namam Salih, and Alain Préat. Optimum formulation design and properties of drilling fluids incorporated with green uncoated and polymer-coated magnetite nanoparticles. *Arabian Journal of Chemistry*, 17(2):105492, feb 2024.

[72] Shama Perween, Nitu Kumari Thakur, Mukarram Beg, Shivanjali Sharma, and Amit Ranjan. Enhancing the properties of water based drilling fluid

using bismuth ferrite nanoparticles. *Colloids and Surfaces A: Physicochemical and Engineering Aspects*, 561:165–177, jan 2019.

[73] Mukarram Beg, Himanshu Kesarwani, and Shivanjali Sharma. Effect of CuO and ZnO Nanoparticles on Efficacy of Poly 4-Styrenesulfonic Acid-Co-Maleic Acid Sodium Salt for Controlling HPHT Filtration. In *Day 1 Mon, November 11, 2019*, Abu Dhabi, UAE, nov 2019. SPE.

[74] Adnan Aftab, Muhammad Ali, Muhammad Arif, Sallahudin Panhwar, Noori M.Cata Saady, Emad A. Al-Khdheeawi, Omar Mahmoud, Abdul Razak Ismail, Alireza Keshavarz, and Stefan Iglauer. Influence of tailor-made TiO2/API bentonite nanocomposite on drilling mud performance: Towards enhanced drilling operations. *Applied Clay Science*, 199(March):105862, 2020.

[75] Srawanti Medhi, Satyajit Chowdhury, Dharmender Kumar Gupta, and Aryab Mazumdar. An investigation on the effects of silica and copper oxide nanoparticles on rheological and fluid loss property of drilling fluids. *Journal of Petroleum Exploration and Production Technology*, 10(1):91–101, jan 2020.

[76] Shama Perween, Mukarram Beg, Ravi Shankar, Shivanjali Sharma, and Amit Ranjan. Effect of zinc titanate nanoparticles on rheological and filtration properties of water based drilling fluids. *Journal of Petroleum Science and Engineering*, 170:844–857, nov 2018.

[77] Pitchayut Dejtaradon, Hossein Hamidi, Michael Halim Chuks, David Wilkinson, and Roozbeh Rafati. Impact of ZnO and CuO nanoparticles on the rheological and filtration properties of water-based drilling fluid. *Colloids and Surfaces A: Physicochemical and Engineering Aspects*, 570:354–367, 2019.

[78] Ali Ghayedi and Arezoo Khosravi. Laboratory investigation of the effect of GO-ZnO nanocomposite on drilling fluid properties and its potential on H2S removal in oil reservoirs. *Journal of Petroleum Science and Engineering*, 184(November 2019):106684, 2020.

[79] R. Saboori, S. Sabbaghi, M. Barahoei, and M. Sahooli. Improvement of Thermal Conductivity Properties of Drilling Fluid by CuO Nanofluid. *Nano and Micro Scales*, 5(2):97–101, 2017.

[80] Adnan Aftab, Muhammad Ali, Muhammad Faraz Sahito, Udit Surya Mohanty, Nilesh Kumar Jha, Hamed Akhondzadeh, Muhammad Rizwan Azhar, Abdul Razak Ismail, Alireza Keshavarz, and Stefan Iglauer. Environmental Friendliness and High Performance of Multifunctional Tween 80/ZnO-Nanoparticles-Added Water-Based Drilling Fluid: An Experimental Approach. *ACS Sustainable Chemistry and Engineering*, 8(30):11224–11243, aug 2020.

[81] Rahmatallah Saboori, Samad Sabbaghi, Azim Kalantariasl, and Dariush Mowla. Improvement in filtration properties of water-based drilling fluid by nanocarboxymethyl cellulose/polystyrene core–shell nanocomposite. *Journal of Petroleum Exploration and Production Technology*, 8(2):445–454, jun 2018.

[82] Jamal Nasser, Anna Jesil, Tariq Mohiuddin, Majid Al Ruqeshi, Geetha Devi, and Shahjahan Mohataram. Experimental Investigation of Drilling Fluid Performance as Nanoparticles. *World Journal of Nano Science and Engineering*, 03(03):57–61, 2013.

[83] Yang Xuan, Guancheng Jiang, and Yingying Li. Nanographite Oxide as Ultrastrong Fluid-Loss-Control Additive in Water-Based Drilling Fluids. *Journal of Dispersion Science and Technology*, 35(10):1386–1392, 2014.

[84] Babak Fazelabdolabadi, Abbas Ali Khodadadi, and Mostafa Sedaghatzadeh. Thermal and rheological properties improvement of drilling fluids using functionalized carbon nanotubes. *Applied Nanoscience (Switzerland)*, 5(6):651–659, aug 2015.

[85] Lan Ma, Pingya Luo, Yi He, Liyun Zhang, Yi Fan, and Zhenju Jiang. Improving the stability of multi-walled carbon nano-tubes in extremely environments:

Applications as nano-plugging additives in drilling fluids. *Journal of Natural Gas Science and Engineering*, 74(November 2019), 2020.

[86] B. C. Liu, S. Q. Liu, Z. R. Chen, Q. N. Meng, and Chuang Li. Oxide and diamond nanoparticles modified drilling fluid for deep, complicated drilling conditions. *Journal of Nanoscience and Nanotechnology*, 16(12):13007–13013, 2016.

[87] Chengyi Wu, Dandan Wang, Huimin Wu, and Youmeng Dan. Synthesis and characterization of macroporous sodium alginate-g-poly(AA-co-DMAPMA) hydrogel. *Polymer Bulletin*, 73(12):3255–3269, dec 2016.

[88] Abdullah Özkan, Nilay Hayriye Asker, and Vildan Özkan. Experimental Investigation of MWCNTs Decorated with ZnO Nanoparticles as a Novel Additive in Conventional Water-based Drilling Mud. *ECS Journal of Solid State Science and Technology*, 10(9):091001, sep 2021.

[89] Dmitry V. Kosynkin, Gabriel Ceriotti, Kurt C. Wilson, Jay R. Lomeda, Jason T. Scorsone, Arvind D. Patel, James E. Friedheim, and James M. Tour. Graphene oxide as a high-performance fluid-loss-control additive in water-based drilling fluids. *ACS Applied Materials and Interfaces*, 4(1):222–227, jan 2012.

[90] Norasazly Mohd Taha, Sean Lee, and Scomi Kmc. IPTC-18539-MS Nano Graphene Application Improving Drilling Fluids Performance. Technical report, 2015.

[91] Abdul Razak Ismail, W. R. W Sulaiman, M. Z. Jaafar, A. Aftab, A. A. Razi, and Z. H. Ibupoto. The application of MWCNT to enhance the rheological behavior of drilling fluids at high temperature. *Malaysian Journal of Fundamental and Applied Sciences*, 12(3):95–98, 2017.

[92] Anirudh Bardhan, Ankit Singh, Harshwardhanam Nishanta, Shivanjali Sharma, Abhay Kumar Choubey, and Shailesh Kumar. Biogenic Copper Oxide

Nanoparticles for Improved Lubricity and Filtration Control in Water-Based Drilling Mud. *Energy & Fuels*, 38(10):8564–8578, may 2024.

[93] Jörg Stetefeld, Sean A. McKenna, and Trushar R. Patel. Dynamic light scattering: a practical guide and applications in biomedical sciences. *Biophysical Reviews*, 8(4):409–427, 2016.

[94] A. Einstein. Zur Elektrodynamik bewegter Körper. *Annalen der Physik*, 322(10):891–921, 1905.

[95] Mohd Omar Fatehah, Hamidi Abdul Aziz, and Serge Stoll. Stability of ZnO Nanoparticles in Solution. Influence of pH, Dissolution, Aggregation and Disaggregation Effects. *Journal of Colloid Science and Biotechnology*, 3(1):75–84, 2014.

[96] Ladan Rashidi. Magnetic nanoparticles: synthesis and characterization. In *Magnetic Nanoparticle-Based Hybrid Materials*, pages 3–32. Elsevier, 2021.

[97] P Scherrer. Nachr Ges wiss goettingen. *Math. Phys.*, 2:98–100, 1918.

[98] Anurag Pandey, Syed Feraz Qamar, Sumanta Das, Surita Basu, Himanshu Kesarwani, Amit Saxena, Shivanjali Sharma, and Jayati Sarkar. Advanced multiwall carbon nanotube-optimized surfactant-polymer flooding for enhanced oil recovery. *Fuel*, 355(August 2023):129463, jan 2024.

[99] A. Stanković, S. Dimitrijević, and D. Uskoković. Influence of size scale and morphology on antibacterial properties of ZnO powders hydrothemally synthesized using different surface stabilizing agents. *Colloids and Surfaces B: Biointerfaces*, 102:21–28, 2013.

[100] Stefan Christian Endres, Lucio Colombi Ciacchi, and Lutz Mädler. A review of contact force models between nanoparticles in agglomerates, aggregates, and films. *Journal of Aerosol Science*, 153:105719, mar 2021.

[101] American Petroleum Institute. Recommend Practice for Field Testing Water-Based Drilling Fluids - 13B-1, 2017.

[102] Eugene Cook Bingham. *Fluidity and plasticity*. Number 1992. McGraw-Hill.

[103] M. Enamul Hossain and Abdulaziz Abdullah Al-Majed. *Fundamentals of Sustainable Drilling Engineering*. John Wiley & Sons, Inc., Hoboken, NJ, USA, feb 2015.

[104] Jayachandran Perumalsamy, Pawan Gupta, and Jitendra S. Sangwai. Performance evaluation of esters and graphene nanoparticles as an additives on the rheological and lubrication properties of water-based drilling mud. *Journal of Petroleum Science and Engineering*, 204(October 2020):108680, 2021.

[105] OECD. *Global Plastics Outlook*. OECD, feb 2022.

[106] Anthony L. Andrady and Mike A. Neal. Applications and societal benefits of plastics. *Philosophical Transactions of the Royal Society B: Biological Sciences*, 364(1526):1977–1984, jul 2009.

[107] Chuanwei Zhuo and Yiannis A. Levendis. Upcycling waste plastics into carbon nanomaterials: A review, feb 2014.

[108] Aftab Hussain Arain, Syahrir Ridha, Suhaib Umer Ilyas, Mysara Eissa Mohyaldinn, and Raja Rajeswary Suppiah. Evaluating the influence of graphene nanoplatelets on the performance of invert emulsion drilling fluid in high-temperature wells. *Journal of Petroleum Exploration and Production Technology*, apr 2022.

[109] Anirudh Bardhan. Graphene as a Surfactant Carrier: A Performance Study for Enhanced Oil Recovery Applications. In *SPE Annual Technical Conference and Exhibition*, page 204263. SPE, oct 2020.

[110] A K Geim and K S Novoselov. The rise of graphene. *Nature Materials*, 6(3):183–191, 2007.

[111] Seyed Hasan Hajiabadi, Hamed Aghaei, Mahdieh Ghabdian, Mina Kalateh-Aghamohammadi, Ehsan Esmaeilnezhad, and Hyoung Jin Choi. On the attributes of invert-emulsion drilling fluids modified with graphene oxide/inorganic complexes. *Journal of Industrial and Engineering Chemistry*, 93:290–301, jan 2021.

[112] Chai Yee Ho, Suzana Yusup, Chok Vui Soon, and Mohamad Taufiq Arpin. Rheological Behaviour of Graphene Nano-sheets in Hydrogenated Oil-based Drilling Fluid. *Procedia Engineering*, 148:49–56, 2016.

[113] H. Gudarzifar, S. Sabbaghi, A. Rezvani, and R. Saboori. Experimental investigation of rheological & filtration properties and thermal conductivity of water-based drilling fluid enhanced. *Powder Technology*, 368:323–341, may 2020.

[114] Rabia Ikram, Badrul Mohamed Jan, Jana Vejpravova, M. Iqbal Choudhary, and Zaira Zaman Chowdhury. Recent Advances of Graphene-Derived Nanocomposites in Water-Based Drilling Fluids. *Nanomaterials*, 10(10):2004, oct 2020.

[115] Eny Kusrini, Felix Oktavianto, Anwar Usman, Dias Puspitaning Mawarni, and Muhammad Idrus Alhamid. Synthesis, characterization, and performance of graphene oxide and phosphorylated graphene oxide as additive in water-based drilling fluids. *Applied Surface Science*, 506, mar 2020.

[116] Srawanti Medhi, Satyajit Chowdhury, Naman Bhatt, Dharmendra K. Gupta, Sravendra Rana, and Jitendra S. Sangwai. Analysis of high performing graphene oxide nanosheets based non-damaging drilling fluids through rheological measurements and CFD studies. *Powder Technology*, 377:379–395, jan 2021.

[117] Ali Rafieefar, Farhad Sharif, Abdolnabi Hashemi, and Ali Mohammad Bazargan. Rheological Behavior and Filtration of Water-Based Drilling Fluids

Containing Graphene Oxide: Experimental Measurement, Mechanistic Understanding, and Modeling. *ACS Omega*, 6(44):29905–29920, nov 2021.

[118] Jiankang Guo, Jienian Yan, Weiwang Fan, and Hongjing Zhang. Applications of strongly inhibitive silicate-based drilling fluids in troublesome shale formations in Sudan. *Journal of Petroleum Science and Engineering*, 50(3-4):195–203, mar 2006.

[119] Hazlina Husin, Khaled Abdalla Elraies, Hyoung Jin Choi, and Zachary Aman. Influence of graphene nanoplatelet and silver nanoparticle on the rheological properties of water-based mud. *Applied Sciences (Switzerland)*, 8(8), aug 2018.

[120] Azeem Rana, Ibrahim Khan, Shahid Ali, Tawfik A. Saleh, and Safyan A. Khan. Controlling shale swelling and fluid loss properties of water-based drilling Mud via ultrasonic impregnated SWCNTs/PVP nanocomposites. *Energy and Fuels*, 34(8):9515–9523, aug 2020.

[121] E VanOort, search Rijswijk, D Ripley, I Ward, JW Chapman, BW Mud Aberdeen, R Wtlhamson, Mobtl NSL Aberdeen, and M Aston. IADC/SPE 35059 Silica.te-Based Drilling Fluids: Competent, Cost-effective and Benign Solut1ons to Wellbore Stability Problems* BP Exploration (XTP) Sunbury *SPE Members **IADC Members * SPE members. Technical report, 1996.

[122] Sandeep Pandey, Manoj Karakoti, Sunil Dhali, Neha Karki, Boddepalli SanthiBhushan, Chetna Tewari, Sravendra Rana, Anurag Srivastava, Anand B. Melkani, and Nanda Gopal Sahoo. Bulk synthesis of graphene nanosheets from plastic waste: An invincible method of solid waste management for better tomorrow. *Waste Management*, 88:48–55, 2019.

[123] Anjanay Pandey, Krishna Raghav Chaturvedi, Japan Trivedi, and Tushar Sharma. Assessment of polymer based carbonation in weak/strong alkaline media for energy production and carbon storage: An approach to address carbon emissions. *Journal of Cleaner Production*, 328(June):129628, 2021.

[124] Nanda Gopal Sahoo, Sandeep Pandey, Manoj Karakoti, and V D Punetha. A process of Manufacturing Graphene, 2016.

[125] Yi Shen and Baoliang Chen. Sulfonated Graphene Nanosheets as a Superb Adsorbent for Various Environmental Pollutants in Water. *Environmental Science and Technology*, 49(12):7364–7372, jun 2015.

[126] Baghir Suleimanov, Elchin Veliyev, and Vladimir Vishnyakov. *Nanocolloids for petroleum engineering : fundamentals and practices*. 2022.

[127] G. Srinivas, Yanwu Zhu, Richard Piner, Neal Skipper, Mark Ellerby, and Rod Ruoff. Synthesis of graphene-like nanosheets and their hydrogen adsorption capacity. *Carbon*, 48(3):630–635, mar 2010.

[128] S. Q. Liu, Z. R. Chen, Q. N. Meng, H. L. Zhou, C. Li, and B. C. Liu. Effect of Graphene and Graphene Oxide Addition on Lubricating and Friction Properties of Drilling Fluids. *Nanoscience and Nanotechnology Letters*, 9(4):446–452, apr 2017.

[129] Rabia Ikram, Badrul Mohamed Jan, Akhmal Sidek, and George Kenanakis. Utilization of eco-friendly waste generated nanomaterials in water-based drilling fluids: state of the art review, aug 2021.

[130] Mansoor Ali Khan, Hikmat Said Al-Salim, and Leila Niloofar Arsanjani. Development of high temperature pressure (HTHP) water based drilling mud using synthetic polymers, and nanoparticles. *Journal of Advanced Research in Fluid Mechanics and Thermal Sciences*, 47(1):172–182, 2018.

[131] Koorosh Tookallo. Analyzing Effects of Various Kinds of Multi-Wall Carbo Nanotubes (MWCNT) on Performance of Water Base Mud (WBM). *COJ Reviews and Research*, 1(2):1–11, 2018.

[132] Seyed Hasan Hajiabadi, Hamed Aghaei, Mina Kalateh-Aghamohammadi, and Marzieh Shorgasthi. An overview on the significance of carbon-based nanomaterials in upstream oil and gas industry, mar 2020.

[133] Takahiro Maruyama. Carbon nanotubes. In *Handbook of Carbon-Based Nanomaterials*, pages 299–319. Elsevier, 2021.

[134] Jian Wang, Yingzhong Yuan, Liehui Zhang, and Ruihe Wang. The influence of viscosity on stability of foamy oil in the process of heavy oil solution gas drive. *Journal of Petroleum Science and Engineering*, 66(1-2):69–74, may 2009.

[135] Abdul Razak Ismail, Wan Rosli Wan Sulaiman, Mohd Zaidi Jaafar, Issham Ismail, and Elisabet Sabu Hera. Nanoparticles performance as fluid loss additives in water based drilling fluids. *Materials Science Forum*, 864:189–193, 2016.

[136] Emeka E. Okoro, Anita A. Zuokumor, Ikechukwu S. Okafor, Kevin C. Igwilo, and Kale B. Orodu. Determining the optimum concentration of multiwalled carbon nanotubes as filtrate loss additive in field-applicable mud systems. *Journal of Petroleum Exploration and Production Technology*, 10(2):429–438, 2020.

[137] Muhammad Awais Ashfaq Alvi, Mesfin Belayneh, Arild Saasen, and Sulalit Bandyopadhyay. Impact of Various Nanoparticles on the Viscous Properties of Water Based Drilling Fluids. In *Volume 10: Petroleum Technology*, pages 1–11. American Society of Mechanical Engineers, jun 2021.

[138] Roozbeh Rafati, Sean Robert Smith, Amin Sharifi Haddad, Rizky Novara, and Hossein Hamidi. Effect of nanoparticles on the modifications of drilling fluids properties: A review of recent advances, feb 2018.

[139] E. I. Lysakova, A. D. Skorobogatova, A. L. Neverov, M. I. Pryazhnikov, V. Ya. Rudyak, and A. V. Minakov. A comprehensive study of the effect of multiwalled carbon nanotubes as an additive on the properties of oil-based drilling fluids. *Journal of Materials Science*, 59(11):4513–4532, mar 2024.

[140] Anurag Pandey, Syed Feraz Qamar, Sumanta Das, Surita Basu, Himanshu Kesarwani, Amit Saxena, Shivanjali Sharma, and Jayati Sarkar. Advanced multi-

wall carbon nanotube-optimized surfactant-polymer flooding for enhanced oil recovery. *Fuel*, 355:129463, jan 2024.

[141] A. Tomova, G. Gentile, A. Grozdanov, M. E. Errico, P. Paunovic, M. Avella, and A. T. Dimitrov. Functionalization and characterization of MWCNT produced by different methods. *Acta Physica Polonica A*, 129(3):405–408, 2016.

[142] D. G. Larrude, P. Ayala, M. E.H. Maia Da Costa, and F. L. Freire. Multiwalled carbon nanotubes decorated with cobalt oxide nanoparticles. *Journal of Nanomaterials*, 2012(March 2012), 2012.

[143] S. Costa, E. Borowiak-Palen, M. Kruszyñska, A. Bachmatiuk, and R. J. Kaleńczuk. Characterization of carbon nanotubes by Raman spectroscopy. *Materials Science- Poland*, 26(2):433–441, 2008.

[144] M. Zdrojek, W. Gebicki, C. Jastrzebski, T. Melin, and A. Huczko. Studies of multiwall carbon nanotubes using raman spectroscopy and atomic force microscopy. *Solid State Phenomena*, 99-100(May 2014):265–268, 2004.

[145] Gennady J. Kabo, Eugene Paulechka, Andrey V. Blokhin, Olga V. Voitkevich, Tatsiana Liavitskaya, and Andrey G. Kabo. Thermodynamic properties and similarity of stacked-cup multiwall carbon nanotubes and graphite. *Journal of Chemical and Engineering Data*, 61(11):3849–3857, 2016.

[146] Mojtaba Moazzen, Amin Mousavi Khaneghah, Nabi Shariatifar, Mahsa Ahmadloo, Ismail Eş, Abbas Norouzian Baghani, Saeed Yousefinejad, Mahmood Alimohammadi, Ali Azari, Sina Dobaradaran, Noushin Rastkari, Shahrokh Nazmara, Mahdieh Delikhoon, and GholamReza Jahed Khaniki. Multi-walled carbon nanotubes modified with iron oxide and silver nanoparticles (MWCNT-Fe3O4/Ag) as a novel adsorbent for determining PAEs in carbonated soft drinks using magnetic SPE-GC/MS method. *Arabian Journal of Chemistry*, 12(4):476–488, may 2019.

[147] Won-Chun Oh, Feng-Jun Zhang, and Ming-Liang Chen. Characterization and photodegradation characteristics of organic dye for Pt–titania combined multi-walled carbon nanotube composite catalysts. *Journal of Industrial and Engineering Chemistry*, 16(2):321–326, mar 2010.

[148] Zhaoguang Yuan, Jerome Schubert, Catalin Teodoriu, and Paolo Gardoni. HPHT Gas Well Cementing Complications and its Effect on Casing Collapse Resistance. In *SPE Oil and Gas India Conference and Exhibition, Mumbai, India*. SPE, mar 2012.

[149] Hitoshi Yusa and Tetsu Watanuki. X-ray diffraction of multiwalled carbon nanotube under high pressure: Structural durability on static compression. *Carbon*, 43(3):519–523, 2005.

[150] M.S.P. Shaffer, X. Fan, and A.H. Windle. Dispersion and packing of carbon nanotubes. *Carbon*, 36(11):1603–1612, nov 1998.

[151] V. Datsyuk, M. Kalyva, K. Papagelis, J. Parthenios, D. Tasis, A. Siokou, I. Kallitsis, and C. Galiotis. Chemical oxidation of multiwalled carbon nanotubes. *Carbon*, 46(6):833–840, may 2008.

[152] Yoon Jin Kim, Taek Sun Shin, Hyung Do Choi, Jong Hwa Kwon, Yeon-Choon Chung, and Ho Gyu Yoon. Electrical conductivity of chemically modified multiwalled carbon nanotube/epoxy composites. *Carbon*, 43(1):23–30, 2005.

[153] Juan Amaro-Gahete, Almudena Benítez, Rocío Otero, Dolores Esquivel, César Jiménez-Sanchidrián, Julián Morales, Álvaro Caballero, and Francisco J. Romero-Salguero. A comparative study of particle size distribution of graphene nanosheets synthesized by an ultrasound-assisted method. *Nanomaterials*, 9(2), feb 2019.

[154] T. I.T. Okpalugo, P. Papakonstantinou, H. Murphy, J. McLaughlin, and N. M.D. Brown. High resolution XPS characterization of chemical functionalised MWCNTs and SWCNTs. *Carbon*, 43(1):153–161, 2005.

[155] Harry Bennettand and Graham J Ouver. High Resolution XPS of Organic Polymers. *Journal of Chemical Education*, 73(4):A92, apr 1996.

[156] Yuexin Tian, Xiangjun Liu, Pingya Luo, Jinjun Huang, Jian Xiong, Lixi Liang, and Wenfei Li. Study of a Polyamine Inhibitor Used for Shale Water-Based Drilling Fluid. *ACS Omega*, 6(23):15448–15459, jun 2021.

[157] Hanqing Chen, Bing Wang, Di Gao, Ming Guan, Lingna Zheng, Hong Ouyang, Zhifang Chai, Yuliang Zhao, and Weiyue Feng. Broad-spectrum antibacterial activity of carbon nanotubes to human gut bacteria. *Small*, 9(16):2735–2746, 2013.

[158] Boldoo, Ham, and Cho. Comparison Study on Photo-Thermal Energy Conversion Performance of Functionalized and Non-Functionalized MWCNT Nanofluid. *Energies*, 12(19):3763, oct 2019.

[159] Krishna Raghav Chaturvedi, Rakesh Kumar, Japan Trivedi, James J. Sheng, and Tushar Sharma. Stable Silica Nanofluids of an Oilfield Polymer for Enhanced CO 2 Absorption for Oilfield Applications. *Energy & Fuels*, 32(12):12730–12741, dec 2018.

[160] Min Hoon Baik and Seung Yeop Lee. Colloidal stability of bentonite clay considering surface charge properties as a function of pH and ionic strength. *Journal of Industrial and Engineering Chemistry*, 16(5):837–841, 2010.

[161] Benjamin Werner, Velaug Myrseth, and Arild Saasen. Viscoelastic properties of drilling fluids and their influence on cuttings transport. *Journal of Petroleum Science and Engineering*, 156(December 2016):845–851, 2017.

[162] Pengxiang Xu, Jiaping Lin, and Liangshun Zhang. Distinct Viscoelasticity of Nanoparticle-Tethering Polymers Revealed by Nonequilibrium Molecular Dynamics Simulations. *The Journal of Physical Chemistry C*, 121(50):28194–28203, dec 2017.

[163] Mursal Zeynalli, Muhammad Mushtaq, Emad W. Al-Shalabi, Umar Alfazazi, Anas M. Hassan, and Waleed AlAmeri. *A comprehensive review of viscoelastic polymer flooding in sandstone and carbonate rocks*, volume 13. Nature Publishing Group UK, 2023.

[164] Lixian Song, Shalin Patil, Yingze Song, Liang Chen, Fucheng Tian, Le Chen, Xueyu Li, Liangbin Li, and Shiwang Cheng. Nanoparticle Clustering and Viscoelastic Properties of Polymer Nanocomposites with Non-Attractive Polymer-Nanoparticle Interactions. *Macromolecules*, 2022.

[165] M Sedaghatzadeh, A A Khodadadi, and M R Tahmasebi Birgani. An Improvement in Thermal and Rheological Properties of Water-based Drilling Fluids Using Multiwall Carbon Nanotube (MWCNT). *Iranian Journal of Oil & Gas Science and Technology*, 1(1):55–65, 2012.

[166] Mukarram Beg. *Design of Water Based Drilling Fluids for Fluid Loss Reduction and Shale Stabilization*. PhD thesis, Rajiv Gandhi Institute of Petroleum Technology, Jais, 2021.

[167] Jay Karen Maria William, Swaminathan Ponmani, Robello Samuel, R. Nagarajan, and Jitendra S. Sangwai. Effect of CuO and ZnO nanofluids in xanthan gum on thermal, electrical and high pressure rheology of water-based drilling fluids. *Journal of Petroleum Science and Engineering*, 117:15–27, 2014.

[168] Yuan Lin, Qizhong Tian, Peiwen Lin, Xinghui Tan, Huaitao Qin, and Jiawang Chen. Effect of Nanoparticles on Rheological Properties of Water-Based Drilling Fluid. *Nanomaterials*, 13(14):2092, jul 2023.

[169] Afrah Atri, Mosaab Echabaane, Amel Bouzidi, Imen Harabi, Bernabe Mari Soucase, and Rafik Ben Chaâbane. Green synthesis of copper oxide nanoparticles using Ephedra Alata plant extract and a study of their antifungal, antibacterial activity and photocatalytic performance under sunlight. *Heliyon*, 9(2):1–16, 2023.

[170] O. Anwar Bég, D. E.Sanchez Espinoza, Ali Kadir, Md Shamshuddin, and Ayesha Sohail. Experimental study of improved rheology and lubricity of drilling fluids enhanced with nano-particles. *Applied Nanoscience (Switzerland)*, 8(5):1069–1090, 2018.

[171] Arif Nazir, Mohsan Raza, Mazhar Abbas, Shaista Abbas, Abid Ali, Zahid Ali, Umer Younas, Samiah H. Al-Mijalli, and Munawar Iqbal. Microwave assisted green synthesis of ZnO nanoparticles using Rumex dentatus leaf extract: photocatalytic and antibacterial potential evaluation. *Zeitschrift für Physikalische Chemie*, 236(9):1203–1217, sep 2022.

[172] Elwy A. Mohamed. Green synthesis of copper & copper oxide nanoparticles using the extract of seedless dates. *Heliyon*, 6(1):e03123, 2020.

[173] Kiran Kumar Prem Kumar, Nandipura D. Dinesh, and Satish Kumar Murari. Microwave assisted green synthesis of ZnO and Ag doped ZnO nanoparticles as antifungal and antibacterial agents using Colocasia esculenta leaf extract. *International Journal of Nanoparticles*, 11(3):239–263, 2019.

[174] K. Parvathalu, K. Rajitha, B. Chandrashekar, K. Sathvik, K. Pranay Bhasker, B. Sreenivas, M. Pritam, P. Pushpalatha, K. Moses, and P. Bala Bhaskar. Biomimetic Synthesis of Copper Nanoparticles Using Tinospora Cordifolia Plant Leaf Extract for Photocatalytic Activity Applications. *Plasmonics*, 2023.

[175] Deepak Kumar Prajapati, Anirudh Bardhan, and Shivanjali Sharma. Microwave-assisted synthesis of zinc oxide nanoflowers for improving the rheological and filtration performance of high-temperature water-based drilling fluids. *Journal of Dispersion Science and Technology*, 0(0):1–13, dec 2023.

[176] Shalu Yadav, Ankit Singh, and Abhay Kumar Choubey. Composition dependent variation in structural, morphological, optical and magnetic properties of

biogenic CuO/NiO mixed oxides nanoparticles. *Journal of Alloys and Compounds*, 979:173422, apr 2024.

[177] Preeti Dauthal and Mausumi Mukhopadhyay. Noble Metal Nanoparticles: Plant-Mediated Synthesis, Mechanistic Aspects of Synthesis, and Applications. *Industrial & Engineering Chemistry Research*, 55(36):9557–9577, sep 2016.

[178] Sk Mehebub Rahaman, Anirudh Bardhan, Trishna Mandal, Madhuparna Chakraborty, Kripasindhu Karmakar, Subhendu Dhibar, Shivanjali Sharma, Manab Chakravarty, Samia M. Ibrahim, and Bidyut Saha. Understanding the effect of surfactants' hydrophobicity on the growth of lanthanum sulfide nanospheres in water-in-oil microemulsions: a detailed dynamic light scattering, small angle X-ray scattering, and microscopy study. *New Journal of Chemistry*, 47(21):10309–10321, 2023.

[179] Sk Mehebub Rahaman, Madhuparna Chakraborty, Sandip Kundu, Subhendu Dhibar, Dileep Kumar, Samia M. Ibrahim, Manab Chakravarty, and Bidyut Saha. Controlled synthesis of samarium trifluoride nanoparticles in a water-in-oil microemulsion: Effects of water-to-surfactant ratio on particles and phosphate removal. *Journal of Hazardous Materials Advances*, 11:100348, aug 2023.

[180] Damian C. Onwudiwe. Microwave-assisted synthesis of PbS nanostructures. *Heliyon*, 5(3):e01413, 2019.

[181] Hengbo Yin, Tetsushi Yamamoto, Yuji Wada, and Shozo Yanagida. Large-scale and size-controlled synthesis of silver nanoparticles under microwave irradiation. *Materials Chemistry and Physics*, 83(1):66–70, jan 2004.

[182] Jignasa N. Solanki and Zagabathuni Venkata Panchakshari Murthy. Reduction of Nitro Aromatic Compounds over Ag/Al 2 O 3 Nanocatalyst Prepared in Water-in-Oil Microemulsion: Effects of Water-to-Surfactant Mole Ratio

and Type of Reducing Agent. *Industrial & Engineering Chemistry Research*, 50(12):7338–7344, jun 2011.

[183] Guang Wei Lu and Ping Gao. *Emulsions and Microemulsions for Topical and Transdermal Drug Delivery*. 2010.

[184] Vânia Serrão Sousa and Margarida Ribau Teixeira. Aggregation kinetics and surface charge of CuO nanoparticles: The influence of pH, ionic strength and humic acids. *Environmental Chemistry*, 10(4):313–322, 2013.

[185] A B Bodade, M A Taiwade, and G N Chaudhari. Bioelectrode based chitosan-nano copper oxide for application to lipase biosensor. *Journal of Applied Pharmaceutical Research (JAPTRonline*, 5(1):30–39, 2017.

[186] Srawanti Medhi, Satyajit Chowdhury, Jitendra S. Sangwai, and Dharmender Kumar Gupta. Effect of Al2O3 nanoparticle on viscoelastic and filtration properties of a salt-polymer-based drilling fluid. *Energy Sources, Part A: Recovery, Utilization and Environmental Effects*, 2019.

[187] Mohammed Al-Shargabi, Shadfar Davoodi, David A. Wood, Ameen Al-Musai, Valeriy S. Rukavishnikov, and Konstantin M. Minaev. Nanoparticle applications as beneficial oil and gas drilling fluid additives: A review. *Journal of Molecular Liquids*, 352:118725, 2022.

[188] E. I. Mikhienkova, S. V. Lysakov, A. L. Neverov, V. A. Zhigarev, A. V. Minakov, and V. Ya Rudyak. Experimental study on the influence of nanoparticles on oil-based drilling fluid properties. *Journal of Petroleum Science and Engineering*, 208(PB):109452, 2022.

[189] Maen Moh'd Husein, Mohammad F. Zakaria, and Geir Hareland. Novel Nanoparticle-Containing Drilling Fluids to Mitigate Fluid Loss, 2013.

[190] Abdul Razak Ismail, Tan Chee Seong, Nor Aziah Buang, Wan Rosli, and Wan Sulaiman. Improve Performance of Water-based Drilling Fluids. *Sriwi-*

jaya International Seminar on Energy-Environmental Science and Technology, 1(1):43–47, 2014.

[191] Tianle Liu, Guosheng Jiang, Ping Zhang, Jiaxin Sun, Huicui Sun, Ren Wang, and Mingming Zheng. A new low-cost drilling fluid for drilling in natural gas hydrate-bearing sediments. *Journal of Natural Gas Science and Engineering*, 33:934–941, jul 2016.

[192] Azim Kalantariasl, Abbas Zeinijahromi, and Pavel Bedrikovetsky. SPE 168144 External Filter Cake Buildup in Dynamic Filtration: Mechanisms and Key Factors. Technical report, 2014.

[193] Yeoh Jun Jie Jason, Heoy Geok How, Yew Heng Teoh, and Hun Guan Chuah. A study on the tribological performance of nanolubricants. *Processes*, 8(11):1–33, 2020.

[194] Ehsan Pakdaman, Shahriar Osfouri, Reza Azin, Khodabakhsh Niknam, and Abbas Roohi. Improving the rheology, lubricity, and differential sticking properties of water-based drilling muds at high temperatures using hydrophilic Gilsonite nanoparticles. *Colloids and Surfaces A: Physicochemical and Engineering Aspects*, 582, dec 2019.

[195] Corina Birleanu, Marius Pustan, Mircea Cioaza, Andreia Molea, Florin Popa, and Glad Contiu. Effect of TiO2 nanoparticles on the tribological properties of lubricating oil: an experimental investigation. *Scientific Reports*, 12(1):1–17, 2022.

[196] Jacek Wojnarowicz, Tadeusz Chudoba, and Witold Lojkowski. A review of microwave synthesis of zinc oxide nanomaterials: Reactants, process parameters and morphoslogies. *Nanomaterials*, 10(6), 2020.

[197] Srawanti Medhi, D. K. Gupta, and Jitendra S. Sangwai. Impact of zinc oxide nanoparticles on the rheological and fluid-loss properties, and the hydraulic

performance of non-damaging drilling fluid. *Journal of Natural Gas Science and Engineering*, 88, apr 2021.

[198] Pitchayut Dejtaradon, Hossein Hamidi, Michael Halim Chuks, David Wilkinson, and Roozbeh Rafati. Impact of ZnO and CuO nanoparticles on the rheological and filtration properties of water-based drilling fluid. *Colloids and Surfaces A: Physicochemical and Engineering Aspects*, 570:354–367, jun 2019.

[199] J. Abdo, R. Zaier, E. Hassan, H. AL-Sharji, and A. Al-Shabibi. ZnO–clay nanocomposites for enhance drilling at HTHP conditions. *Surface and Interface Analysis*, 46(10-11):970–974, oct 2014.

[200] Muhammad Hasibul Ahasan, Md Fazla Alahi Alvi, Nayem Ahmed, and Md Saiful Alam. An investigation of the effects of synthesized zinc oxide nanoparticles on the properties of water-based drilling fluid. *Petroleum Research*, 7(1):131–137, 2022.

[201] M. Danish Haneef and J. Abdo. Growth of ZnO nanorods in clay matrix to ensure uniform dispersion in drilling fluids. *Technical Proceedings of the 2012 NSTI Nanotechnology Conference and Expo, NSTI-Nanotech 2012*, 1:652–655, 2012.

[202] Melanie M. Tomczak, Maneesh K. Gupta, Lawrence F. Drummy, Sophie M. Rozenzhak, and Rajesh R. Naik. Morphological control and assembly of zinc oxide using a biotemplate. *Acta Biomaterialia*, 5(3):876–882, 2009.

[203] Kai Dai, Guangping Zhu, Zhongliang Liu, Qingzhuang Liu, Zheng Chen, and Luhua Lu. Facile preparation and growth mechanism of zinc oxide nanopencils. *Materials Letters*, 67(1):193–195, 2012.

[204] Yude Wang, Xiaoyan Cai, Bingqian Han, Shaojuan Deng, Yan Wang, Chengjun Dong, and Igor Djerdj. Hydrothermal growth of ZnO nanorods on Zn substrates and their application in degradation of azo dyes under ambient conditions. *CrystEngComm*, 16(33):7761–7770, 2014.

[205] Q. Ahsanulhaq, A. Umar, and Y. B. Hahn. Growth of aligned ZnO nanorods and nanopencils on ZnO/Si in aqueous solution: Growth mechanism and structural and optical properties. *Nanotechnology*, 18(11), 2007.

[206] Ruri Agung Wahyuono, Christa Schmidt, Andrea Dellith, Jan Dellith, Martin Schulz, Martin Seyring, Markus Rettenmayr, Jonathan Plentz, and Benjamin Dietzek. ZnO nanoflowers-based photoanodes: Aqueous chemical synthesis, microstructure and optical properties. *Open Chemistry*, 14(1):158–169, 2016.

[207] Anirudh Bardhan, Ankit Singh, Harshwardhanam Nishanta, Shivanjali Sharma, Abhay Kumar Choubey, and Shailesh Kumar. Biogenic Copper Oxide Nanoparticles for Improved Lubricity and Filtration Control in Water-Based Drilling Mud. *Energy & Fuels*, 38(10):8564–8578, may 2024.

[208] Mahesh Chandra Patel, Mohammed Abdalla Ayoub, Anas Mohammed Hassan, and Mazlin Bt Idress. A Novel ZnO Nanoparticles Enhanced Surfactant Based Viscoelastic Fluid Systems for Fracturing under High Temperature and High Shear Rate Conditions: Synthesis, Rheometric Analysis, and Fluid Model Derivation. *Polymers*, 14(19):4023, sep 2022.

[209] Mortadha T. Alsaba, Mohammed F. Al Dushaishi, and Ahmed K. Abbas. Application of nano water-based drilling fluid in improving hole cleaning. *SN Applied Sciences*, 2(5):1–7, 2020.

[210] Muili Feyisitan Fakoya and Subhash Nandlal Shah. Rheological properties of surfactant-based and polymeric nano-fluids. In *Society of Petroleum Engineers - Coiled Tubing and Well Intervention Conference and Exhibition 2013*, pages 321–337, Texas, 2013.

[211] Yili Kang, Jiping She, Hao Zhang, Lijun You, and Minggu Song. Strengthening shale wellbore with silica nanoparticles drilling fluid. *Petroleum*, 2(2):189–195, jun 2016.

[212] Mustafa Verşan Kök and Berk Bal. Effects of silica nanoparticles on the performance of water-based drilling fluids. *Journal of Petroleum Science and Engineering*, 180(May):605–614, 2019.

[213] Saket M. Javeri, Zishaan W. Haindade, and Chaitanya B. Jere. Mitigating Loss Circulation And Differential Sticking Problems Using Silicon Nanoparticles. In *SPE/IADC Middle East Drilling Technology Conference and Exhibition, Muscat, Oman*. SPE, oct 2011.

[214] Zisis Vryzas, Lori Nalbandian, Vassilis T. Zaspalis, and Vassilios C. Kelessidis. How different nanoparticles affect the rheological properties of aqueous Wyoming sodium bentonite suspensions. *Journal of Petroleum Science and Engineering*, 173:941–954, feb 2019.

[215] Anwar Ahmed, Erum Pervaiz, and Tayyaba Noor. Applications of Emerging Nanomaterials in Drilling Fluids. *ChemistrySelect*, 7(43), nov 2022.

[216] Neetish Kumar Maurya, Prabhakar Kushwaha, and Ajay Mandal. Studies on interfacial and rheological properties of water soluble polymer grafted nanoparticle for application in enhanced oil recovery. *Journal of the Taiwan Institute of Chemical Engineers*, 70:319–330, 2016.

Anirudh Bardhan

Drilling Fluids Design Laboratory
Department of Petroleum Engineering & Geoengineering
Rajiv Gandhi Institute of Petroleum Technology, Jais
Phone: (+91) 9872494478
Email: anirudhb@rgipt.ac.in
ORCID: 0000-0001-8320-505X
www.linkedin.com/in/anirudh-bardhan

EDUCATION

Ph.D. Petroleum Engineering	Rajiv Gandhi Institute of Petroleum Technology Jais, India	2024
M.Tech Petroleum Engineering	Pandit Deendayal Energy University Gandhinagar, India	2020
B.E. Petroleum Engineering	Chandigarh University Mohali, India	2018

HONORS AND AWARDS

1st Place Master's Div, South Asia	SPE Regional Student Paper Contest Society of Petroleum Engineers International	2020
SPI 10/10 3rd and 4th Semester	M.Tech. Petroleum Engineering Pandit Deendayal Energy University, India	2020
Rank 2 by Merit	B.E. Petroleum Engineering Chandigarh University, India	2018
INSPIRE Award	Kendriya Vidyalaya Garden Reach Department of Science and Technology, India	2020

RESEARCH EXPERIENCE

2021-Present

Senior Research Fellow, Drilling Fluids Design Laboratory
Rajiv Gandhi Institute of Petroleum Technology, India
Advisors: Dr. Shivanjali Sharma and Dr. Shailesh Kumar
Thesis: *Multifunctional Nano Additives for High-Performance Drilling Fluids: An Experimental Investigation for High-Temperature Applications*

2019-2020

Graduate Research Assistant, School of Petroleum Technology
Pandit Deendayal Energy University, India
Advisors: Dr. Shivakumar P.
Dissertation: *Graphene - A Potential Surfactant Carrier for Enhanced Oil Recovery Applications*

EXPERIENCE

2021-Present

Teaching/Research Assistant, Petroleum Engingeering and Geoengineering
Rajiv Gandhi Institute of Petroleum Technology, India

- Helped establish the Undergraduate Reservoir Engineering Laboratory and Postgraduate Research Lab on Net-Zero and Sustainability.
- Assisted in multiple industry-sponsored research projects.
- Taught Laboratory courses on Drilling Fluids Testing, Reservoir Engineering, Workshop Practices, and Industrial Pollution Control to undergraduate petroleum engineering and chemical engineering students.
- Assisted in conducting exams and coordinating lab sessions.
- Managed the day-to-day operations of the Drilling Fluids Design Laboratory including research scholars, undergraduate students, equipment, and facility.
- Developed and implemented laboratory policies and procedures to ensure compliance with safety, performance, and quality standards.
- Documented and maintained laboratory records in accordance with applicable regulations.
- Provided guidance and assistance with laboratory troubleshooting and problem-solving.

2018-2020

Teaching Assistant, School of Petroleum Technology
Pandit Deendayal Energy University, India

- Taught Drilling Fluids Preparation and Laboratory Testing, Reservoir Engineering Laboratory, and Basics of Petroleum Software (CMG and Kappa Workstation) to petroleum engineering undergraduate students (around 120 students).
- Developed quizzes, exams, and coordinated lab sessions.
- Assisted the faculty member in preparing the lab manual.

PUBLICATIONS

Journal Publications

1. **Bardhan, A.**, Kumar, S., Basu, S., Pandey, A., Kesarwani, H., Saxena, A., Sarkar, J., Sharma, S., Kumar, S., "Mechanistic Performance of Modified Carbon Nanotubes Stabilized in Water-based Drilling Fluids for High-Temperature Applications," ACS Energy Fuels, I.F. 5.2, vol. 38, no. 17, pp. 16066-16078, 2024.
   https://doi.org/ 10.1021/acs.energyfuels.4c02548

2. Khan, F., **Bardhan, A.**, Kumar, P., Yadawa, Y., Sharma, S., Saxena, A., Ranjan, A., "Performance Assessment of Bismuth Ferrite Nanoparticles in Enhancing Oil Well Cement Properties: Implications for Sustainable Construction," SPE Journal, I.F. 3.2, vol. 29, no. 09, pp. 4596-4607, 2024.
   https://doi.org/10.2118/221469-PA

3. **Bardhan, A.**, Singh, A., Nishanta, H., Srivastava, S., Sharma, S., Choubey, A. K., Kumar, S., "Biogenic Copper Oxide Nanoparticles for Improved Lubricity and Filtration Control in Water-Based Drilling Mud" ACS Energy Fuels, I.F. 5.2, vol. 38, no. 10, pp. 8564-8578, 2024.
   https://doi.org/10.1021/acs.energyfuels.4c00635

4. **Bardhan, A.,** Vats, S., Prajapati, D. K., Halari, D., Sharma, S., Saxena, A., "Utilization of Mesoporous Nano-Silica as High-Temperature Water-based Drilling Fluids Additive: Insights into the Fluid Loss Reduction and Shale Stabilization Potential," Geoenergy Science and Engineering (formerly Journal of Petroleum Science and Engineering, I.F. 5.1), vol. 232, part A, 212436, ISSN 2949-8910, 2024.
   https://doi.org/10.1016/j.geoen.2023.212436

5. Prajapati, D. K., **Bardhan, A.**, Sharma, S., "Microwave-assisted Synthesis of Zinc Oxide Nanoflowers for Improving the Rheological and Filtration Performance of High-Temperature Water-based Drilling Fluids," Journal of Dispersion Science and Technology, I.F. 1.9, pp.1-13, 2023.
   https://doi.org/10.1080/01932691.2023.2294303

6. Rahaman, S. M., **Bardhan, A.**, Mandal, T., Chakraborty, M., Khatun, M., Layek, M., Sharma, S., Chakravarty, M., Saha, R., Saha, B., "An effect of hydrophobicity of cosurfactant on the growth of cerium tetrafluoride hexagonal nanorods in water-in-oil microemulsion template," Journal of Molecular Liquids, I.F. 5.3, vol. 391, part A, pp. 123333, 2023.
   https://doi.org/10.1016/j.molliq.2023.123333

7. Rahaman, S. M., **b**, Mandal, T., Chakraborty, M., Karmakar, K., Dhibar, S., Sharma, S., Chakravarty, M., Ibrahim, S. M., Saha, B., "Understanding the effect of surfactants' hydrophobicity on the growth of lanthanum sulfide nanospheres in water-in-oil microemulsions: a detailed dynamic light scattering, small angle X-ray scattering, and microscopy study," New Journal of

Chemistry, I.F. 3.3, vol. 47, no. 21, pp. 10309-10321, 2023.
https://doi.org/10.1039/D3NJ00935A

Conference Papers

1. **Bardhan, A.**, Khan, F., Kesarwani, H., Vats, S., Sharma, S., Kumar, S., "Performance Evaluation of Novel Silane Coated Nanoparticles as an Additive for High-Performance Drilling Fluid Applications," International Petroleum Technology Conference, Bangkok, Thailand, March 1-3, 2023, Paper no. IPTC-22878-MS.
https://doi.org/10.2523/IPTC-22878-MS

2. **Bardhan, A.** "Graphene as a Surfactant Carrier: A Performance Study for Enhanced Oil Recovery Applications," SPE Annual Technical Conference and Exhibition, Virtual, October 26-29, 2020, Paper no. SPE-204263-STU.
https://doi.org/10.2118/204263-STU

PRESENTATIONS AND INVITED LECTURES

Oral Presentations

1. "Influence Of Morphology And Dispersion Stability On The Properties Of High-performance Water-based Drilling Fluids: A Comparative Study On Zinc Oxide Nanostructures" *NANO 2024 - 17th International Conference on Nanostructured Materials*, Abu Dhabi, United Arab Emirates. November 4, 2024.

2. "Exploring the Role of Vinyl Copolymers in Next-Generation Water-Based Drilling Fluids for Geothermal Well" *International Conference on Petroleum, Hydrogen and Decarbonization*, Indian Institute of Technology Guwahati, India. November 2, 2023.

3. "Performance Evaluation of Novel Silane Coated Nanoparticles as an Additive for High-Performance Drilling Fluid Applications," *International Petroleum Technology Conference*, Bangkok, Thailand. March 2, 2023.

Invited Lectures

1. "Drilling Fluids Preparation," SPE Weeks 11.0 (Feb 2019) and 14.0 (Feb 2020).

PROFESSIONAL TRAINING

20 June 2019 to 31 July 2019

Joshi Technologies International Inc. – India Projects , Dholka
Summer Intern

- Workover and Production Practices: A Case Study of Acid Job Workover, Surface Facilities and Production Optimization by Echometer Survey.

1 January 2018 to 30 June 2018

Corrtech International Private Limited , Ahmedabad
Field Intern

- Palanpur-Vadodara Pipeline Project (Hindustan Petroleum Corporation Limited) – Pipeline Laying and Associated Works.

16 June 2016 to 20 July 2016

Drilling Mentor Private Limited , Ahmedabad
Project Intern

- Well Control Procedure – Practices in India and Recommendations

---

PROFESSIONAL AFFILIATIONS

2014 - Present

Society of Petroleum Engineers International
Student and Professional Member

LANGUAGES

English: Advanced Listening & Speaking, Distinguished Reading & Writing.
Bangla: Native Language.
Hindi: Distinguished Listening & Speaking, Advanced Reading & Writing.

EQUIPMENT HANDLED

Rheology: Anton Paar MCR 302e (with customized high-pressure assembly), Fann Viscometer 32SA.
Drilling Fluid Preparation & Testing: Fann EP/Lubricity Tester, OFITE Capillary Suction Timer, Mud balance, Sand Content kit, Shearometer, Retort Kit, Roller Oven, pH, Resistivity, Emulsion stability tester.
Cement Preparation & Testing: Fann Constant Speed Mixer Model 686CS, Atmospheric Consistometer, Cement Curing Autoclave, CTE Ultrasonic Cement Analyzer, Universal Testing Machine.
Drilling Fluid & Cement Filtration: Fann API Filter Press 300 Series, Fann HPHT Filter Press 175 mL, CTE Stirred Fluid Loss Tester.
Material Synthesis & Treatment: NuWav Pro UV-Microwave Digestor, Centrifuge, Ultrasonic Probe, and bath sonicators.
Material Characterization: Malvern ZetaSizer Nano-ZS, Kruss Dynamic Foam Analyzer.
Rock Characterization: Helium Porosimeter, Gas Permeameter, Mercury Injection Capillary Pressure, Porous Plate Capillary Pressure, Goniometer, Core Resistivity meter.
Carbon Utilization & Sequestration: HPHT Goniometer, Carbonated Water Generation Assembly, Carbon Adsorption High-Pressure Stirred Reactor.

COMPUTER SKILLS

Programming: Basics of Python, C and MATLAB.
Applications: Overleaf and TEXstudio LaTeX, OriginPro, CanvaPro, GraphPad Prism, MS Office (Excel, Word, PowerPoint), KAPPA (Saphir, Topaze, Rubis), CMG (IMEX).

OTHER

- Spearheaded the event management as the **Student Convener** at the **International Conference on Transforming Upstream: Breakthrough Technologies and Sustainability 2024**, Rajiv Gandhi Institute of Petroleum Technology, September 2024.
- Founded an online community **PetroVidya®** for petroleum engineering undergraduates and graduates for knowledge sharing in August 2020.
- Served as the **Managing Editor and Content Writer** for **SPT Mirror** (the Official Magazine of the School of Petroleum Technology), Pandit Deendayal Petroleum University from August 2019 to June 2020.

REFERENCES

Dr. Shivanjali Sharma
Associate Professor, Department of Petroleum Engineering & Geo-Engineering
Associate Dean, Faculty Affairs
Rajiv Gandhi Institute of Petroleum Technology, India
Email: ssharma@rgipt.ac.in

Dr. Shailesh Kumar
Assistant Professor, Department of Petroleum Engineering & Geo-Engineering
Rajiv Gandhi Institute of Petroleum Technology, India
Email: shaileshk@rgipt.ac.in

Dr. Amit Saxena
Assistant Professor, Department of Petroleum Engineering & Geo-Engineering
Rajiv Gandhi Institute of Petroleum Technology, India
Email: asaxena@rgipt.ac.in